# DIRECT, CATALYTIC, INTERMOLECULAR ANTI-MARKOVNIKOV HYDROACETOXYLATIONS OF ALKENES ENABLED VIA PHOTOREDOX CATALYSIS, AND INVESTIGATIONS INTO THE MECHANISM OF THE POLYMERIZATION OF 4-METHOXYSTYRENE INITIATED BY PYRYLIUM SALTS

Andrew Perkowski

A dissertation submitted to the faculty of the University of North Carolina at Chapel Hill in partial fulfillment of the requirements for the degree of Doctor of Philosophy in the Department of Chemistry.

Chapel Hill
2014

Approved by:

David A Nicewicz

Erik Alexanian

Marcey Waters

Maurice Brookhart

Joseph Templeton

## ABSTRACT

Andrew Perkowski: Direct, Catalytic, Intermolecular Anti-Markovnikov Hydroacetoxylations of Alkenes Enabled via Photoredox Catalysis, and Investigations into the Mechanism of the Polymerization of 4-Methoxystyrene Initiated by Pyrylium Salts
(Under the Direction of David A. Nicewicz)

**I. Intermolecular Anti-Markovnikov Addition of Oxygen Nucleophiles to Alkenes: Direct and Indirect Catalytic Methods to Address a Fundamental Challenge**

Markovnikov versus anti-Markovnikov functionalization of alkenes is discussed, as well as the inherent challenge in overcoming Markovnikov selectivity. Stoichiometric and catalytic methods for anti-Markovnikov functionalization are discussed and appraised.

**II. Anti-Markovnikov Addition of Oxygen Nucleophiles to Alkene Cation Radical Intermediates**

The formation of alkene cation radicals is disccused, as well as examples of anti-Markovnikov nucleophilic addition to alkene cation radicals.

**III. The Direct Anti-Markovnikov Addition of Carboxylic Acids to Alkenes Using Photoredox Catalysis**

The conception and optimization of a photoredox catalysis system for the anti-Markovnikov addition of carboxylic acids to alkenes under visible light irradiation is described.

**IV. Investigations Into the Mechanism of the Polymerization of 4-Methoxystyrene Initiated by Pyrylium Salts Under Visible Light Irradiation**

Polymerization of 4-methoxystyrene using 2,4,6-tri(p-tolyl)pyrylium tetrafluoroborate as a photoinitiator is found to proceed via a cationic propagation mode. The effects of alcohol additives on the polymerization are discussed, and a proposal for the mechanism of their influence is put forward. Experiments to further elucidate the initiation and polymerization mechanism are proposed.

## ACKNOWLEDGEMENTS

I wish to thank my advisor Professor David Nicewicz for his help, support, and guidance over these past five years. I am particularly grateful for his support in my collaboration with the research group of Wei You, and his encouragement to leave the comfortable in pursuit of the unknown. I would also like to thank Professor Wei You for his patient support and guidance as I learned to apply my skills to new problems and new questions.

Additionally, I would like to thank and congratulate my fellow cohort of graduate students David Hamilton, Tien Nguyen, Michelle Riener, and Jean-marc Grandjean who have also attained their doctorates this year. I am proud of the research we have conducted, the laboratory we have founded, and the legacy and culture of comradery and civility that we are leaving behind in the Nicewicz group.

I would like to thank my family for their love and support, and my parents in particular for fostering within me a love of learning for as long as I can remember. Thank you also for the considerable sacrifices in time and money that you made so I could receive the best education available to me.

Finally, I would like to thank my wife, Ellen. You have been my greatest support long before we came to Chapel Hill as a newly married couple. More than anyone else you have seen the blood, sweat, toil, and tears that have gone into these past five years. Our relationship is stronger, deeper, and richer for it. I cannot thank you enough for loving not only who I am but who you knew I could be, pushing me to work harder, to be better, to continue even at times

when I thought I could not, to give more than I knew I could give. You are an inspiration to me, and I love you.

## TABLE OF CONTENTS

## LIST OF FIGURES

## LIST OF ABBREVIATIONS AND SYMBOLS

| | |
|---|---|
| %Conv. | Percent Conversion |
| %v/v | percent volume per volume |
| µL | microliter |
| µm | micrometer |
| 1° | Primary |
| $^{13}$C NMR | Carbon Thirteen Nuclear Magnetic Resonance |
| $^{1}$H NMR | Proton Nuclear Magnetic Resonance |
| 2° | Secondary |
| Å | Angstrom |
| Ac | Acetyl |
| BDE | Bond Dissociation Energy |
| BET | Back Electron Transfer |
| BQ | Benzoquinone |
| cat. | catalytic |
| CBz | Carboxybenzyl |
| C-C | carbon-carbon single bond |
| C-H | carbon-hydrogen single bond |
| CN | cyano or nitrile |
| CT | Charge Transfer |
| C-X | carbon-heteroatom single bond |
| d.r. | diastereomeric ratio |
| DCE | 1,2-Dichloroethane |

| | |
|---|---|
| DCM | Dichloromethane |
| DMA | Dimethylacetamide |
| E | *Entgegen* |
| $E_{0,0}$ | Excitation Energy |
| $E_{ox}$ | Electrochemical Oxidation Potential |
| equiv. | equivalents |
| $E_{red}$ | Electrochemical Reduction Potential |
| ESI | Electrospray Ionization |
| *et al.* | and others |
| FMO | Frontier Molecular Orbital |
| GPC | Gel Permeation Chromatography |
| H-Atom | Hydrogen Atom |
| HBQ | Hydroquinone |
| HOAc | Acetic Acid |
| HOMO | Highest Occupied Molecular Orbital |
| hrs | hours |
| Hz | hertz |
| hυ | photon of light |
| int | intermediate |
| *i*PrOH | *iso*-propanol |
| IR | Infrared |
| ISC | Intersystem Crossing |
| kcal | kilocalories |

| | |
|---|---|
| LED | Light Emitting Diode |
| LRMS | Low Resolution Mass Spectrometry |
| LUMO | Lowest Unoccupied Molecular Orbital |
| *m* | *meta* |
| *m/z* | mass to charge ratio |
| Me | methyl |
| MeCN | acetonitrile |
| MeOH | Methanol |
| mg | milligram |
| MHz | megahertz |
| mL | milliliter |
| mmol | millimolar |
| $M_n$ | Number Average Molecular Weight |
| mol | moles |
| mol% | molar percentage |
| MPa | Megapascals |
| MW | Molecular Weight |
| $M_w$ | Weight Average Molecular Weight |
| NaOAc | Sodium Acetate |
| nm | nanometer |
| NMP | *N*-Methylpyrrolidinone |
| NMR | Nuclear Magnetic Resonance |
| NOCAS | Nucleophile-Olefin Combination, Aromatic Substitution |

| | |
|---|---|
| *o* | *ortho* |
| OAc | Acetate |
| *p* | *para* |
| PDI | Polydispersity Index |
| PET | Photoinduced Electron Transfer |
| Ph | Phenyl |
| Phth | phthalimide |
| $_{p}$Ka | Logarithm of Acidity Equilibrium Constant |
| ppm | parts per million |
| rbf | round-bottom flask |
| rt | room temperature |
| S | generic solvent molecule |
| $S_0$ | Singlet ground state |
| $S_1$ | First singlet excited state |
| SCE | Saturated Calomel Electrode |
| SET | Single Electron Transfer |
| $T_1$ | First triplet state |
| *t*BuOH | *tert*-butanol |
| TfOH | triflic acid |
| THF | tetrahydrofuran |
| TLC | Thin Layer Chromatography |
| UV | Ultraviolet |
| V | Voltz |

| | |
|---|---|
| Z | *Zusammen* |
| $\Delta G$ | Free Energy Change |
| $\Delta G^{\ddagger}$ | Transition State Energy |
| $\lambda_{max}$ | Lambda maximum |
| $\chi$ | Pauling electronegativity |
| $\chi_B$ | Pauling electronegativity of boron |
| $\chi_H$ | Pauling electronegativity of hydrogen |

# CHAPTER 1. INTERMOLECULAR ANTI-MARKOVNIKOV ADDITION OF OXYGEN NUCLEOPHILES TO ALKENES: DIRECT AND INDIRECT METHODS TO ADDRESS A FUNDAMENTAL CHEMICAL CHALLENGE

## 1.1. Markovnikov Regioselectivity

In 1870,[1] Vladimir Markovnikov disclosed investigations into the regioselectivity of the reaction of alkenes with halogenic acids. In the conclusion of his studies, Markovnikov noted: "…when an unsymmetrical alkene combines with a hydrohalic acid, the halogen adds on to the carbon atom containing the fewer hydrogen atoms, that is the carbon that is more under the influence of other carbons." While Markovnikov's original studies were conducted with halogenic acids, this regioselectivity has been widely observed more generally in reactions between alkenes and Brønsted acids. Over the past century, further studies have correlated this regioselectivity with the inherent electronic polarization of those alkenes.[2] Kinetically, the initial protonation of the alkene occurs preferentially on the less substituted, more partially negative carbon of the alkene. The resulting carbocation exists as an empty *p*-orbital, $p(C^+)$ situated on the more substituted carbon of the former alkene, and is stabilized by the overlap of neighboring carbon-carbon and carbon-hydrogen sigma bonds, $\sigma$(C-C) and $\sigma$(C-H) respectively. The relative thermodynamic stabilities of the resulting products generally reflects the relative stabilities of these carbocationic intermediates. A similar orbital analysis of the products points to the overlap of the neighboring carbon-carbon and carbon-hydrogen sigma bonds ($\sigma$(C-C) and $\sigma$(C-H) respectively) with the carbon-heteroatom sigma anti-bonding orbital, $\sigma^*$(C-X), also known as hyperconjugation. Such overlap weakens the carbon-heteroatom bond somewhat, but is overall stabilizing. These kinetic and thermodynamic effects are summarized in Figure 1.1 below.

**Figure 1.1. Thermodynamic and Kinetic Factors Contributing to Markovnikov Selectivity**

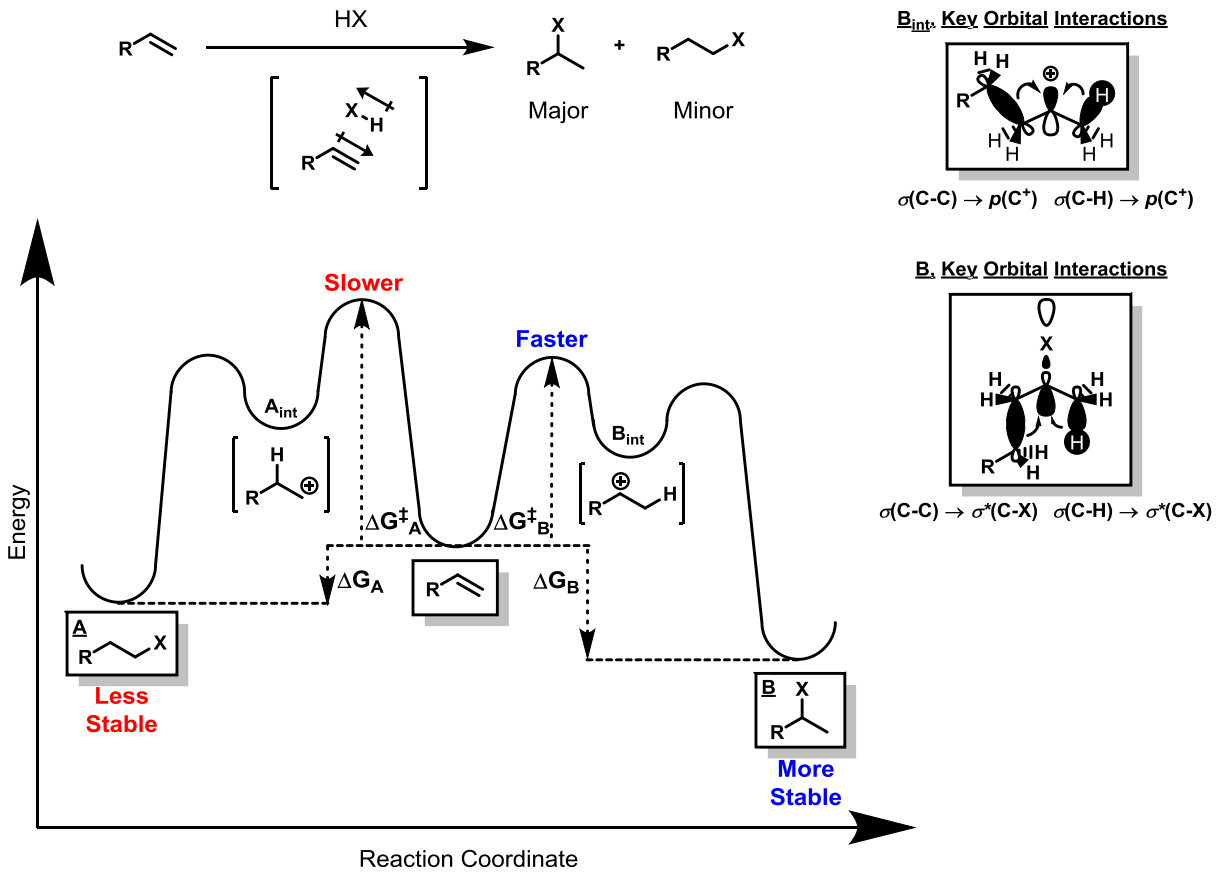


## 1.2. Reversing Markovnikov Selectivity: Brown Hydroboration

Reversing the inherent regioselectivity of these reactions has been an ongoing challenge throughout the twentieth and twenty first centuries. Perhaps the most widely used method to generate the anti-Markovnikov oxy-functionalized product of a corresponding alkene is the hydroboration/oxidation sequence disclosed by H. C. Brown.[3,4,5] The method, in its most general form, involves the reaction of borane with an alkene, often in an ethereal solvent, to give an intermediate alkyl borane exhibiting anti-Markovnikov selectivity. Oxidation of the alkyl borane (using oxidants such as hydrogen peroxide under basic conditions) gives the net anti-Markovnikov heteroatom substituted product (Figure 1.2). While the oxidation of organoboranes

using alkaline hydrogen peroxide had been noted as early as 1938,[6] it was not until the mid-1950's that a method was developed for the facile preparation of alkyl borane species. It appears the precipitating event may have been the serendipitous discovery that ethereal solvents greatly enhance the rate of reactivity of borane.[4,7] Prior to this, the most facile route to alkyl borane species appears to have been reaction of an organolithium or Grignard reagent with a boric ester.

**Figure 1.2. Brown Hydroboration/Oxidation General Sequence**

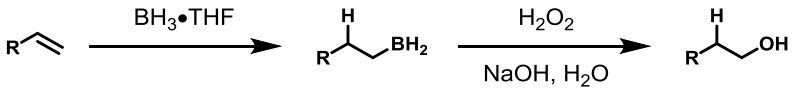


Two particular properties of boron account for the reactivity and regioselectivity observed in the reaction of borane and its analogues with alkenes. Boron has only six valence electrons, and thus its compounds possess an empty *p*-orbital on boron, making them Lewis acidic. The electronegativity of boron ($\chi_B$ =2.04) is lower than that of hydrogen ($\chi_H$ = 2.20) causing the boron hydrogen bond to be oppositely polarized to that of most other hydrogen heteroatom bonds (particularly with elements of group 15, 16, and 17).[8,9] The Lewis acidity of borane causes initial nucleophilic attack of the alkene to occur upon boron, and the polarized nature of the boron-hydrogen bond promotes concomitant delivery of a hydride to the more substituted (more partially positive) carbon of the alkene. A summarization of these properties and the regioselectivity obtained in the reaction of borane with a selection of alkenes of varying patterns of substitution are depicted below in Figure 1.3. Additionally, steric interactions further reinforce anti-Markovnikov regioselectivity.

Unlike reaction of an alkene with a Brønsted acid, hydroboration also exhibits strong stereoselectivity in its reaction with substituted alkenes. The boron hydrogen bond of borane is

broken with simultaneous formation of the boron-carbon and hydrogen-carbon bonds and, consequently, there is a high degree of syn-selectivity between boron and hydrogen.

**Figure 1.3. Anti-Markovnikov Regioselectivity in the Hydroboration of Alkenes.**

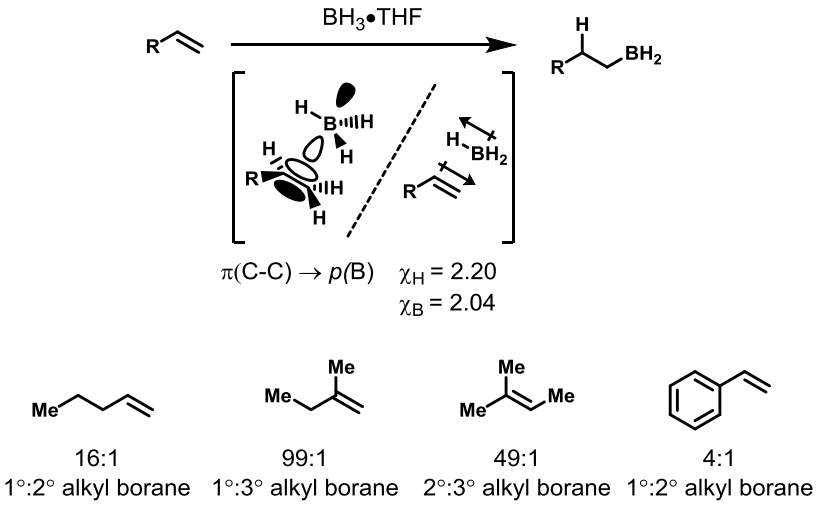


The oxidation of the product alkyl borane using alkaline hydrogen peroxide occurs by nucleophilic attack of a peroxide anion on boron, forming a borate (Figure 1.4). Migration of the carbon-boron bond to oxygen is followed by loss of hydroxide, and occurs with retention of stereochemistry at carbon, this happens twice more to generate a boric ester which can be hydrolyzed to give the desired alcohol.

**Figure 1.4. Mechanism of the Oxidation of Alkyl Boranes to Alcohol and Boric Acid**

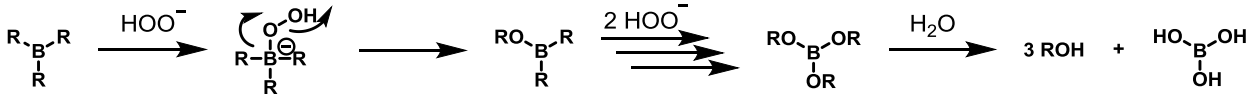


While Brown hydroboration has proven to be one of the most effective and widely applied methods for the anti-Markovnikov hydrofunctionalization of alkenes, it exhibits certain limitations. The overall transformation requires two stoichiometric reactions: first, hydroboration of the alkene; second, oxidation of the intermediate alkyl borane. Borane and borane complexes (e.g. dimethyl sulfide, tetrahydrofuran adducts) generally require inert, moisture free conditions

for storage. From the perspective of both cost and waste generation, a method which would directly provide anti-Markovnikov functionalized products from alkenes using air and moisture stable reagents could potentially offer advantages over hydroboration/oxidation chemistry. The development of a direct, catalytic solution to this problem has proven challenging. While much recent work has been reported in the context of intermolecular anti-Markovnikov hydroamination,[10–18] there have been comparatively fewer solutions to the challenge of intermolecular anti-Markovnikov oxyfunctionalization. Nevertheless, the past several years have seen several creative and compelling attempts to solve this challenge.[19]

### 1.3. Palladium Catalyzed Aerobic Allylic Acetoxylation of Terminal Alkenes

In 2010, Stahl *et al.*[20] disclosed a terminally selective allylic acetoxylation reaction, and demonstrated a one-pot, three step sequence that could arrive at the net anti-Markovnikov hydration products of the starting alkenes. The system employed palladium as catalyst and 4,5-diazafluorenone (**1**) as a supporting ligand (Figure 1.5). A wide range of allyl substituted esters, amides, electron rich to electron neutral aryl groups, and carbonyls were tolerated. Among the bipyridyl and phenanthryl ligands screened, **1** was unique in its ability to effect this reaction aerobically.

**Figure 1.5. Terminally Selective Palladium Catalyzed Allyic Acetoxylations**

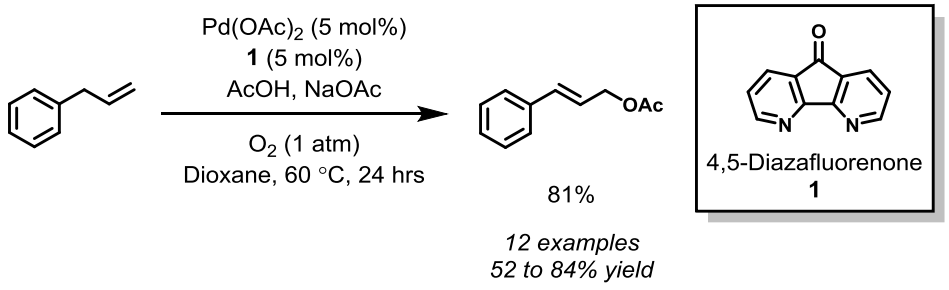

After allyic acetoxylation, the reaction mixture could be directly treated with potassium carbonate in methanol, and then stirred with added activated carbon under an atmosphere of hydrogen to achieve a net anti-Markovnikov hydration reaction. Stahl and coworkers demonstrated this procedure using allyl benzene (Figure 1.6).

**Figure 1.6. One-pot Net Anti-Markovnikov Hydration Procedure**

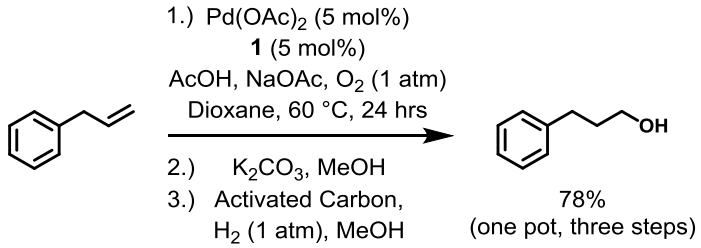


Palladium catalyzed allylic acetoxylation reactions require a stoichiometric oxidant for catalyst turn over, and benzoquinone is most commonly employed.[21] Mechanistic studies carried out in the course of the development of this reaction suggested that under anaerobic conditions benzoquinone serves not only to oxidize $Pd^0$ to $Pd^{II}$, but may also influence other steps of the catalytic cycle. When palladium-π-allyl complexes with 4,4'-di-*tert*-butyl-2,2'-bipyridine as a supporting ligand were prepared in a stoichiometric fashion, no reaction with acetate anion was observed either under anaerobic conditions (nitrogen atmosphere) or aerobic conditions (3 atm oxygen). When 2 equivalents of benzoquinone were employed, however, complete consumption of the (4,4'-di-*tert*-butyl-2,2'-bipyridyl)$Pd^{II}$($\eta^3$-allyl) complex occurred to give an 88% yield of allyl acetate. In contrast, the corresponding $Pd^{II}$($\eta^3$-allyl) complex with **1** generated allyl acetate under all of the same conditions, though at differing rates: 24 hours to complete conversion under nitrogen, 3 hours under 3 atm of oxygen, and 1 hour in the presence of 2 equivalents of benzoquinone. This suggests that benzoquinone (and possibly oxygen as well, though to a lesser extent) may serve to promote the attack of acetate anion on the $Pd^{II}$($\eta^3$-allyl) species.

In an attempt to further understand the role of **1** as ligand, the reversibility of C-O bond formation was also investigated in the presence and absence of oxidants. With cinnamyl acetate as substrate, in the absence of oxidant, $d_3$-acetate exchange was facile with **1** as ligand but did not occur with 4,4'-di-*tert*-butyl-2,2'-bipyridine. When oxygen or benzoquinone was included with **1** as ligand, $d_3$-acetate exchange diminished greatly. The amount of exchange decreased in proportion to the oxygen pressure employed in the reaction, presumably due to oxygen reacting rapidly with the $Pd^0$-alkene product complex to displace the cinnamyl acetate. Based on these studies, Stahl and coworkers propose that **1** circumvents the need for benzoquinone by destabilizing the $Pd^{II}(\eta^3$-allyl) intermediate due to a larger bite-angle (versus the other tested bipyridyl and phenanthryl ligands) thus promoting nucleophilic attack by acetate. After formation of the allyl acetate product, oxygen is a competent oxidant to regenerate $Pd^{II}$. In systems employing other ligands, benzoquinone appears to be necessary to promote nucleophilic attack on the $Pd^{II}(\eta^3$-allyl) in addition to re-oxidation of the palladium catalyst. The general mechanism of the aerobic allylic acetoxylation of terminal alkenes is presented below in Figure 1.7.

**Figure 1.7. Mechanism of Palladium Catalyzed Aerobic Allylic Acetoxylation**

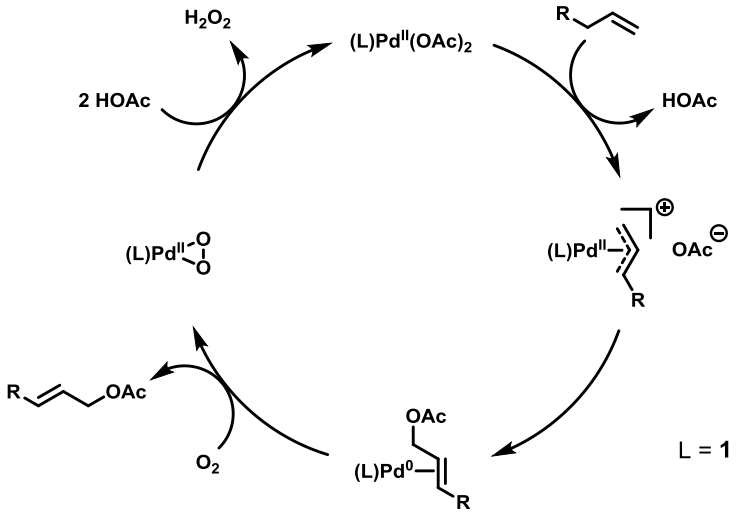


### 1.4. Tandem Hydroformylation/Reduction of 1-Decene

Nozaki and coworkers,[22] also in 2010, reported a formal anti-Markovnikov hydration method involving tandem hydroformylation and hydrogenation of 1-decene, producing the terminal alcohol product in up to 90% yield and selectivity of 22 to 1 for the linear alcohol product (Figure 1.8). The reaction is carried out at elevated temperatures under an atmosphere of syngas (1 to 1 hydrogen to carbon monoxide), with a rhodium(I) complex supported by a Xantphos ligand (**2**) which carries out the hydroformylation step, while Shvo's catalyst (**3**) reduces the resulting aldehyde.

The choice of **2** is highly important for the observed selectivity. Controlling the ratio of linear (*n*, normal) to branched (*i*, iso) aldehyde products in the hydroformylation of alkenes is not a trivial challenge. Leeuwen and coworkers[23] studied the effects of ligands of varying bite-angle and rigidity on the selectivity of the hydroformylation of 1-octene. Selectivity for *n*-aldehyde products generally increased with increasing diphosphine bite-angle (as determined by molecular

**Figure 1.8 One-pot Hydroformylation/Reduction of 1-Decene**

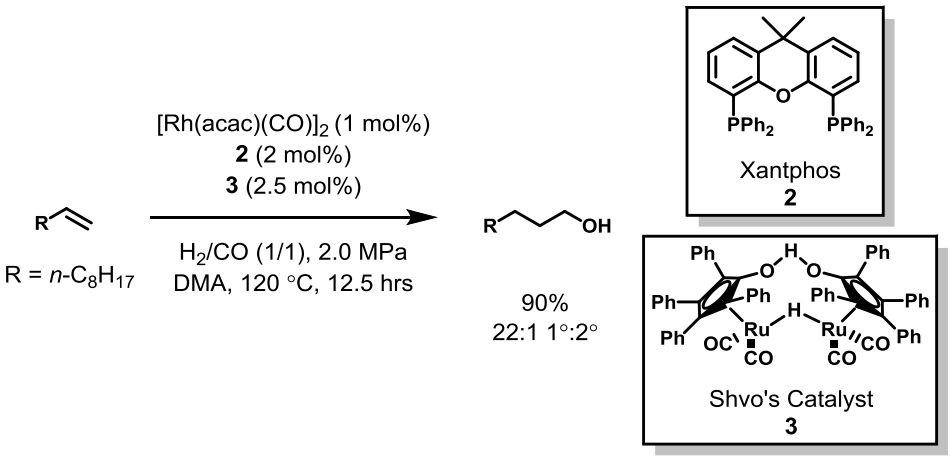


mechanics calculcations of the ligands), with an optimum between 112 and 120°. Ligands with even greater bite-angles did not form distinct, monomeric rhodium complexes, and exhibited drastically reduced selectivities. In addition to bite-angle, ligand rigidity (the variation of bite-angle produced within a given window of strain energy) was also found to be an important factor in selectivity. More rigid ligands, those which varied less from their natural bite-angle for a given amount of strain energy, contributed to greater *n*-aldehyde selectivity and less isomerization of 1-octene to 2-octene. Overall, rigid ligands with large bite-angles (such as **2**) assist in the formation of a distinct, defined "docking site" in the complex for the alkene substrate which sterically better accommodates linear alkyl intermediates, and lead to *n*-aldehyde products. Nozaki and coworkers chose **3** for its selectivity in the hydrogenation of the intermediate aldehyde over the starting alkene substrate.[24] The ruthenium complex activates dihydrogen in a heterolytic manner, formally generating an equivalent of ruthenium hydride and an equivalent of proton. This polar activation of dihydrogen greatly increases the rate of reduction of polar functionalities, such as aldehyde or ketones, over that of non-polarized functionalities such as carbon-carbon double bonds thus allowing for the selectivity necessary to

efficiently carry out both the hydroformylation and the hydrogenation in a single reaction vessel. A general representation of the overall transformation is depicted below in Figure 1.9.

**Figure 1.9. Overall Hydroformylation/Reduction Sequence to Produce 1-Decanol**

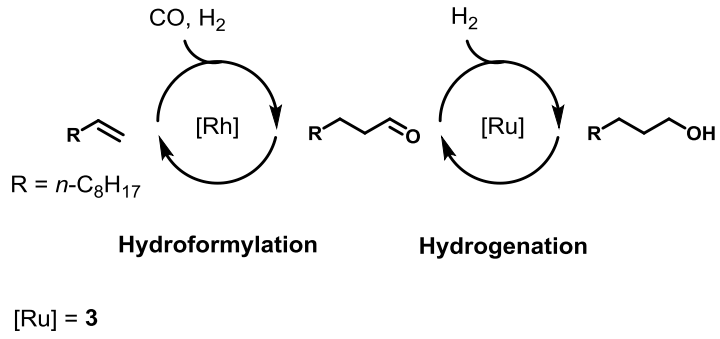


While this strategy produces linear alcohols in great yield and selectivity, the product includes a one carbon homologation relative to the starting alkene due to the hydroformylation necessary to install the oxygen functionality. Judicious choice of starting alkene could compensate for this necessary homologation for many desired primary alcohol targets, classifying this method as a formal anti-Markovnikov hydration.

### 1.5. Anti-Markovnikov Hydration of Styrenes by Triple Relay Catalysis

A notable method was disclosed by Grubbs *et al.* in 2011,[25] depicted below in Figure 1.10. Terminally unsubstituted styrenyl olefins could be transformed into the corresponding primary alcohols with good selectivity (>20:1) making use of a triple relay catalysis system. Initial Wacker-type oxidation of the olefin with *tert*-butanol results in a *tert*-butylvinyl ether, followed by acid hydrolysis of the resulting vinyl ether, and finally transfer hydrogenation from *iso*-propanol of the resulting aldehyde catalyzed by **3**. The triple relay catalytic sequence is summarized in Figure 1.11. Copper(II) chloride salts were found to be important to inhibit direct

**Figure 1.10. Anti-Markovnikov Hydration of Terminal Styrenes by Triple Relay Catalysis**

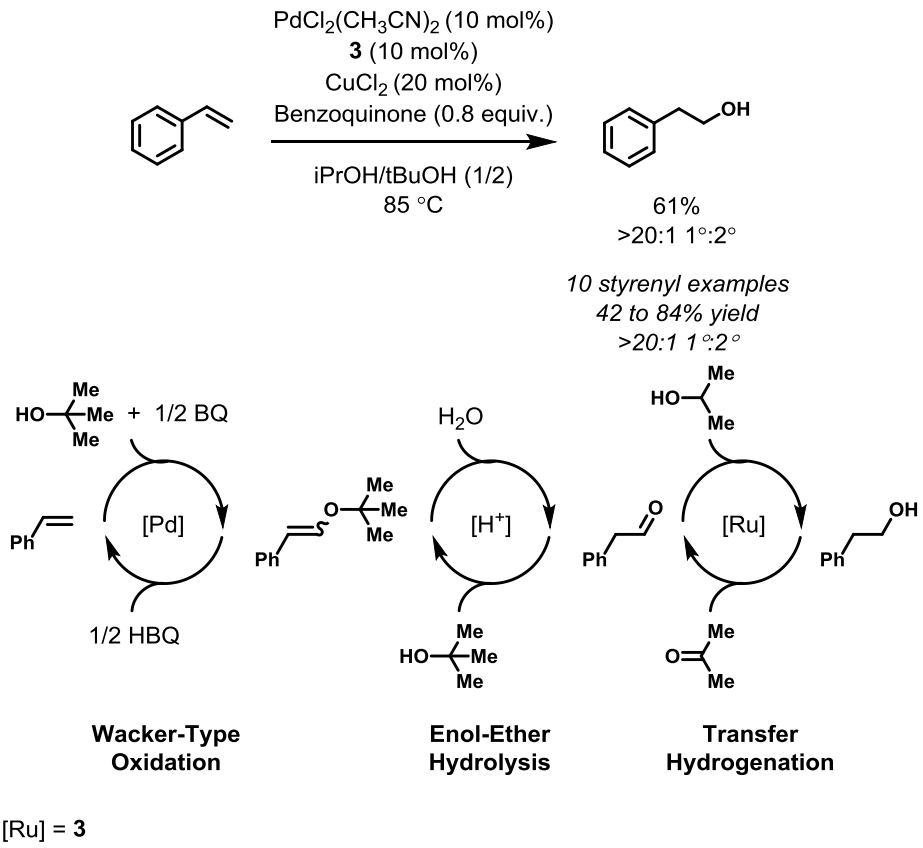


[Ru] = **3**

reduction of the alkene, and benzoquinone was necessary for *in situ* re-oxidation of palladium.

Good selectivity and reactivity were observed for a range of styrenyl alkenes, however terminal alkyl olefins were found to react poorly and with little to no selectivity (Figure 1.11).

**Figure 1.11. Hydration of Non-Styrenyl Terminal Olefins by Triple Relay Catalysis**

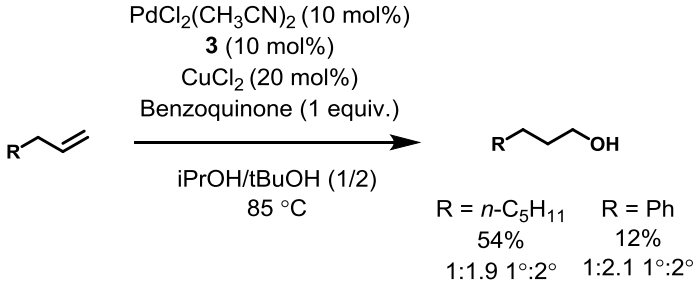


In the context of terminal styrenyl olefins, this method is perhaps closest to a direct, catalytic solution to the challenge of anti-Markovnikov hydrofunctionalization using oxygen

nucleophiles. Practically, though, a large amount of catalysts and additives are necessary for efficient reactivity. A combined 50 mol% of ruthenium, palladium, and copper relative to starting alkene are employed, in some cases resulting in an only slightly greater amount of the desired product (for example, 61 mol% in the case of styrene). Nevertheless, the method is catalytic in nature and is a significant contribution to addressing this challenge.

### 1.6. Ruthenium Catalyzed Anti-Markovnikov Reductive Hydration of Terminal Alkynes

In a recent publication, Herzon and coworkers disclosed a ruthenium catalyzed anti-Markovnikov reductive hydration of terminal alkynes providing great selectivity and a broad substrate scope (Figure 1.12).[26]

The reaction shares similarities, conceptually, with those systems put forward by Nozaki

**Figure 1.12. Anti-Markovnikov Reductive Hydration of Terminal Alkynes**

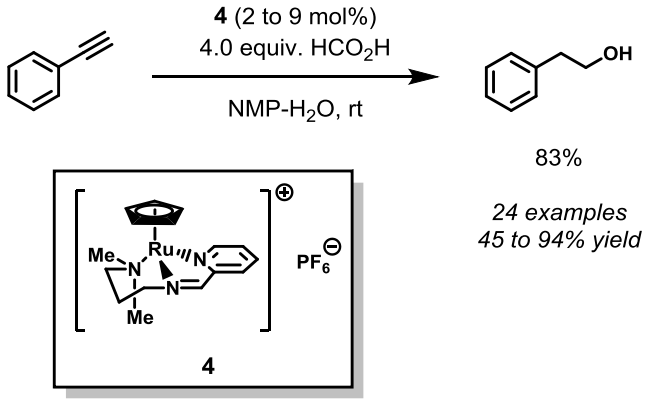


and Grubbs (above). In this case, the intermediate aldehyde is formed via terminal alkyne hydration catalyzed by a ruthenium complex (**4**) possessing a cyclopentadienyl ligand and an iminopyridine ligand with a pendant amine, while the reduction is carried out by the same catalyst after generation of a ruthenium hydride from decarboxylation of formic acid. Study into the mechanism of this transformation revealed a complex system involving three cycles: hydration of the terminal alkyne, reduction of the resulting aldehyde, and reversible

decarboxylation of formic acid into dihydrogen and carbon dioxide.Under neutral conditions, **4** is coordinatively saturated and can be stored under air in a dessicator.

The overall mechanistic sequence of the ruthenium catalyzed anti-Markovnikov reductive hydration of alkynes is presented in Figure 1.13 below. Protonation of **4** by formic acid causes the pendant amine to become labile, opening up a coordination site on ruthenium. Formate can occupy this site forming a formate complex **5**, which can lead either to decarboxylation and formation of a ruthenium hydride (**7**), or solvent can displace the formate generating a solvent coordinated complex, **6**. Complex **6** is then capable of terminally selective hydration of the alkyne substrate **8** to generate an aldehyde (**9**). Dissociation must occur for **9** to come into contact with an equivalent of **7**, which can reduce the aldehyde to the corresponding alcohol providing the net anti-Markovnikov hydration product.

This method is efficient for generating the anti-Markovnikov hydrofunctionalization product of a variety of corresponding theoretical terminal alkenes. The need to use alkynes to achieve this transformation, however, exhibits two particular limitations. First, products corresponding to the formal anti-Markovnikov hydrofuntionalization of more highly substituted alkenes are not accessible. Second, alkenes are a ubiquitous functionality in both natural products and petrochemical derivatives, while alkynes are less broadly found, generally requiring additional synthetic steps for their formation. Still, the method makes use of a single transition metal complex which plays an impressive dual role, requiring only added formic acid and water to achieve the desired transformation.

**Figure 1.13. Overall Anti-Markovnikov Reductive Hydration of Alkynes**

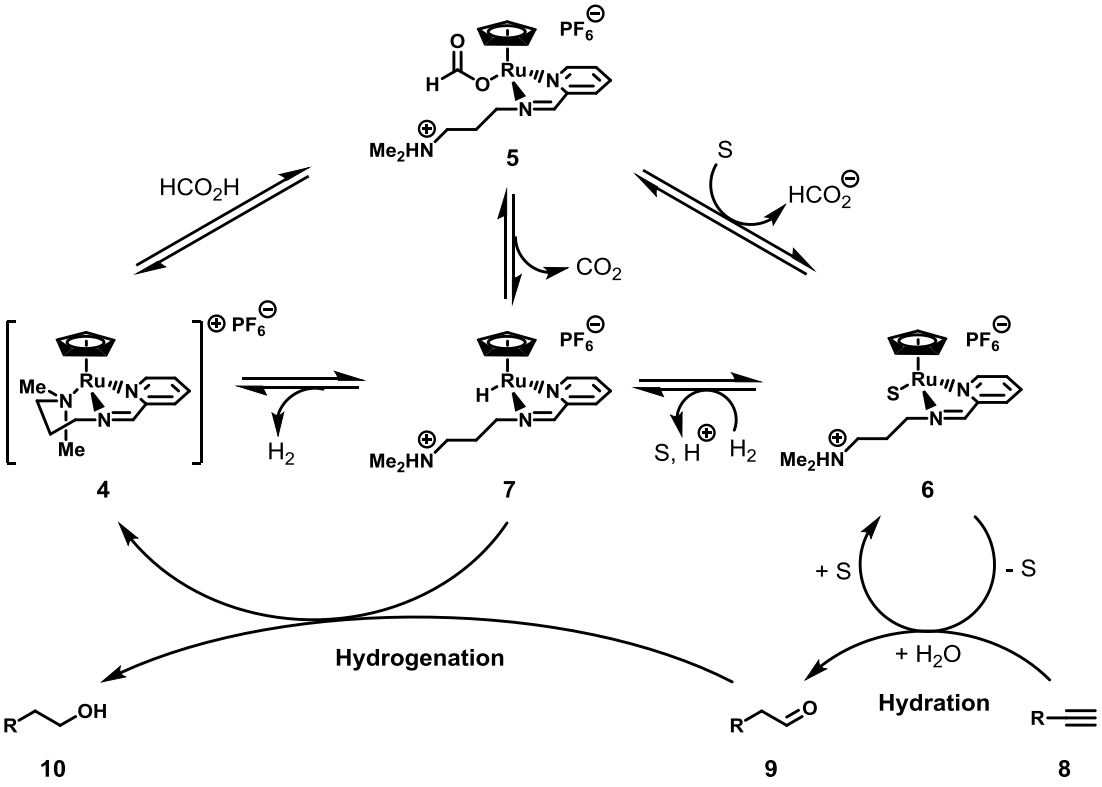


## 1.7. Overview of Current Methods for Catalytic Anti-Markovnikov Oxyfunctionalization

Important strides have been made over the past several years towards a direct, catalytic method for the intermolecular anti-Markovnikov oxyfuntionalization of alkenes. The leading methods make use of transition metal catalysis of varying modes, including creative solutions employing tandem catalysis, sequential catalysis, and catalysts that play dual roles within the reaction. Certain limitations still exist, however. Substrates scopes are generally limited to terminal alkenes, and necessitate homologation or transposition of the alkene prior to further functionalization to arrive at the net anti-Markovnikov functionalized product. The method of Grubbs *et al.* is limited to terminal styrenyl alkenes though has the advantage of directly forming the anti-Markovnikov product from the corresponding alkene without intervening steps or

homologation. The reductive hydration of terminal alkynes reported by Herzon and coworkers possesses an impressive substrate scope, but requires beginning with terminal alkynes precluding the formation of anti-Markovnikov oxyfunctionalization products corresponding to alkenes of greater substitution. Given this, there is room for additional approaches to address this challenge.

## CHAPTER 2. ANTI-MARKOVNIKOV ADDITION OF OXYGEN NUCLEOPHILES TO ALKENE CATION RADICAL INTERMEDIATES

### 2.1. Earliest Reports of Alkene Cation Radical Nucleophilic Addition

Another potential means of addressing the challenge of direct, catalytic anti-Markovnikov oxyfunctionalization of alkenes is via single electron oxidized intermediates known as alkene cation radicals. The first report of nucleophilic addition to an alkene via its cation radical intermediate was published by Arnold and coworkers in 1973.[27] They observed that (2-methoxyethane-1,1-diyl)dibenzene was the exclusive product of the irradiation of a methanol solution of 1,1-diphenylethene and 4-cyanobenzoate (**1**) by a high-pressure xenon-mercury vapor lamp (Figure 2.1). Similar irradiation using 2-propanol as solvent gave (2-isopropoxyethane-1,1-diyl)dibenzene as the exclusive product. Based on transient absorbance studies, Arnold concluded that the reaction proceeded through the 1,1-diphenylethene cation radical, generated via photoinduced electron transfer (PET) to 4-cyanobenzoate followed by nucleophilic trapping by solvent. Subsequent studies by Arnold and other researches have confirmed this pattern of alkene cation radical reactivity with a number of alkenes and nucleophiles.

**Figure 2.1. PET Promoted Anti-Markovnikov Hydromethoxylation of 1,1-Diphenylethene**

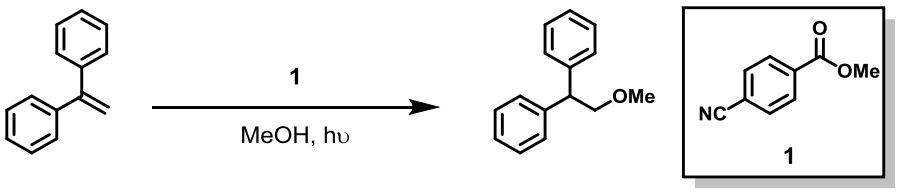

## 2.2. Generating Alkene Cation Radicals via Photoinduced Electron Transfer

Photoinduced electron transfer (PET) is a common method for the generation of radical cationic intermediates. Before discussing the PET process in particular, it is wise to review the general photophysical processes involved in photo-excitation of organic molecules.[28,29] To aid in understanding and visualization of this process, reference will be made to a Jablonski diagram, depicted in Figure 2.2. below.

**Figure 2.2. Jablonski Diagram**

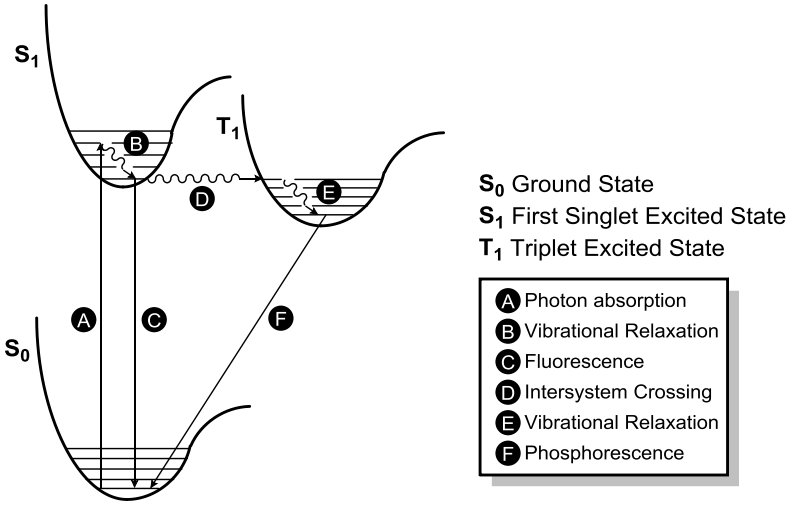


Most organic molecules are closed shell species in their ground state (all electrons are paired), represented by the energy surface $\mathbf{S_0}$ in Figure 2.2. Absorption of a photon of light of appropriate energy promotes the molecule to its first electronically excited singlet state represented by the energy surface $\mathbf{S_1}$. For absorption to occur, the energy of the photon must correspond with the gap in energy between the ground state, $\mathbf{S_0}$, and the excited state, $\mathbf{S_1}$ (Figure 2.2, **A**). The excited state, $\mathbf{S_1}$, is a singlet state as transition directly to a triplet excited state is forbidden due to the necessity for conservation of overall angular momentum of the system. Transitions are more probable between states of similar geometry, and electron transitions are orders of magnitude faster than the vibrational motions of nuclei, so the newly excited molecule

has a geometry similar to the ground state from which it came. This geometry seldom corresponds to the lowest energy level within $\mathbf{S_1}$, and thus vibrational relaxation occurs to a geometry that corresponds to a lower lying energy level within $\mathbf{S_1}$ (Figure 2.2, **B**).

Generally, singlet excited states have one of three possible fates. First, radiationless decay can occur (not pictured) in which the molecule gives off energy in the form of heat to surrounding molecules (e.g. solvent) through vibrational relaxation. The probability of radiationless decay decreases as the difference in energy between $\mathbf{S_0}$ and $\mathbf{S_1}$ increases. The magnitude of this gap is affected primarily by the structure of the particular molecule. Second, fluorescence can occur (Figure 2.2, **C**) wherein the excited state of the molecule emits a photon of energy corresponding to the gap in energy between the excited state, $\mathbf{S_1}$, and some energy level within the ground state, $\mathbf{S_0}$, due to the same geometrical considerations of discussed above for excitation. The probability of fluorescence increases as the difference in energy between $\mathbf{S_0}$ and $\mathbf{S_1}$ increases. The energy of the emitted photon is always lower in energy than the absorbed photon due to the vibrational relaxation that occurs between absorption and emission.

The third possibility is intersystem crossing, which involves a change in electron spin multiplicity (from the singlet state with no unpaired electrons, to the triplet state with two unpaired electrons). This can occur if the energy and geometry of the molecule in the excited state, $\mathbf{S_1}$, matches closely the energy and geometry of a state on the triplet excited state energy surface, $\mathbf{T_1}$ (Figure 2.2, **D**). Such excited triplet states are normally energetically lower than the starting excited singlet state, and intersystem crossing is followed by vibrational relaxation to a low lying energy level within $\mathbf{T_1}$ (Figure 2.2, **E**). Formally, the electronic transition involved in intersystem crossing is spin forbidden for the same reasons stated above with regards to the initial excitation. Transitions from singlet excited states to triplet excited states generally proceed

via spin-orbit coupling. In a simplistic sense, when the energy and geometry of a particular state on the excited singlet energy surface (**$S_1$**) are close to the energy and geometry of a state on the excited triplet energy surface (**$T_1$**), an electron can exchange with an orthogonal orbital altering the angular momentum of that orbital, while the movement of that electron simultaneously alters the electronic spin-angular momentum providing an overall conservation of angular momentum with concomitant change in the electron multiplicity. The existence of states that possess the right energy and geometry to allow for this coupling is a function, primarily, of the structure of particular molecules. Along these same lines, organic molecules containing "heavier" atoms (i.e. atoms of rows 3, 4, and 5) undergo intersystem crossing more rapidly because of the greater degree of spin-orbit coupling that occurs inherently in *d* and *f* orbitals. Because a return from the triplet excited state, **$T_1$**, to the starting ground state, **$S_0$**, is also spin forbidden, triplet excited states tend to be relatively long lived ($\tau_p = 10^{-3}$ to $10^{1}$s for triplet excited states versus $\tau_f = 10^{-8}$ to $10^{-5}$s, where $\tau_x$ represents the lifetime of the excited species, calculated as the inverse rate, *k*, of emission from either state, $\tau_x = 1/k_x$). Emission eventually occurs (Figure 2.2, **F**) producing a photon of less energy than both the initial absorption (Figure 2.2, **A**) as well as the alternate pathway of fluorescence (Figure 2.2, **C**).

With this photophysical foundation, attention can be turned towards the PET process, the general sequence of which can be described through frontier molecular orbital (FMO) analysis. Examining the respective HOMO and LUMO of some acceptor, **A**, and some donor, **D**, with frontier orbitals as depicted in panel **I** of Figure 2.3, single electron transfer (SET) from **D** to **A** is not a thermodynamically favorable process as the LUMO of **A** is too high in energy relative to the HOMO of **D**. Excitation of **A** with a photon of light (denoted "hυ"), however, will move an

electron from the HOMO to the LUMO of **A**. This excited state, **A*** (panel **II**, Figure 2.3), now possesses an electron hole in its HOMO, which is lower in energy than the HOMO of **D**, making

**Figure 2.3. FMO Analysis of PET**

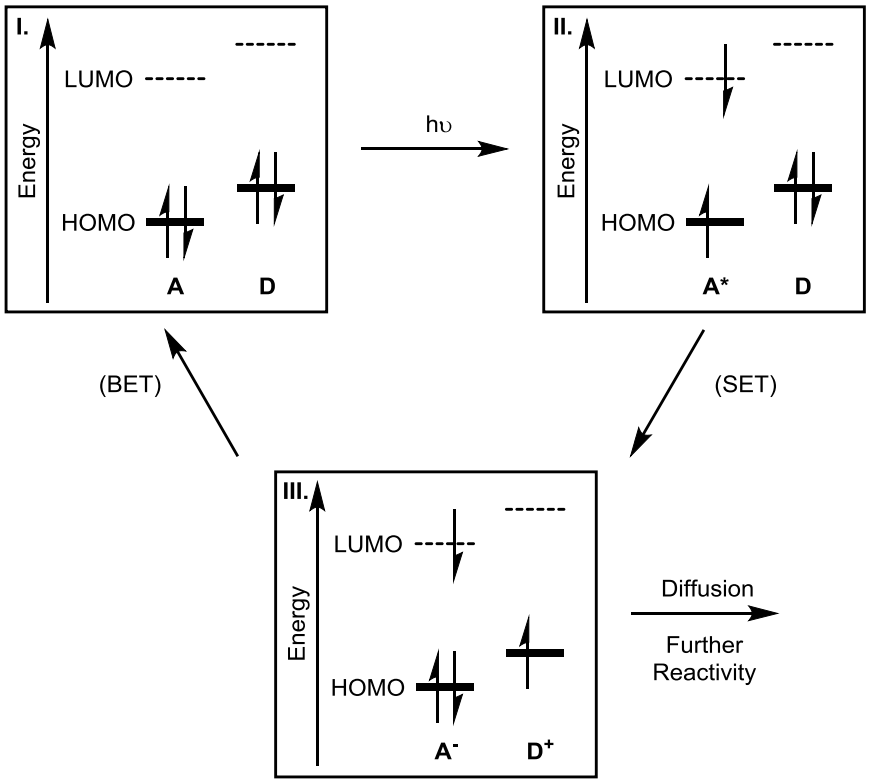


SET thermodynamically favorable. After SET from **D** to **A***(panel **III**, Figure 2.3), we have two new species: $\mathbf{A}^-$ which is formally an anion radical, and $\mathbf{D}^+$ which is formally a cation radical. If these species remain in contact (for example, due to Coulombic attraction) then back electron transfer (BET) can occur bringing the process back to where it began. If these species diffuse away from one another, then further reactivity can occur, potentially with other species present in solution.

The free energy of this transfer can be calculated by the equation below, a modified version of the Weller equation (Figure 2.4), where $E_{Red}$ is the ground state reduction potential of the acceptor, $E_{Ox}$ is the oxidation potential of the donor, and $E_{0,0}$ is the gain in energy of the

acceptor upon excitation by a photon. Reduction and oxidation potentials of molecules are generally measured using electrochemical methods such as cyclic voltammetry, and are always reported relative to a standard reference electrode. Comparisons are most informative between measurements using the same reference electrode under similar conditions of solvent, electrolyte, and temperature. The gain in energy of excited states relative to ground states, $E_{0,0}$, must be estimated from other data, such as the peak wavelength of fluorescent emission.

This information allows for the prediction of the thermodynamic driving force for electron transfer from a given donor to a given excited state acceptor. A general diagram of representative oxidation and reduction potentials of a selection of species appears in Figure 2.4, all relative to the standard calomel electrode (SCE). The diagram is organized such that if a particular oxidant (electron acceptor) is further to the right of a particular reductant (electron donor) then electron transfer from that reductant to that oxidant should be thermodynamically favorable.

**Figure 2.4. Electrochemical Potentials of Species of Interest and Modified Weller Equation**

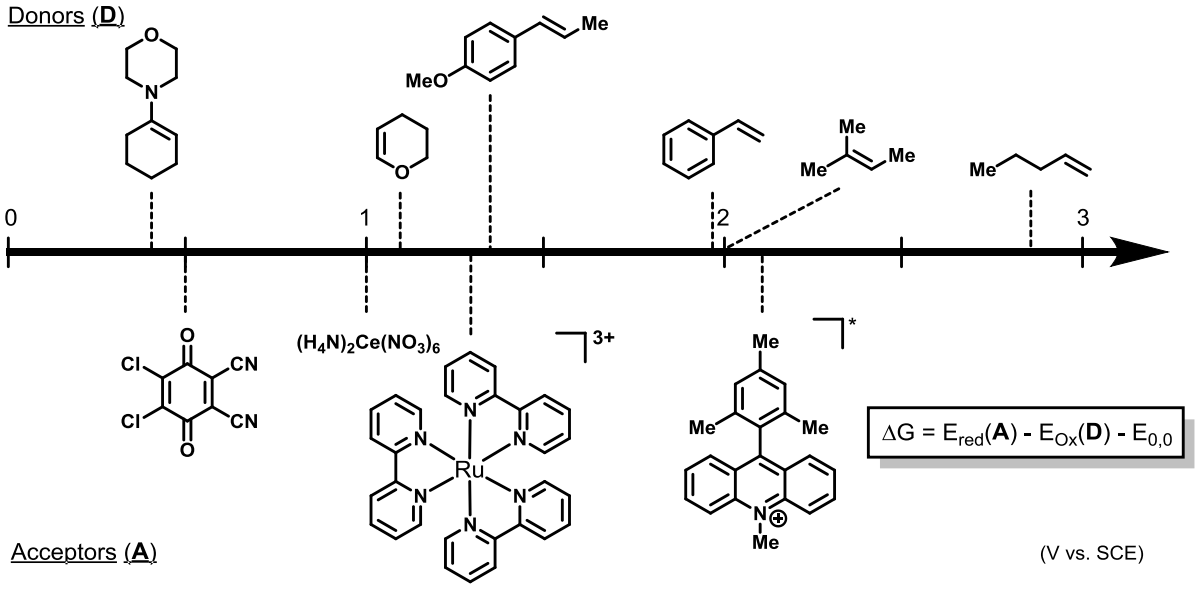

## 2.3 Early Investigations Into PET Promoted Anti-Markovnikov Alkene Addition

After the initial disclosure by Arnold in 1973, further research into PET promoted additions to alkenes by Arnold's laboratory and Gassman's laboratory over the next several decades sought to understand the cause of the observed regioselectivity. In 1975,[30] Arnold and Shigemitsu submitted three phenyl substituted cyclic alkenes (phenylnorbornene, phenycyclohexene, and phenylcyclopentene) to irradiation using medium-pressure mercury vapor lamps in solutions containing either **1** or 1-cyanonaphthalene (**2**) and a nucleophilic solvent component (Figure 2.5). Yields ranged from good to modest, and complete regioselectivity was observed. Except in the case of phenylnorbornene, the products exhibited little to no diastereoselectivity.

**Figure 2.5. PET Promoted Anti-Markovnikov Additions to Phenyl Substituted Alkenes**

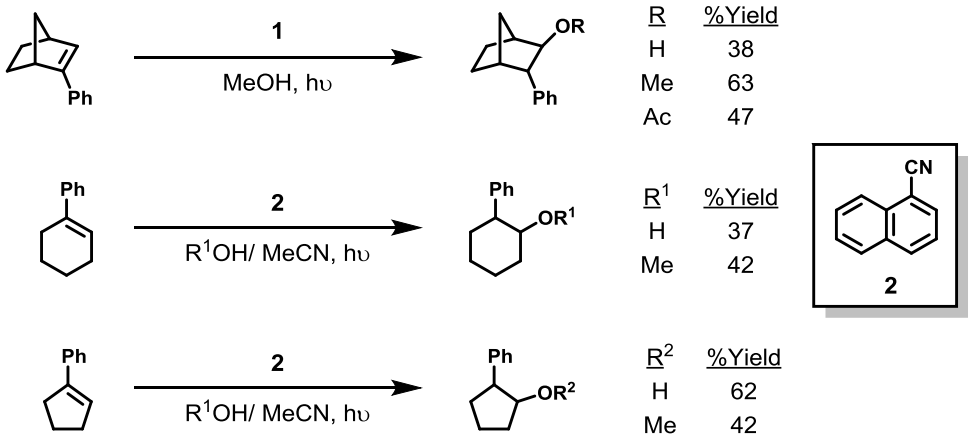


Gassman and coworkers further investigated the reactivity of 1-methylcyclohexene under similar conditions in 1987, using biphenyl (**3**) as a co-sensitizer to increase the efficiency of the reaction by reducing BET.[31] While modest yields were generally obtained, complete regioselectivity was also observed in all cases (Figure 2.6).

**Figure 2.6 PET Promoted Anti-Markovnikov Additions to 1-Methylcyclohexene**

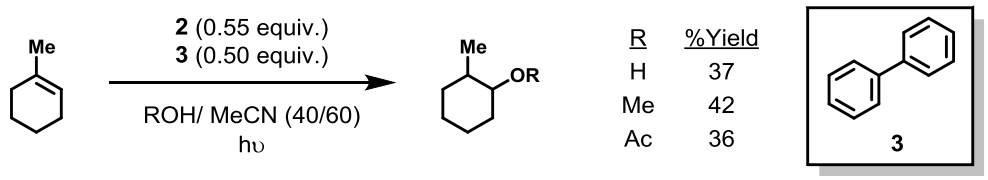


Beyond these initial studies detailing the fundamental pattern of nucleophile additions to alkenes under PET conditions, few reports expanding the synthetic scope and utility of anti-Markovnikov intermolecular additions of oxygen nucleophiles to alkenes within this manifold appeared in the literature. Three notable publications by Inoue and coworkers, however, do report attempts at inducing asymmetry in the addition of methanol and water to prop-1-ene-1,1-diyldibenzene under PET conditions using chiral photosensitizers,[32,33] or by complexation with cyclodextrins.[34] In all cases modest yields and modest enantioselectivities were observed. Overall, most PET promoted additions to alkenes reported in the literature suffer from limited substrate scope, relatively modest yields, and the necessity for stoichiometric or near-stoichiometric quantities of photosensitizers, as well as ultraviolet irradiation which can lead to undesired side reactions.

## 2.4 The Photochemical Nucleophile-Olefin Combination, Aromatic Substitution Reaction

The current understanding of the reactivity patterns of alkene cation radicals towards nucleophiles was elucidated by the studies of Arnold and coworkers into the photochemical nucleophile-olefin combination, aromatic substitution (photo-NOCAS) reaction.[35] In 1984[36], in a study of the reactivity of dicyanobenzene isomers with alkenes under ultraviolet irradiation in solutions containing nucleophilic co-solvents, cyanoarene-alkene-nucleophile adducts were

**Figure 2.7. Selected Examples of Photo-NOCAS Reactions**

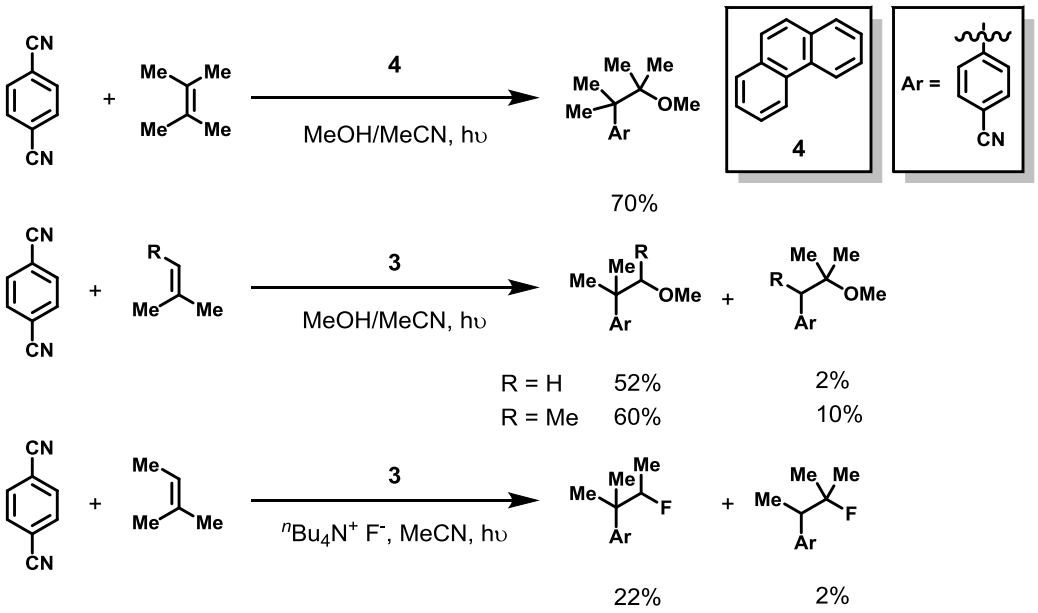


detected. Subsequent studies found this reactivity pattern to be fairly general upon the irradiation of mixtures of dicyanobenzenes, alkyl olefins, and nucleophiles.[37–41] Selected examples of photo-NOCAS reactions are listed in Figure 2.7 above.

After careful study of the reaction by experimental and computational means, Arnold and coworkers put forward a mechanism for the photo-NOCAS reaction (Figure 2.8). This reaction similarly begins with photoinduced electron transfer from an alkene (**6**) to 1,4-dicyanobenzene (**5**) to form a radical cationic alkene and a 1,4-dicyanobenzene radical anion. Nucleophilic capture of the cation radical intermediate occurs such that the unpaired electron resides on the more substituted carbon producing the more stable regioisomer of the distonic cation radical species, **7**. The distonic cation radical then undergoes deprotonation and coupling with the radical anionic 1,4-dicyanobenzene, followed by loss of cyanide, generating the final aryl substituted product **8**.

**Figure 2.8. Mechanism of the Photo-NOCAS Reaction**

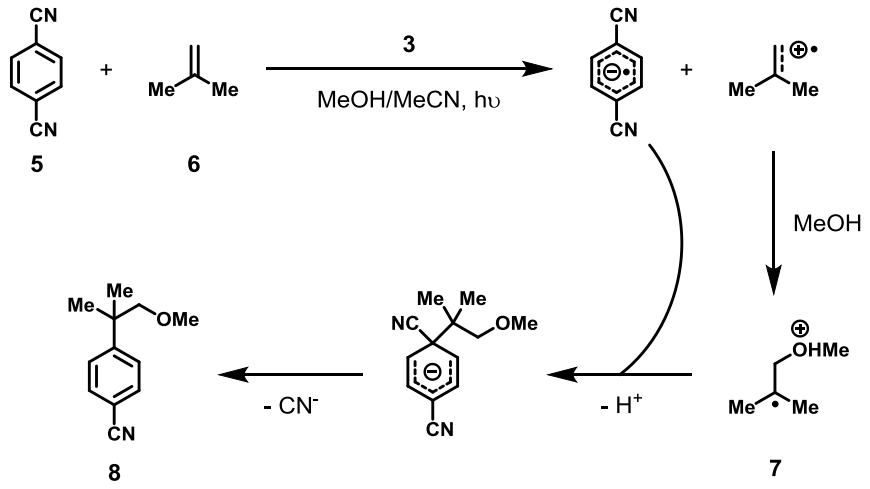


This reaction mechanism exhibits all of the fundamental steps involved in the reaction of nucleophiles and alkenes under PET conditions. Arnold concluded from computational studies that the driving force for anti-Markovnikov regioselectivity was formation of the more stable radical species after nucleophilic addition.

## 2.5. Photoredox Catalysis for the Anti-Markovnikov Hydroetherification of Alkenols

Recently, literature reports of visible light promoted PET processes to carry out a range of interesting transformations have exploded.[42–45] In 2012, the development of an anti-Markovnikov selective intramolecular cyclization of alkenols in our laboratory was reported by Hamilton and Nicewicz.[46] The transformation made use of 9-mesityl-10-methylacridinium perchlorate (**9**) as a visible light photosensitizer and 2-phenylmalononitrile (**10**) as a redox active hydrogen atom donor additive (Figure 2.9). The system was notable with regards to its selectivity for the anti-Markovnikov regioisomer over a wide range of alkenols. No products corresponding to Markovnikov regioselectivity were observed in any cases.

**Figure 2.9. Visible Light Photoredox Anti-Markovnikov Hydroetherification of Alkenols**

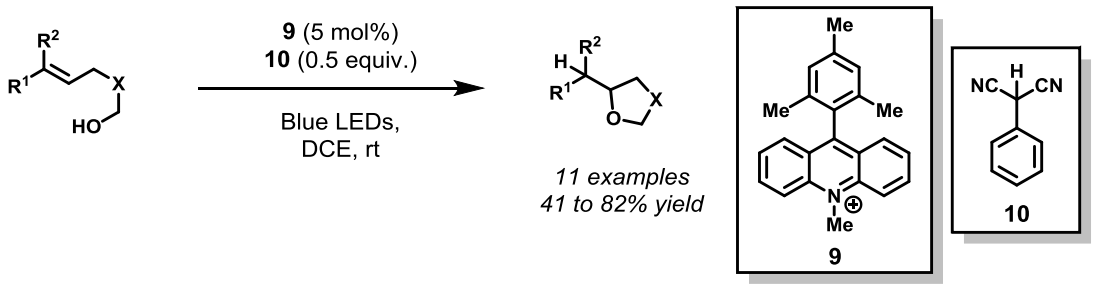


Photosensitizer **9** (as the perchlorate salt) has been applied to other PET promoted oxidations,[47–50] and was chosen for its high excited state reduction potential ($E_{1/2}^{red}* = +2.15$ V vs SCE for the singlet excited state, and $E_{1/2}^{red}* = +1.45$ V for the triplet state) giving access to a range of oxidizable alkenol substrates, and highly reversible redox behavior ($E_{1/2}^{Ox} = -0.57$ V vs SCE for the 9-mesityl-10-methylacridine radical), along with visible light excitation ($\lambda_{max} = 440$ nm).[51] These properties are summarized below in Figure 2.10. The authors presumed that redox reversibility of the photosensitizer would be important to transfer an electron from **11** back to intermediates of the type **7** to achieve net anti-Markovnikov hydrofunctionalization in preference to other side reactions such as photosensitizer incorporation (as in the photo-NOCAS reaction). Additionally, **9** exhibits a long excited state lifetime which should increase the likelihood of encountering and oxidizing an alkenol substrate. The nature of the excited state of **9** responsible for single electron transfer has been the subject of debate in the literature. It is proposed based on spectroscopic evidence and transient absorption techniques that the excited state of **9** responsible for PET is either an abnormally long-lived charge-transfer (CT) state between the mesityl group and the acridinium chromophore,[52–54] or a somewhat long-lived triplet state localized on the acridinium chromophore.[51,55–58] Any attempt to weigh in on this ongoing scientific discussion is beyond the scope of this current chapter.

**Figure 2.10. Summary of 9-Mesityl-10-methylacridinium Photophysical Properties**

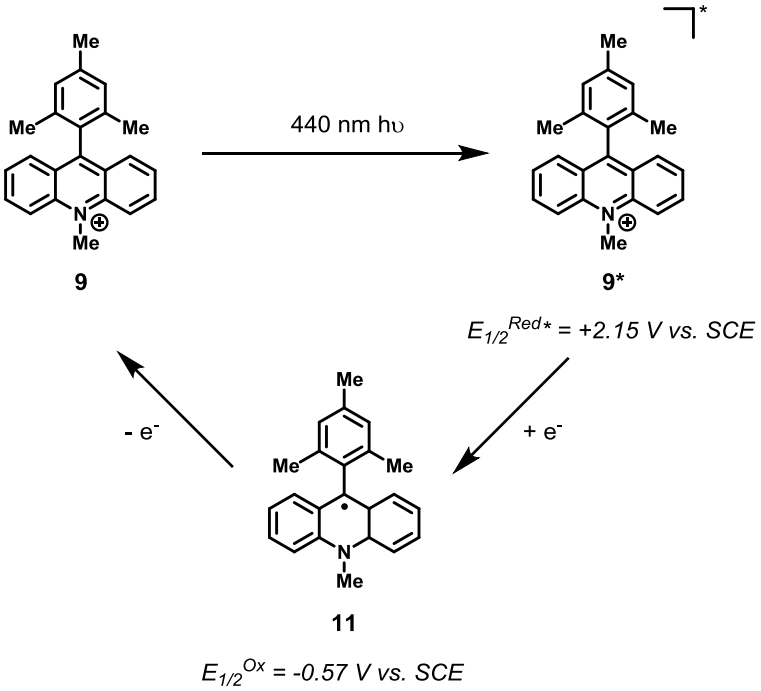


Key to the efficiency of the transformation was the inclusion of the redox-active hydrogen atom donor additive, **10** (Figure 2.11). In the cyclization of **12** to **13**, if the reaction was carried out without **10** then a reduced yield of **13** was obtained without significant change to conversion of **12**, obtaining instead byproducts from what the authors identified as apparent subsequent radical side reactions. There are three properties of **10** which explain its suitability as a redox-active hydrogen atom donor in this reaction. First, the homolytic bond dissociation energy (BDE) of the carbon-hydrogen bond of **10** is 77 kcal/mol making hydrogen atom transfer to most carbon centered tertiary radicals (such as **7**) thermodynamically favorable. Second, the reduction potential of the 2-phenylmalononitrile radical, **14**, is -0.19 V vs SCE making oxidation of **11** by **14** thermodynamically favorable. Finally, while **10** is a weak acid (*p*Ka of 4.2), the conjugate base of 2-phenylmalononitrile, **15**, should be capable of deprotonating the equivalent of strong acid generated from alcohol trapping of the alkene cation radical.

**Figure 2.11. 2-Phenylmalononitrile as Redox Active Hydrogen Atom Donor**

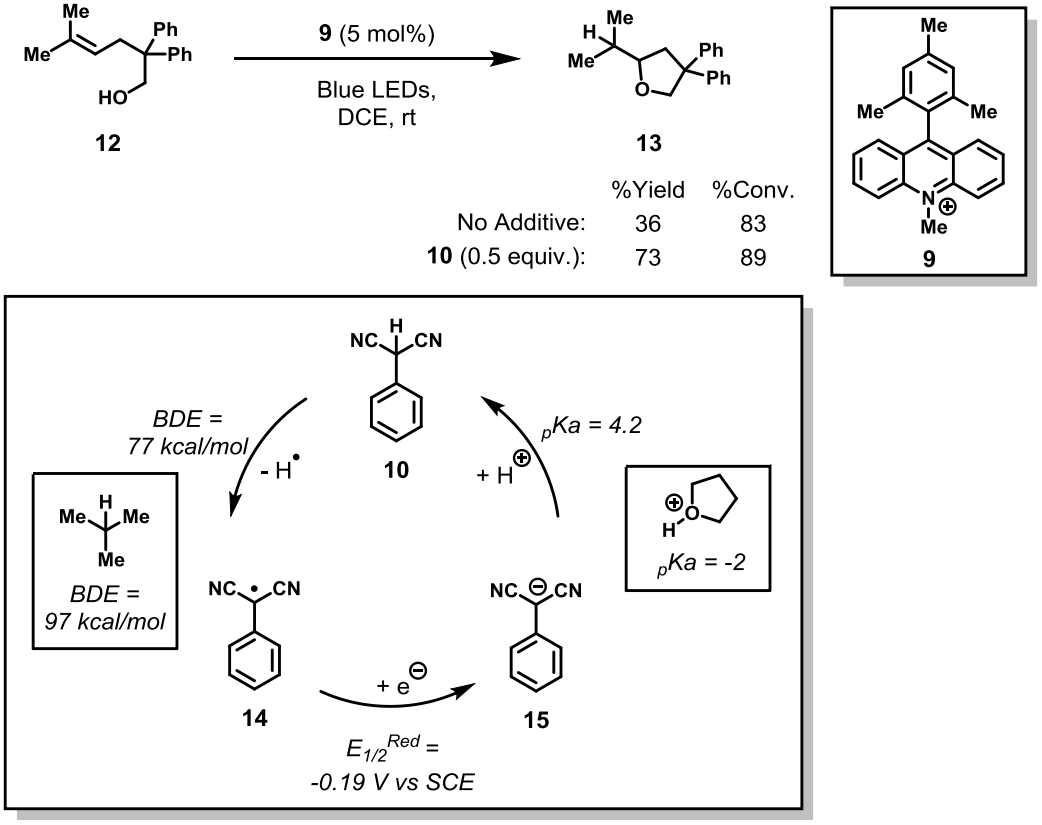


A notable example which clearly demonstrates the strong preference for anti-Markovnikov regioselectivity is in the cyclization of 4-phenylpent-4-en-1-ol (**16**) to 3-phenyltetrahydro-2*H*-pyran (**17**) under photoredox conditions (Figure 2.12). This cyclization is counter to the preference expected using the guidelines outlined by Baldwin in 1976.[59] If the same substrate is submitted to acid catalyzed cyclization conditions, then 2,3,3-trimethyl-2-phenyltetrahydrofuran (**18**) is the exclusive product in accordance with Markovnikov selectivity and Baldwin's rules. The mechanism proposed by Nicewicz and coworkers for the anti-Markovnikov hydroetherification of alkenols is outlined in Figure 2.13.

**Figure 2.12. Anti-Markovnikov Selectivity in Reaction with a 1,1-Disubstituted Alkene**

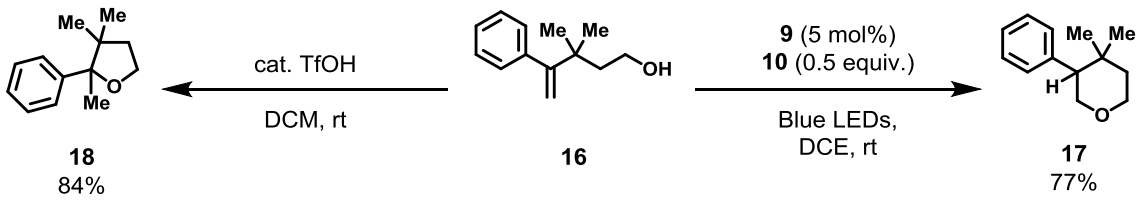


The reaction begins with excitation of **9** to its excited state **9***. Single electron transfer then occurs between **12** and **9*** to form the alkene cation radical **19** and the reduced photosensitizer **11**. The alkene cation radical **19** can rearrange to the distonic cation radical **20**, producing the more stable carbon-centered radical species. Deprotonation of the distonic cation radical gives the neutral radical **21**, which undergoes hydrogen atom transfer from **10**, affording

**Figure 2.13. Proposed Mechanism of Anti-Markovnikov Cycloetherification**

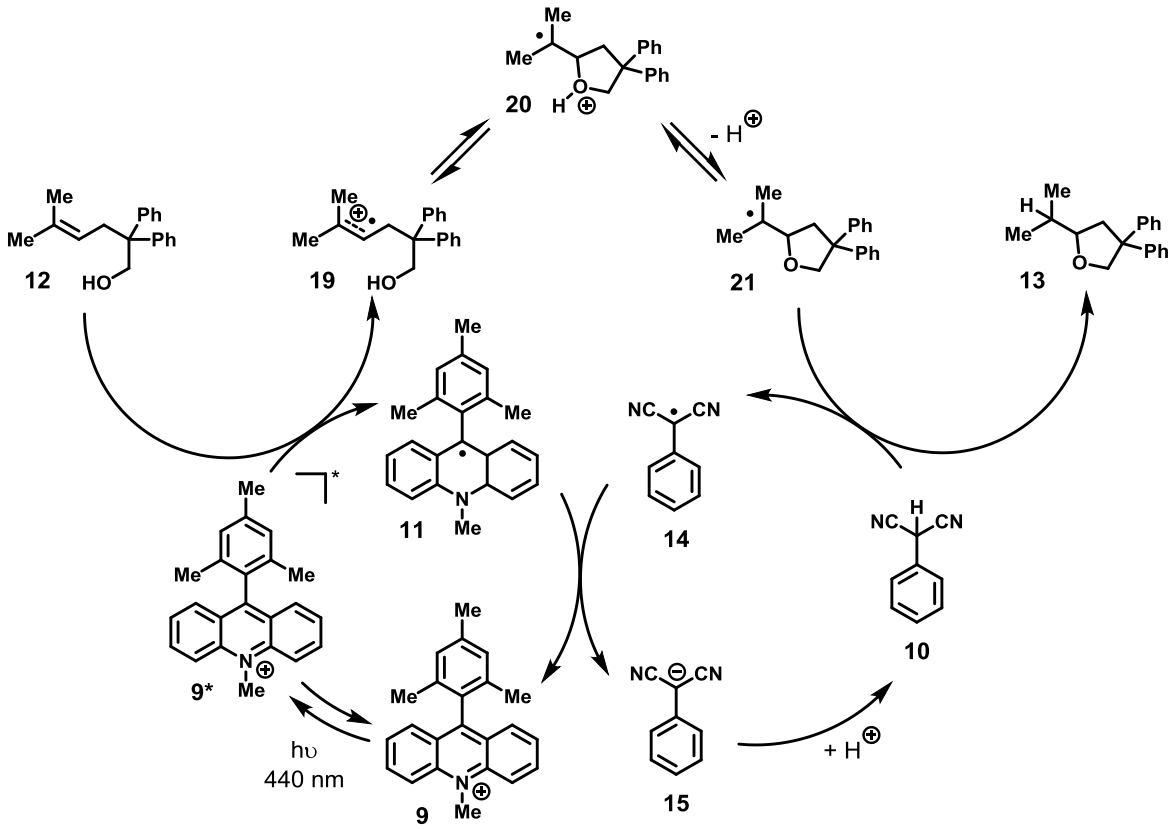

the product **13** and the 2-phenylmalononitrile radical (**14**). The newly formed radical **14** then oxidizes **11** to regenerate the photosensitizer **9**. Protonation of the anion **15** then regenerates the hydrogen atom donor **10**.

While this method is notable for its strong regioselectivity, it does exhibit certain limitations. Reaction times are generally prolonged, sometimes exceeding 96 hours. The redox-active hydrogen atom donor additive **10** is needed in relatively high loadings, and in some cases stoichiometric amounts of 2-phenylmalononitrile are required for efficient reactivity. Super-stoichiometric amounts of **10** can lead to reduced reaction times and elevated yields in some cases. For example, 2.0 equivalents of **10** were used to achieve the intermolecular hydromethoxylation of *p*-anethole (**22**), giving **23** in an 81% yield as the exclusive product (Figure 2.14).

**Figure 2.14. Intermolecular Anti-Markovnikov Hydromethoxylation of *p*-Anethole**

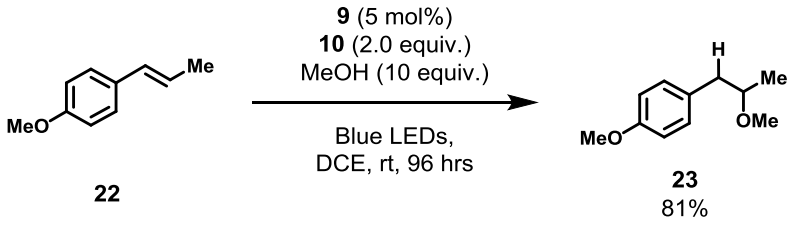


**22** **23** 81%

The use of large amounts of an additive for efficient reactivity, however, moves away from an ideal solution to the challenge of direct, catalytic intermolecular anti-Markovnikov oxyfunctionalization of alkenes. Nevertheless, this general mode of catalysis was seen as very promising in our laboratory for the further development of a direct, catalytic intermolecular anti-Markovnikov oxyfunctionalization of alkenes.

# CHAPTER 3. THE DIRECT ANT-MARKOVNIKOV ADDITION OF CARBOXYLIC ACIDS TO ALKENES USING PHOTOREDOX CATALYSIS

## 3.1. Anti-Markovnikov Additions of Carboxylic Acids to Alkenes, Initial Optimization

Given the impressive results achieved using 9-mesityl-10-methylacridinium tetrafluoroborate (**1**) in combination with 2-phenylmalononitrile (**2**) for the anti-Markovnikov cycloetherification of alkenols demonstrated by Hamilton and Nicewicz, we were interested in taking advantage of this system to develop an intermolecular anti-Markovnikov oxyfunctionalization reaction. The precedent demonstrated the possibility of a direct, catalytic solution through the intermediacy of alkene cation radicals generated via visible light PET. We chose to investigate the addition of carboxylic acids to alkenes. Carboxylic acids were of particular interest as they could be used to synthesize a diverse array of esters depending on the choice of alkene and acid. Additionally, reactions with simple acids such as acetic acid or benzoic acid could potentially be used in complex target synthesis as a simultaneous anti-Markovnikov hydration and alcohol protection.

Early exploration of reaction conditions using the previously applied hydrogen atom donor **2**, along with **1**, identified that base was required for efficient reactivity. Of the bases screened, 2,6-lutidine (**3**) was found to be the most effective. The optimum conditions identified resulted in a complete conversion of *p*-anethole **4** to 1-(4-methoxyphenyl)propan-2-yl acetate (**5**) in an 82% yield ($^1$H NMR) after 5 days of irradiation in dilute acetic acid using 2.5 equivalents of **2** (Figure 3.1). The reaction exhibited complete anti-Markovnikov regioselectivity ($^1$H NMR), based on comparison with reported NMR spectra in the literature, and an independently synthesisized sample of **5**. Despite the encouraging regioselectivity, prolonged reaction times,

high loadings of **2**, and the need to use acetic acid as solvent generated immediate interest in further optimization of this reaction.

The focus of additional optimization turned to the identification of alternate hydrogen atom donors, particularly ones that might allow for reduced loadings and, decreased reaction times, and use of solvents other than acetic acid. Initial success was achieved using 9-cyanofluorene, **6**. Using only 1 equivalent of **6**, the reaction could now be carried out in dichloroethane, achieving complete conversion in 48 hours, and resulting in 88% yield of **5**. This improvement is likely attributable to the slightly lower carbon-hydrogen BDE of **6** (75 kcal/mol) versus **2** (77 kcal/mol).[60] Attempts to further lower the loading of **6** resulted in prolonged reaction times and diminished yields.

A further screen of hydrogen atom donors, in substoichiometric amounts (0.25 equivalents) was carried out (Figure 3.2). In this screen, benzenesulfinic acid (**8**) was found to exhibit markedly reduced reaction times, albeit with modestly reduced yield at complete conversion compared to the higher loadings of either **2** or **6** previously employed. The balance of the material was difficult to characterize, but appeared to most likely consist of oligomeric species. Furthermore, sodium benzene sulfinate (**9**) was capable of replacing both **8** and **3**. This was particularly appealing as **9** is a commercially available bench stable reagent, while sulfinic acids are hygroscopic and prone to oxidation under ambient conditions. Further attempts to optimize the hydroacetoxylation reaction using **9** as a hydrogen atom donor precursor did not result in improved yields or reaction times. It was necessary to use anhydrous acetic acid prepared by addition of acetic anhydride (5 %v/v).

**Figure 3.1. Initial Optimized Conditions for Anti-Markovnikov Hydroacetoxylation**

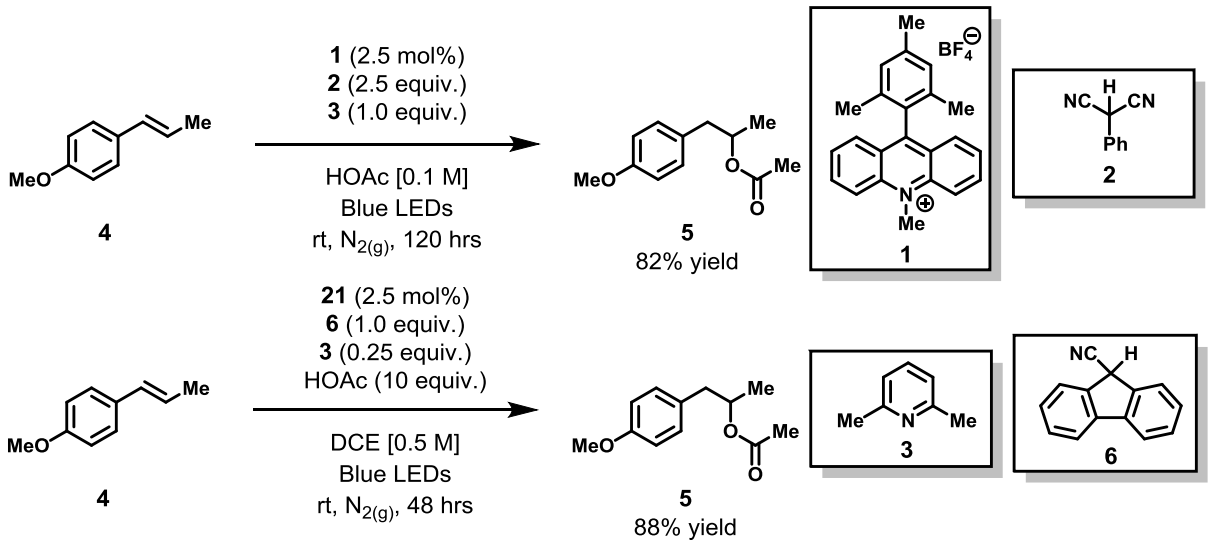


The improvement in reaction rate is likely due to the more electrophilic nature of the hydrogen-

**Figure 3.2. Hydrogen Atom Donor Screen**

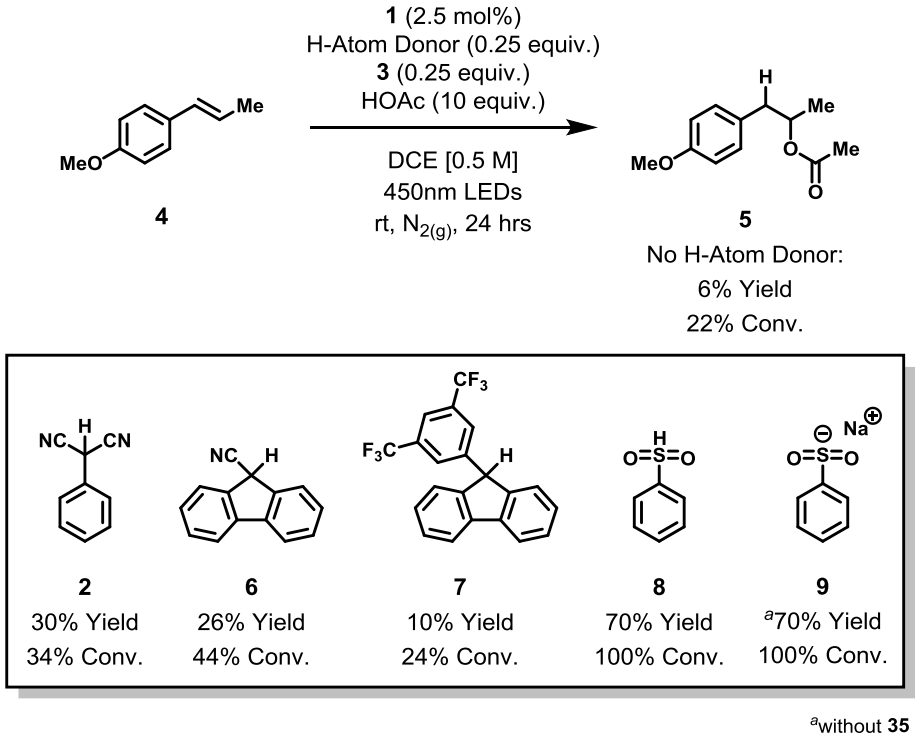


sulfur bond in **8** versus the carbon-hydrogen bonds of **2**, **6**, or **7**. These effects have been observed before in other systems, and form the basis of polarity-reversal catalysis.[61–63]

**Figure 3.3. Thiophenol and Polarity-Reversal Catalysis in the Reduction of Alkyl Halides**

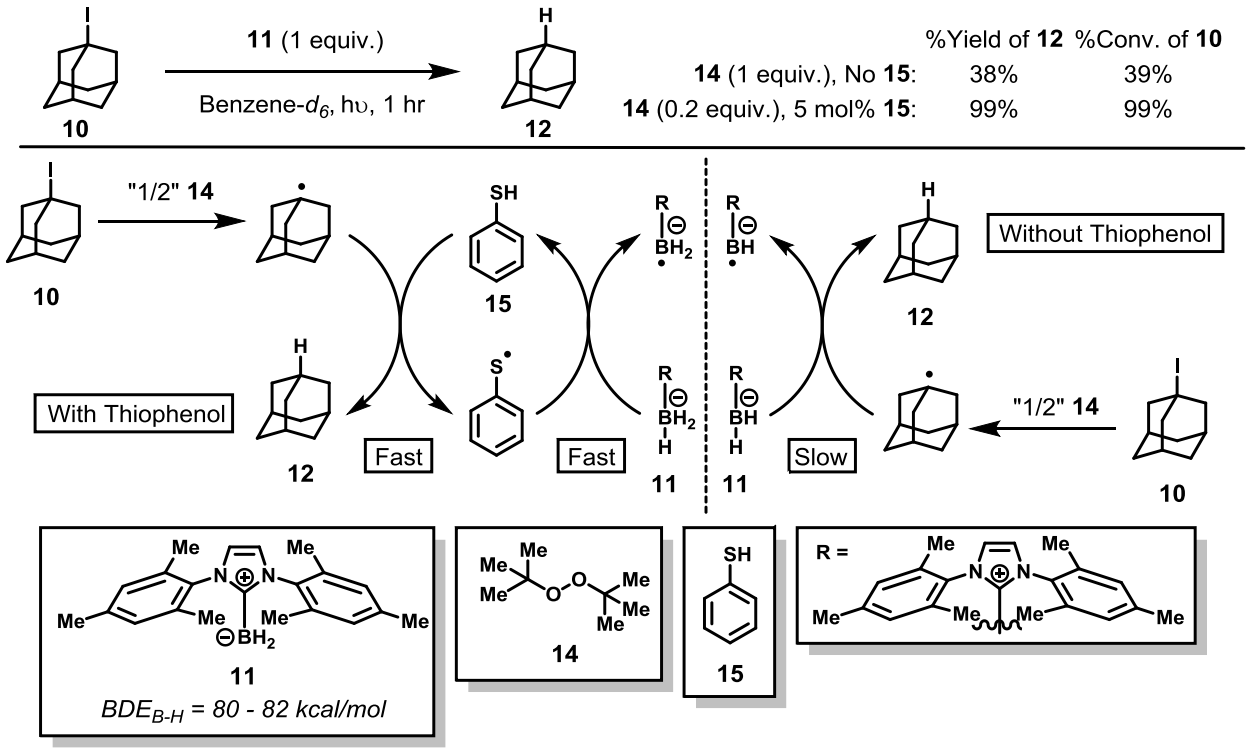


An example of polarity-reversal catalysis in the reduction of alkyl halides demonstrated by Curran and coworkers[64] is depicted above in Figure 3.3. The stoichiometric hydrogen atom donor 1,3-dimesitylimidazol-2-ylidene borane (**11**) reduces adamantyl iodide (**10**) to adamantane (**12**) much more slowly in the absence of thiophenol (**15**) than in the presence of 5 mol% **15**, despite the thermodynamic favorability of the exchange of a boron-hydrogen bond (80 – 82 kcal/mol) of **11** for a tertiary carbon-hydrogen bond (~97 kcal/mol) such as that of adamantane.[65] The authors propose that it is primarily the electrophilic character of the sulfur-hydrogen bond of **15**, along with its relatively low homolytic BDE (~79 kcal/mol), that allows it to shuttle hydrogen atoms between the nucleophilic hydrogen atom source **11** and the nucleophilic adamantyl radical intermediate on the way to **12**.

### 3.2. Anti-Markovnikov Hydroacetoxylation of Styrenes, Substrate Scope

With a system that had been satisfactorily optimized in regards to reaction time, yield, and hydrogen atom donor loading, the scope of styrenyl alkenes was investigated (Figure 3.4). In

**Figure 3.4. Anti-Markovnikov Hydroacetoxylation of Styrenes, Scope of Substrates**

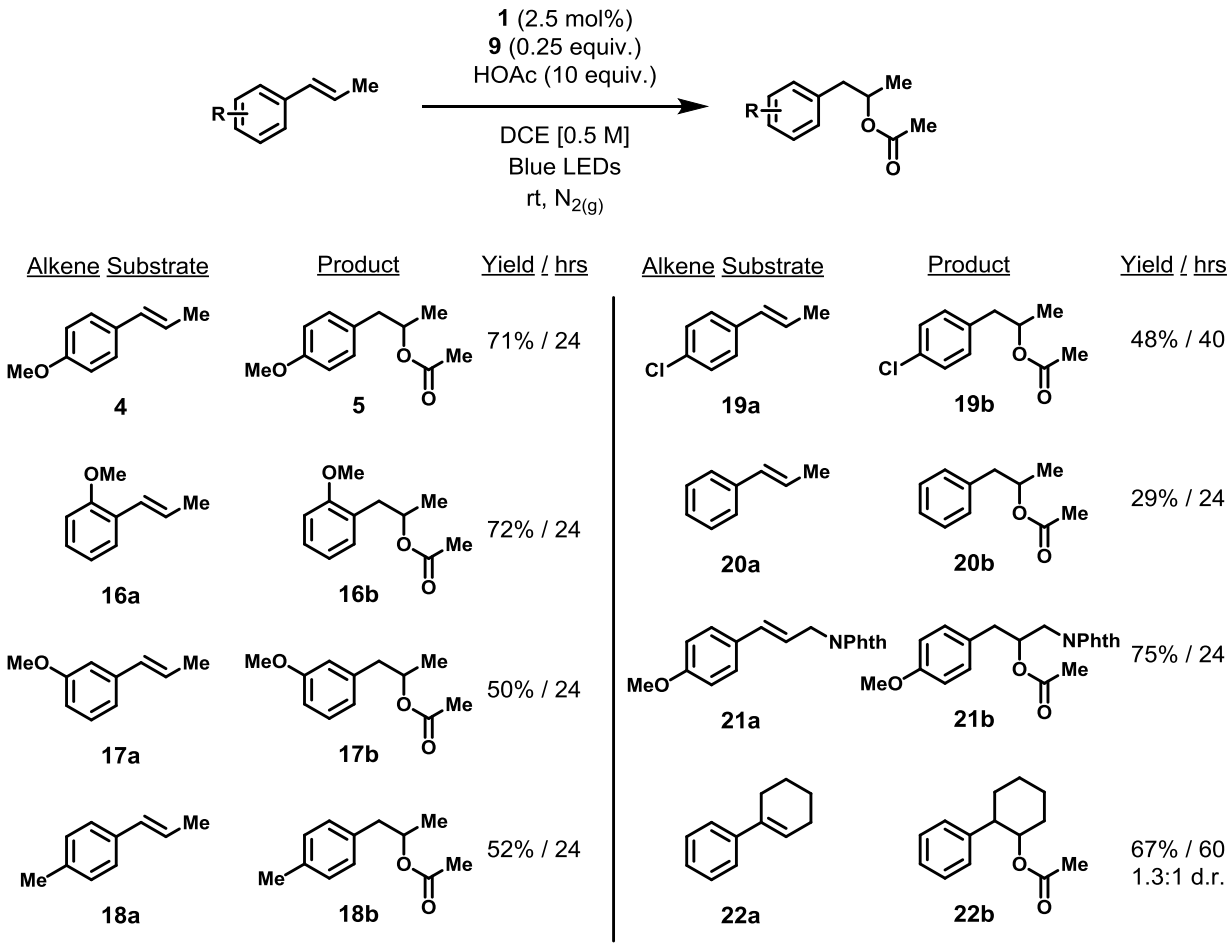


all cases, only the anti-Markovnikov regioisomer was detected. No products resulting from Markovnikov addition were either detected or isolated. Each yield listed is the average of at least two isolated yields carried out on a scale of 1.0 mmol starting alkene. Both **4** and *o*-anethole (**16a**) gave good yields of the corresponding anti-Markovnikov hydroacetoxylation products (**5** and **16b**, respectively) after 24 hours (71% and 72%, respectively), whereas *m*-anethole (**17a**) gave reduced yields (50%) of the corresponding product, **17b**. The somewhat less electron rich

4-methyl-*β*-methylstyrene (**18a**) also gave moderate yields of the corresponding anti-Markovnikov product (52%), **18b**. Moderate yields were also achieved (48%) in the case of the reaction of 4-chloro-*β*-methylstyrene (**19a**) to form **19b**, while somewhat longer reaction times were necessary for complete consumption of the starting material. Only modest yields (29%), however, were obtained under the standard reaction conditions with *β*-methylstyrene (**20a**) to give the product **20b**. While alcohol protecting groups such as silyl ethers decomposed under the reaction conditions, phthalimide protected amines were tolerated. The phthalimide derivate of *p*-anethole (**21a**) reacted efficiently under the standard conditions to give a 75% yield of the anti-Markovnikov hydroacetoxylation product (**21b**). Phenylcyclohexene (**22a**), a trisubstituted alkene, also required longer reaction times (40 hours) but reacted to give 67% of the corresponding hydroacetoxylation product (**22b**) with complete regioselectivity, albeit with nearly no diastereomeric selectivity. Reactions with terminally unsubstituted styrenes resulted in complex reaction mixtures. While $^{1}$H NMR analysis suggested the formation of very low yields of anti-Markovnikov hydroacetoxylation products (< 15% based on internal standard) no products could be isolated in a pure form for further verification. Non-styrenyl alkenes, such as 2-methyl-2-butene and 2-methylcyclopentene, were unreactive under these conditions despite oxidation potentials below the excited state reduction potential of **1**.

### 3.3. Anti-Markovnikov Additions of Other Carboxylic Acids to *p*-Anethole

The range of carboxylic acids that could be used in this anti-Markovnikov hydrocarboxylation reaction was of great interest. The use of other acids under the standard conditions developed for anti-Markovnikov hydroacetoxylation resulted in inseparable mixtures of esters, as a small amount of acetic anhydride was required for efficient reactivity using **9**. At this time aromatic thiols were found to be highly effective hydrogen atom donors for other

intramolecular anti-Markovnikov hydrofunctionalization reactions in our laboratory.[66] Aromatic thiols, such as **15**, were initially overlooked as potential hydrogen atom donors due to their relatively low oxidation potentials ($E_{ox}$ of **15** ~1.4 V vs SCE[67]), and their proclivity towards thiol-ene chemistry under similar reaction conditions.[68,69] Regardless, replacement of **9** with 0.20 equivalents of **15** and 0.25 equivalents of **3** (with the otherwise standard conditions) efficiently produced a range of esters from reaction with **4** (Figure 3.5).

Reactions between propionic acid, *n*-butyric acid, *i*-butyric acid and **4** resulted in excellent yields of the corresponding anti-Markovnikov substitution products **23** (99%), **24** (97%), and **25** (98%), respectively. All yields are the average of two isolated yields on a 1.0 mmol scale of **4**. The time to complete conversion increased in proportion to the relative steric demands of the acid nucleophiles, and in the case of pivalic acid only a 30% yield of the corresponding ester product **26** was formed after 96 hours. Benzoic acid was also a competent nucleophile, giving the benzoate ester **27** in 94% yield after 30 hours.

**Figure 3.5. Anti-Markovnikov Additions of a Variety of Carboxylic Acids to *p*-Anethole**

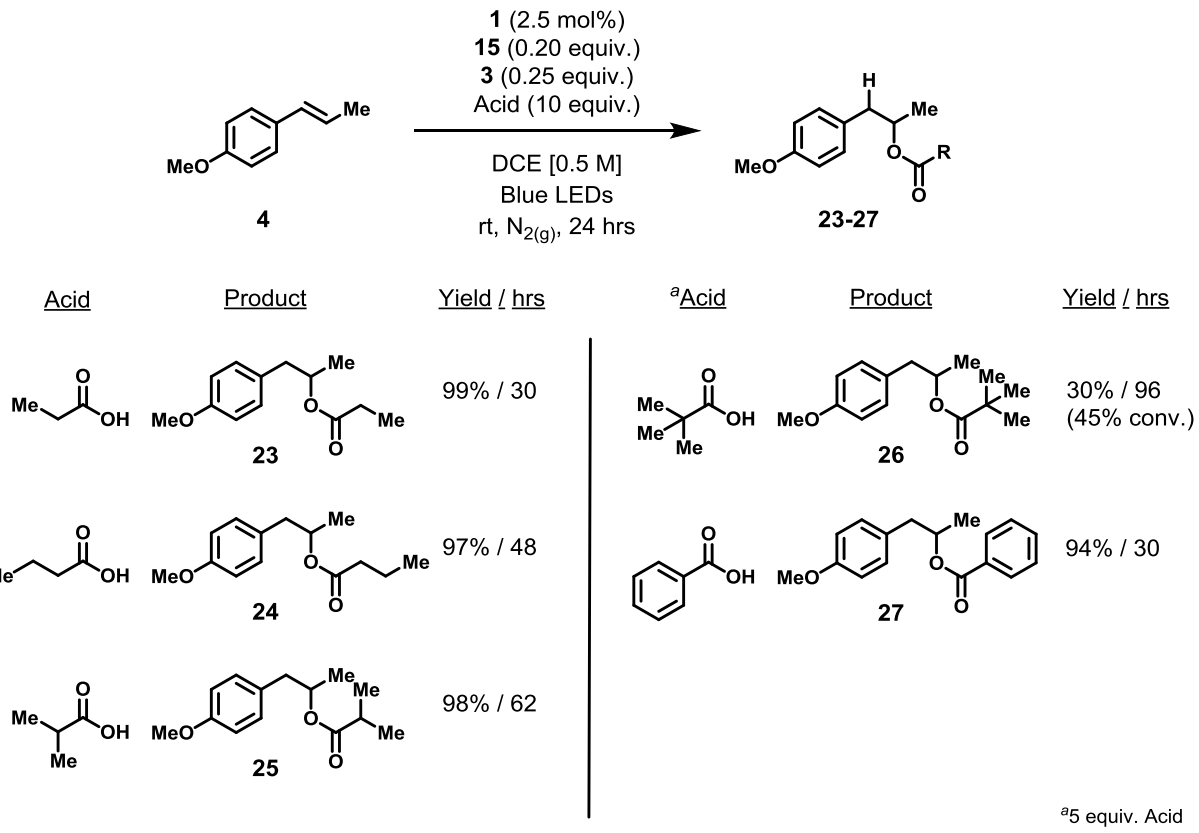


### 3.4. Anti-Markovnikov Hydroacetoxylations of Non-Styrenyl Alkenes

The efficiency which **15** exhibited in reactions between various carboxylic acids and **4** renewed interest in reactions with non-styrenyl alkenes (Figure 3.6). Despite prolonged reaction times, **15** proved effective for the hydroacetoxylation of 2-methyl-2-butene (**28a**) which proceeded to give a 74% yield of the desired product solely as the anti-Markovnikov regioisomer (**28b**). Additionally, 1-methylcyclopentene (**29a**) gave a 61% yield of the corresponding anti-Markovnikov hydroacetoxylation product **29b**, with a modest diastereoselectivity of 1.9 to 1 after similarly long reaction times. Due to the low boiling points of **28b** and **29b,** accurate isolated yields could not be obtained. Yields were determined for these products by $^{1}$H NMR of the crude reactions using hexamethyldisiloxane as internal standard. Each yield was the average

**Figure 3.6. Anti-Markovnikov Addition of Carboxylic Acids to Non-Styrenyl Alkenes**

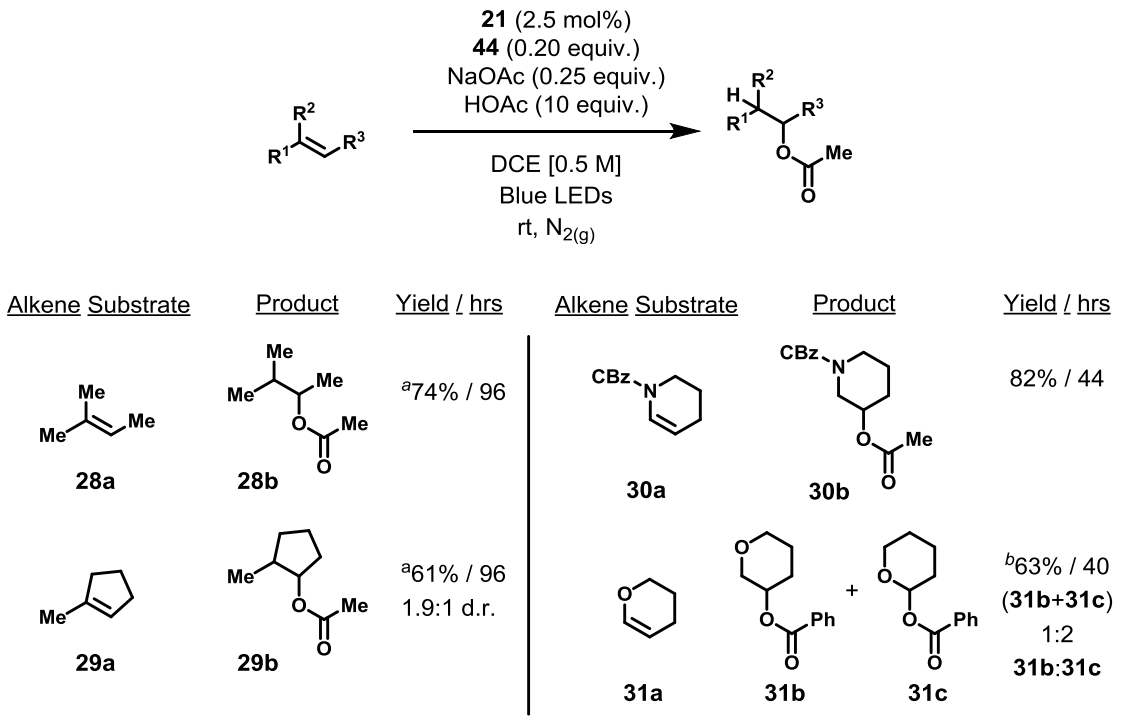


[a]Based on $^1$H NMR Internal Standard
[b]0.25 equiv. **35** instead of NaOAc,
5 equiv. Benzoic Acid instead of Acetic Acid

of two separate reactions carried out at a 2.0 mmol scale of starting alkene. The cyclic enamide benzyl 3,4-dihydropyridine-1(2*H*)-carboxylate (**30a**) reacted to complete conversion after 44 hours to give an impressive 82% yield of the corresponding acetate ester **30b**, still retaining complete anti-Markovnikov regioselectivity. Only the particularly acid sensitive enol-ether 3,4-dihydro-2*H*-pyran (**31a**), reacted with benzoic acid to give a mixture of anti-Markovnikov (**31b**) and Markovnikov (**31c**) regioisomers in a 1 to 2 ratio in a combined 63% yield after 40 hours.

### 3.5. Proposed Mechanism for Anti-Markovnikov Hydroacetoxylation

Presumably, the mechanism of this transformation is similar to that proposed for the intramolecular anti-Markovnikov hydroetherification of alkenols. The proposed mechanism for the intermolecular anti-Markovnikov hydroacetoxylation of **4** is depicted below in Figure 3.7. A

**Figure 3.7. Proposed Mechanism for the Anti-Markovnikov Hydroacetoxylation of Alkenes**

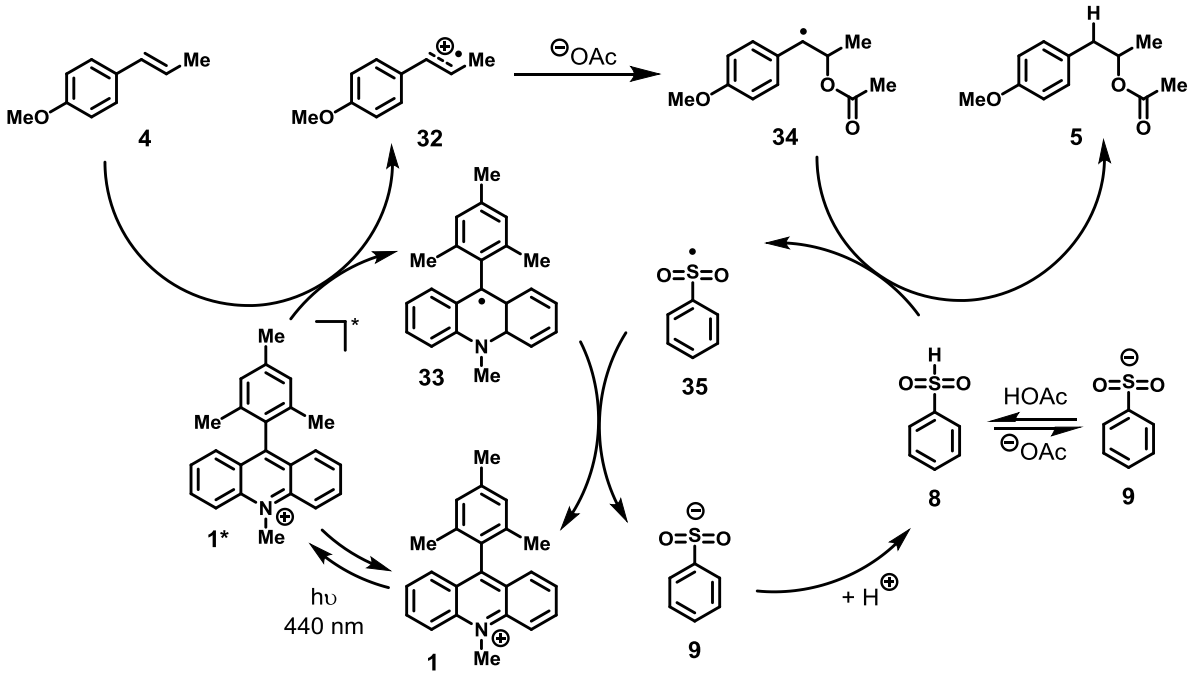


photon of light absorbed by **1** promotes the organic dye to its electronically excited state, **1***. Single electron transfer then occurs from **4** to **1***, generating the corresponding alkene cation radical **32** and the reduced acridine radical **33**. Nucleophilic addition of acetate (from protonation of benzenesulfinate **9** to give benzenesulfinic acid **8**) to **32** gives the radical **34**, which can undergo hydrogen atom transfer from **8,** giving the anti-Markovnikov ester product **5** and the benzenesulfinyl radical **35**. Finally, electron transfer from **33** to **35** regenerates the acridinium organic dye **1** and the hydrogen atom donor precursor **9**.

The use of **9** as both a base and a hydrogen-atom donor precursor permitted a deuterium labeling study to help probe the proposed mechanism (Figure 3.8). By substituting acetic acid-$d_4$ (**37**) in place of the protio-acetic acid under otherwise standard conditions, 87% deuterium incorporation was observed at one of the benzylic sites of the hydroacetoxylation product **38**. The 13% protium incorporation likely comes from the added acetic anhydride, necessary for efficient reactivity, hydrolyzing to give protio-acetic acid. Perhaps more intriguing was the

greatly increased reaction times. After 120 hours of irradiation a 93% conversion of **4** was achieved with a modest 38% yield of the product **38**. The remaining mass balance was difficult to definitely characterize, but appeared composed of oligomeric byproducts. This result lends evidence towards hydrogen atom transfer as being the rate limiting step in this anti-Markovnikov hydroacetoxylation of alkenes.

**Figure 3.8. Anti-Markovnikov Hydroacetoxylation Deuterium-Labeling Study**

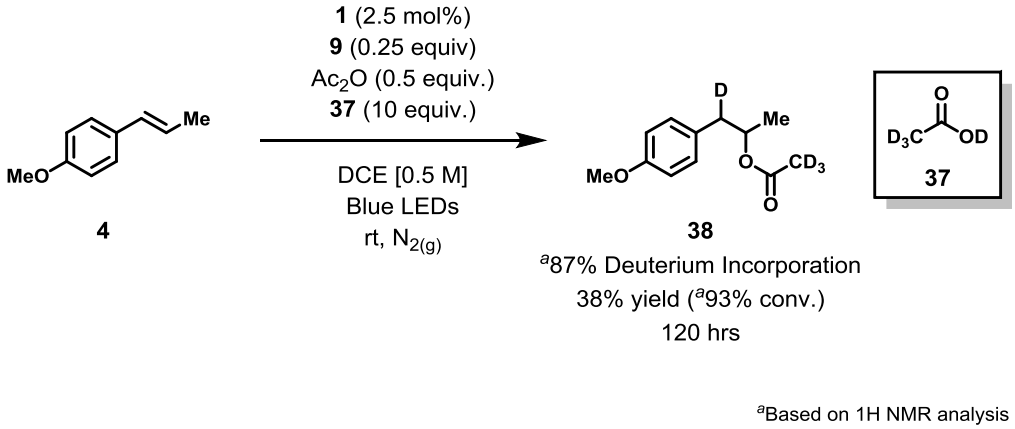


## 3.6. Conclusions, Future Directions, and Further Studies of Interest

In this chapter, a method for the intermolecular anti-Markovnikov regioselective addition of carboxylic acids to alkenes was detailed. The reaction is enabled by a photoredox catalysis system making use of an organic dye photosensitizer and a hydrogen atom donor additive. The hydroacetoxylation of twelve alkenes was demonstrated, as well as the addition of five different carboxylic acids to *p*-anethole (**4**). The method is a direct addition of carboxylic acids to alkenes with complete anti-Markovnikov regioselectivity for all alkenes except the most acid sensitive, and is driven by visible light irradiation. A deuterium labelling study provides evidence that hydrogen atom transfer is likely the rate limiting step of the reaction.

The method does possess certain limitations. Reaction times, particularly for non-styrenyl alkenes, are still prolonged. Furthermore, super-stoichiometric amounts of carboxylic acids are

necessary for efficient reactivity with the current system. Inconsistent yields and reaction times were observed when less than 10 equivalents of carboxylic acid were employed. Both of these limitations may be addressed by further optimization of the hydrogen atom donor additive. Recent work[16] in our laboratory has found that diphenyldisulfide can operate as a competent hydrogen atom donor precursor for intermolecular anti-Markovnikov hydroamination using only 1.5 equivalents of the trifluorosulfonamide nucleophile, and preliminary unpublished data suggest that reaction rates of intramolecular anti-Markovnikov hydroetherification are generally shorter using diphenyldisulfide. In addition to the investigation of disulfides, the effect of steric and electronic substitution on the phenyl ring of both thiophenol and sulfinic acid are of interest in the continued optimization of this reaction.

To expand the scope of alkene substrates, photosensitizers with greater excited state reduction potentials will be key. One potential class of such organic dyes may be pyrylogens (Figure 3.8).[70,71] Pyrylogens are dicationic organic salts that possess two separate, distinct, and reversible single electron ground state electrochemical reduction potentials, in addition to exhibiting blue light absorption. Using the phosphorescent emission of various pyrylogens in combination with their ground state reduction potentials, Clennan and coworkers have estimated the excited state reduction potentials of some pyrylogens to be greater than 2.5 V vs. SCE, which

**Figure 3.9 Pyrylogen Dyes, Notable Properties**Error! Bookmark not defined.

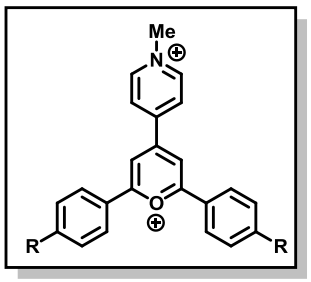


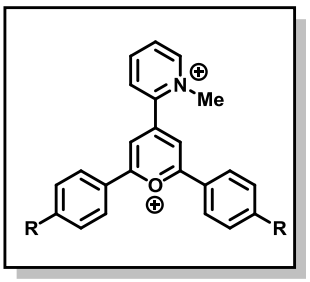


| | $^{a}E_{Red}$* (V) | $\lambda_{max}$ (nm) |
|---|---|---|
| **39**, R = H | 2.51 | 435 |
| **40**, R = Cl | 2.49 | 440 |
| **41**, R = $CF_3$ | 2.84 | 415 |

| | $^{a}E_{Red}$* (V) | $\lambda_{max}$ (nm) |
|---|---|---|
| **42**, R = H | 2.51 | 435 |
| **43**, R = $CF_3$ | 2.65 | 410 |

[a]vs. SCE, estimated based on electrochemical reduction potentials and phosphorescent emission

could expand the current alkene substrate scope.

## 3.7. Methods, Experimental Data, and Spectra

### General Methods

Infrared (IR) spectra were obtained using a Jasco 260 Plus Fourier transform infrared spectrometer. Proton and carbon magnetic resonance spectra ($^{1}$H NMR and $^{13}$C NMR) were recorded on a Bruker model DRX 400, or a Bruker AVANCE III 600 CryoProbe ($^{1}$H NMR at 400 MHz, 600 MHz and $^{13}$C NMR at 100, 150 MHz) spectrometer with solvent resonance as the internal standard ($^{1}$H NMR: $CDCl_3$ at 7.26 ppm; $^{13}$C NMR: $CDCl_3$ at 77.0 ppm). $^{1}$H NMR data are reported as follows: chemical shift, multiplicity (s = singlet, d = doublet, t = triplet, dd = doublet of doublets, dt = doublet of triplets, td = triplet of doublets, m = multiplet, brs = broad singlet, bm = broad multiplet), coupling constants (Hz), and integration. Mass spectra were obtained using a Micromass (now Waters Corporation, 34 Maple Street, Milford, MA 01757) Quattro-II, Triple Quadrupole Mass Spectrometer, with a Z-spray nano-Electrospray source design, in combination with a NanoMate (Advion 19 Brown Road, Ithaca, NY 14850) chip based

electrospray sample introduction system and nozzle. Flash chromatography was performed using SiliaFlash P60 silica gel (40-63 μm) purchased from Silicycle. Dichloroethane was purchased from Sigma-Aldrich Corporation and stored over activated 4Å molecular sieves. Irradiation of photochemical reactions was carried out using a 15W PAR38 blue LED floodlamp purchased from EagleLight (Carlsbad, CA), with borosilicate glass vials purchased from Fisher Scientific. All reagents were purchased from Sigma-Aldrich corporation or Fisher Scientific corporation. *p*-Anethole was distilled under vacuum prior to use. All other purchased reagents were used without additional purification unless otherwise noted.

## Preparation of Photosensitizer

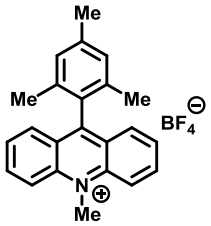


9-Mesityl-10-methylacridinium tetrafluoroborate
(**1**)

9-mesityl-10-methylacridinium tetrafluoroborate. Prepared according to literature procedure[46] using tetrafluoroboric acid diethyl ether complex instead of perchloric acid; spectral data were in agreement with literature values.

## Preparation of Substrates

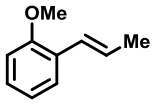


(*E*)-1-methoxy-2-(prop-1-en-1-yl)benzene
(**16a**)

(E)-1-methoxy-2-(prop-1-en-1-yl)benzene (**16a**). Prepared as a mixture of geometric isomers (4:1 (*Z*):(*E*) ratio) according to a literature procedure; spectral data were in agreement with literature values.

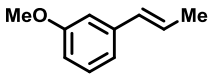


(*E*)-1-methoxy-3-(prop-1-en-1-yl)benzene
(**17a**)

(E)-1-methoxy-3-(prop-1-en-1-yl)benzene (**17a**). Prepared as a mixture of geometric isomers (4:1 (*Z*):(*E*) ratio) according to a literature procedure[72]; spectral data were in agreement with literature values.

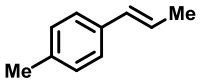


(*E*)-1-methyl-4-(prop-1-en-1-yl)benzene
(**18a**)

(E)-4-methyl-2-(prop-1-en-1-yl)benzene (**18a**). Prepared as a mixture of geometric isomers (4:1 (*Z*):(*E*) ratio) according to a literature procedure[73]; spectral data were in agreement with literature values.

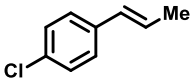


(*E*)-1-chloro-4-(prop-1-en-1-yl)benzene
(**19a**)

(E)-1-Chloro-4-(prop-1-en-1-yl)benzene (**19a**). Prepared as a mixture of geometric isomers (3.5:1 (*E*):(*Z*) ratio) according to a literature procedure[74]; spectral data were in agreement with literature values.

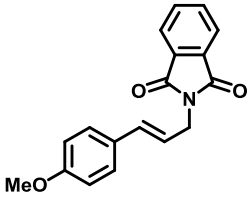


(*E*)-2-(3-(4-methoxyphenyl)allyl)isoindoline-1,3-dione
(**21a**)

(*E*)-2-(3-(4-Methoxyphenyl)allyl)isoindoline-1,3-dione (**21a**). Prepared according to a literature procedure[75]; spectral data were in agreement with literature values.

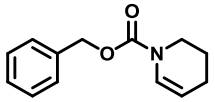

benzyl 3,4-dihydropyridine-1(2*H*)-carboxylate
(**30a**)

Benzyl 3,4-dihydropyridine-1(2*H*)-carboxylate (**30a**). Prepared according to a literature procedure[76]; spectral data were in agreement with literature values.

**Method A**

To a one dram vial equipped with a Teflon coated stir bar was added 10 mg (0.025 mmol, 2.5 mol%) of 9-mesityl-10-methylacridinium tetrafluoroborate, followed by 41 mg (0.25 mmol, 25 mol%) of sodium benzene sulfinate. The vial was then sealed with a Teflon coated septum cap, cooled to 0 °C in an ice bath, and flushed with nitrogen for five minutes. To the vial was then added 1.5 mL of anhydrous dichloroethane, followed by 570 μL of acetic acid (10 mmol, 10 equivalents, containing 5% v/v acetic anhydride) via syringe. The solution was sparged with nitrogen at 0 °C for 15 minutes. Then, 150 μL (1.0 mmol, 1.0 equivalent) of *p*-anethole was added to the solution via syringe, followed by an additional 5 minutes of sparging with nitrogen. The vial was then irradiated with 450 nm blue LEDs under positive nitrogen pressure, and monitored by TLC (15/85 Acetone/Hexanes) for the disappearance of starting material. After disappearance of starting material was observed by TLC, the reactions were transferred to a 500 mL separatory funnel and diluted with 100 mL of diethyl ether. The organic layer was then washed with two 100 mL portions of saturated sodium bicarbonate. The organic layer was separated and dried with magnesium sulfate, and then filtered via filter paper. The solvent was reduced under vacuum, and silica gel chromatography was carried out using a gradient of 1 to 5% acetone in hexanes.

**Method B**

To a one dram vial equipped with a Teflon coated stir bar was added 10 mg (0.025 mmol, 2.5 mol%) of 9-mesityl-10-methylacridinium tetrafluoroborate. The vial was then sealed with a Teflon coated septum cap, cooled to 0 °C in an ice bath, and flushed with nitrogen for five minutes. To the vial was then added 1.3 mL of anhydrous dichloroethane, followed by 750 μL of propionic acid (10 mmol, 10 equivalents), 21 μL (0.20 mmol, 20 mol%) of thiophenol, and 30 μL (0.25 mmol, 25 mol%) 2,6-lutidine, respectively, via syringe. The solution was sparged with nitrogen at 0 °C for 15 minutes. Then, 150 μL (1.0 mmol, 1.0 equivalent) of *p*-anethole was added to the solution via syringe, followed by an additional 5 minutes of sparging with nitrogen. The vial was then irradiated with 450 nm blue LEDs under positive nitrogen pressure, and monitored by TLC (15/85 Acetone/Hexanes) for the disappearance of starting material. After disappearance of starting material was observed by TLC, the reactions were transferred to a 500 mL separatory funnel and diluted with 100 mL of diethyl ether. The organic layer was then washed with two 100 mL portions of saturated sodium bicarbonate. The organic layer was separated and dried with magnesium sulfate, and then filtered via filter paper. The solvent was reduced under vacuum, and silica gel chromatography was carried out using a gradient of 1 to 5% acetone in hexanes.

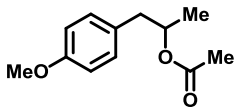


1-(4-methoxyphenyl)propan-2-yl acetate
(**5**)

1-(4-methoxyphenyl)propan-2-yl acetate (**5**) was produced using method A, above, from *p*-anethole (1.0 mmol scale), after 24 hours. Column chromatography on silica gel (1 to 5%

acetone/hexanes gradient) yielded 149 mg (72%) of a colorless oil. Analytical data were in agreement with those reported in the literature.[77]

Analytical data for **5**: $^{1}$H NMR (400 MHz, $CDCl_3$): δ 7.10 (d, *J* = 8.3 Hz, 2H), 6.83 (d, *J* = 8.3 Hz, 2H), 5.06 (sextet, *J* = 6.4 Hz, 1H), 3.79 (s, 3H), 2.86 (dd, *J* = 6.8 Hz, *J* = 13.7 Hz, 1H), 2.69 (dd, *J* = 6.8 Hz, *J* = 13.7 Hz, 1H), 2.00 (s, 3H), 1.20 (d, J = 6.3 Hz, 3H); $^{13}$C NMR ($CDCl_3$, 100 MHz): δ 170.59, 158.19, 130.33, 129.62, 113.69, 71.62, 55.19, 41.28, 21.33, 19.33

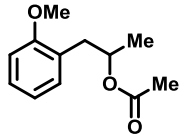


1-(2-methoxyphenyl)propan-2-yl acetate
(**16b**)

1-(2-methoxyphenyl)propan-2-yl acetate (**16b**) was produced using method A, above, from *o*-anethole (1.0 mmol scale), after 24 hours. Column chromatography on silica gel (1 to 5% acetone/hexanes gradient) yielded 157 mg (75%) of a colorless oil. Analytical data were in agreement with those reported in the literature.[78]

Analytical data for **16b**: $^{1}$H NMR (400 MHz, $CDCl_3$): δ 7.20 (td, *J* = 1.7 Hz, *J* = 8.0 Hz, 1H), 7.12 (dd, *J* = 1.7 Hz, *J* = 7.5 Hz, 1H), 6.93 – 6.80 (multiplet, 2H), 5.18 (sextet, *J* = 6.5 Hz, 1H), 3.82 (s, 3H), 2.90 – 2.81 (multiplet, 2H), 1.96 (s, 3H), 1.21 (d, *J* = 6.3 Hz, 3H); $^{13}$C NMR ($CDCl_3$, 100 MHz): δ 170.54, 157.64, 131.12, 127.75, 126.03, 120.13, 110.22, 70.50, 55.20, 36.54, 21.28, 19.65

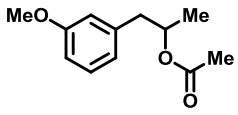


1-(3-methoxyphenyl)propan-2-yl acetate
(**17b**)

1-(3-methoxyphenyl)propan-2-yl acetate (**17b**) was produced using method A, above, from *m*-anethole (1.0 mmol scale), after 24 hours. Column chromatography on silica gel (1 to 5%

acetone/hexanes gradient) yielded 117 mg (56%) of a colorless oil. Analytical data were in agreement with those reported in the literature.[79]

Analytical data for **17b**: $^{1}$H NMR (400 MHz, $CDCl_3$): δ 7.20 (t, *J* = 7.8 Hz, 1H), 6.82 – 6.72 (multiplet, 4H), 5.11 (sextet, *J* = 6.4 Hz, 1H), 3.80 (s, 3H), 2.92 (dd, *J* = 6.7 Hz, *J* = 13.6 Hz, 1H), 2.72 (dd, *J* = 6.7 Hz, *J* = 13.6 Hz, 1H), 2.01 (s, 3H), 1.22 (d, *J* = 6.3 Hz, 3H); $^{13}$C NMR ($CDCl_3$, 100 MHz): δ 170.49, 159.53, 139.13, 129.24, 121.75, 115.07, 111.78, 71.34, 55.09, 42.20, 21.28, 19.42

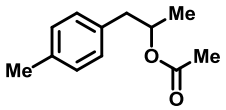


1-(*p*-tolyl)propan-2-yl acetate
(**18b**)

1-(*p*-tolyl)propan-2-yl acetate (**18b**) was produced using method A, above, from 1-methyl-4-(prop-1- en-1-yl)benzene (1.0 mmol scale), after 24 hours. Column chromatography on silica gel (1 to 5% acetone/hexanes gradient) yielded 121 mg (63%) of a colorless oil.

Analytical data for **18b**: $^{1}$H NMR (400 MHz, $CDCl_3$): δ 7.12-7.07 (m, 4H), 5.10 (sextet, *J* = 6.5 Hz, 1H) 2.90 (dd, *J* = 6.6 Hz, *J* = 13.6 Hz, 1H) 2.72 (dd, *J* = 6.7 Hz, *J* = 13.6 Hz, 1H) 2.32 (s, 3H) 2.00 (s, 3H), 1.21 (d, *J* = 6.4 Hz, 3H); $^{13}$C NMR ($CDCl_3$, 150 MHz): δ 170.5, 135.9, 134.5, 129.3, 129.0, 71.5, 41.8, 21.3, 21.0, 19.4 ; IR (thin film): 2978.5, 2927.4, 2858.9, 1736.6, 1515.8, 1452.1, 1372.1, 1243.9 cm-1; LRMS (+ESI): *m/z* calculated for [M+H]+: 193.12; found: 193.00

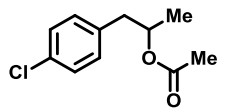


1-(4-chlorophenyl)propan-2-yl acetate
(**19b**)

1-(4-chlorophenyl)propan-2-yl acetate (**19b**) was produced using method A, above, from 1-chloro-4- (prop-1-en-1-yl)benzene (1.0 mmol scale), after 40 hours. Column chromatography on silica gel (1 to 5% acetone/hexanes gradient) yielded 110 mg (52%) of a colorless oil.

Analytical data for **19b**: $^{1}$H NMR (400 MHz, $CDCl_3$): δ 7.25 (d, *J* = 8.4 Hz, 2H), 7.12 (d, *J* = 8.4 Hz, 2H), 5.07 (sextet, *J* = 6.4 Hz, 1H), 2.88 (dd, J = 7.0 Hz, J = 13.6 Hz, 1H), 2.73 (dd, J = 6.5 Hz, J = 13.6 Hz, 1H), 1.98 (s, 3H), 1.21 (d, J = 6.4 Hz, 3H); $^{13}$C NMR ($CDCl_3$, 100 MHz): δ 170.47, 136.34, 130.72, 128.46, 71.11, 41.54, 21.26, 19.45 ; IR (thin film): 3028.7, 2979.5, 2931.3, 2854.1, 1737.6, 1597.7, 1493.6, 1448.3, 1408.8, 1372.1, 1242.9 cm-1; LRMS (+ESI): *m/z* calculated for [M+H]+: 213.07; found: 213.12

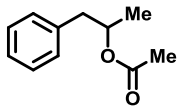


1-phenylpropan-2-yl acetate
(**20b**)

1-phenylpropan-2-yl acetate (**20b**) was produced using method A, above, from *β*-methylstyrene (1.0 mmol scale), after 24 hours. Column chromatography on silica gel (1 to 5% acetone/hexanes gradient) yielded 58 mg (33%) of a colorless oil. Analytical data were in agreement with those reported in the literature.[80]

Analytical data for **20b**: $^{1}$H NMR (400 MHz, $CDCl_3$): δ 7.31-7.27 (m, 2H), 7.23-7.19 (m, 3H), 5.12 (sextet, J = 6.5 Hz , 1H) 7.17 (d, *J* = 8.4 Hz, 2H) 6.83 (d, *J* = 8.4 Hz, 2H) 5.32 (sextet, *J* = 6.5 Hz, 1H), 2.93 (dd, J = 6.5 Hz, J = 13.8 Hz, 1H) 2.75 (dd, J = 6.5 Hz, J = 13.8, 1H) 2.00 (s, 3H) 1.22 (d, J = 6.5 Hz, 3H); $^{13}$C NMR ($CDCl_3$, 100 MHz): δ 170.5, 137.6, 129.4, 128.3, 126.4, 71.4, 42.2, 21.3, 19.4

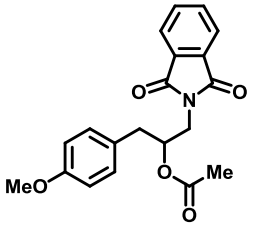


1-(1,3-dioxoisoindolin-2-yl)-3-(4-methoxyphenyl)propan-2-yl acetate
(**21b**)

1-(1,3-dioxoisoindolin-2-yl)-3-(4-methoxyphenyl)propan-2-yl (**21b**) acetate was produced using method A, above, from (E)-2-(3-(4-methoxyphenyl)allyl)isoindoline-1,3-dione (1.0 mmol scale), after 24 hours. Column chromatography on silica gel (1 to 15% acetone/hexanes gradient) yielded 222 mg (76%) of a white solid.

Analytical data for **21b**: $^{1}$H NMR (600 MHz, $CDCl_3$): 7.84 (dd, *J* = 5.4, 3.1 Hz, 1H), 7.72 (dd, *J* = 5.4, 3.0 Hz, 1H), 7.15 (d, *J* = 8.6 Hz, 1H), 6.81 (d, *J* = 8.6 Hz, 1H), 5.34 (dq, *J* = 8.0, 5.5 Hz, 1H), 3.88 (d, *J* = 5.3 Hz, 1H), 3.77 (s, 2H), 2.96 – 2.79 (m, 1H), 1.92 (s, 1H).; $^{13}$C NMR ($CDCl_3$, 150 MHz): δ 170.64, 168.22, 158.34, 134.03, 131.89, 130.18, 128.50, 123.34, 113.83, 72.36, 55.17, 40.78, 37.50, 20.93; IR (thin film): 3446.2, 2938.0, 2836.8, 1773.23, 1715.4, 1684.5, 1652.7, 1636.3, 1615.1, 1513.9, 1466.6, 1426.1, 1395.3, 1374.0 cm-1; LRMS (+ESI): *m/z* calculated for [M+H]+: 354.13; found: 354.19

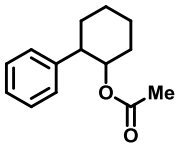


2-phenylcyclohexyl acetate
(**22b**)

2-phenylcyclohexyl acetate (**22b**) was produced using method A, above, from 1-phenylcyclohexene (1.0 mmol scale) in a 1.3:1 diastereomeric ratio, after 40 hours. Column chromatography on silica gel (1 to 5% acetone/hexanes gradient) yielded 150 mg (69%) of a colorless oil. Analytical data were in agreement with those reported in the literature.[81]

Analytical data for **22b**: $^{1}$H NMR (600 MHz, $CDCl_3$): δ 7.30 – 7.26 (multiplet, 2H), 7.24 – 7.17 (multiplet, 3H), 5.15 (s, 0.60 H), 4.97 (td, *J* = 4.4 Hz, *J* = 10.6 Hz, 0.40H), 2.78 (dt, *J* = 3.0 Hz, *J* = 12.9 Hz, 0.60H), 2.65 (td, *J* = 4.0 Hz, *J* = 12.4 Hz, 0.40H), 2.18 – 1.99 (multiplet, 2H), 1.98 – 1.69 (multiplet, 6H), 1.68 – 1.29 (multiplet, 3H); $^{13}$C NMR ($CDCl_3$, 150 MHz): δ 170.36,

170.30, 143.26, 143.09, 128.20, 128.07, 127.74, 127.47, 126.37, 126.36, 75.86, 73.12, 49.67, 46.52, 33.76, 32.30, 30.65, 25.92, 25.89, 25.79, 24.73, 21.13, 20.97, 20.12

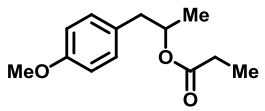


1-(4-methoxyphenyl)propan-2-yl propionate
(**23**)

1-(4-methoxyphenyl)propan-2-yl priopionate (**23**) was produced using method B, above, from *p*-anethole (1.0 mmol scale), after 30 hours. Column chromatography on silica gel (1 to 5% acetone/hexanes gradient) yielded 221 mg (99%) of a colorless oil.

Analytical data for **23**: $^{1}$H NMR (400 MHz, $CDCl_3$): δ 7.11 (d, *J* = 8.7 Hz, 2H), 6.82 (d, *J* = 8.7 Hz, 2H), 5.08 (sextet, *J* = 6.3 Hz, 1H), 3.78 (s, 3H), 2.86 (dd, *J* = 6.3, Hz, *J* = 13.7 Hz, 1H), 2.70 (dd, *J* = 6.6 Hz, *J* = 13.6 Hz, 1H), 2.27 (quartet, *J* = 7.7 Hz, 2H), 1.15 (d, *J* = 6.1 Hz, 3H), 1.09 (t, *J* = 7.7 Hz, 3H); $^{13}$C NMR ($CDCl_3$, 150 MHz): δ 173.9, 158.2, 130.3, 129.7, 113.7, 71.4, 55.2, 41.3, 27.9, 19.4, 9.1; IR (thin film): 2979.5, 2935.1, 2836.8, 1731.8, 1613.2, 1584.2, 1513.9, 1462.7, 1422.2, 1369.2, 1336.4, 1301.7, 1248.7, 1190.8, 1134.9 cm-1; LRMS (+ESI): *m/z* calculated for [M+H]+: 223.13; found: 223.09

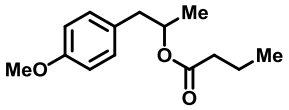


1-(4-methoxyphenyl)propan-2-yl butyrate
(**24**)

1-(4-methoxyphenyl)propan-2-yl butyrate (**24**) was produced using method B, above, from *p*-anethole (1.0 mmol scale), after 48 hours. Column chromatography on silica gel (1 to 5% acetone/hexanes gradient) yielded 229 mg (97%) of a colorless oil.

Analytical data for **24**: $^{1}$H NMR (400 MHz, $CDCl_3$): δ 7.13 – 7.08 (multiplet, 2H), 6.85 – 6.79 (multiplet, 2H), 5.08 (sextet, *J* = 6.42 Hz, 1H), 3.78 (s, 3H), 2.86 (dd, *J* = 6.7 Hz, *J* = 13.7 Hz,

1H), 2.70 (dd, *J* = 6.4 Hz, *J* = 13.9 Hz, 1H), 2.22 (t, *J* = 7.4 Hz, 2H), 1.62 (sextet, *J* = 7.4 Hz, 2H), 1.20 (d, *J* = 6.3 Hz, 3H), 0.89 (t, *J* = 7.41 Hz, 3H); $^{13}$C NMR ($CDCl_3$, 150 MHz): δ 173.11, 158.18, 130.31, 129.70, 113.67, 71.29, 55.17, 41.35, 36.50, 19.40, 18.41, 13.56; IR (thin film): 3033.5, 2965.0, 2934.2, 2875.3, 2836.8, 1730.8, 1613.2, 1584.2, 1513.9, 1462.7, 1420.3, 1379.8, 1338.4, 1301.7, 1298.7 cm-1; LRMS (+ESI): *m/z* calculated for [M+H]+: 237.15; found: 237.13

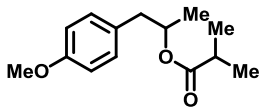


1-(4-methoxyphenyl)propan-2-yl isobutyrate
(**25**)

1-(4-methoxyphenyl)propan-2-yl isobutyrate (**25**) was produced using method B, above, from *p*-anethole (1.0 mmol scale), after 62 hours. Column chromatography on silica gel (1 to 5% acetone/hexanes gradient) yielded 233 mg (99%) of a colorless oil. Analytical data were in agreement with those reported in the literature.[82]

Analytical data for **25**: $^{1}$H NMR (400 MHz, $CDCl_3$): δ 7.14 – 7.08 (multiplet, 2H), 6.85 – 6.78 (multiplet, 2H), 5.07 (sextet, *J* = 6.4 Hz, 1H), 3.78 (s, 3H), 2.85 (dd, *J* = 6.9 Hz, *J* = 13.9 Hz, 1H), 2.71 (dd, *J* = 6.3 Hz, *J* = 13.8 Hz, 1H), 2.47 (septet, *J* = 6.3 Hz, *J* = 13.8 Hz, 1H), 1.20 (d, 6.4 Hz, 3H), 1.11 (d, *J* = 7.0 Hz, 3H), 1.09 (d, *J* = 7.0 Hz, 3H); $^{13}$C NMR ($CDCl_3$, 100 MHz): δ 176.58. 158.17, 130.34, 129.73, 113.64, 71.17, 55.17, 41.33, 34.14, 19.37, 18.92, 18.85

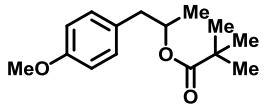


1-(4-methoxyphenyl)propan-2-yl pivalate
(**26**)

1-(4-methoxyphenyl)propan-2-yl pivalate (**26**) was produced using method B, above, from *p*-anethole (1.0 mmol scale), using 5.0 equivalents (5.0 mmol) pivalic acid. After irradiation for 96 hours, conversion of *p*-anethole was found to be 45% (determined by $^{1}$H NMR internal standard

using 5.0 μL of hexamethyldisiloxane). Column chromatography on silica gel (1 to 5% acetone/hexanes gradient) yielded 87 mg (35%) of a yellow oil.

Analytical data for **26**: $^{1}$H NMR (400 MHz, $CDCl_3$): δ 7.15 – 7.07 (multiplet, 2H), 6.85 – 6.76 (multiplet, 2H), 5.04 (sextet, *J* = 6.3 Hz, 1H), 3.78 (s, 3H), 2.84 (dd, *J* = 6.9 Hz, *J* = 13.8 Hz, 1H), 2.72 (dd, *J* = 6.3 Hz, *J* = 13.8 Hz, 1H); $^{13}$C NMR ($CDCl_3$, 150 MHz): δ 178.0, 158.1, 130.4, 129.8, 113.6, 71.2, 55.2, 41.3, 38.6, 27.1, 19.4; IR (thin film): 3648.7, 2974.7, 2933.2, 2871.5, 2835.8, 2359.5, 1723.1, 1613.2, 1513.9, 1457.9, 1396.2, 1283.4, 1248.1, 1366.3 cm-1; LRMS (+ESI): *m/z* calculated for [M+H]+: 251.16; found: 251.05

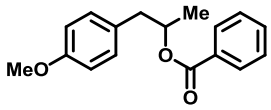


1-(4-methoxyphenyl)propan-2-yl benzoate (**27**)

1-(4-methoxyphenyl)propan-2-yl benzoate (**27**) was produced using method B, above, from *p*-anethole (1.0 mmol scale), using 5.0 equivalents (5.0 mmol) of benzoic acid, after 30 hours. Column chromatography on silica gel (1 to 5% acetone/hexanes gradient) yielded 253 mg (94%) of a colorless oil.

Analytical data for **27**: $^{1}$H NMR (600 MHz, $CDCl_3$): δ 8.02 (d, *J* = 7.8 Hz, 2H), 7.55 (t, 7.5 Hz, 1H), 7.43 (t, 7.8 Hz, 2H) 7.17 (d, *J* = 8.4 Hz, 2H) 6.83 (d, *J* = 8.4 Hz, 2H) 5.32 (sextet, *J* = 6.2 Hz, 1H) 3.78 (s, 3H) 3.02 (dd, J = 6.2 Hz, J = 13.8 Hz, 1H) 2.84 (dd, J = 6.8 Hz, J = 13.8, 1H) 1.33 (d, J = 6.1 Hz, 3H); $^{13}$C NMR ($CDCl_3$, 150 MHz): δ 166.0, 158.2, 132.7, 130.7, 130.5, 129.6, 129.5, 128.3, 113.7, 72.3, 55.2, 41.4, 19.4 ; IR (thin film): 3410.5, 3062.4, 3033.5, 2977.6, 2933.2, 2834.9, 1714.4, 1612.2, 1584.2, 1512.9, 1491.7, 1452.1 cm-1 LRMS (+ESI): *m/z* calculated for [M+H]+: 271.13; found: 271.15

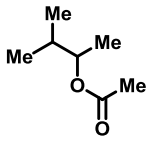


3-methylbutan-2-yl acetate
(**28b**)

3-methylbutan-2-yl acetate (**28b**) was produced using method B (employing sodium acetate instead of 2,6-lutidine) from 2-methyl-2-butene (2.0 mmol scale). The reaction was determined to be complete after 96 hours based on $^{1}$H NMR analysis of crude aliquots. The yield of 3-methylbutan-2-yl acetate was determined by $^{1}$H NMR internal standard (due to product volatility), using 20.0 μL of hexamethyldisiloxane, to be 1.54 mmol (77%). The title compound was subjected to column chromatography on silica gel (1 to 5% diethyl ether/pentane) to yield a volatile colorless oil. Analytical data were in agreement with those reported in the literature.[80] Analytical data for **28b**: $^{1}$H NMR (600 MHz, $CDCl_3$): δ 4.72 (quintet, $J$ = 6.26 Hz, 1H), 1.76 (octet, $J$ = 6.7 Hz, 1H), 1.15 (d, $J$ = 6.6 Hz, 3H), 0.99 (d, $J$ = 6.9 Hz, 6H); $^{13}$C NMR ($CDCl_3$, 150 MHz): δ 170.85, 75.20, 32.60, 18.06, 17.98, 16.66

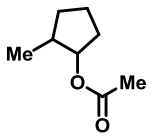


2-methylcyclopentyl acetate
(**29b**)

2-methylcyclopentyl acetate (**29b**) was produced using method B (employing sodium acetate in place of 2,6-lutidine), from 1-methylcyclopentene (2.0 mmol scale) in a 1.9:1 diastereomeric ratio. The reaction was determined to be complete after 96 hours based on $^{1}$H NMR analysis of crude aliquots. The yield of 2-methylcyclopentyl acetate was determined by $^{1}$H NMR internal standard (due to product volatility), using 25.0 μL of hexamethyldisiloxane, to be 1.30 mmol (65%). The title compound was subjected to column chromatography on silica gel (1 to 5%

diethyl ether/pentane) to yield a volatile colorless oil. Analytical data were in agreement with those reported in the literature.[83]

Analytical data for 2-methylcyclopentyl acetate: $^{1}$H NMR (400 MHz, $CDCl_3$): δ 5.11 (td, $J$ = 2.6 Hz, $J$ = 5.5 Hz, 0.83H), 4.70 – 4.64 (m, 0.17H), 2.10 – 1.85 (m, 5H), 1.82 – 1.48 (m, 4H); $^{13}$C NMR ($CDCl_3$, 100 MHz): δ 170.98, 82.60, 78.69, 39.90, 38.37, 32.19, 31.84, 31.57, 31.35, 22.36, 22.18, 21.35, 21.19, 18.20, 13.82

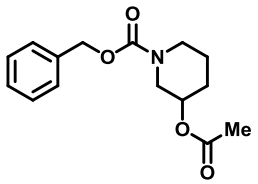


benzyl 3-acetoxypiperidine-1-carboxylate
(**30b**)

Benzyl 3-acetoxypiperidine-1-carboxyate (**30b**) was produced using method B (employing sodium acetate instead of 2,6-lutidine) from benzyl 3,4-dihydropyridine-1(2*H*)-carboxylate (1.0 mmol scale), after 44 hours. Column chromatography on silica gel (1 to 15% acetone/hexanes gradient) yielded 245 mg (88%) of a viscous, light yellow oil. Analytical data were in agreement with those reported in the literature.[84]

Analytical data for **30b**: $^{1}$H NMR (600 MHz, $CDCl_3$) 7.38 – 7.27 (m, 5H), 5.25 – 5.00 (broad multiplet, 2H) 4.80 (broad singlet, 1H) 3.70 – 3.27 (broad multiplet, 4H), 2.07 – 1.63 (broad multiplet, 6H), 1.60 – 1.45 (broad singlet, 1H); $^{13}$C NMR ($CDCl_3$, 150 MHz): δ 170.30, 155.42, 136.70, 128.45, 127.95, 127.79, 67.73, 67.05, 47.37, 44.04, 28.98, 21.48, 21.02

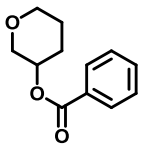


tetrahydro-2*H*-pyran-3-yl benzoate
(**31b**)

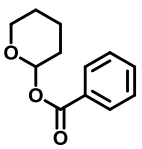


tetrahydro-2*H*-pyran-2-yl benzoate
(**31c**)

Tetrahydro-2H-pyran-3-yl benzoate (**31b**) and tetrahydro-2H-pyran-2-yl benzoate (**31c**) were produced in a 2 to 1 ratio in an overall 72% yield (1.0 mmol scale), using method B, above, with 5.0 equivalents of benzoic acid, after 40 hours. The mixture was purified by column chromatography on silica gel (1 to 5% acetone/hexanes) to yield a colorless oil.

Analytical data for **31c** were in agreement with those reported in the literature.[85]

Analytical data for **31c**: $^{1}$H NMR (400 MHz, $CDCl_3$): δ 8.11 - 8.08 (m, 2H), 7.58 to 7.54 (m, 1H), 7.46 - 7.24 (m, 2H), 6.25 (t, *J* = 2.8 Hz, 1H), 3.99 (td, *J* = 10.7 Hz, *J* = 2.8 Hz, 1H), 3.75 (m, 1H), 2.00 - 1.81 (m, 3H), 1.79 - 1.60 (m, 3H); $^{13}$C NMR ($CDCl_3$, 100 MHz): δ 166.0, 133.0, 130.2, 129.6, 128.3, 93.0, 63.1, 29.2, 24.9, 18.5

Analytical data for **31b**: $^{1}$H NMR (400 MHz, $CDCl_3$): δ 8.07 (d, *J* = 7.5 Hz, 2H), 7.56 (t, *J* = 7.3 Hz, 1H), 7.44 (t, *J* = 7.6 Hz, 2H), 5.10 – 5.00 (m, 1H), 3.88 (dd, *J* = 2.7 Hz, *J* = 11.6 Hz, 1H), 3.75 – 3.67 (m, 3H), 2.10 – 2.01 (m, 1H), 2.00 – 1.82 (m, 2H), 1.71 – 1.58 (m, 1H); $^{13}$C NMR ($CDCl_3$, 100 MHz): δ 165.9, 133.0, 130.3, 129.6, 128.3, 69.7, 68.5, 67.9, 28.3, 23.1; IR (thin film): 3749.9, 3734.5, 3063.4, 2953.5, 2849.3, 1716.3, 1602.6, 1451.2, 1315.2, 1274.7 cm-1; LRMS (+ESI): *m/z* calculated for [M+H]+: 207.10; found: 207.11

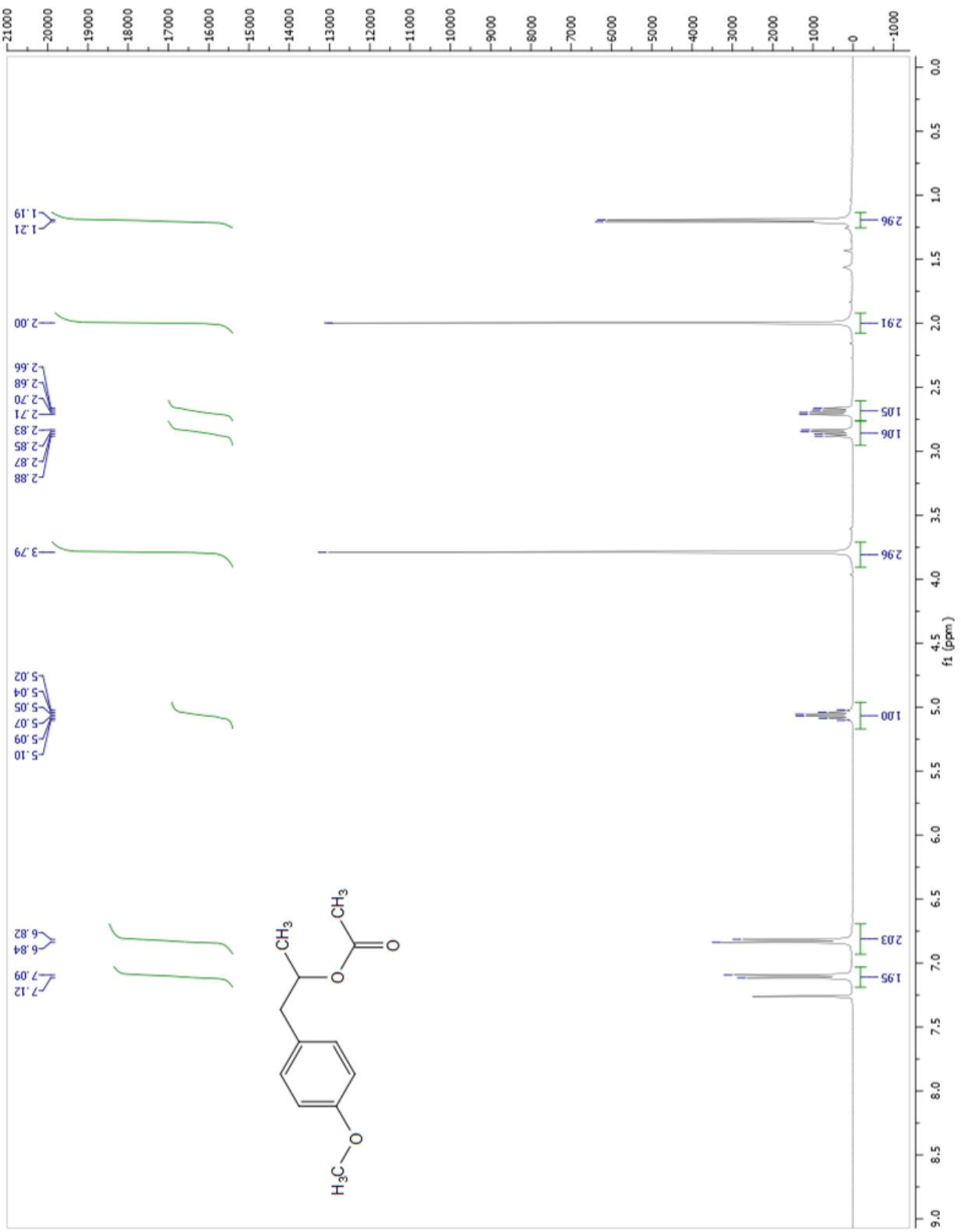
f1 (ppm)
1.19
1.21
2.00
2.66
2.68
2.70
2.71
2.83
2.85
2.87
2.88
3.79
5.02
5.04
5.05
5.07
5.09
5.10
6.82
6.84
7.09
7.12
2.96
2.91
1.05
1.06
2.96
1.00
2.03
1.95
CH3
CH3
O
O
H3C
O

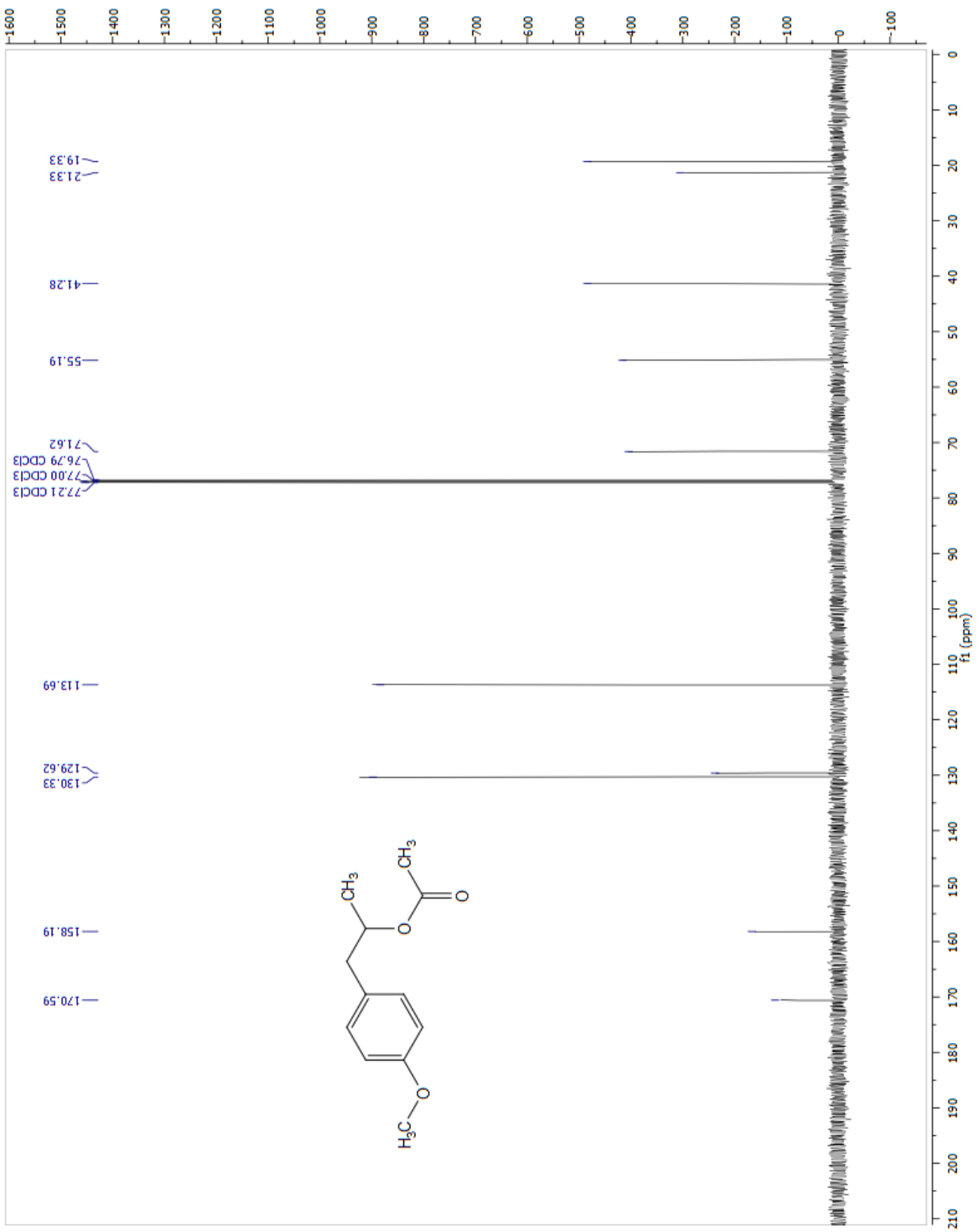
19.33
21.33
41.28
55.19
71.62
76.79 CDCl3
77.00 CDCl3
77.21 CDCl3
113.69
129.62
130.33
158.19
170.59
f1 (ppm)


f1 (ppm)
3.05
0.33
0.54
0.59
2.93
1.00
1.92
1.92
1.20
1.19
2.00
2.66
2.68
2.70
2.71
2.83
2.83
2.85
2.85
2.87
2.88
3.79
5.03
5.04
5.06
5.07
5.09
6.81
6.82
6.82
6.83
6.84
6.85
7.09
7.26
D
D
D
CH3
O
O
H
D
O
H3C


f1 (ppm)
3.23
2.95
1.04
1.04
3.01
1.00
2.94
1.00
1.22
1.21
2.01
2.00
2.69
2.71
2.74
2.89
2.90
2.92
2.94
3.80
5.07
5.09
5.10
5.12
5.14
5.15
6.74
6.75
6.76
6.76
6.78
6.80
7.18
7.20
7.22
CH3
CH3
O
O
O
CH3

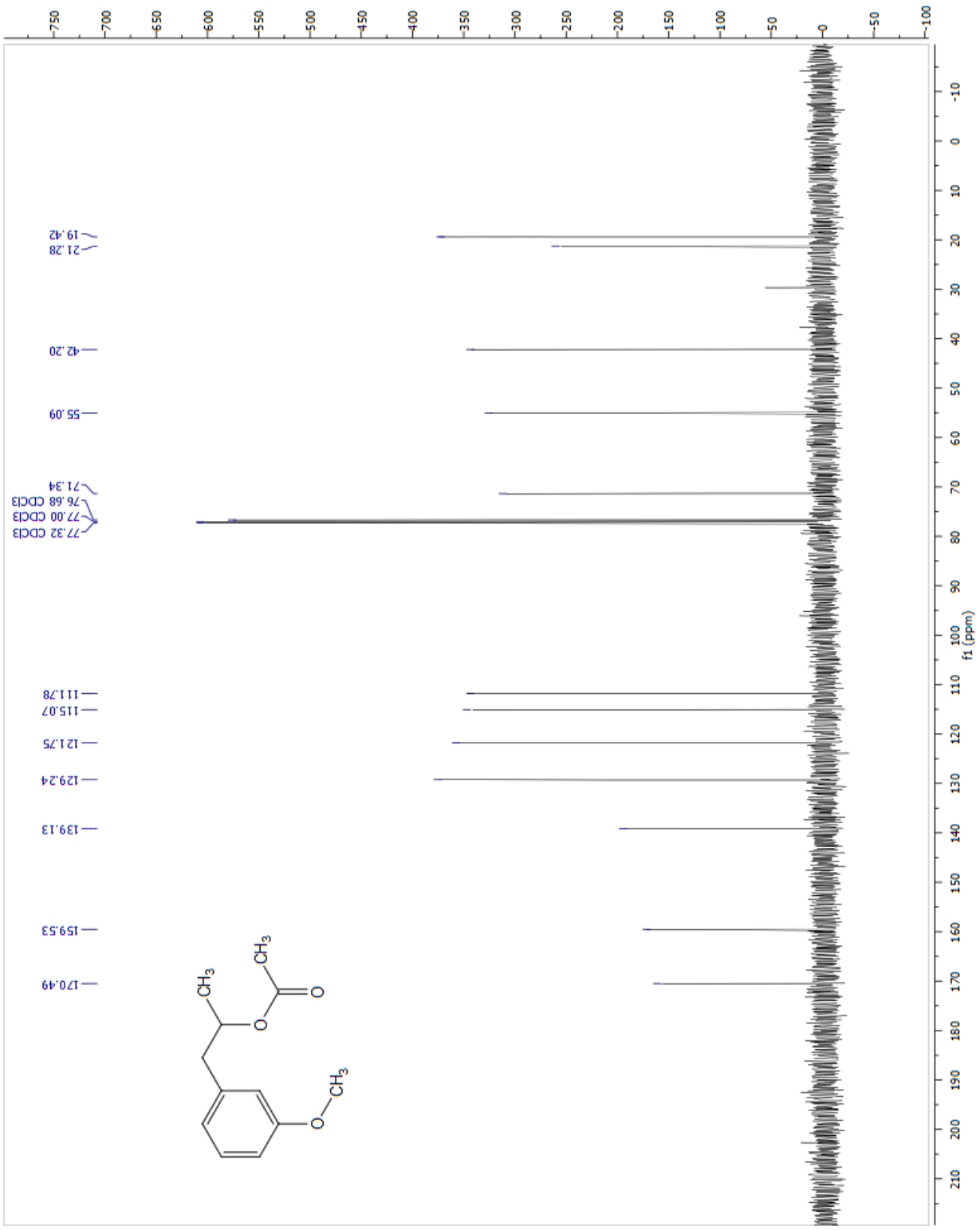
170.49
159.53
139.13
129.24
121.75
115.07
111.78
77.32 CDCl3
77.00 CDCl3
76.68 CDCl3
71.34
55.09
42.20
21.28
19.42
f1 (ppm)

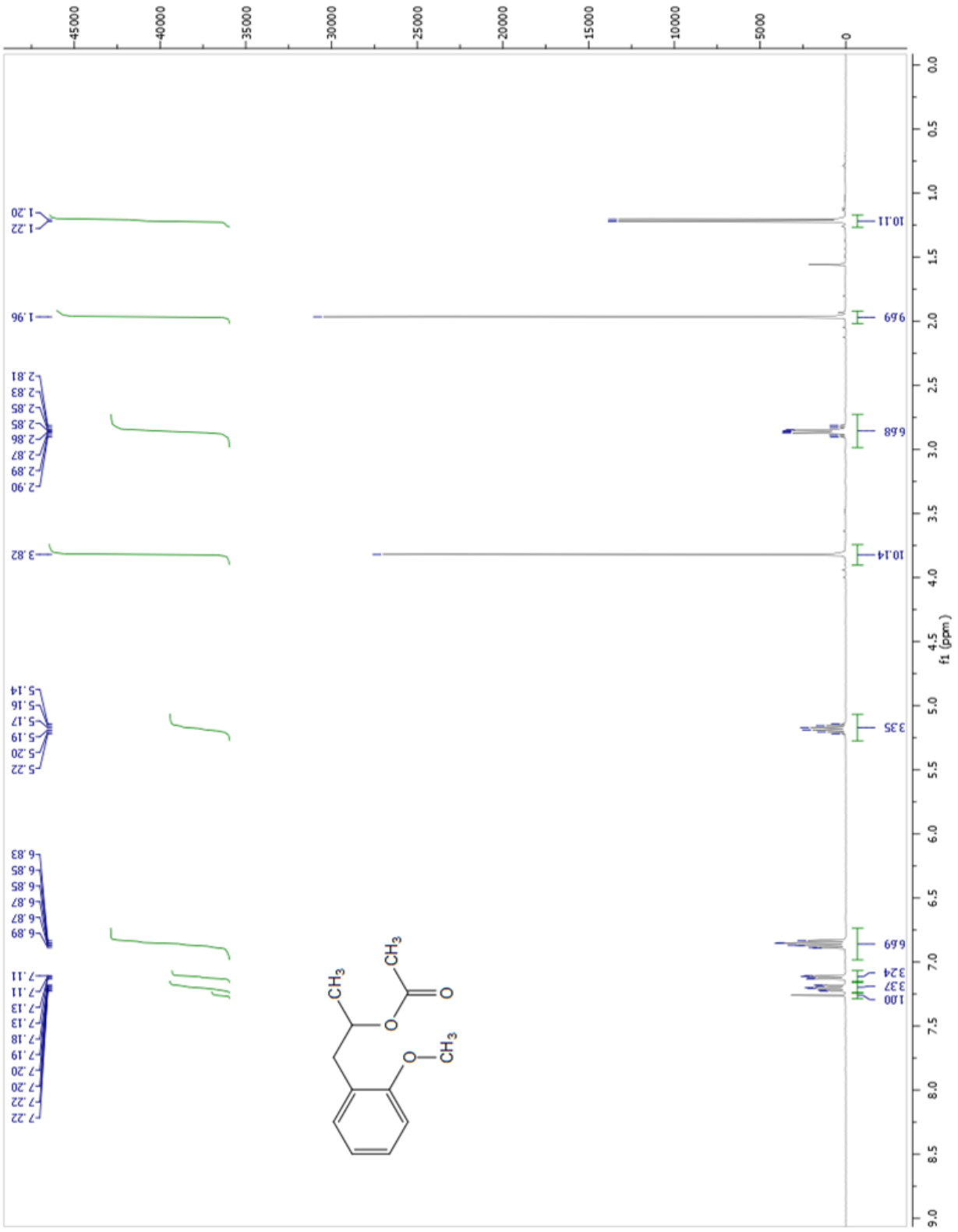
f1 (ppm)
CH3
CH3
O
O
O
CH3

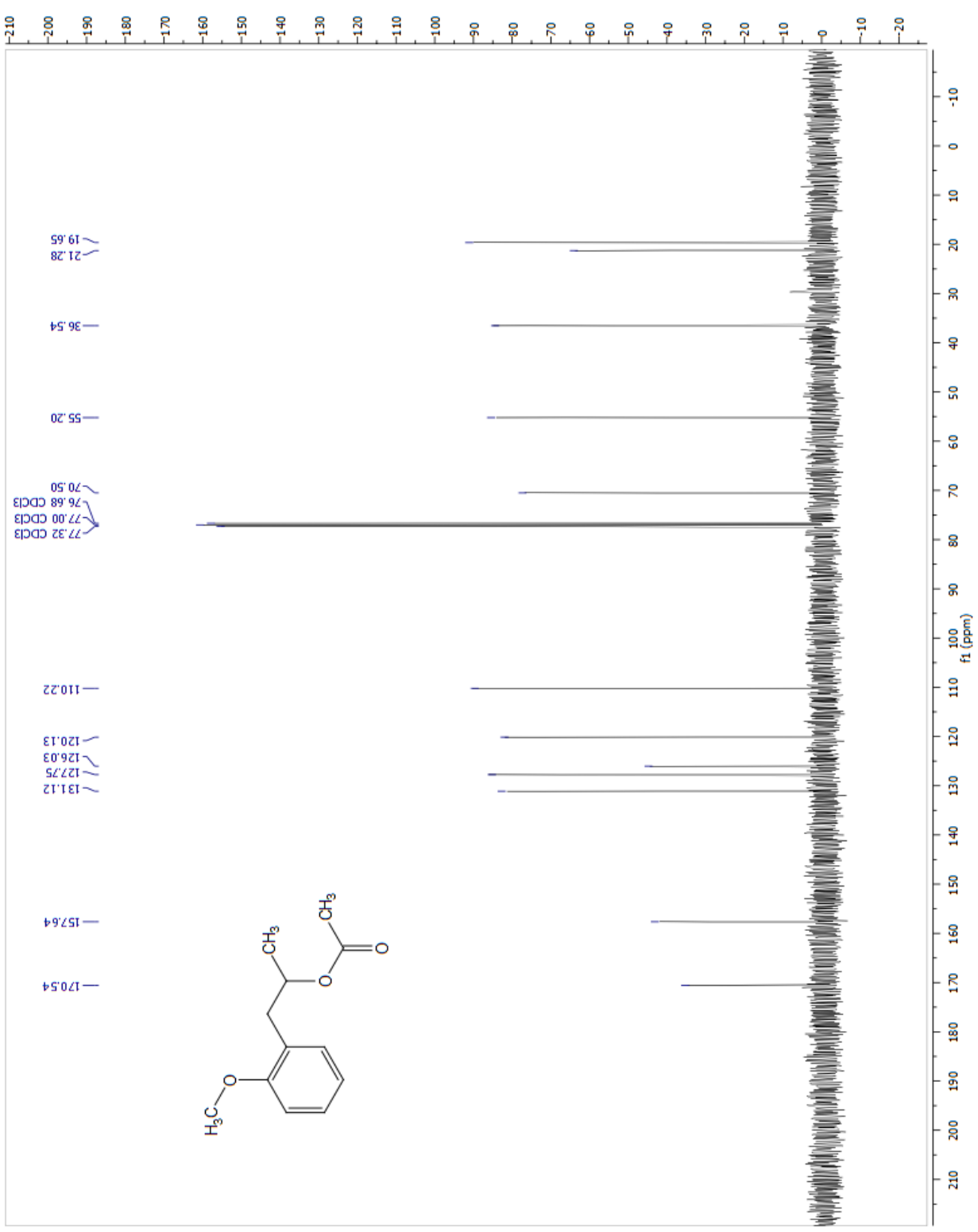
170.54
157.64
131.12
127.75
126.03
120.13
110.22
77.32 CDCl3
77.00 CDCl3
76.68 CDCl3
70.50
55.20
36.54
21.28
19.65
f1 (ppm)


f1 (ppm)
CH3
CH3
O
O
H3C

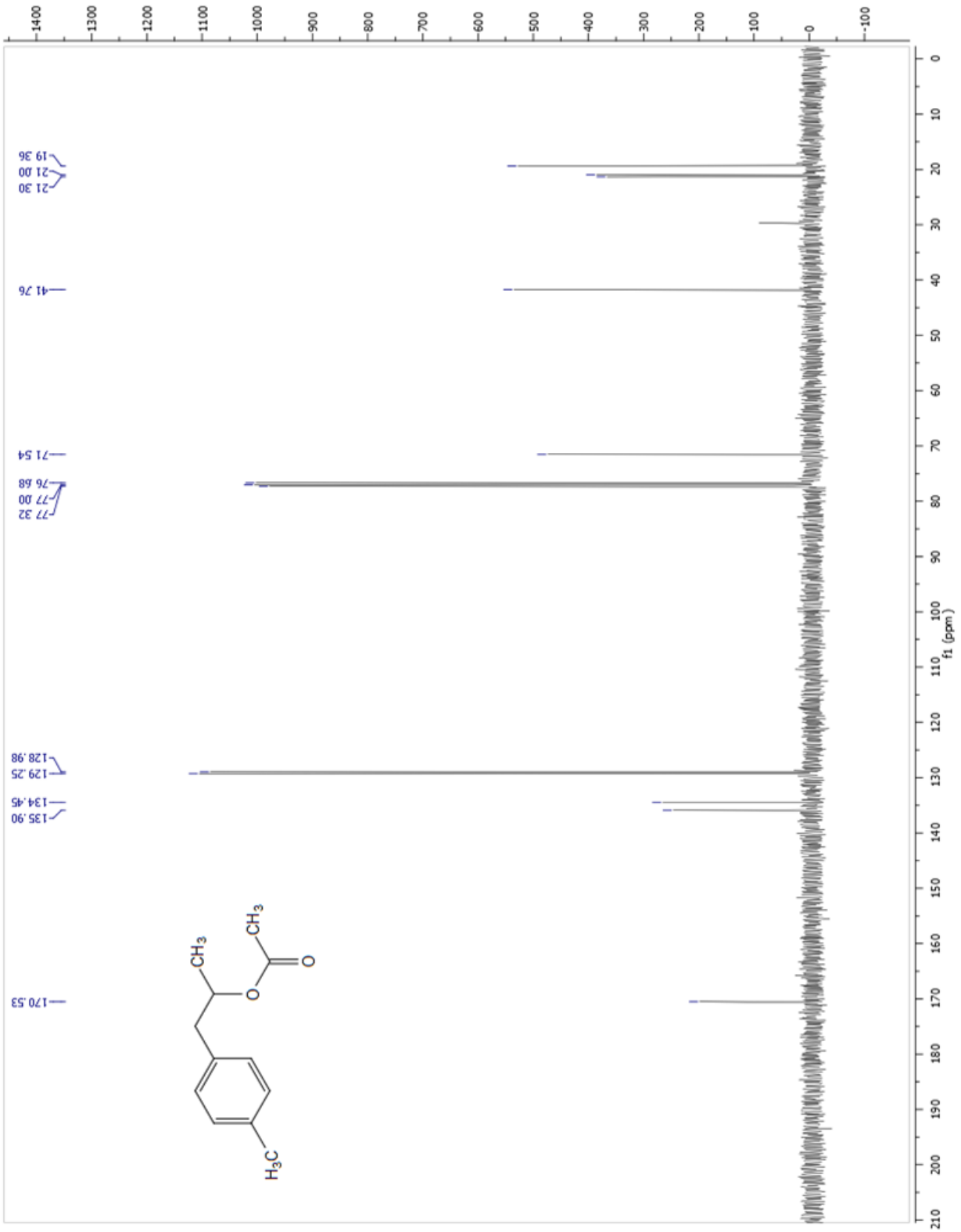
170.53
135.90
134.45
129.25
128.98
77.32
77.00
76.68
71.54
41.76
21.30
21.00
19.36
f1 (ppm)
CH3
CH3
O
O
H3C

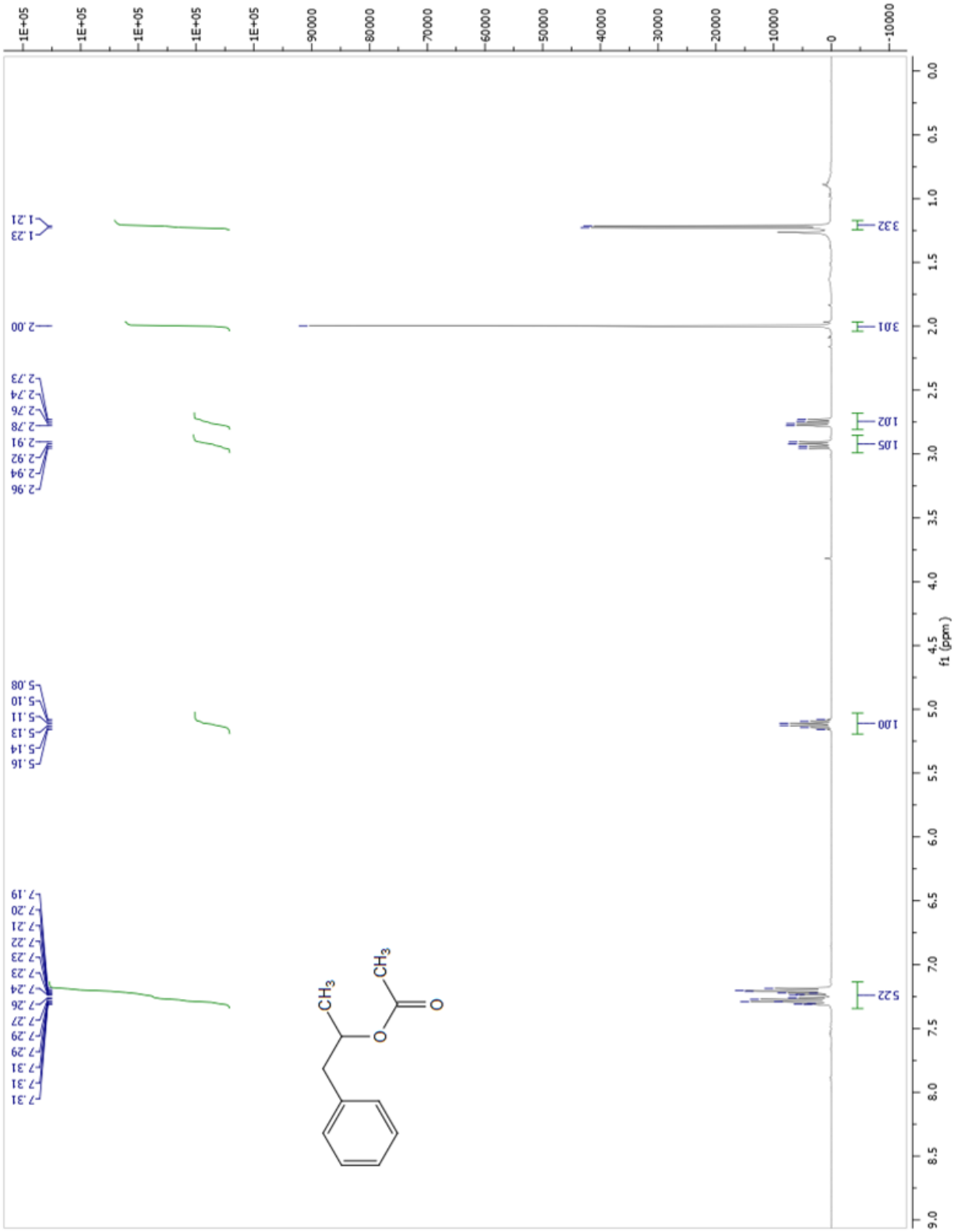
1.21
1.23
2.00
2.73
2.74
2.76
2.78
2.91
2.92
2.94
2.96
5.08
5.10
5.11
5.13
5.14
5.16
7.19
7.20
7.21
7.22
7.23
7.23
7.24
7.26
7.27
7.29
7.29
7.31
7.31
7.31
3.32
3.01
1.02
1.05
1.00
5.22
CH3
CH3
O
O
f1 (ppm)

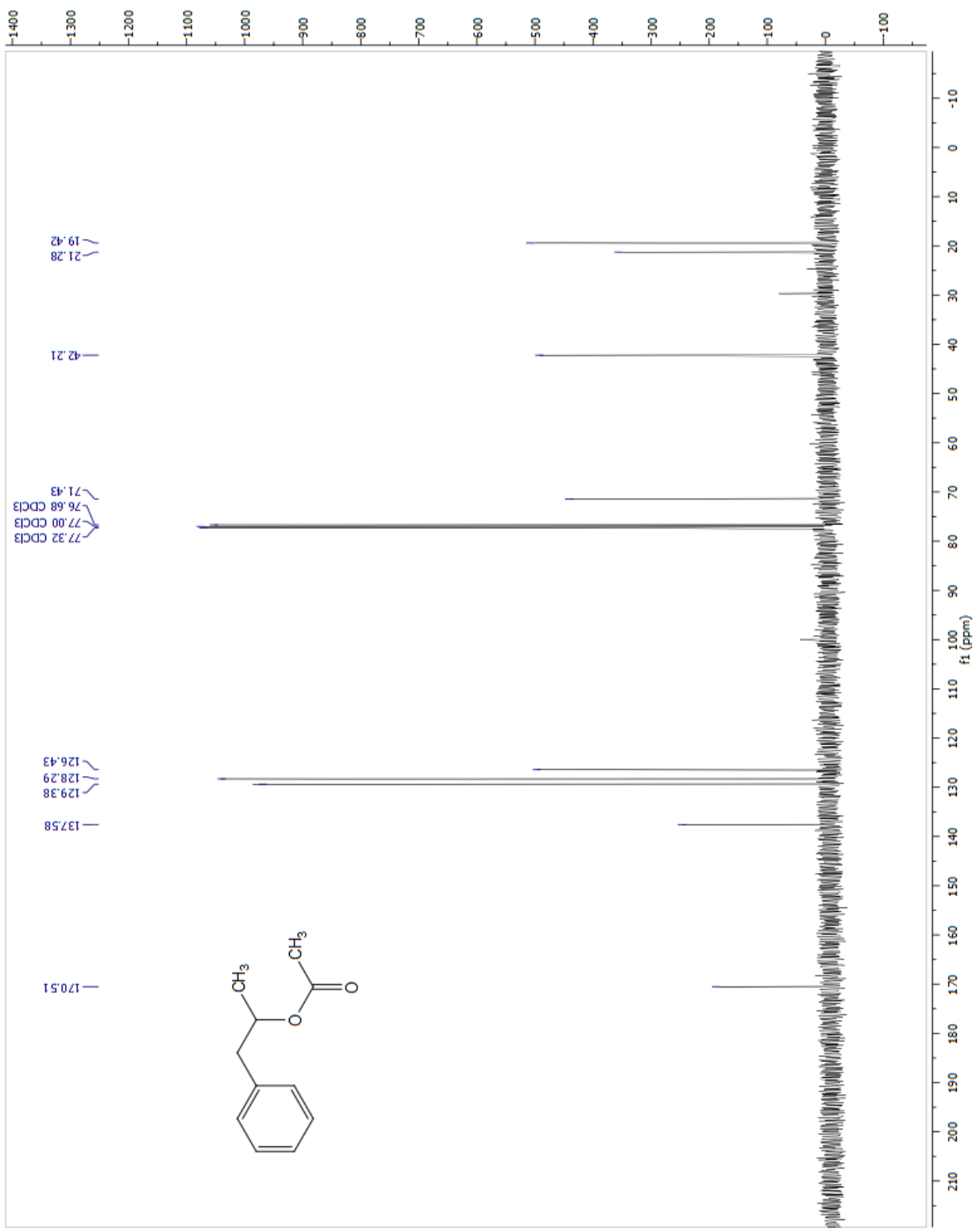
170.51
137.58
129.38
128.29
126.43
77.32 CDCl3
77.00 CDCl3
76.68 CDCl3
71.43
42.21
21.28
19.42
f1 (ppm)

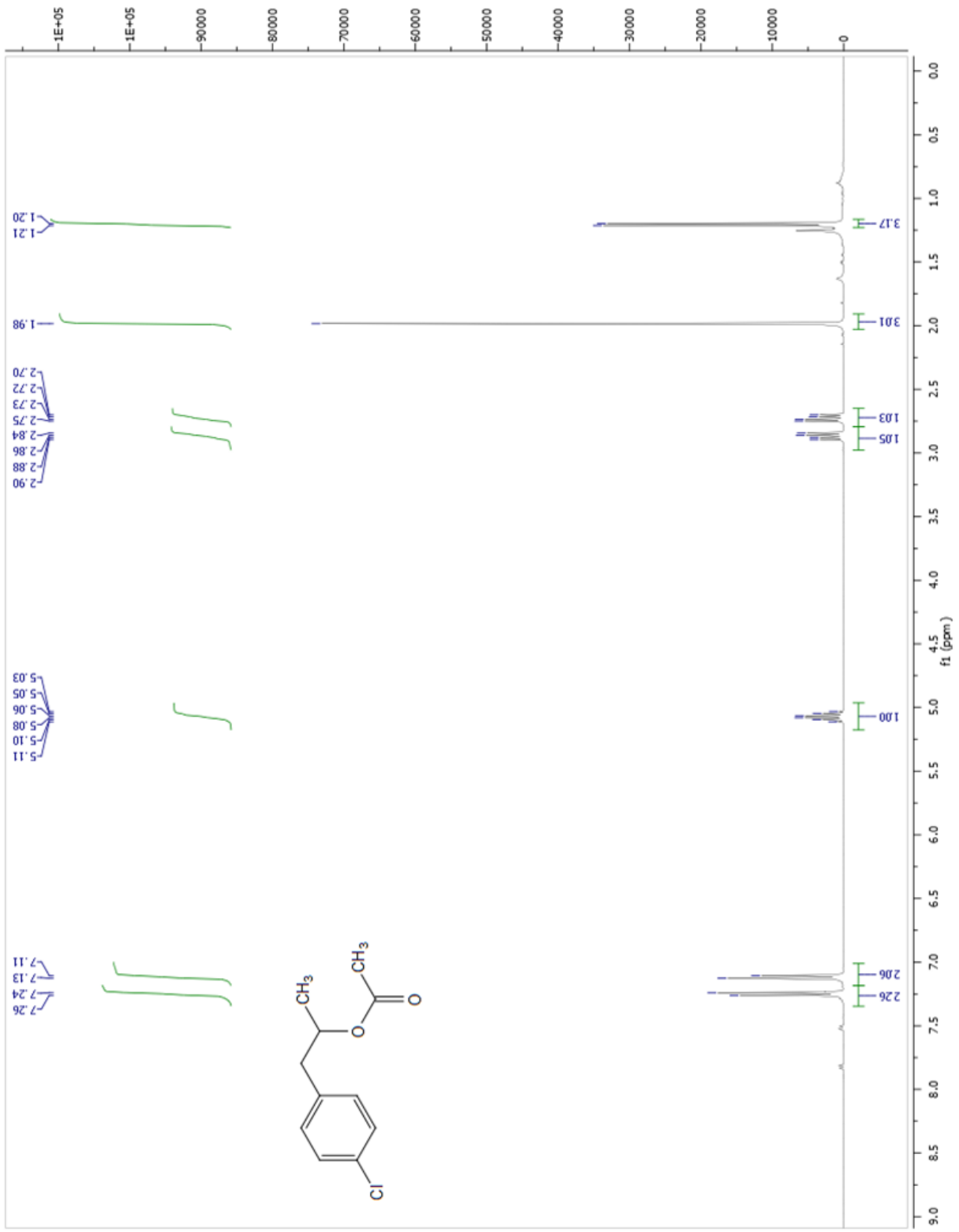
1.21
1.20
1.98
2.70
2.72
2.73
2.75
2.84
2.86
2.88
2.90
5.03
5.05
5.06
5.08
5.10
5.11
7.11
7.13
7.24
7.26
3.17
3.01
1.03
1.05
1.00
2.06
2.26
CH3
CH3
O
O
Cl
f1 (ppm)

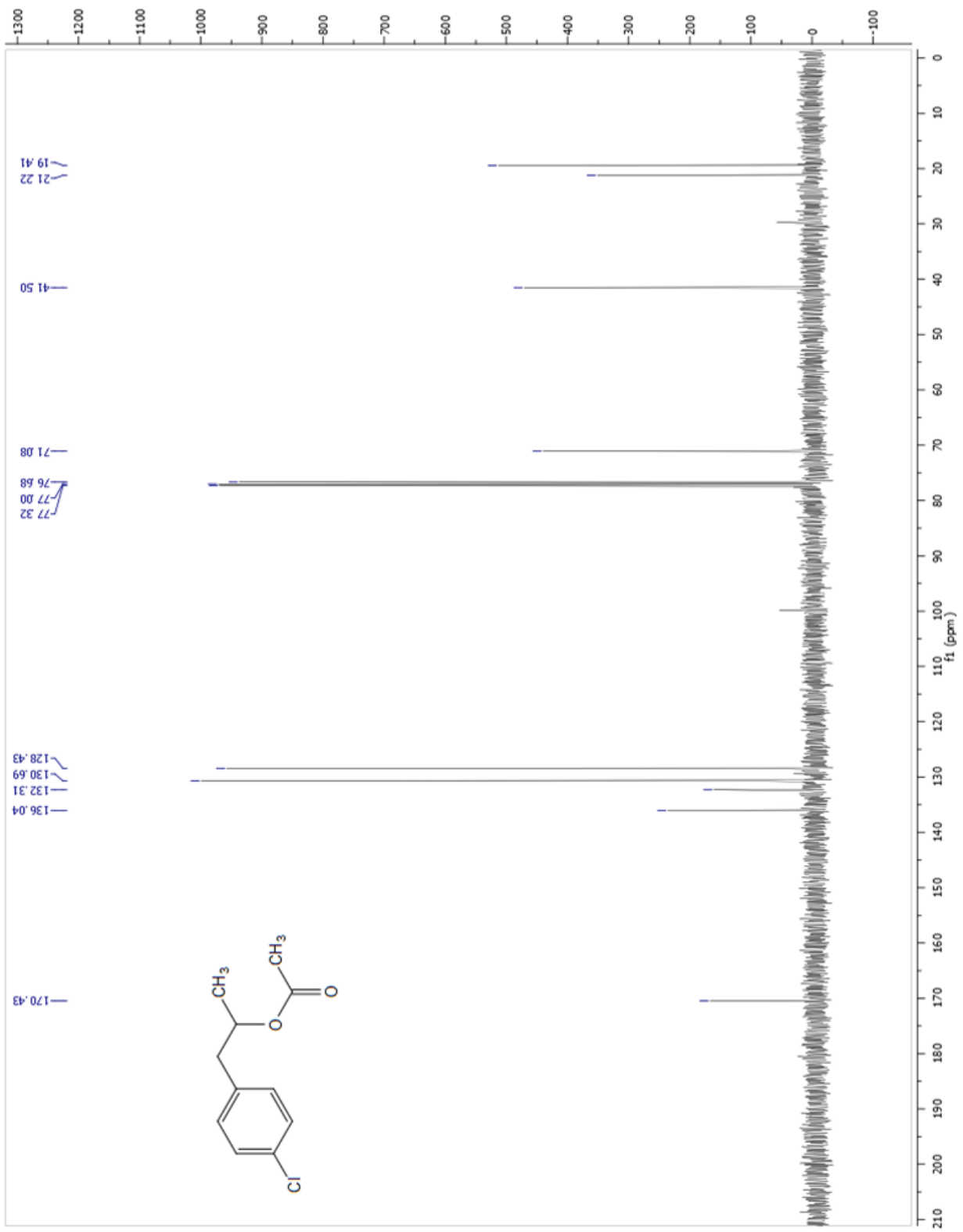
19.41
21.22
41.50
71.08
76.68
77.00
77.32
128.43
130.69
132.31
136.04
170.43
CH3
CH3
O
O
Cl
f1 (ppm)

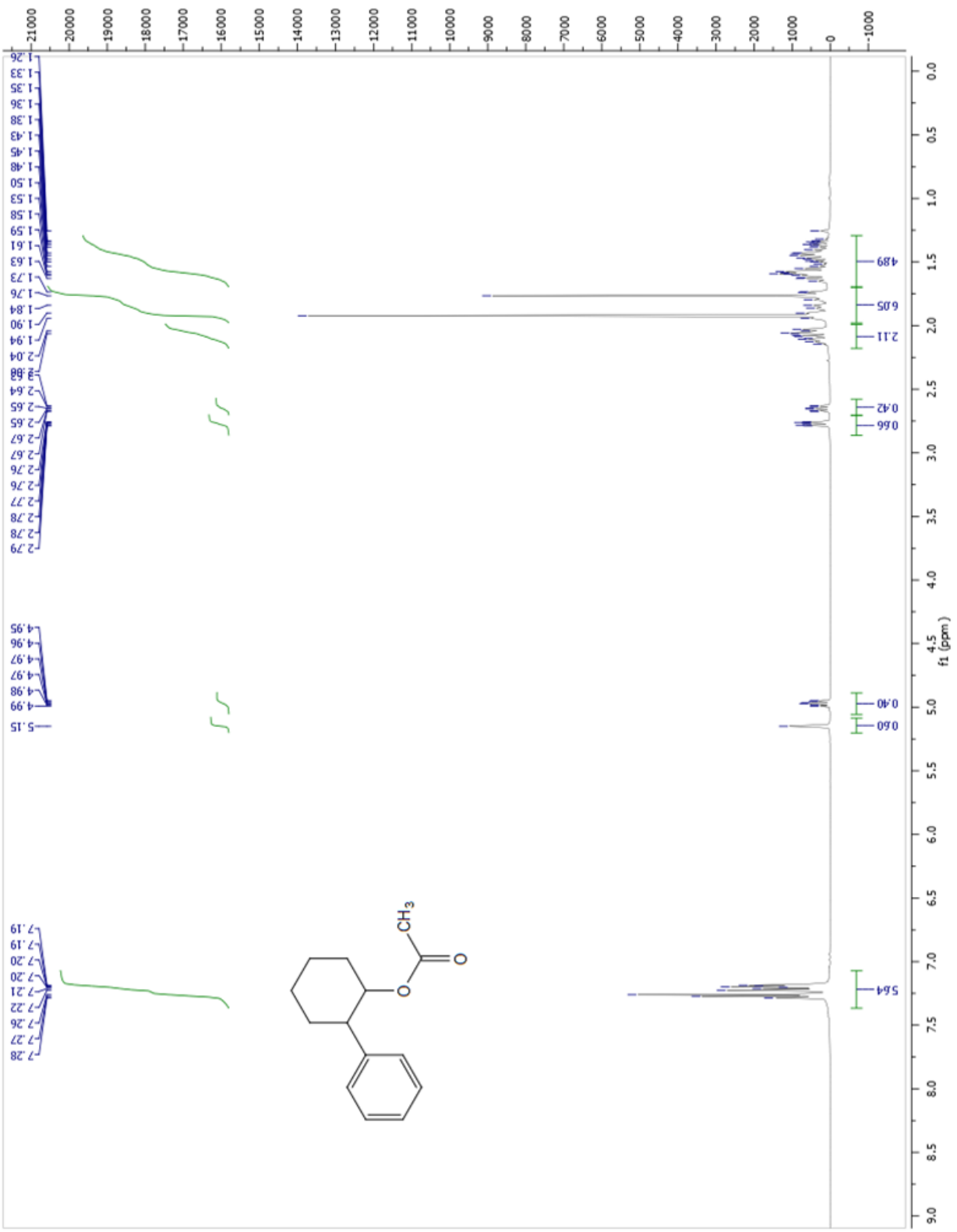
CH3
O
O
f1 (ppm)

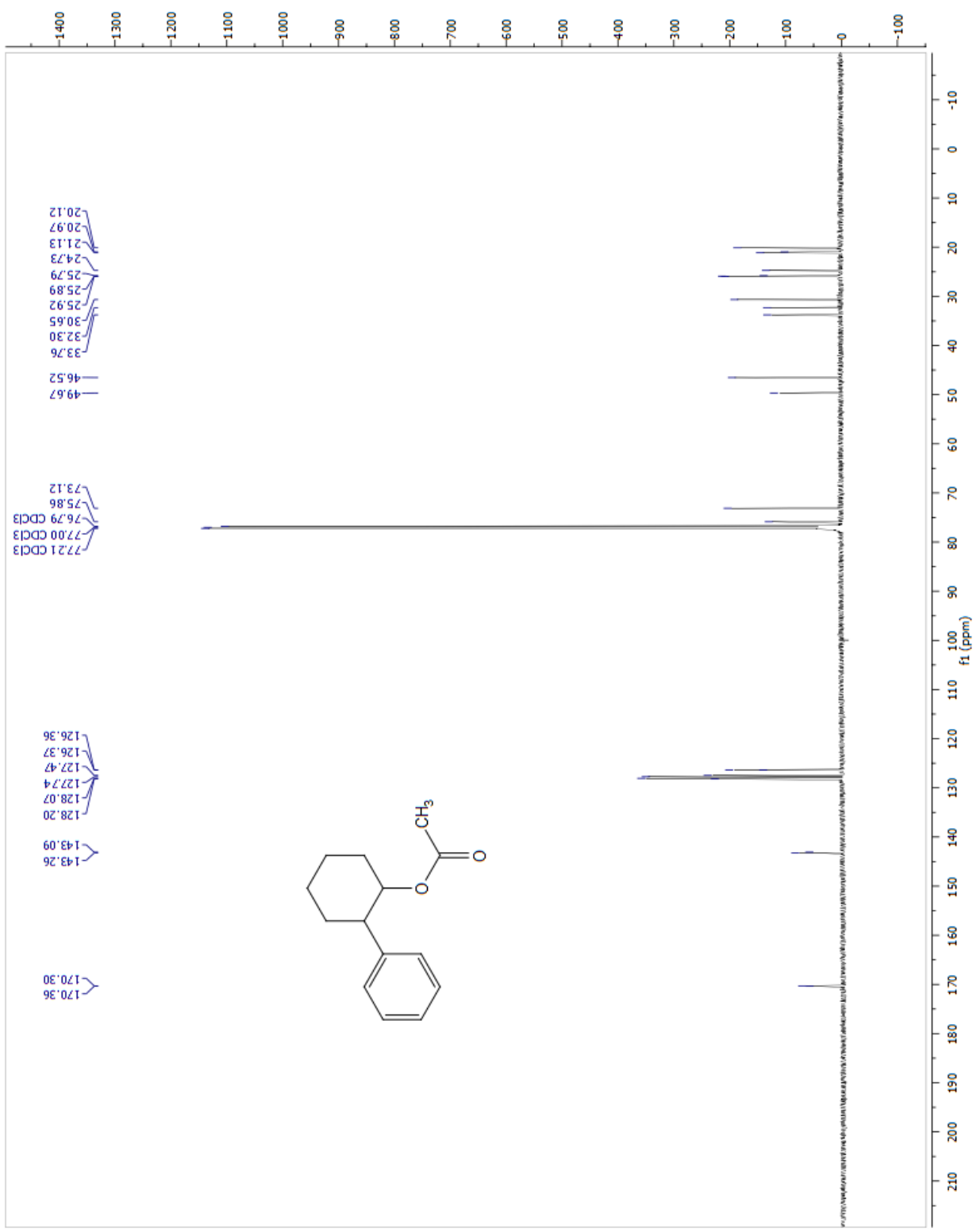
170.36
170.30
143.26
143.09
128.20
128.07
127.74
127.47
126.37
126.36
77.21 CDCl3
77.00 CDCl3
76.79 CDCl3
75.86
73.12
49.67
46.52
33.76
32.30
30.65
25.92
25.89
25.79
24.73
21.13
20.97
20.12
CH3
O
O
f1 (ppm)

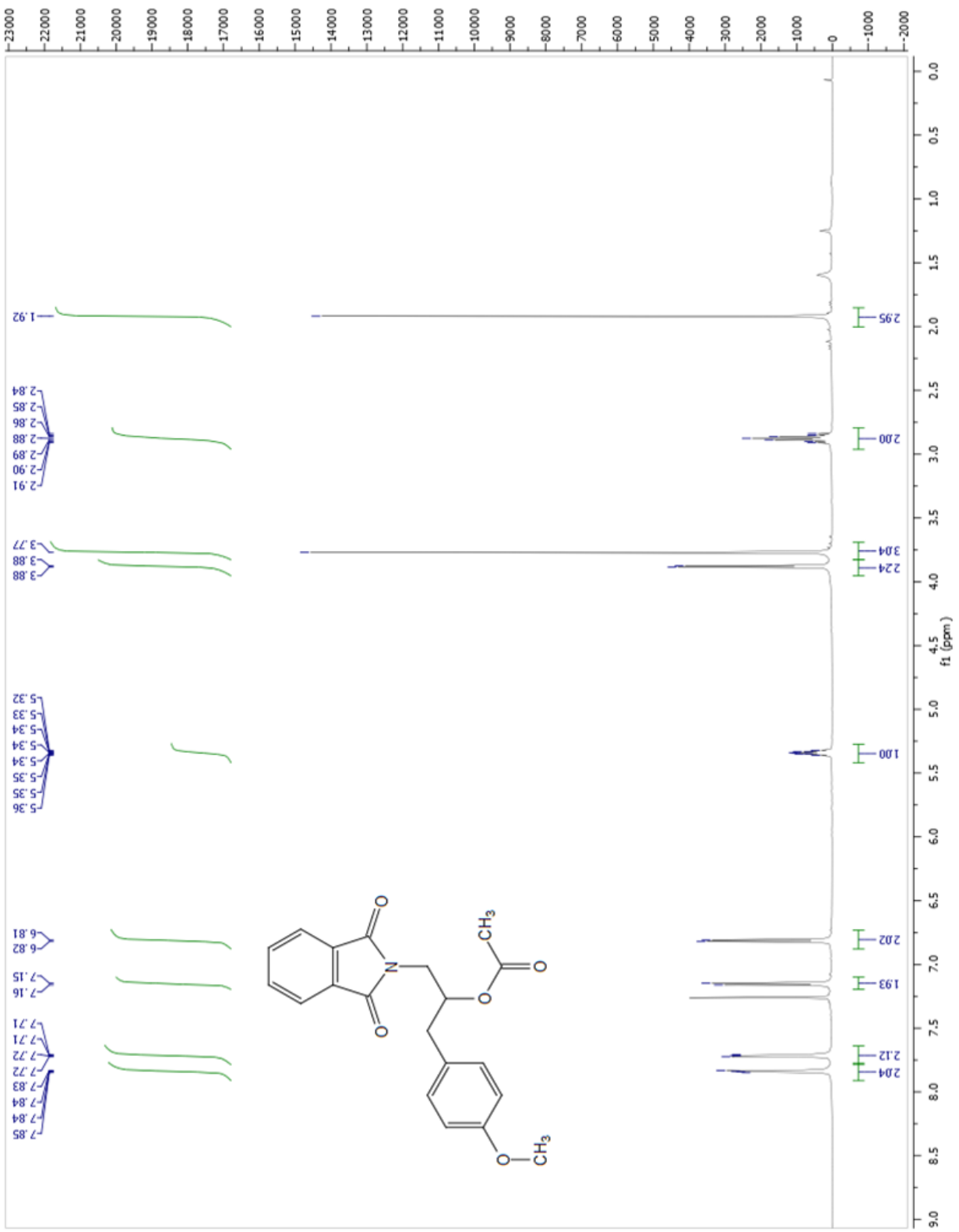
f1 (ppm)
O
N
O
O
O
CH3
O
CH3


20.93
37.50
40.78
55.17
72.36
76.79
77.00
77.21
113.83
123.34
128.50
130.18
131.89
134.03
158.34
168.22
170.64
f1 (ppm)

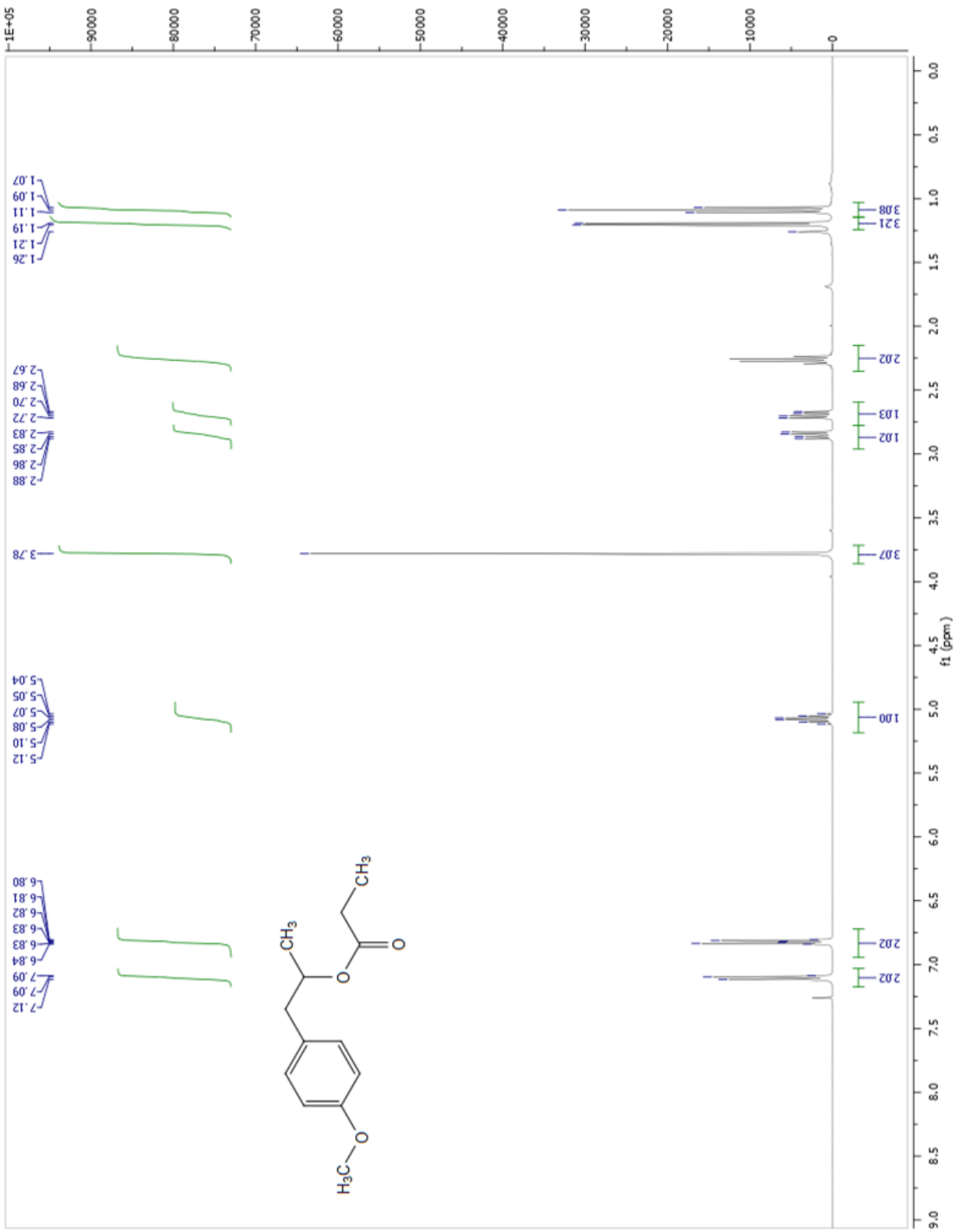
1E+05
90000
80000
70000
60000
50000
40000
30000
20000
10000
0
f1 (ppm)
1.07
1.09
1.11
1.19
1.21
1.26
2.67
2.68
2.70
2.72
2.83
2.85
2.86
2.88
3.78
5.04
5.05
5.07
5.08
5.10
5.12
6.80
6.81
6.82
6.83
6.83
6.84
7.09
7.09
7.12
3.08
3.21
2.02
1.03
1.02
3.07
1.00
2.02
2.02
CH3
CH3
O
O
O
H3C

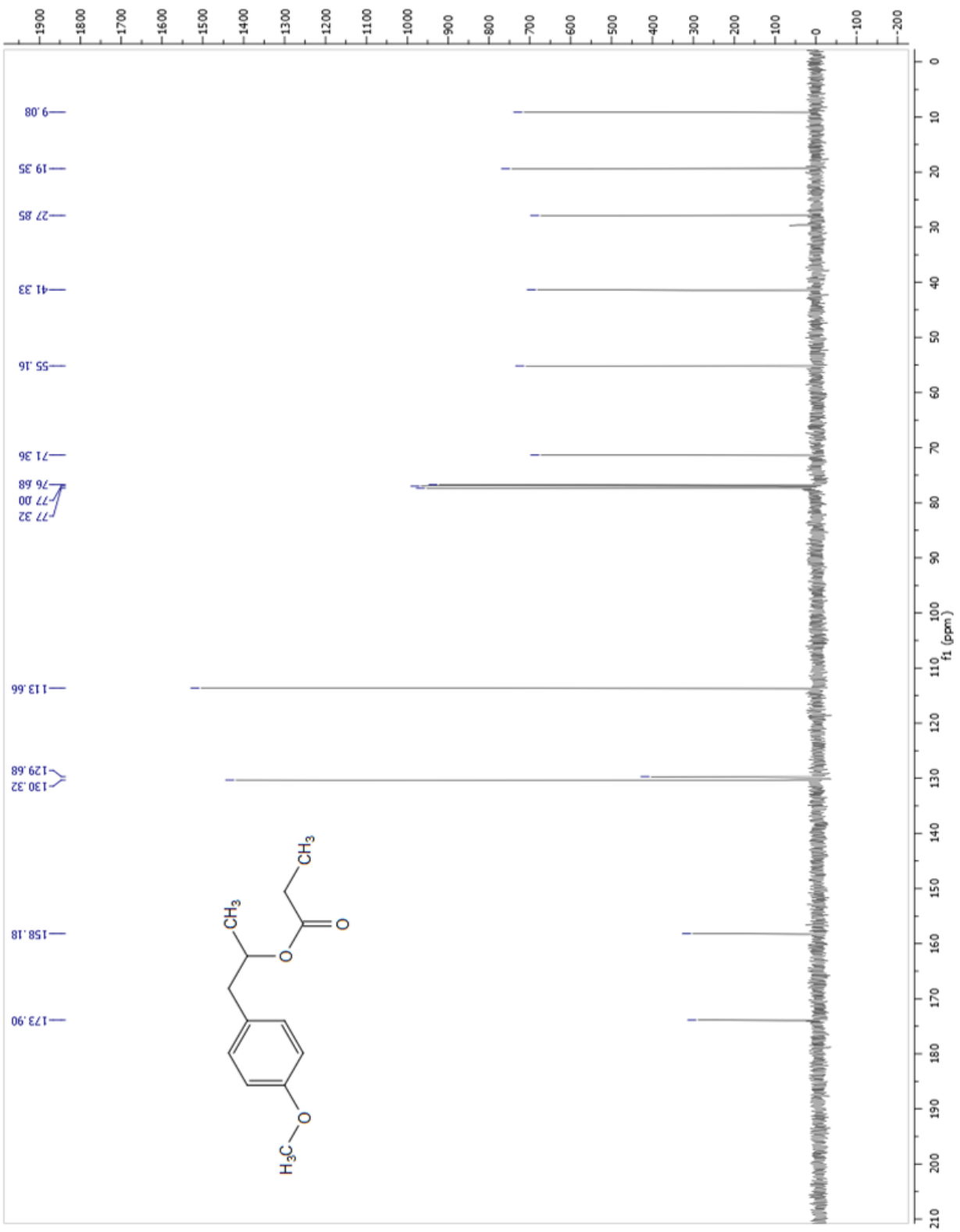
9.08
19.35
27.85
41.33
55.16
71.36
76.68
77.00
77.32
113.66
129.68
130.32
158.18
173.90
f1 (ppm)

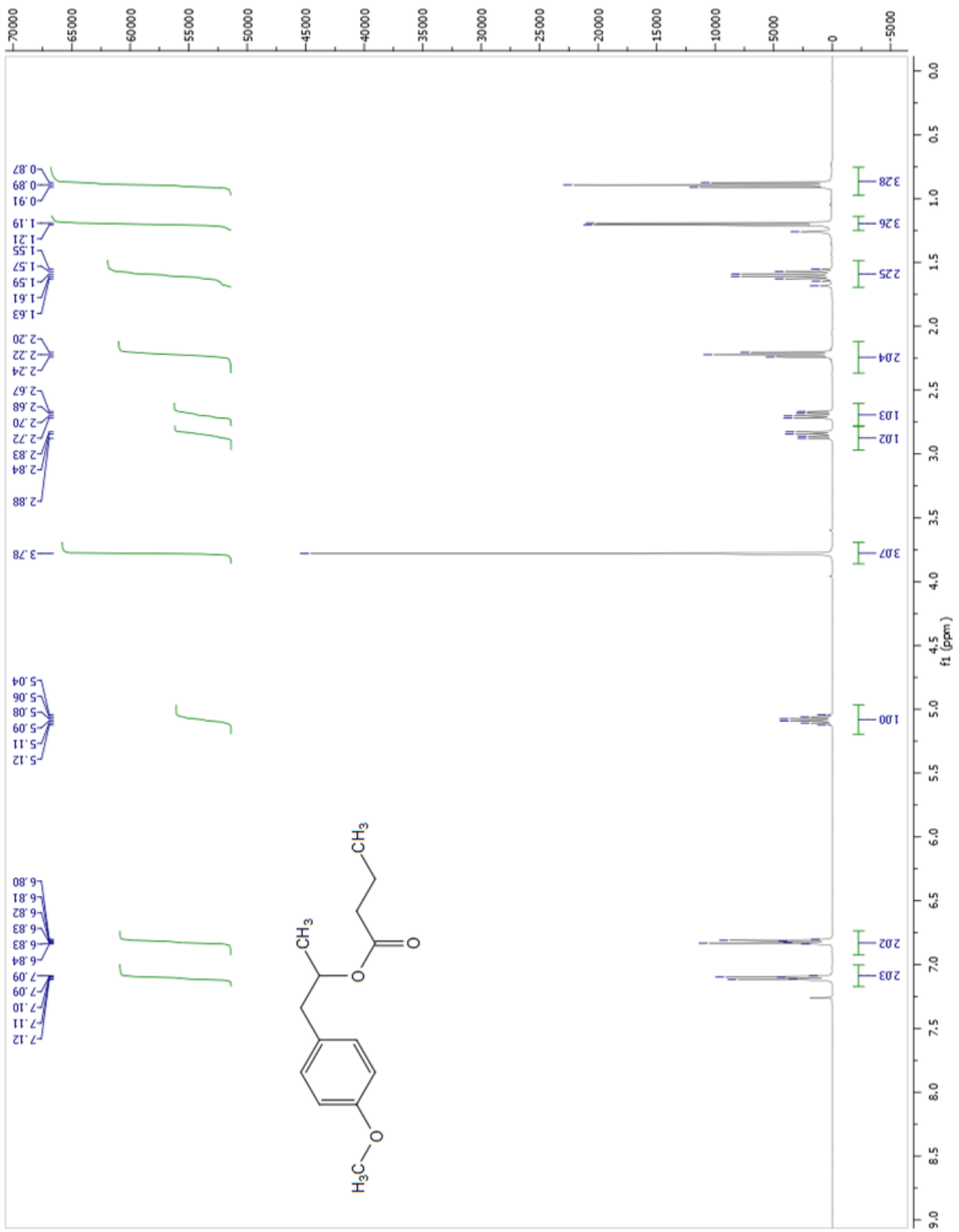
f1 (ppm)
CH3
CH3
O
O
O
H3C

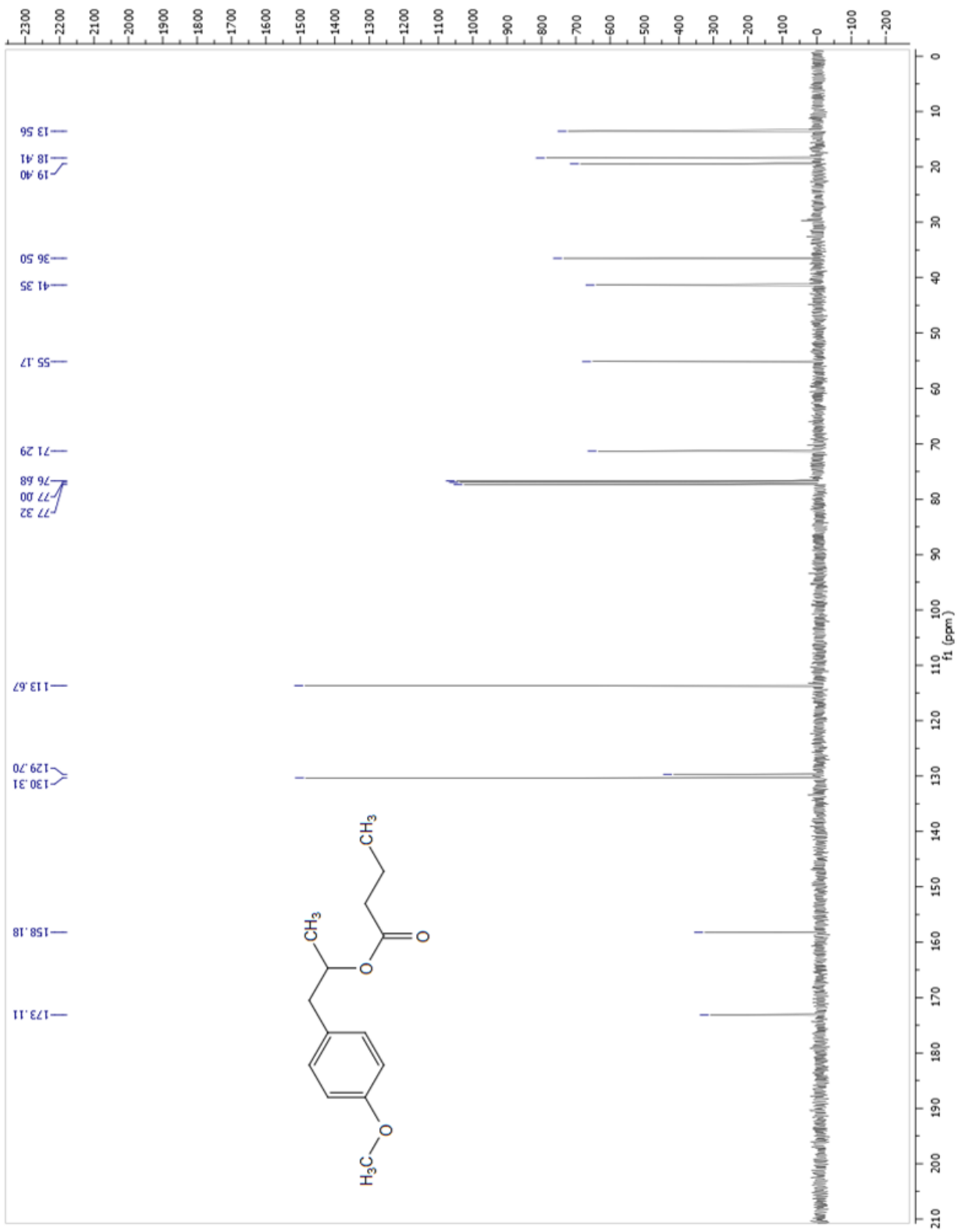
13.56
18.41
19.40
36.50
41.35
55.17
71.29
76.68
77.00
77.32
113.67
129.70
130.31
158.18
173.11
f1 (ppm)

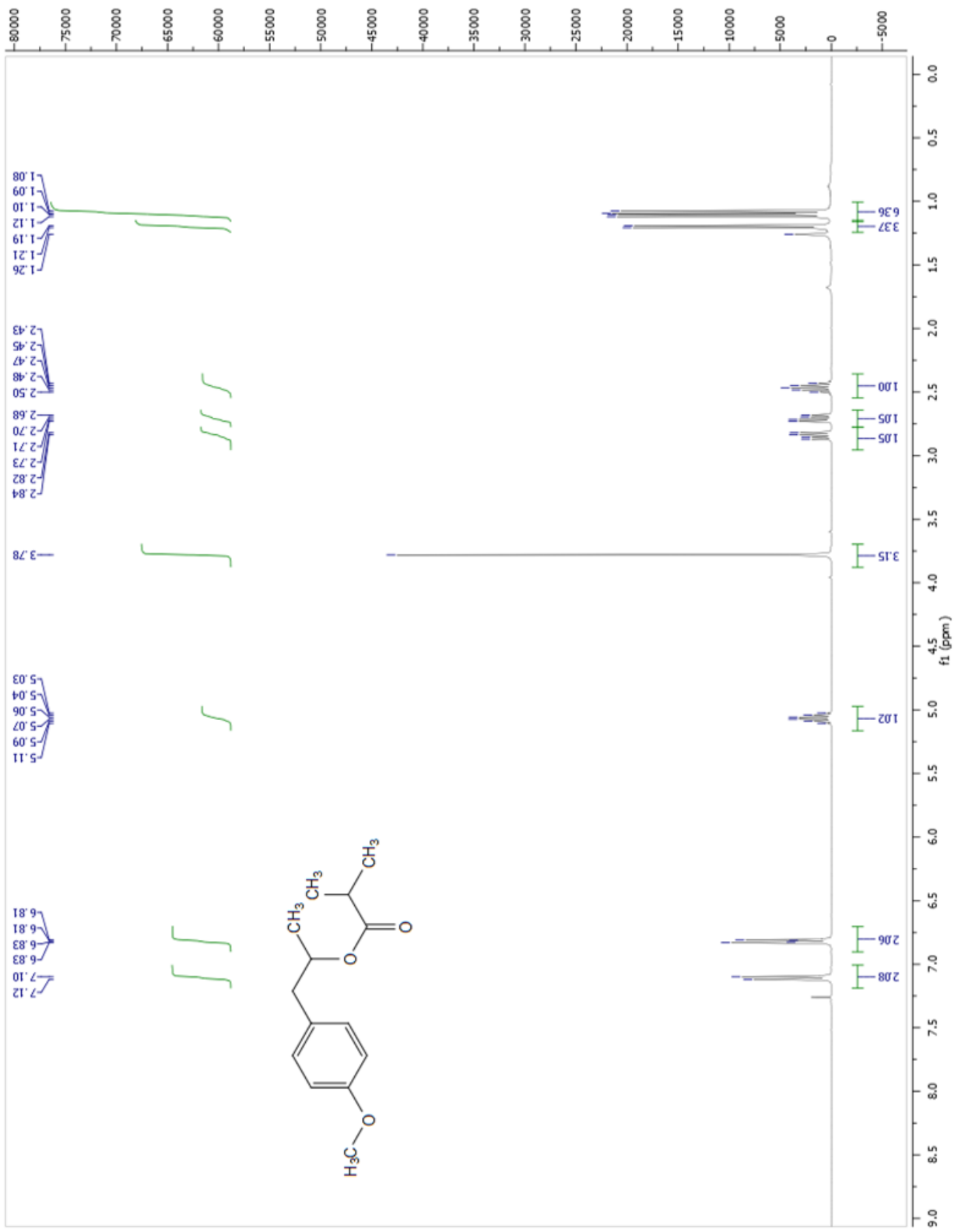
f1 (ppm)
CH3
CH3
CH3
O
O
H3C
O

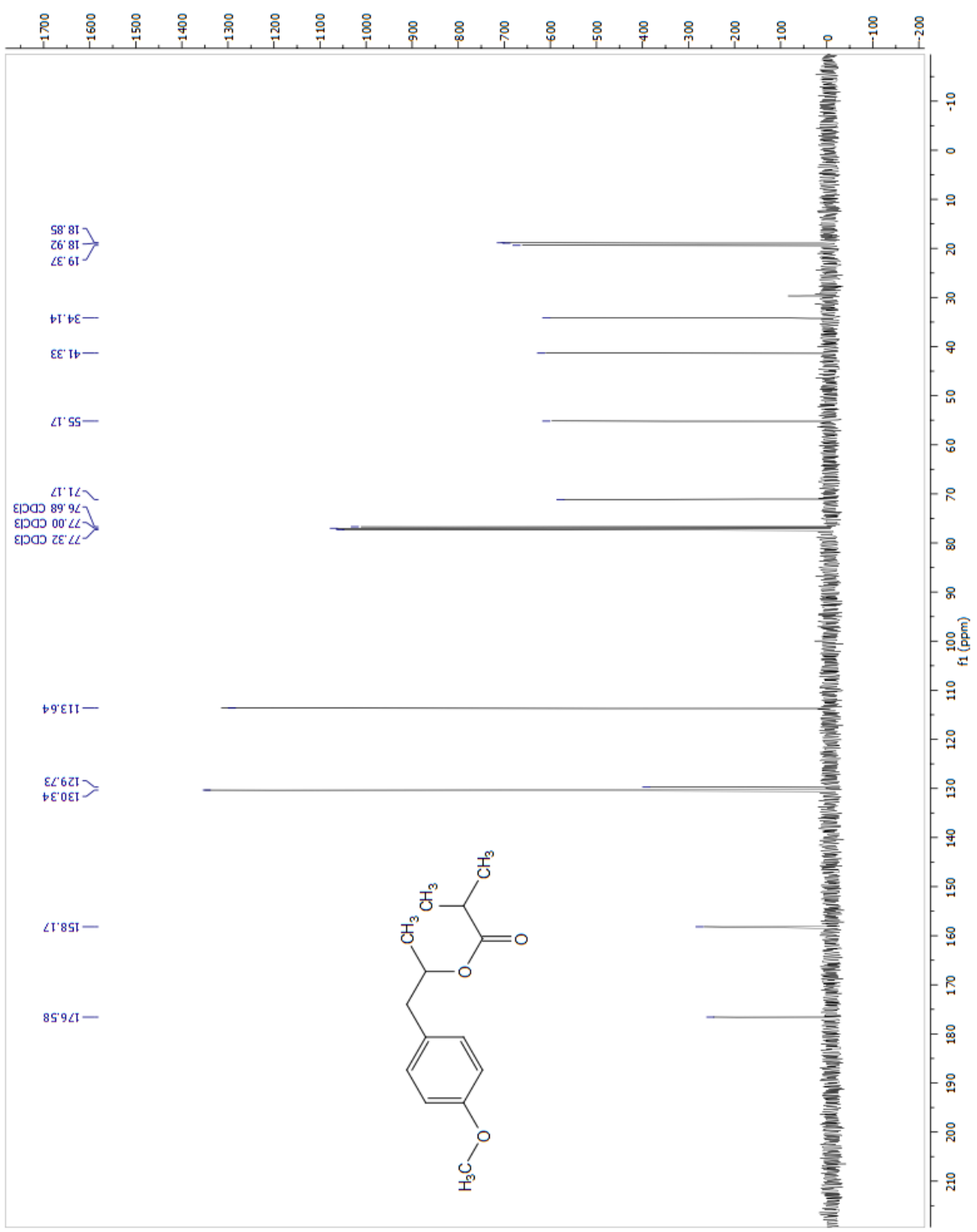
18.85
18.92
19.37
34.14
41.33
55.17
71.17
76.68 CDCl3
77.00 CDCl3
77.32 CDCl3
113.64
129.73
130.34
158.17
176.58
CH3
CH3
CH3
O
O
H3C
O
f1 (ppm)

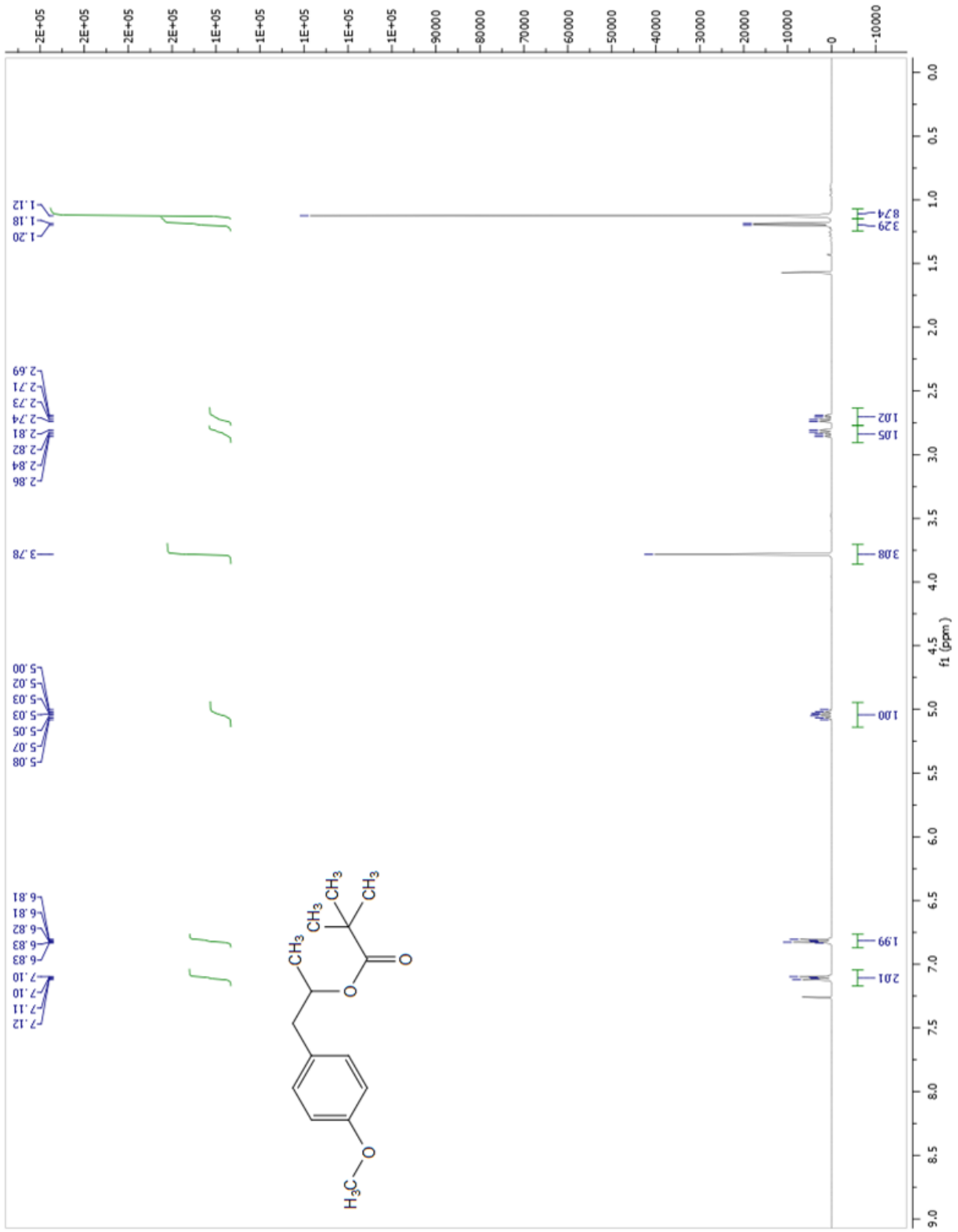
1.20
1.18
1.12
2.86
2.84
2.82
2.81
2.74
2.73
2.71
2.69
3.78
5.08
5.07
5.05
5.03
5.03
5.02
5.00
6.83
6.83
6.82
6.81
6.81
7.12
7.11
7.10
7.10
CH3
CH3
CH3
O
O
O
H3C
874
329
102
105
308
100
199
201
f1 (ppm)

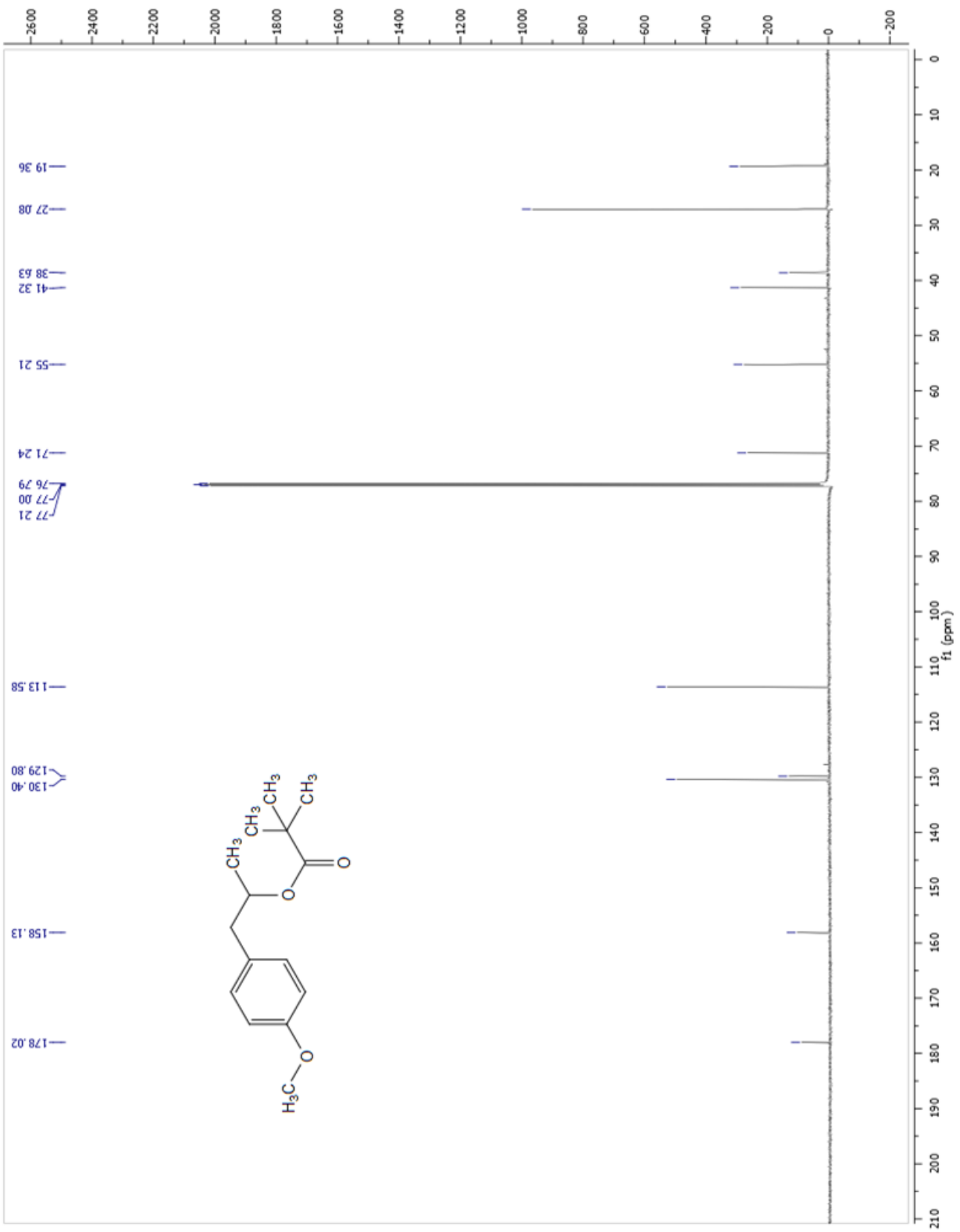
19.36
27.08
38.63
41.32
55.21
71.24
76.79
77.00
77.21
113.58
129.80
130.40
158.13
178.02
f1 (ppm)

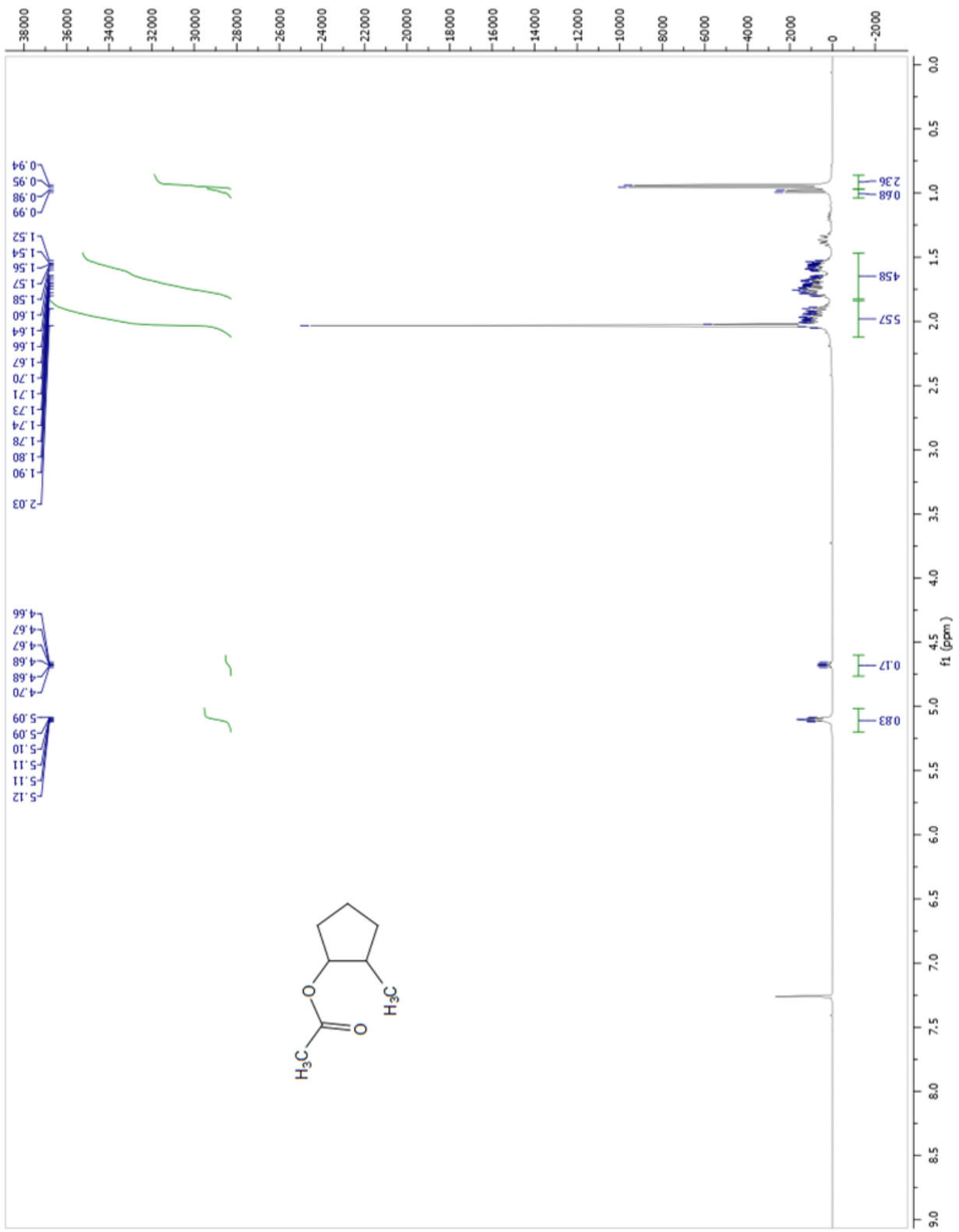
f1 (ppm)
2.36
0.68
4.58
5.57
0.17
0.83
H3C
O
O
H3C

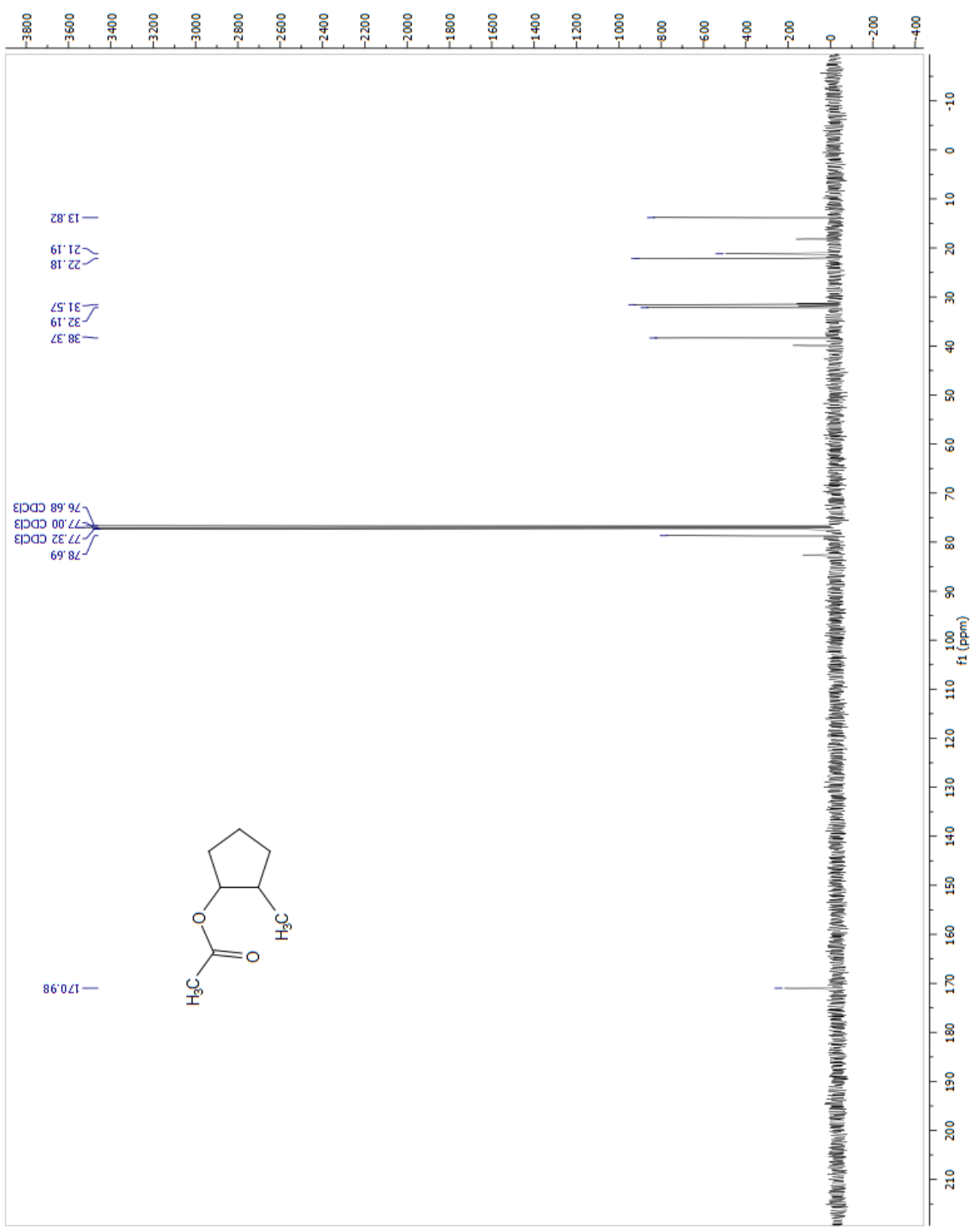
170.98
78.69
77.32 CDCl3
77.00 CDCl3
76.68 CDCl3
38.37
32.19
31.57
22.18
21.19
13.82
O
O
H3C
H3C
f1 (ppm)

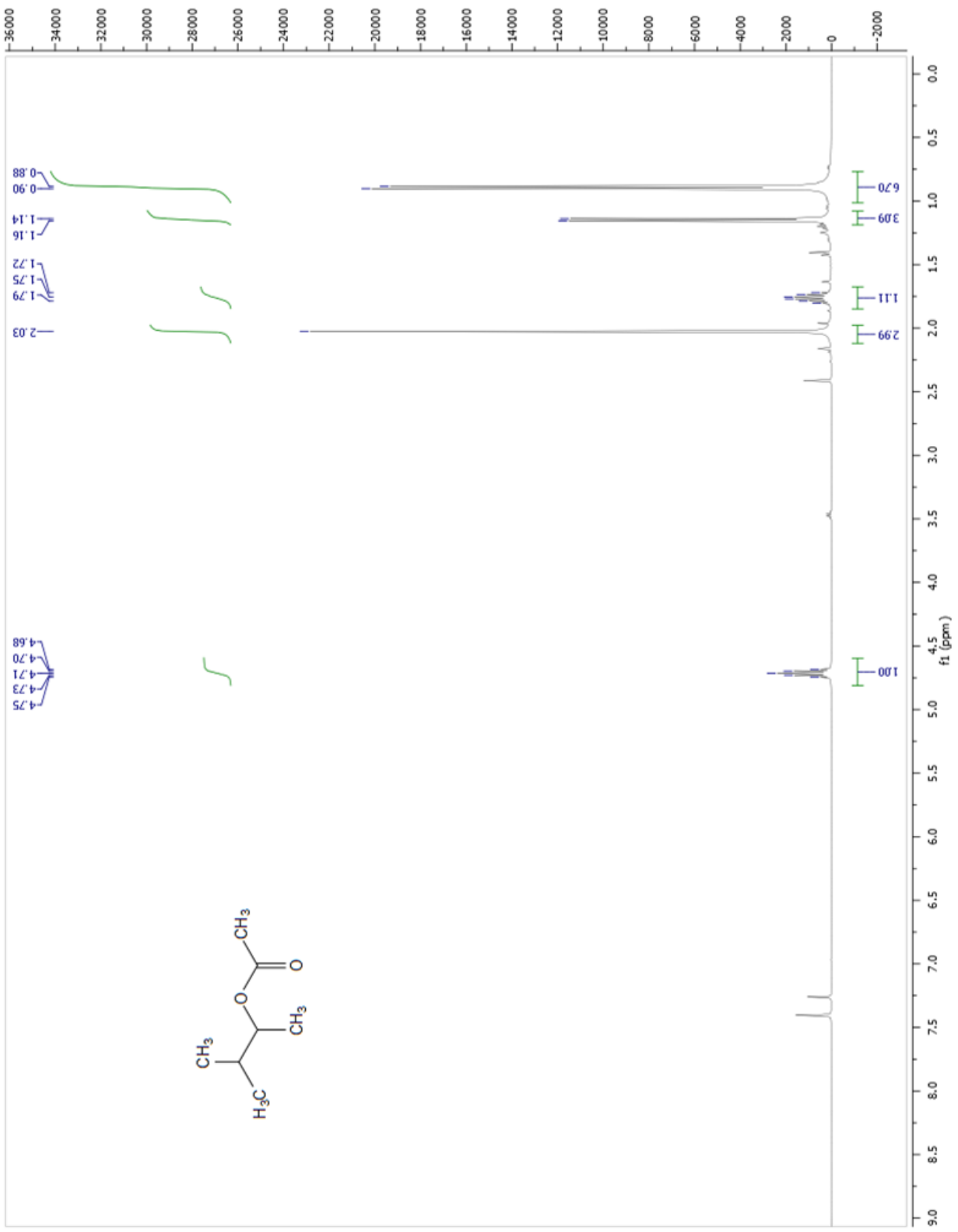
f1 (ppm)
6.70
3.09
1.11
2.99
1.00
0.88
0.90
1.14
1.16
1.72
1.75
1.79
2.03
4.68
4.70
4.71
4.73
4.75
CH3
O
O
CH3
CH3
H3C

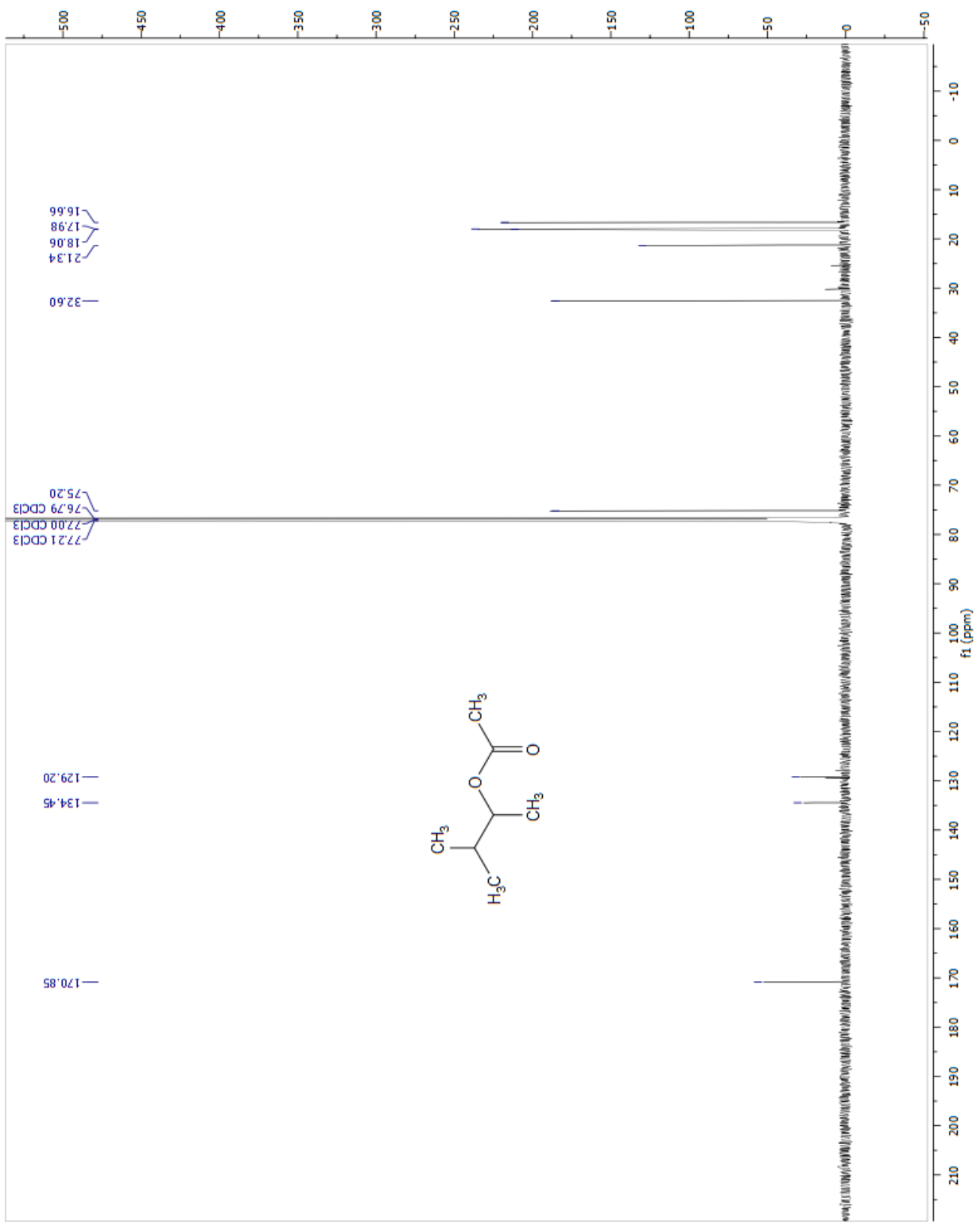
170.85
134.45
129.20
77.21 CDCl3
77.00 CDCl3
76.79 CDCl3
75.20
32.60
21.34
18.06
17.98
16.66
f1 (ppm)

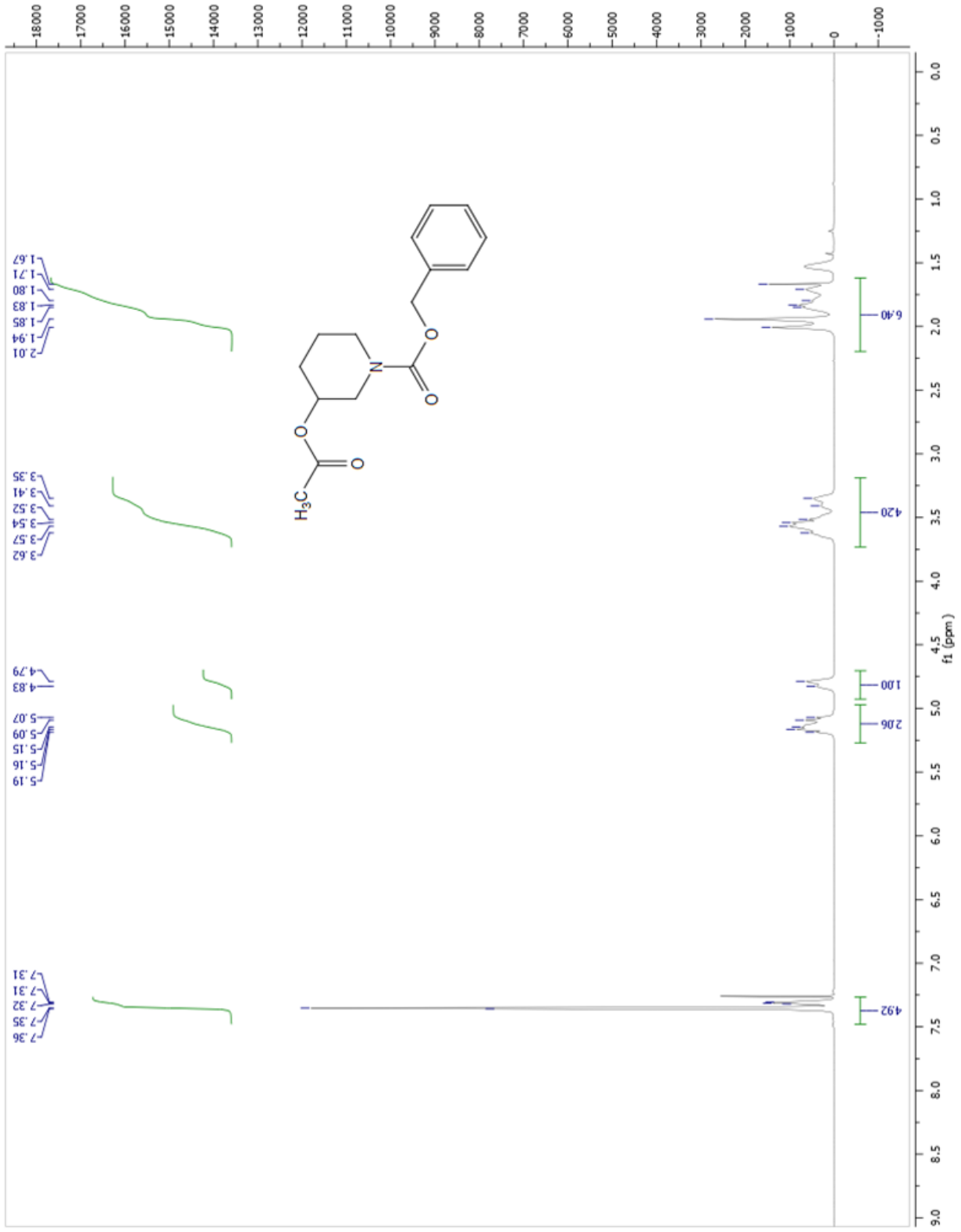
7.36
7.35
7.32
7.31
7.31
5.19
5.16
5.15
5.09
5.07
4.83
4.79
3.62
3.57
3.54
3.52
3.41
3.35
2.01
1.94
1.85
1.83
1.80
1.71
1.67
4.92
2.06
1.00
4.20
6.40
f1 (ppm)


21.02
21.48
28.98
44.04
47.37
67.05
67.73
76.79 CDCl3
77.00 CDCl3
77.21 CDCl3
127.79
127.95
128.45
136.70
155.42
170.30
f1 (ppm)

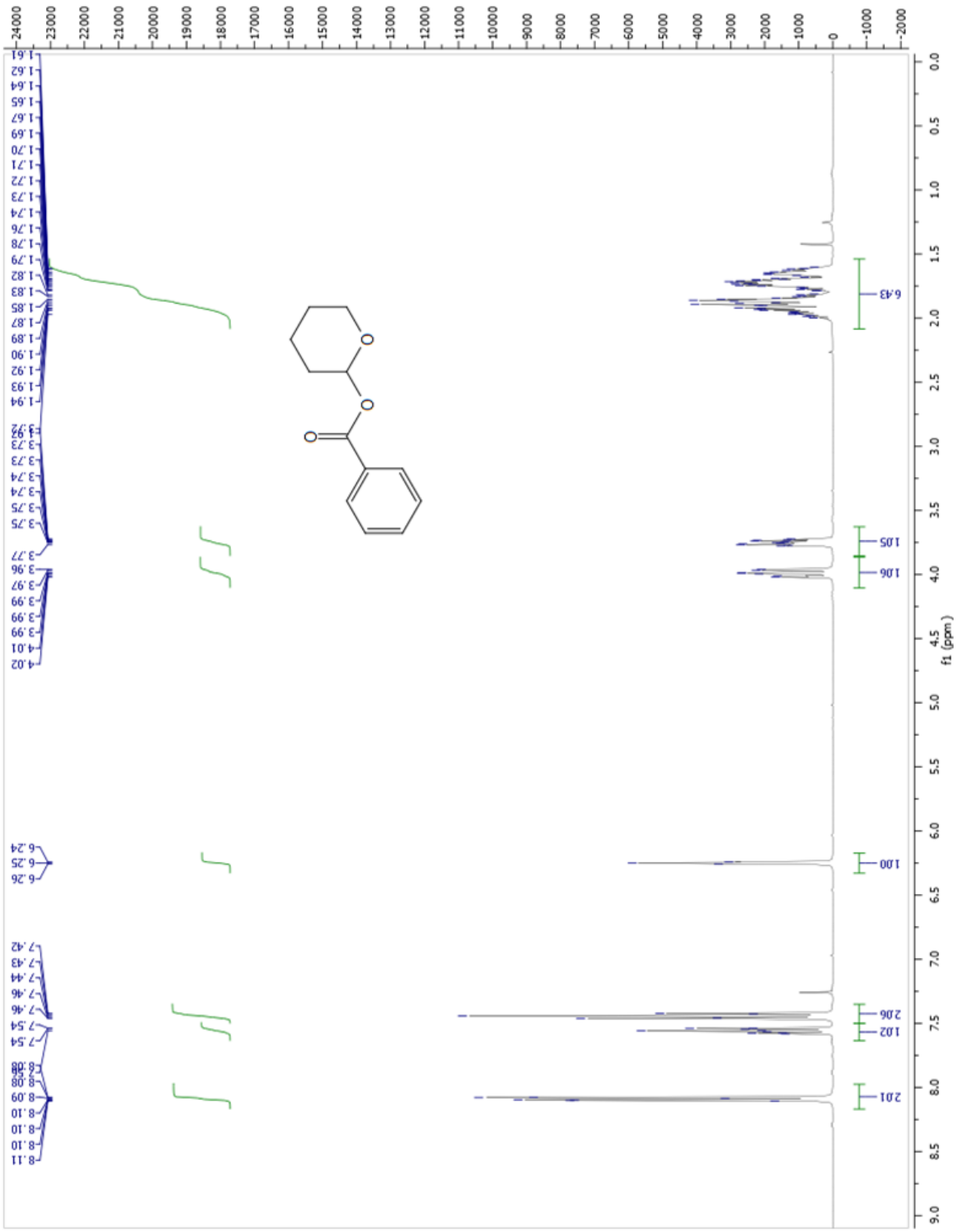
f1 (ppm)
6.43
1.05
1.06
1.00
2.06
1.02
2.01


18.50
24.93
29.18
63.07
76.68 CDCl3
77.00 CDCl3
77.32 CDCl3
93.01
128.28
129.62
130.23
133.00
165.03
f1 (ppm)

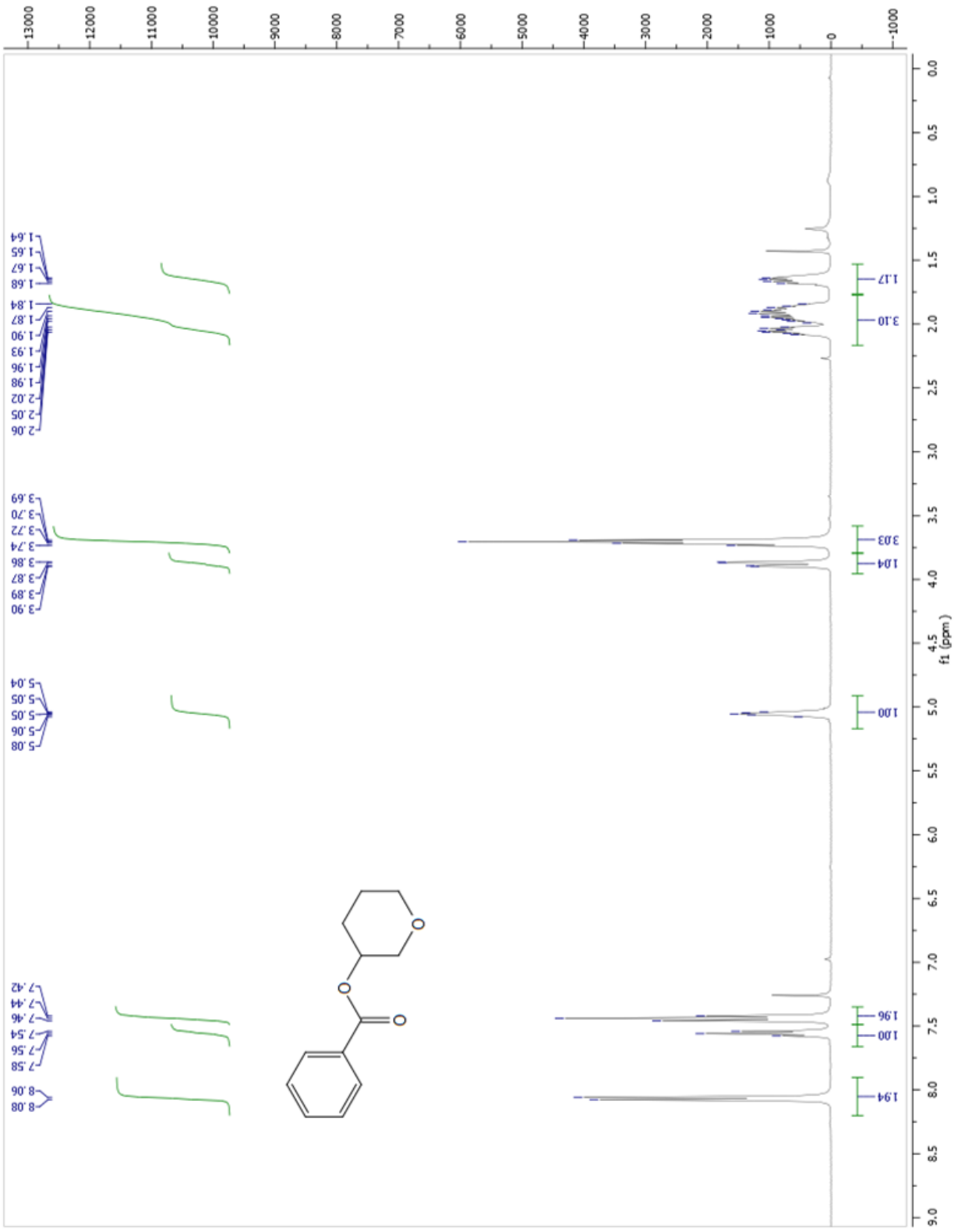
f1 (ppm)

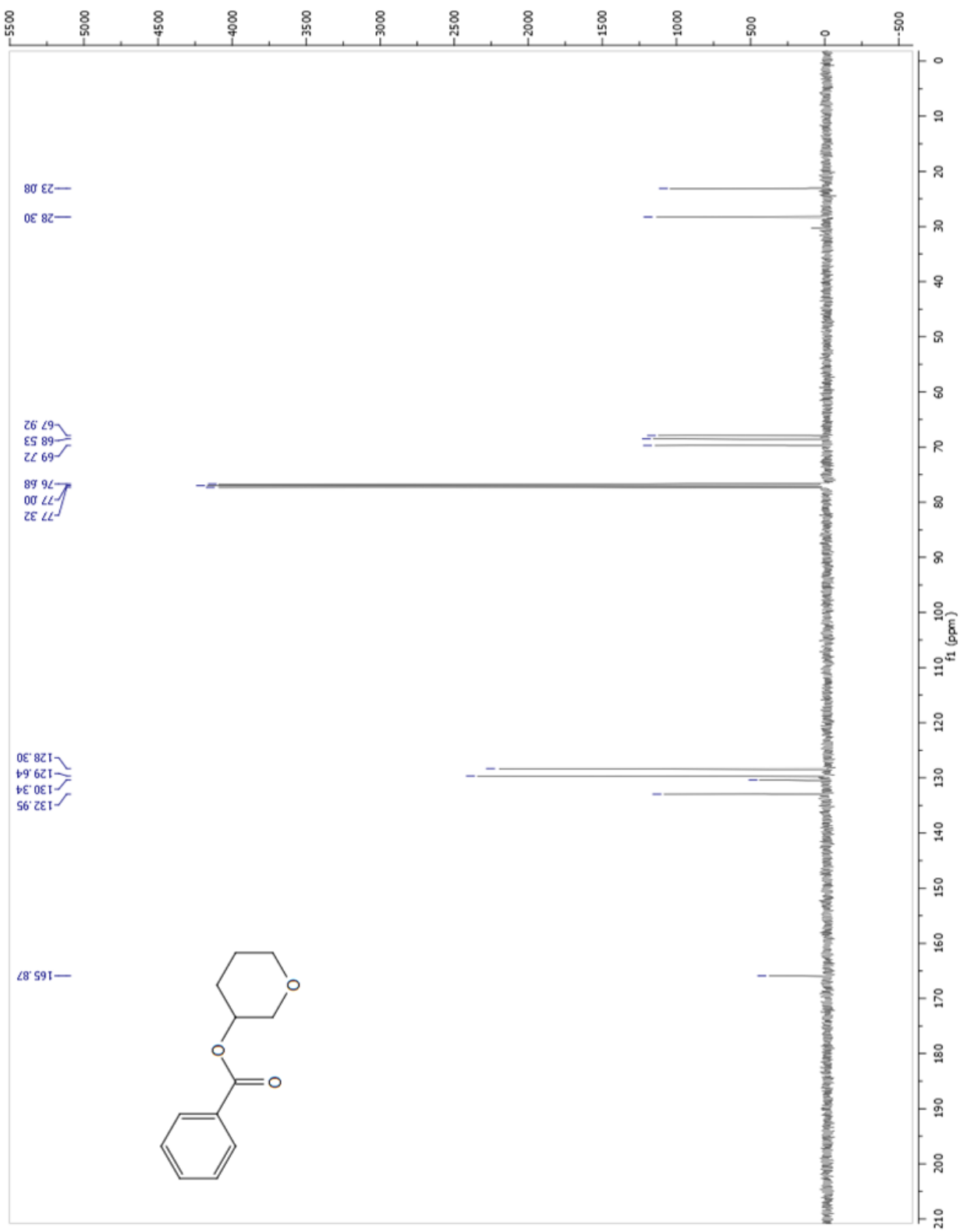
23.08
28.30
67.92
68.53
69.72
76.68
77.00
77.32
128.30
129.64
130.34
132.95
165.87
f1 (ppm)

# CHAPTER 4. INVESTIGATION INTO THE MECHANISM OF THE POLYMERIZATION OF 4-METHOXYSTYRENE INITIATED BY PYRYLIUM SALTS UNDER VISIBLE LIGHT IRRADIATION

## 4.1. Dimerization of Styrenyl Substrates via Alkene Cation Radicals Generated via PET

In 2013, Riener and Nicewicz reported the [2+2] dimerization of electron rich styrenyl alkenes to form substituted cyclobutanes catalyzed by 2,4,6-tri(4-methoxyphenyl)pyrylium tetrafluoroborate (**1**) under visible light irradiation.[86] The authors' studies took inspiration from seminal work reported by Bauld and Johnston into the alkene cation radical [2+2] dimerization of oxidizable styrenes.[87,88] Riener and Nicewicz reported the homodimerization of a number of electron rich terminal styrenes, such as 4-methoxystyrene **3** to form cyclobutane **4**, and $\beta$-substituted styrenes such as *p*-anethole **9** to form cyclobutane **10** (Figure 4.1). Demonstrating the utility of this method, the authors reported the synthesis of two natural products of the lignan family. Magnosalin was synthesized in one step in a 50% yield from *E*-asarone (**12**), and endiandrin A was synthesized in a 59% yield over three steps starting from **10**, the corresponding cyclobutane dimer of **9.**

Initially, cycloreversion via the corresponding cyclobutane cation radical was a major unproductive pathway reducing yields of $\beta$-substituted styrenyl alkene dimers, while polymerization reduced yields of the desired dimers in the case of terminal styrenyl alkenes. The key to maintenance of the desired reactivity and minimization of unproductive side reactions proved to be the inclusion of an additive to act as an electron relay between the photosensitizer **1** and the oxidizable alkene. Electron relays (such as anthracene **5**, naphthalene **11**, or

diethylaniline **8**) were chosen for particular substrates based on their oxidation potentials. As a lower limit, the electron relay required an oxidation potential higher than that of the styrenyl alkene to generate the corresponding alkene cation radical for successful dimerization. As an upper limit, the electron relay required an oxidation potential lower than the cyclobutane product to prevent generation of the cyclobutane cation radical. Thus, properly chosen, an electron relay of appropriate oxidation potential would permit the oxidation of the styrene substrate (either directly by the excited state of **1**, or by the cation radical of the electron relay), while inhibiting oxidation of the dimeric products and minimizing deleterious side reactions.

The proposed mechanism for the transformation, and the role of the electron relay, begins with excitation of **1** by a photon of light to generate **1***. Single electron transfer (SET) can then occur between **1*** and **5** (direct oxidation of substrate **14** by **1*** is also possible) to generate the cation radical **13** and the pyranyl radical **12**. A second SET from **14** to **13** generates the alkene cation radical **15**, and regenerates the electron relay **5**. The alkene cation radical **15** undergoes [2+2] dimerization with another equivalent of **14** to form the cyclobutane cation radical **16**. Finally, **16** can oxidize any one of **12**, **5**, or **14** to form the neutral cyclobutane dimer product **17** in addition to **1**, **13**, or **15**, respectively.

The observation of polymerization in the course of these studies generated interest within the Nicewicz and You research groups, and was the impetus for further investigation into the potential for pyrylium salts to initiate photopolymerization. The work discussed herein was carried out in collaboration with the laboratory of Professor Wei You.

**Figure 4.1. Riener and Nicewicz, [2+2] Dimerization of Styrenyl Alkenes via PET**

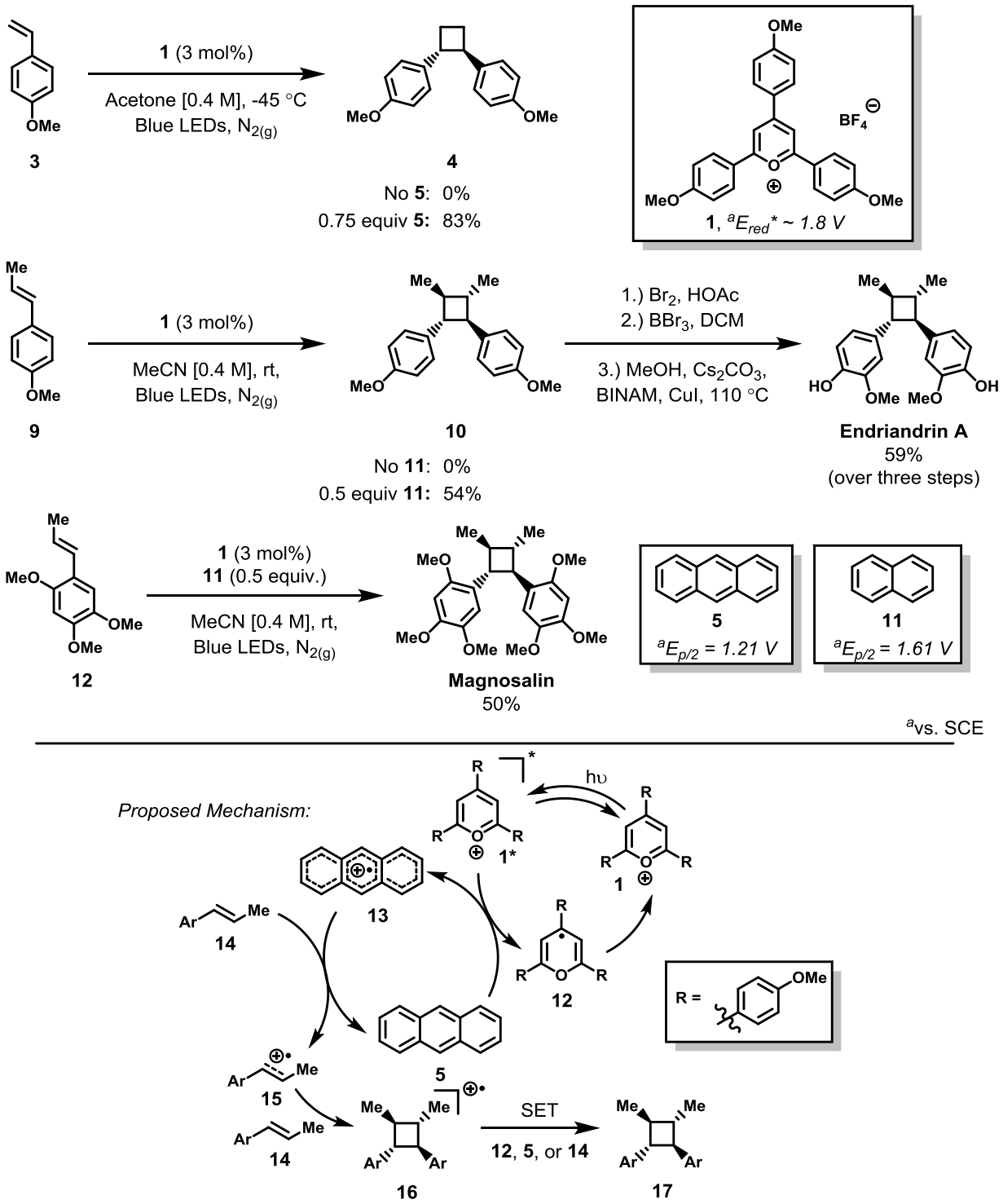

### 4.2. Photoinitiated Polymerization using Organic Salts

Reports of polymerizations using pyrylium salts as photoinitiators or additives are sparse. The use of pyrylium salts as an additive in the solid state polymerization of styrenyl monomers was disclosed by M. J. Rooney.[89] In this publication, 2,4,6-triphenylpyrylium hexafluoroantinomate was employed as an additive in the polymerization of 2-methoxy-4-benzyloxy-styrene in the solid phase using irradiation with ultra-violet (UV) light. While polymerization of the monomer occurred upon UV irradiation with or without added 2,4,6-triphenylpyrylium hexafluoroantinomate, a larger proportion of low molecular weight material was detected by GPC analysis in photopolymerizations incorporating the pyrylium salt.

Nevertheless, the use of other types of organic salts as photoinitiators for polymerization has garnered great interest in both academe and industry.[90–95] The earliest reports were those of Schlessinger who used aryldiazonium salts to initiate the photopolymerization of epoxide monomers under UV irradiation in 1974.[96] Interest in aryldiazonium salt photoinitiators has been limited, likely due to challenges related to their thermal instability. The much more stable diaryliodonium and triarylsulfonium salts are among the most well studied and commonly employed organic salt photoinitiators. Phenacyl onium, pyridinium, and phosphonium salts have also been studied and successfully used as photoinitators.

Onium salts are particularly useful as they initiate cationic polymerization upon UV irradiation. This has two potential advantages in comparison to radical photopolymerization systems which have been studied and employed for nearly a century. First, monomers that do not undergo radical polymerization efficiently (such as epoxides and vinyl ethers) can be employed. This can be an advantage if "shrinkage" of the material is a concern, as monomers such as epoxides can be employed which exhibit a lower loss of volume over the course of

polymerization than, for example, styrenes. Second, and arguably of greater importance, cationic polymerization is insensitive to oxygen, allowing for a wider range of applications under less stringent conditions. Onium salt photopolymerization systems are widely used in products and processes such as coatings, inks used in printers, adhesives, photocurable composites, and many further applications.

Generic structures of diarlyliodonium and triarylsulfonium salts are depicted below in Figure 4.2. The identities of the aryl moieties have a large impact on the wavelength of light

**Figure 4.2. Diaryliodonium and Triarylsulfonium Generic Structures**

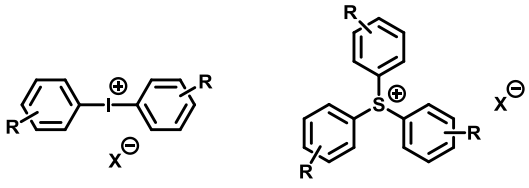


x = $BF_4$, $PF_6$, $SbF_6$, $(C_6F_5)_4B$

absorbed, the extinction coefficient, and the quantum yield of decomposition. Diaryliodonium and triarylsulfonium salts incorporating electron rich and/or polyaromatic aryl groups have even been synthesized which have appreciable absorption within the visible spectrum. The identity of the counter anion has a significant impact on the course of the polymerization. The most straightforward syntheses of diaryliodonium and triarylsulfonium salts generally provide the halide salts, which need to be converted via alkali salt metathesis (e.g. sodium tetrafluoroborate, potassium hexafluorophopshate) to the salts containing non-coordinating anions. Non-coordinating anions (e.g. tetrafluoroborate, hexafluorophosphate, hexafluoroantinomate, tetrakis(pentafluorophenyl)borate) are necessary for efficient polymerizations as they allow for propagation of the cationic center. Coordinating anions (e.g. halides) dramatically reduce the rate of polymerization or suppress it completely.

Studies indicate that onium salts decompose upon irradiation through a process composing two simultaneous and related pathways, both ultimately leading to generation of a strong acid which serves as an initiator.[93,97,98] A summary is depicted below in figure 4.3 with diphenyliodonium tetrafluoroborate (**18**) as an exemplar. The process begins with absorption of a

**Figure 4.3. Photochemical Decomposition of Diphenyliodonium Tetrafluoroborate**

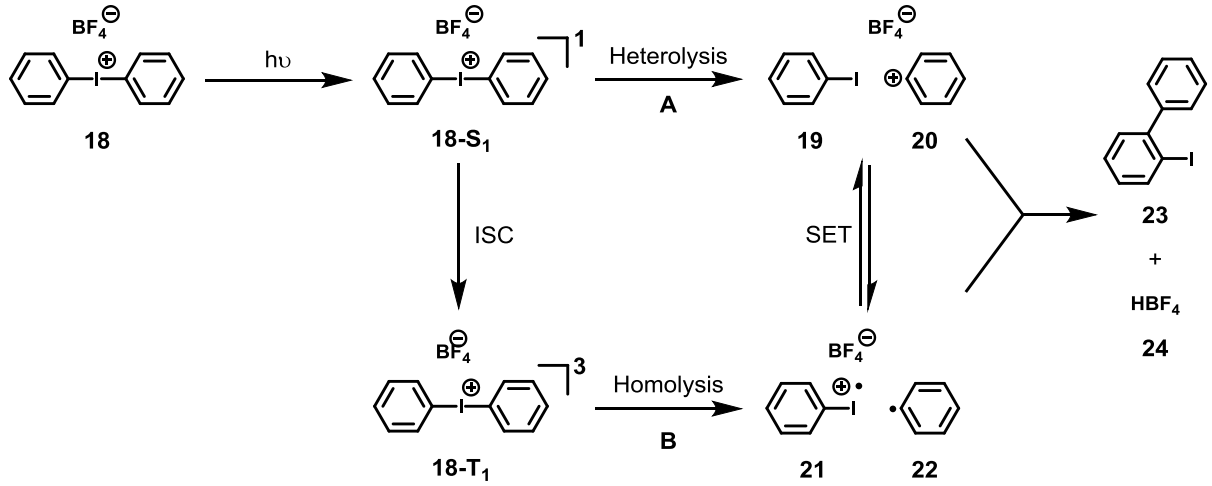


photon of light of appropriate wavelength to generate a singlet excited state, **18-$S_1$**. Heterolytic cleavage (**A**) can occur from this single state to give iodobenzene (**19**) and phenyl cation (**20**). The excited state species **18-$S_1$** can undergoes intersystem crossing (ISC) to give **18-$T_1$**, and homolytic cleavage then occurs (**B**) to give iodobenzene cation radical **21** and phenyl radical **22**. These pathways may interconvert at this point via SET as calculations suggest neither is appreciably more thermodynamically favorable than the other. Recombination of **19** with **20** in pathway **A**, or **21** with **22** in pathway **B**, generates 2-iodo-1,1'-biphenyl **23**, predominantly, and an equivalent of strong Brønsted acid (**24**). Given the very high energy species generated, aspects of initiation in particular polymerization systems are likely influenced by solvent, monomer, and other additives. As pyrylium salts, such as **1**, are not known to decompose in the same fashion as

onium salts, any photopolymerization initiated by pyrylium salts would likely proceed through a different initiation mechanism.

### 4.3. Investigations into the Polymerization of 4-Methoxystyrene Using Pyrylium Salts

Triarylpyrylium salts possess a number of properties which make them particularly appealing for PET applications.[99] They exhibit strong absorption within the visible spectrum ($\lambda_{max}$ = 410 to 450 nm depending on the nature of the substitution on the aryl rings.), and are powerful oxidants in their excited state. The pyranyl radicals generated by PET from a donor species are generally stable, do not undergo fragmentation or other potentially deleterious side reactions, and do not react appreciably with molecular oxygen, though they have been observed to dimerize at low temperatures. They are bench stable salts, are relatively simple to synthesize, can be stored essentially indefinitely, and possess good solubility in a range of polar organic solvents.[100]

To begin investigations into these polymerizations, 2,4,6-tri(*p*-tolyl)pyrylium tetrafluoroborate (**25**) was chosen as an initiator. The pyrylium **25** was more suitable than **1** for these studies as it proved easier to purify by repeated recrystallization from acetic acid. The pyrylium **25** was synthesized by reported literature methods, and dried under vacuum at 70 °C for several days to remove all traces of acetic acid after recrystallization. Investigations into polymerizations initiated by 2,4,6-tri(*p*-tolyl)pyrylium tetrafluoroborate (**25**) were begun using 4-methoxystyrene (**3**) as monomer, as PET from **3** ($E_{1/2}^{OX}$ = 1.49 V) to **25** ($E_{Red}$* ~ 2.3 V) is exergonic (Figure 4.4).[99,101]

**Figure 4.4. Electrochemical Properties of Interest: 4-Methoxystyrene and 2,4,6-Tri(*p*-tolyl)pyrylium Tetrafluoroborate**

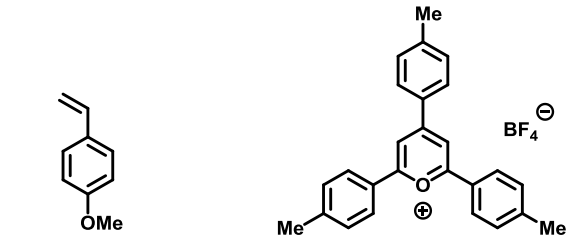


**3** $^{a}E_{1/2}^{ox}$ = 1.49 V

**25** $^{a}E_{red}$* ~ 2.3 V

[a]vs. SCE

Initial attempts at polymerization of **3** using **25** in dichloromethane, using blue LEDs as the irradiation light source, met with success (Figure 4.5). High molecular weight (MW) poly(4-methoxystyrene) was obtained as measured by gel permeation chromatography (GPC), calibrated by reference to polystyrene standards, with a polydispersity index (PDI) around 2. The polymerizations are complete within 5 minutes of irradiation. Polymerization was found to continue even without continuous irradiation, albeit at an apparently slower rate (entries 4 and 5).

**Figure 4.5. Polymerization of 4-Methoxystyrene Using 2,4,6-Tri(*p*-tolyl)pyrylium Salt**

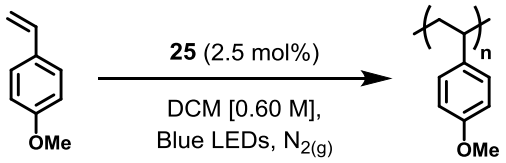


| Entry | Irradiation Time (min) | [a]$M_n$ | [a]$M_w$ | PDI | Entry | Irradiation Time (min) | [a]$M_n$ | [a]$M_w$ | PDI | [b]Conv. (%) |
|---|---|---|---|---|---|---|---|---|---|---|
| 1 | 5 | 140000 | 299000 | 2.13 | 4 | [c]1 | 134000 | 239000 | 1.78 | 23 |
| 2 | 5 | 149000 | 308000 | 2.07 | 5 | [d]1 | 292000 | 445000 | 1.52 | >95 |
| 3 | 5 | 152000 | 300000 | 1.98 | | | | | | |

[a]Daltons, relative to polystyrene standard
[b]Based on $^{1}$H NMR internal standard
[c]1 min. irradiation then quench
[d]1 min. iradiation then 59 min dark

### 4.4. Probing the Dominant Propagation Mode of Polymerization Initiated by Pyrylium Salt

Photopolymerization of 4-methoxystyrene initiated by **25** would likely begin with PET from **3** to **25** generating an alkene cation radical. Such styrenyl alkene cation radicals undergo rapid dimerization to give the corresponding cyclobutane cation radical. To a first approximation, polymerization could then conceivably occur by either radical or cationic propagation, or possibly a mixture of the two propagation modes. Additionally, radical polymerization could potentially be initiated by the pyranyl radical generated by PET from **3** to **25**.

To investigate the propagation mode of this polymerization, a series of additives were chosen as "probes" of either radical propagation or cationic propagation (Figure 4.6). If the

**Figure 4.6. Results of Polymerizations in the Presence of Radical or Cation Probes**

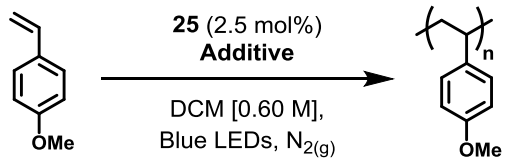


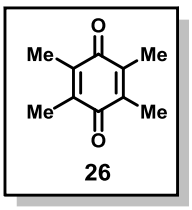


**26**

| Entry | Additive (mol%) | [a]$M_n$ | [a]$M_w$ | PDI | [b]Conv. (%) |
|---|---|---|---|---|---|
| 1 | [c]None | 129000 | 289000 | 2.24 | >95 |
| 2 | **26 (2.5)** | 22600 | 48600 | 2.15 | 87 |
| 3 | **27 (2.5)** | - | - | - | 9 |
| 4 | [d]**25-Chloride (2.5)** | - | - | - | 11 |
| 5 | [d,e]**25-Chloride (2.5)** | - | - | - | 44 |
| 6 | **$CH_3OH$ (6.5)** | 7510 | 8590 | 1.14 | >95 |

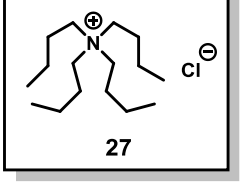


**27**

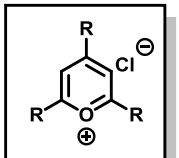


**25-Chloride**

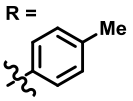


[a]Daltons, relative to polystyrene standard
[b]Based on $^1$H NMR internal standard
[c]5 min. irradiation, [d]in place of **25**, [e]4.5 hrs irradiation

polymerization were predominantly radical in nature then duroquinone (**26**), which reacts with carbon-centered radicals via addition to a $\pi_{C\text{-}O}$ orbital to generate a stable oxygen-centered radical,[102] should inhibit polymerization. If the polymerization were predominantly cationic in nature then tetrabutylammonium chloride (**27**) should inhibit polymerization via nucleophilic addition of chloride to the propagating cation. Duroquinone (**26**) showed some impact on the terminal MW of the poly(4-methoxystyrene), but did not suppress polymerization. Irradiation of a reaction with added **27** resulted in no isolatable polymer. Similarly, if chloride anion was introduced as the counter anion of the pyrylium (**25-Chloride**), polymerization was not observed. To verify that oxidation of **3** was still occurring, a reaction employing **25-Chloride** was submitted to prolonged irradiated (4.5 hours) resulting in a 44% conversion of **3** giving only cyclobutane **4** in 24% yield ($^1$H NMR) and oligomeric species.

The most intriguing results were observed when methanol was included in the reaction. In the presence of 6.5 mol% methanol (relative to **3**), the terminal MW of poly(4-methoxystyrene) was markedly lower with a narrower than expected range of polymer MWs indicated by the relatively low PDI of 1.14. Given the complete suppression of polymerization in the presence of chloride, and the marked attenuation in the presence of methanol, versus the more minor impact of **26**, the polymerization was tentatively concluded to be cationic.

### 4.5. The Effects of Methanol on the Polymerization of 4-Methoxystyrene

To further explore the impact of added methanol on the resulting polymer, a range of methanol loadings were investigated, from 1.6 mol% to 52 mol% of methanol relative to **3**. The data is summarized below in Figure 4.7. Methanol influences both the MW and the PDI of the resulting polymers. While the PDI has a relatively small variance over the range of methanol

loading (1.18 ± 0.06) the weight average MW ($M_w$) and the number average MW ($M_n$) decreases as a function of methanol loading. This was a rather curious result, as the theoretical lower limit for the terminal MW of a given polymerization can be calculated, to a first approximation, by multiplying the ratio of monomer to initiator by the MW of the monomer. From this simple calculation, the theoretical lower MW limit for poly(4-methoxystyrene) is 5520 Daltons. One potential explanation for this behavior is that at high concentrations methanol may behave as a chain transfer agent. Unfortunately, complete isolation of all polymer precipitate from residual **25** was not successful, foiling attempts to calculate accurate mass recovery, though all reactions

**Figure 4.7. Effect of Methanol Loading on $M_w$, $M_n$, and PDI**

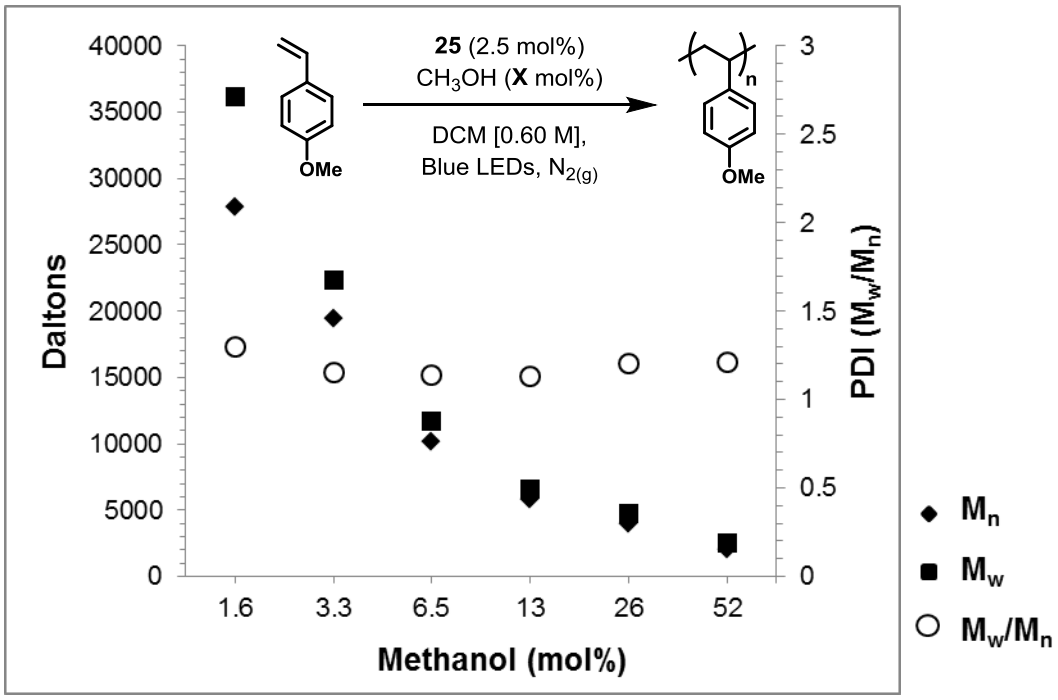


achieved complete conversion of monomer based on $^1$H NMR analysis using an internal standard. Polymerizations with added methanol up to 13 mol% were complete within the 25 min standard reaction time employed, while greater methanol loadings required extended reaction times to achieve complete conversion of **3**. With 26 mol% methanol added the polymerization

was complete within 50 min, and 2 hrs with 54 mol% methanol, (all conversions are based on $^1$H NMR analysis of crude reactions using hexamethyldisiloxane as an internal standard). The crude reaction mixtures where elevated methanol loadings were employed (> 26 mol%) exhibited elevated yields of the [2+2] cyclobutane dimer (between 10 and 5%), while those with lower methanol loadings (< 26 mol%) were accompanied by low yields of the dimer (< 5%).

Given that low MW material could be prepared under conditions of high methanol loading, end group analysis by $^1$H NMR was possible. Poly(4-methoxystyrene) with low PDI incorporating a methoxy end group has been prepared previously via a different system and has been characterized by $^1$H NMR.[103] If the polymerization proceeds via a cationic mode, then methanol should be incorporated into the chain end of the polymer. Such incorporation may also suggest that methanol is influencing the course of the polymerization by nucleophilic interaction with the propagating cationic center. To distinguish between methanol incorporated over the course of the reaction and methanol incorporated from precipitation of the polymer, two experiments were carried out. The first experiment (Figure 4.8, a.) employed the standard polymerization conditions with a methanol loading of 52 mol%. The second experiment (Figure 4.8, b.) employed identical conditions, but used methanol-$d_3$ ($CD_3OH$). A chemical shift corresponding to a methoxy group derived from the methanol added to the reaction should be observed in the $^1$H NMR of the polymer from the first reaction, but not in the second. A methoxy group detected in both experiments would suggest that the group was incorporated when the polymer was precipitated from methanol. In addition, if no methoxy end group was observed in either case, then the preliminary assignment of the polymerization as cationic would be in doubt, and would require reevaluation.

The polymer resulting from each experiment was twice precipitated from methanol at -78 °C, and gravity filtered over packed cotton. Analysis by GPC indicated low MW material with relatively narrow PDI (1.19). Analysis by $^{1}$H NMR indicated that the methanol in the reaction was incorporated as an end group (**A**, Figure 4.8 a. versus **A** in Figure 4.8 b). A broad peak near 1.0 ppm (**B**, Figure 4.8 a. and b.) was also identified as a methyl end group base on

**Figure 4.8. Poly(4-methoxystyrene) Deuterium Labeling Study and End Group Analysis**

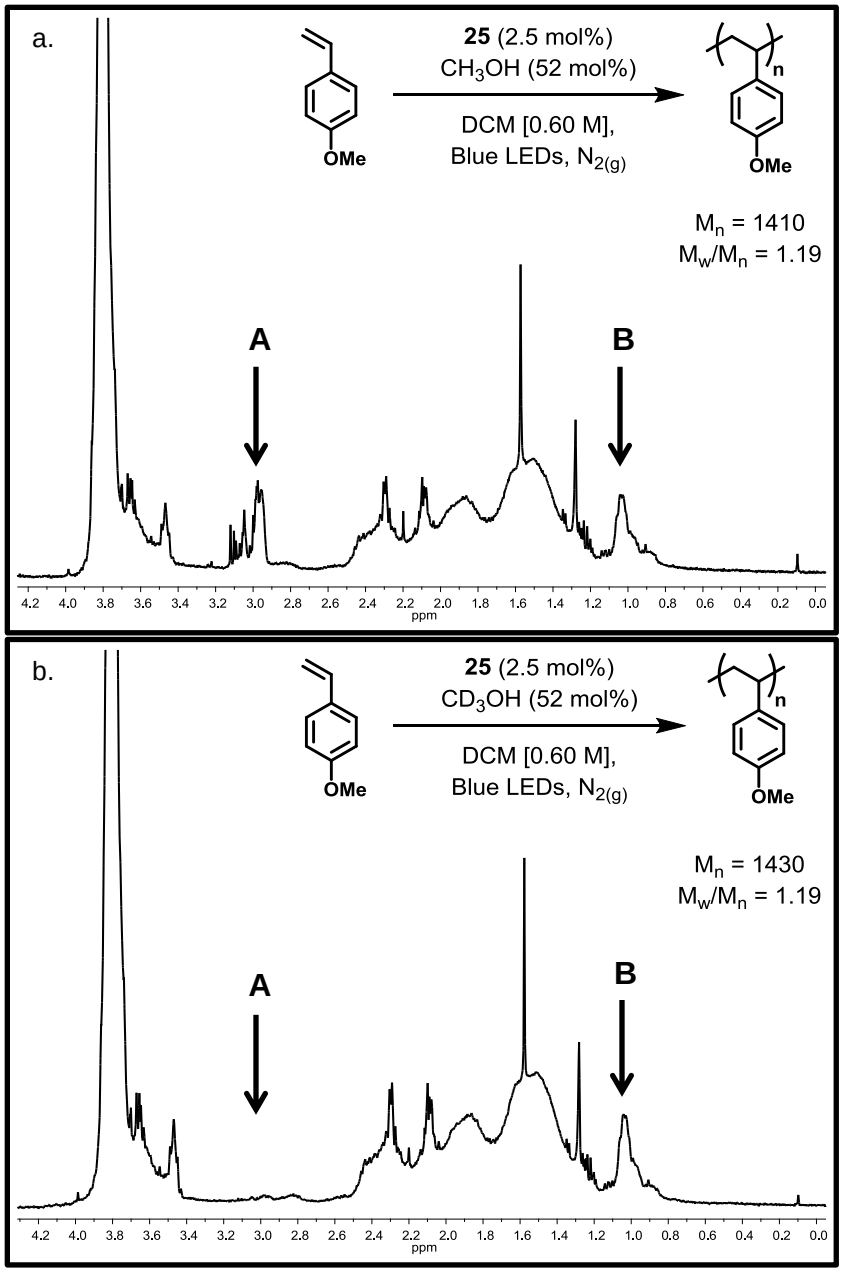

comparison with spectra reported in the literature. This indicated that under the polymerization conditions employed, the polymer chains were initiated by protonation of **3**.

### 4.6. The Influence of Other Alcohols on Pyrylium Initiated Polymerization of 4-Methoxystyrene

Accumulated evidence suggested that the polymerization under question is cationic, and that methanol influences the polymerization via a nucleophilic interaction. If this picture were accurate, then the MW and PDI should be influenced by the nucleophilicity of the alcohol additive. A series of alcohols with increasing steric encumbrance near the hydroxyl functional group (e.g. ethanol, 2-propanol, 2-methyl-2-propanol) should exhibit a diminishing influence over the polymerization, and MW and PDI should increasingly tend towards the MW and PDI achieved in the absence of any additives. Experiments substituting these alcohols for methanol were carried out (Figure 4.9). Additionally trifluoroethanol was included in the series as it is sterically similar to ethanol but considerably less nucleophilic. Diethyl ether was also included in

**Figure 4.9. Influence of Various Additives on Molecular Weight and PDI**

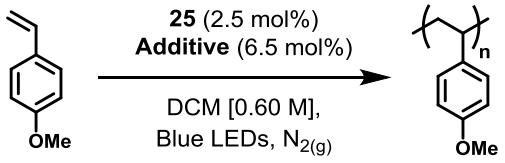


| Entry | Additive | [a]$M_n$ | [a]$M_w$ | PDI | Entry | Additive | [a]$M_n$ | [a]$M_w$ | PDI |
|---|---|---|---|---|---|---|---|---|---|
| 1 | None | 135000 | 309000 | 2.53 | 5 | 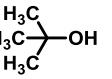 | 37500 | 63000 | 1.68 |
| 2 | $CH_3OH$ | 7090 | 8350 | 1.18 | 6 | $CF_3CH_2OH$ | 65900 | 141000 | 2.14 |
| 3 | $CH_3CH_2OH$ | 8730 | 10700 | 1.22 | 7 | $(CH_3CH_2)_2O$ | 36600 | 80600 | 2.20 |
| 4 | 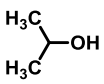 | 15100 | 19200 | 1.27 | 8 | [b]$H_2O$ | 114000 | 191000 | 1.67 |

[a]Daltons, relative to polystyrene standard
[b]immiscible under reaction conditions

the series. As the nucleophilicity of the additive becomes attenuated relative to methanol (for reasons of sterics or electronics), MW and PDI generally increases. This evidence is in agreement with a model that suggests methanol interacts with a propagating cationic center in a nucleophilic fashion to influence the MW and PDI.

### 4.7. The Effects of Pyrylium Salt Initiator on the Polymerization of 4-Methoxystyrene

Given the results detailed above, effects of varying the pyrylium salt initiator **25** were of interest for further study. Under the standard conditions with 6.5 mol% methanol, the loading of initiator **25** was varied between 0.13 to 2.5 mol% relative to **3** (Figure 4.10). From 0.5 mol% **25** and below, MW increases as the loading of **25** decreases which fits the current picture of a cationic polymerization. Less initiator yields fewer propagating chains, allowing each

**Figure 4.10. Effect of 2,4,6-Tri(*p*-tolyl)pyrylium Loading on $M_w$, $M_n$, and PDI**

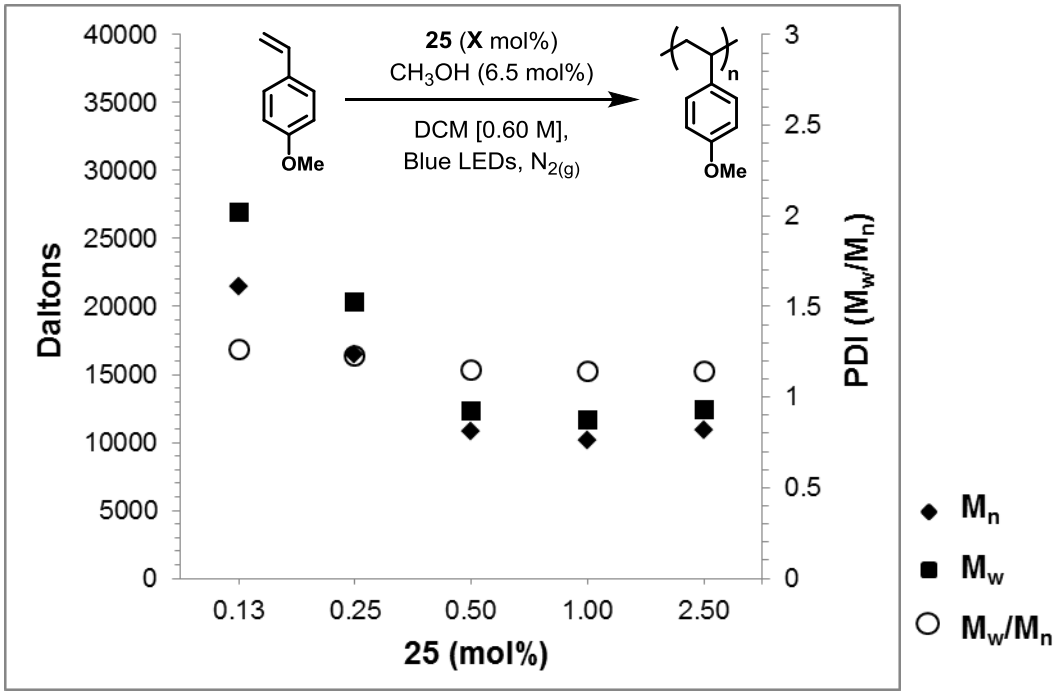


propagating chain to incorporate more monomer. Beginning at 0.5 mol% and moving to higher loadings, however, the terminal MW plateaus. The cause of this behavior has not yet been

determined and is still under investigation. To a first approximation, it appears that above 0.5 mol% **25**, no additional polymer chains are being initiated. The plateau may reflect the limits of irradiation intensity with the current setup. Beginning at or around 0.5 mol% **25**, the pyrylium chromophores may be absorbing as many photons as is possible given the light source being used. Studies examining MW and PDI as a function of mol% **25** in the absence of methanol, as well as studies varying irradiation intensity at a particular loading of **25** are planned for the near future to provide further elucidation.

To determine if the structure of the pyrylium salt photoinitiator has an effect on the terminal MW and PDI of the poly(4-methoxystyrene) produced, two structural isomers of **25** were prepared and tested under the standard conditions (Figure 4.11). While the excited state

**Figure 4.11. Effects of Pyrylium Structure on Polymerization of 4-Methoxystyrene**

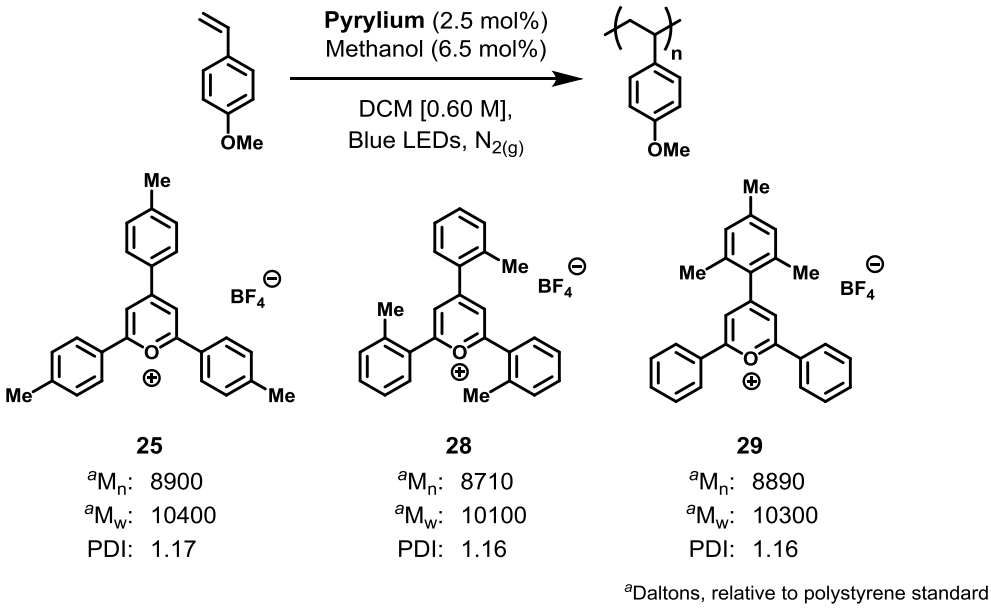


reduction potentials of 2,4,6-tri(*o*-tolyl)pyrylium tetrafluoroborate (**28**), and 2,6-diphenyl-4-mesitylpyrylium tetrafluoroborate (**29**) are not known, they should vary minimally from **25**, and be sufficient for the oxidation of **3**. These structures were chosen primarily for the variation in the steric environment near the pyrylium core. If the pyrylium cation, or its reduced form the

pyryanyl radical, had an impact on the course of the polymerization beyond initiation, differences in the MW and PDI of the poly(4-methoxystyrene) produced using **25**, **28**, or **29** should be detectable. Overall, the properties of the resulting poly(4-methoxystyrene) essentially do not vary with relation to the structure the pyrylium salts tested. The pyrylium cation, or related reduced species, likely do not play a role in the course of the polymerization beyond initiation under the conditions studied. These experiments do not rule out the possibility that more substantial structural and electronic changes may yield more interesting results.

### 4.8. Current Mechanistic Proposal for the Polymerization of 4-Methoxystyrene using 2,4,6-Tri(*p*-tolyl)pyrylium Tetrafluoroborate

The detection of a methyl end group by $^{1}$H NMR suggests that pyrylium **25** is ultimately generating an equivalent of strong acid. Studies of 4-methoxystyrene cation radical dimerization carried out by Schepp and Johnston (Figure 4.12) provide potential elucidation.[88] Using

**Figure 4.12. Cation Radical Mediated Dimerization of 4-Methoxystyrene**

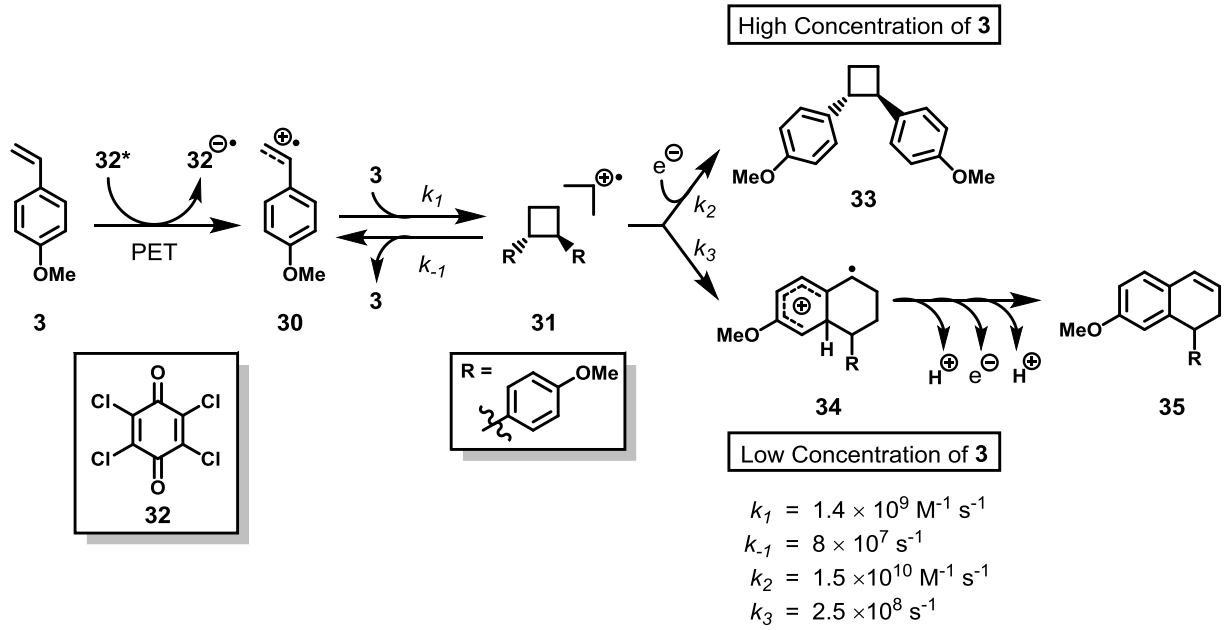

nanosecond and picosecond transient absorption spectroscopy the authors observed the reaction between **3** and the 4-methoxystyrene cation radical **30**, generated via PET to chloranil (**32**), in acetonitrile. They supplemented these studies with analysis of the resulting product mixtures

While **30** possessed too short a lifetime to be observed, the transient formation of the 1,2-bis(4-methoxyphenyl)cyclobutane cation radical **31** was observed in all cases. The subsequent fate of **31** varied depending on the concentration of **3**. Two dimeric products were isolated from the reactions: the [2+2] cyclization product *trans*-1,2-bis(4-methoxyphenyl)cyclobutane (**33**), and a product derived from rearrangement of **31** (likely via **34**), followed by the net loss of two protons and an additional electron, 7-methoxy-1-(4-methoxyphenyl)-1,2-dihydronaphthalene (**35**). The ratio of **33** to **35** depended upon the initial concentration of **3**. Higher initial concentrations of **3** corresponded to greater proportions of **33** over **35**, until **33** was the exclusive product at concentrations of 0.5 M or more. Concentrations below 0.02 M lead to the exclusive formation of **35**.

Based on these studies, initiation likely occurs from the strong acid generated in the course of the transformation of **31** to **35** in the photopolymerization of **3** using pyrylium salts. Attempts to isolate any **35** potentially formed from the reaction mixtures after polymerization are currently underway. Additionally, experiments making use of *in situ* IR monitoring to follow the consumption of **3** over the course of the polymerization to further elucidate the mechanism of initiation are planned.

The accumulated evidence suggests that the photopolymerization of **3** initiated by **25** propagates via a cationic mode. This conclusion is based on the suppression of polymerization in the presence of chloride, the identification of methanol incorporation as an end group by $^{1}H$ NMR analysis, and the strong effects of alcohol additives on the MW and PDI of resulting

poly(4-methoxystyrene). This evidence, particularly the trends in MW and PDI observed in the alcohol series, suggests that methanol influences the course of the polymerization in a nucleophilic fashion. This leads to the proposed mechanism depicted below in Figure 4.13. The process of initiation begins with the oxidation of 4-methoxystyrene (**3**) vie PET to 2,4,6-tri(*p*-tolyl)pyrylium tetrafluoroborate (**25**) to form the 4-methoxystyrene cation radical **30**. Reaction of **30** with another equivalent of **3** forms the cyclobutane cation radical **31**. This species rearranges to **34** followed by net loss of another electron and two protons generating **35**. Protonation of **3** by the strong acid generated in the formation of **35** then initiates cationic polymerization. Methanol then likely influences the course of polymerization via reversible addition (**37**) to the propagating cationic center (**38**).

**Figure 4.13. Proposed Mechanism for Photopolymerization of 4-Methoxystyrene using Pyrylium Salts, Regulated by Methanol**

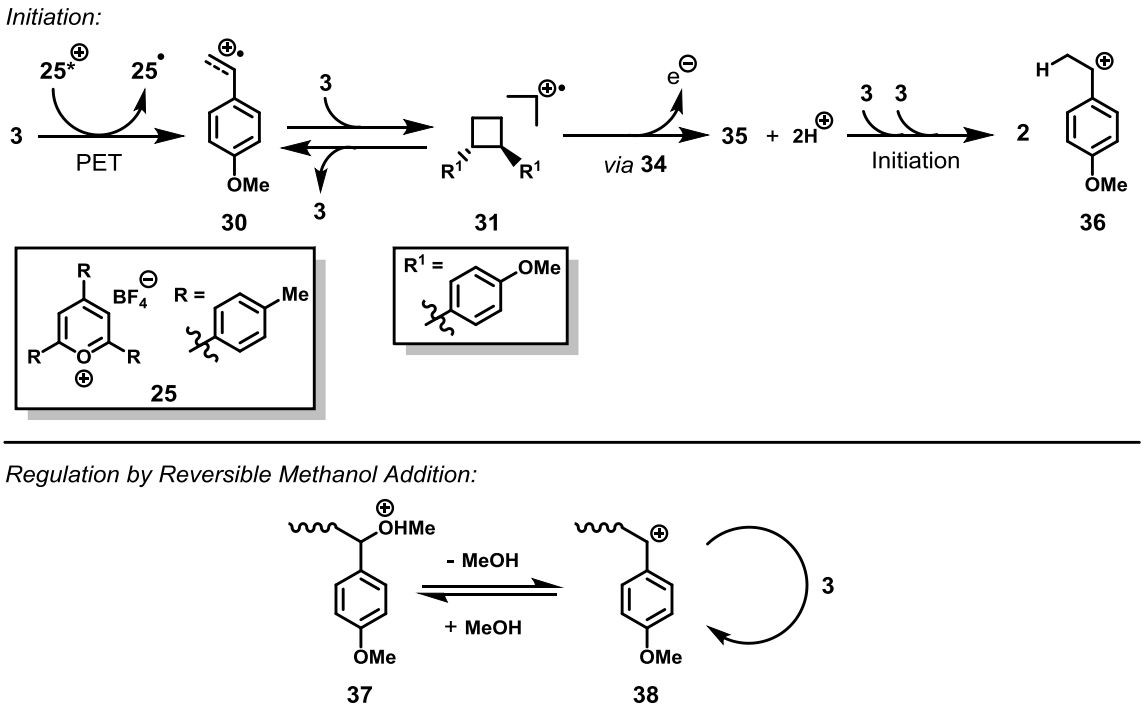


The influence that varying amounts of methanol exhibits over MW of the poly(4-methoxystyrene), particularly at high methanol loadings, may suggest that methanol also behaves

as a chain transfer agent via proton transfer. A potential mechanism for this process is depicted below in Figure 4.14. Excess methanol could potentially be protonated by **37** to generate the methoxy capped poly(4-methoxystyrene) chain **39**. Protonation of **39** would return to **37**, while protonation of another monomer **3** would initiate a new chain. Direct protonation of **3** by a species such as **37** could also be possible. If a chain transfer process such as that depicted in Figure 4.14 occurs, it would likely be more significant at higher methanol concentrations. Experiments using methanol-$d_4$ ($CD_3OD$) followed by subsequent $^1H$ NMR analysis of the

**Figure 4.14. Potential Chain Transfer via Protonation Mediated by Methanol**

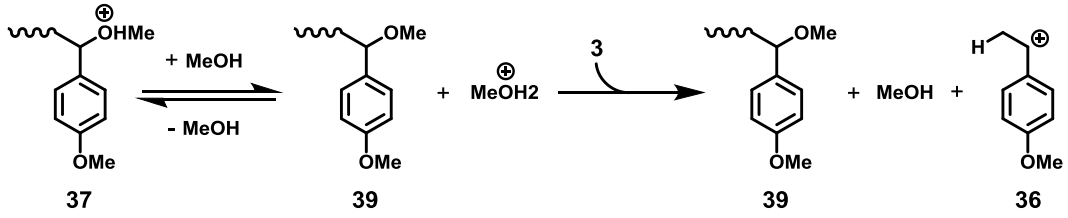


resulting poly(4-methoxystyrene) may shed light on whether this process is occurring. The transfer of additional monomer to a polymerization that has consumed all monomer is another means of investigating this picture. If the MW of the resulting polymer doubles then a chain transfer process such as this is likely not significant. If, however, poly(4-methoxystyrene) with a broad PDI is isolated, or poly(4-methoxystyrene) with a multimodal MW distribution is formed, then a chain transfer mechanism such as depicted in Figure 4.14 is plausible.

### 4.9. Attempts to Reproduce Methanol Effect in Non-Photoinitiated System

If the only role of pyrylium salt **25** is initiating cationic polymerization of **3**, then in principle any suitable cationic initiator under similar conditions in the presence of methanol ought to be capable of producing poly(4-methoxystyrene) with similar properties. In a simple sense, the propagating species in the above discussed polymerizations is a carbocation with an

accompanying tetrafluoroborate anion. Thus tetrafluoroboric acid diethyletherate (**40**) was chosen as a cationic initiator to attempt polymerization of **3** under non-photoinitiating conditions in the presence of methanol. The results of polymerizations of **3** using **40** are detailed below in Figure 4.15. If no methanol is included (entry 1), an insoluble gel is produced which separates from the reaction mixture. Presumably, this material is poly(4-methoxystyrene) containing a high degree of cross-linking due to Friedal-Crafts type electrophilic aromatic substitution reactions

**Figure 4.15. Polymerization of 4-Methoxystyrene using Tetrafluoroboric Acid**

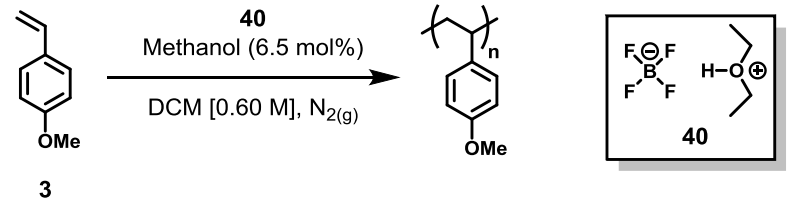


**3**

| Entry | mol% 40 | Temp. (°C) | $^{a}M_n$ | $^{a}M_w$ | PDI |
|---|---|---|---|---|---|
| [a]1 | 2.5 | ambient | - | - | - |
| 2 | 2.5 | ambient | 44300 | 62300 | 1.41 |
| 3 | 2.5 | ambient | 42100 | 84400 | 2.01 |
| 4 | 1.0 | ambient | 19600 | 24700 | 1.26 |
| 5 | 1.0 | ambient | 36800 | 76200 | 2.07 |
| 6 | 1.0 | 0 | 15300 | 23400 | 1.53 |
| 7 | 0.5 | 0 | 12900 | 16300 | 1.27 |
| [b]8 | 1.0 | -78 | - | - | - |

[a]no methanol, insoluble gel formed
[b]quenched with triethylamine after 25 min, no polymer formed

between the styrenyl side chains. The addition of 6.5 mol% methanol produced poly(4-methoxystyrene) of moderate MW (entries 2 and 3). One particular challenge presented by the extreme reactivity of **40** was the difficulty in reproducibility, apparent when comparing entries 2 and 3 or entries 4 and 5. In the case of entries 2 and 4, **40** was added neat via a 10 µL syringe directly into the dichloromethane solution containing methanol and **3** in a dry, inert glovebox. In

entries 3 and 5, **40** was diluted in 0.5 mL dichloromethane and transferred via cannula from one Schlenk flask to another Schlenk flask containing a 2.0 mL solution of **3** and methanol in dichloromethane under nitrogen pressure. Entries 6, 7, and 8 employed this latter method. Moving to lower loadings of **40** and 0 °C (entry 7) poly(4-methoxystyrene) with properties approaching those obtained using **25** under blue light irradiation was produced. Cryogenic temperatures (entry 8) lead to no detectable polymer formation. While **40** is a rather reactive and challenging reagent to work with, our results resembling those observed under the photoinitiation conditions provide some corroboration for the current picture of photopolymeriation of **3** using **25**. More controlled means of carrying out non-photoinitiated polymerizations of the type shown in Figure 4.15 are an area of active interest, particularly to disentangle any dual role methanol may play in the initiation and propagation processes of the photoinitiated polymerizations discussed.

### 4.10. Remaining Questions and Future Directions

Several questions remain to be answered about the photopolymerization of 4-methoxystyrene initiated by **25** in the presence of methanol. Many of these questions have already been mentioned in the sections above. More definitive evidence for the proposed initiation process will be sought. If formation of **35** is key to initiation, then the rate of initiation should exhibit dependence on the concentration of 4-methoxystyrene (see Figure 4.12 and accompanying discussion). Isolation of **35** after polymerization would also provide some evidence for the proposed initiation mechanism. Attempts will also be made to reproduce the influence of methanol on the cationic polymerization of 4-methoxystyrene under non-photoinitiated conditions. Unless methanol also exhibits a strong influence on the process of

initiation of polymerization by **25** (which is within the realm of possibility) similar results should be achievable.

The achievement of relatively narrow PDI by addition of methanol, along with preliminary (though not yet definitive) data suggesting a correlation between MW and monomer conversion, the possibility of a controlled polymerization under the studied conditions is possible, perhaps via a reversible activation-deactivation mechanism (as depicted in Figure 4.13). Very rapid consumption of the monomer under the studied conditions has made investigation of the kinetics of the polymerization challenging. Attempts to slow the polymerization by lower loadings of **25**, and more dilute conditions have so far been insufficient. Carrying out the polymerization at low temperatures (-20 to -10 °C) does slow the consumption of monomer, but also leads to the generation of significant amounts of the cyclobutane dimer **33** (>20%, $^{1}$H NMR). Preliminary data has suggested a correlation between poly(4-methoxystyrene) MW and monomer conversion ($^{1}$H NMR), but here also short reaction times have foiled attempts to quench the polymerization at predictable, reproducible conversions necessary for rigorous analysis. Further attempts will be made to slow the polymerization by moving to less polar solvents (e.g. chloroform, tetrachloromethane) and screening a larger range of additives beyond alcohols (e.g. alkyl thiols, salts with more anions more coordinating than tetrafluoroborate such as triflate, tosylate, mesylate) which may exhibit more nucleophilic behavior towards the propagating cation while still retaining the properties of interest in the resulting polymer. Synthesis of block copolymers by addition of a second monomer capable of cationic polymerization will be attempted, also, as the capability of forming block copolymers is a hallmark of controlled or living polymerizations of all propagation modes and mechanisms.

## 4.11. Methods, Experimental Data, Spectra, and Gel Permeation Chromatograph Traces

### General Methods

Proton and carbon magnetic resonance spectra ($^{1}$H NMR and $^{13}$C NMR) were recorded on a Bruker model DRX 400, or a Bruker AVANCE III 600 CryoProbe ($^{1}$H NMR at 400 MHz, 600 MHz and $^{13}$C NMR at 100, 150 MHz) spectrometer with solvent resonance as the internal standard ($^{1}$H NMR: $CDCl_3$ at 7.26 ppm; $^{13}$C NMR: $CDCl_3$ at 77.0 ppm). $^{1}$H NMR data are reported as follows: chemical shift, multiplicity (s = singlet, d = doublet, t = triplet, dd = doublet of doublets, dt = doublet of triplets, td = triplet of doublets, m = multiplet, brs = broad singlet, bm = broad multiplet), coupling constants (Hz), and integration. Gel permeation chromatography (GPC) was carried out using a Waters Alliance 2695 instrument equipped with a refractive index detector (Waters 2414). Samples were passed through three columns (Waters Styragel HR5, HR4, and HR2) using THF as the mobile phase. All molecular weights (MW) and molecular weights distributions (polydispersity indexes, PDI) were determined by calibration to known, standard polystyrene samples purchased from Polyscience Corporation. Flash chromatography was performed using SiliaFlash P60 silica gel (40-63 μm) purchased from Silicycle. Dichloromethane was purchased from Fisher Scientific corporation, distilled from calcium hydride under dry nitrogen atmosphere, onto activated 4Å molecular sieves and then transferred into a dry, inert glovebox. Basic alumina was activated by the following procedure: dry nitrogen gas was passed through the powder (via a stainless steel needle) contained in a ~100 mL glass container capped with a rubber septum and vented with a needle. The bottle was heated by electric heating tape to between 200 and 230 °C for at least 18 hours. The bottle was allowed to cool, the needles were removed and the septum wrapped in parafilm. The bottle was then moved into a dry, inert glovebox, the septum and parafilm was removed, and a cap screwed on for storage. Irradiation of photochemical reactions was carried out using a 15W PAR38 blue LED

floodlamp purchased from EagleLight (Carlsbad, CA), in 10 mL borosilicate glass Schlenk tubes with an output centered at a wavelength of approximately 450 nm. All reagents were purchased from Sigma-Aldrich corporation or Fisher Scientific corporation and were used without additional purification unless otherwise noted.

**Example Standard Polymerization**

To a clean, dry 10 mL Schlenk flask with a 14/20 ground glass join was placed a Teflon coated magnetic stir bar, followed by 16.7 mg (0.038 mmol, 2.5 mol%) of 2,4,6-tri(*p*-tolyl)pyrylium tetrafluoroborate. At this point, any addition solid additives would also be added. The Schlenk flask was moved into a dry, inert glovebox. Then, approximately 4 to 5 mL of dichloromethane (distilled from calcium hydride under dry nitrogen atmosphere, onto activated 4Å molecular sieves) was filtered through activated basic alumina.(~0.5 to 1.0 mL packed into a plastic 5 mL syringe body equipped with a 0.2 micron Teflon syringe filter) into a clean, dry 1 dram vial. Then, ~ 0.5 to 1.0 mL of 4-methoxystyrene (stabilized with ~1 w/v% tert-butylcatechol) was filtered through activated basic alumina (~0.2 to 0.5 mL packed into a plastic 3 mL syringe body equipped with a 0.2 micron Teflon syringe filter) into a separate clean, dry 1 dram vial. Next, 2.5 mL of the freshly filtered dichloromethane was added via syringe to the Schlenk flask. As this point, any liquid additives would be added, for example: 4.0 µL (0.099 mmol, 3.2 mg, 6.5 mol%) of methanol added via a 10 µL Hamilton syringe. Then, a 250 µL Hamilton syringe was used to dispense 200 uL (202 mg, 1.51 mmol) of 4-methoxystrene into the Schlenk flask. The Schlenk flask was then sealed with a rubber septum, and the stopcock was closed. After removal from the glovebox, the Schlenk flask was submitted to at least three freeze-pump-thaw cycles using liquid nitrogen. The solution was brought up to room temperature and the flask was back filled with dry nitrogen gas. The flask was then irradiated

(standard time 25 minutes, unless otherwise noted) using the blue LED lamp with the flask placed ~1.0 cm from the front of the lamp with stirring rates between 700 and 1100 rpms. After the planned irradiation time, ~13 mg of TEMPO in ~0.5 mL chloroform was added to quench the polymerization, followed by 20.0 µL hexamethyldisiloxane (0.094 mmol) as a $^{1}$H NMR internal standard using a 50 µL Hamilton syringe. At this point, ~100 µL of the reaction was removed via pipet, added to an NMR tube, and diluted with ~0.5 mL chloroform-$d_1$.Monomer conversions were calculated from these samples. Finally, the polymerization reaction was diluted with an additional ~2 mL dichloromethane or chloroform and then precipitated from methanol (~100 to 125 mL) in an Erlenmeyer flask. These flasks were then transferred to a freezer (~ -20 °C) and left at least overnight. Some precipitates were collected via filter paper using a Buchner funnel and an aspirator. In most cases, this method was insufficient. In such cases, samples were reduced under vacuum using a rotary evaporator and then triturated with ~50 to 100 mL of methanol in ~10 mL portions to removed remaining pyrylium and monomer, or gravity filtered overnight over packed cotton (followed by further rinsing with methanol). The isolated solids were then redissolved in dichloromethane, transferred to scintillation vials, and reduced under vacuum. Samples for GPC were dissolved in THF at room temperature, and filtered through a 0.2 TFE micron filter. The remaining material in the methanol supernatant was blown down with air or nitrogen, and any residual solids were dissolved in dichloromethane, transferred to scintillation vials, and reduced under vacuum for storage.

**Preparation of Monomer**

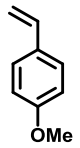


4-Methoxystyrene
(**3**)

4-Methoxystyrene **(3)** was synthesized via Wittig reaction from *p*-anisaldehyde. To a clean, dry 1 L flask was added 12.2 g potassium tert-butoxide (1.1 equiv., 109 mmol), followed by ~400 to 500 mL of anhydrous diethyl ether or tetrahydrofuran (dried by passage over a column of activated alumina). Then, 42.2 g (1.2 equiv., 118 mmol) of methyltriphenylphosphonium bromide was added to the mixture, and the flask was sealed with a septum and placed under positive nitrogen pressure. The mixture was stirred (Teflon coated magnetic stir bar) for ~30 min and quickly became bright yellow. Slowly and by syringe, 12 mL (1.0 equiv., 98.6 mmol, 13.4 g) of *p*-anisaldehyde (freshly distilled from calcium hydride under vacuum) was added to the yellow solution. In the case of diethyl ether, the flask was cooled to 0 °C in an ice bath prior to *p*-anisaldehyde addition, and addition was ceased if solvent refluxing was observed. After complete addition, the reaction was left to stir for at least three hours and sometimes overnight. Next, the reaction was quenched with water, transferred to a 2 L separatory funnel, diluted with ~ 500 to 750 mL diethyl ether and washed a minimum of 5 times with ~200 mL of water. The organic layer was dried, separated, and reduced under vacuum to approximately half its volume by rotary evaporator. The mixture was diluted with pentanes, and placed in the freezer overnight. Then, the solid crystals of triphenylphosphine oxide were filtered off via aspirator suction through a glass frit, the mother liquor was reduced under vacuum, and left under high vacuum overnight with stirring to remove as much residual solvent as possible. Finally, a small amount of *tert*-butylcatechol was placed into the clear oil just prior to distillation

under vacuum from calcium hydride to a round bottom flask with an additional small amount of *tert*-butylcatechol. After distillation, a small amount of the clear oil was removed for NMR analysis, and the remainder was transferred into a dry, inert glovebox and stored at -20 °C when not in use. Yields of 4-methoxystyrene generally ranged between 75 and 90%. Analytical data was in agreement with literature values.[104]

Analytical data for **3**: $^{1}$H NMR (400 MHz, $CDCl_3$): δ 7.35 (m, 2H), 6.87 (m, 2H), 6.67 (dd, *J* = 17.5, 10.8 Hz, 1H), 5.62 (d, *J* = 17.6 Hz, 1H), 5.14 (d, *J* = 10.9 Hz, 1H), 3.82 (s, 3H); $^{13}$C NMR ($CDCl_3$, 100 MHz): δ 159.34, 136.19, 130.41, 127.36, 113.88, 111.55, 55.28.

## Preparation of Pyrylium Salts

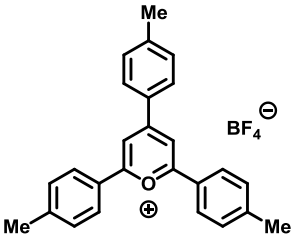


2,4,6-tri-*p*-tolylpyrylium tetrafluoroborate (**25**)

2,4,6-Tri(*p*-tolyl)pyrylium tetrafluoroborate (**25**) was synthesized according to literature procedures in an isolated yield of 2.5 g (31% yield relative to starting *p*-tolualdehyde).[100] The product was recrystallized three times from hot acetic acid and dried for 3 days at 70 °C under high vacuum. The analytical data matched that reported in the literature.

Analytical data for **25**: $^{1}$H NMR (600 MHz, $CDCl_3$): δ 8.43 (s, 2H), 8.27 – 8.22 (m, 4H), 8.22 – 8.16 (m, 2H), 7.55 – 7.48 (m, 4H), 7.23 – 7.17 (m, 2H), 2.48 (s, 6H), 2.15 (s, 3H); $^{13}$C NMR ($CDCl_3$, 150 MHz): δ 169.40, 164.46, 147.10, 147.09, 131.13, 131.01, 130.04, 129.09, 128.42, 125.76, 112.77, 22.03, 21.72.

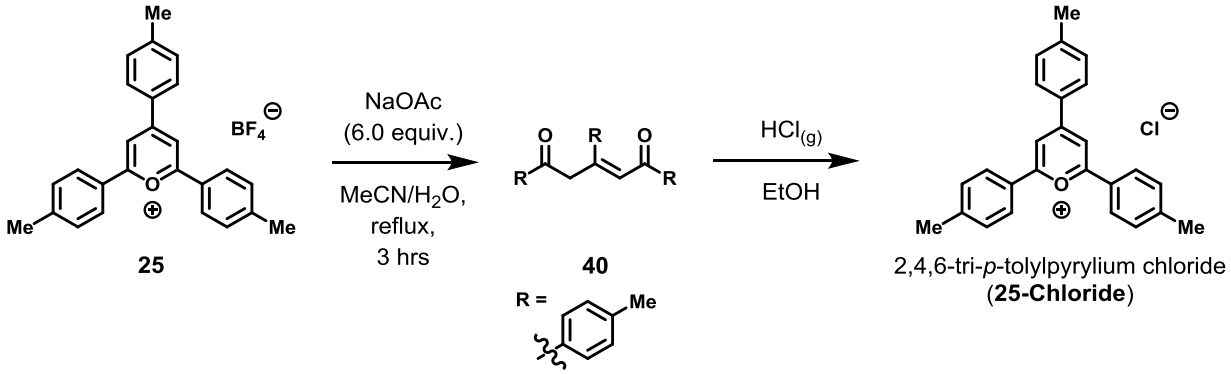


The synthesis of 2,4,6-tri(*p*-tolyl)pyrylium chloride (**25-Chloride**) was adapted from a procedure reported in the literature.[105] To a 9 to 1 solution of acetonitrile water (125 mL) in a 250 mL rbf equipped with a reflux condenser was added 1.0 g (2.28 mmol, 1.0 equiv) of 2,4,6-tri(*p*-tolyl)pyrylium tetrafluoroborate (**25**) followed by 1.12 grams (13.7 mmol, 6.0 equiv). The solution was refluxed for three hours. The solution was then transferred to a separatory funnel, diluted with ~300 mL water, and extracted with 5x 50 mL dichloromethane. The organic layer was separated, dried with sodium sulfate, and filtered through a plug of cotton, then reduced under vacuum using a rotary evaporator to give a red solid. Flash chromatography of the solid (5/95 ethyl acetate/hexanes) gave 380 mg (1.03 mmol, 45%) of a red solid, 1,3,5-tri-p-tolylpent-2-ene-1,5-dione (**41**).This material was dissolved in ~100 mL ethanol in a 250 mL rbf. Anhydrous hydrogen chloride was generated in a separate 100 mL rbf via dropwise addition of sulfuric acid to sodium chloride with vigorous stirring. The gas was transferred to the 250 mL rbf via Teflon tubing, connected to a glass pipet with a short length of Nalgene tubing, and bubbled through the ethanol solution via the pipet inserted through a rubber septum. A second pipet was inserted through the rubber septum as a vent. Throughout the course of bubbling, the solution became yellow. Bubbling lasted for approximately 90 minutes. The solution was then bubbled with dry nitrogen gas for an additional 60 minutes. Then the solvent was reduced under vacuum until a yellow/red solid began to precipitate. The solid was then precipitated from hot methanol

using diethyl ether. The resulting reddish yellow solid was precipitated from acetone using diethyl ether three additional times to give 250 mg (0.65 mmol, 63%) of 2,4,6-tri(*p*-tolyl)pyrylium chloride.

Analytical data for **41**: $^{1}$H NMR (400 MHz, $CDCl_3$): δ 7.96 (d, *J* = 8.2 Hz, 2H), 7.89 (d, *J* = 8.3 Hz, 2H), 7.44 (d, *J* = 10.0 Hz, 3H), 7.32 – 7.16 (m, 4H), 4.84 (s, 2H), 2.51 – 2.34 (m, 9H).; $^{13}$C NMR ($CDCl_3$, 100 MHz): δ 195.88, 190.44, 152.34, 143.72, 143.30, 139.41, 139.10, 136.68, 134.58, 129.40, 129.23, 129.18, 128.40, 126.68, 122.85, 42.58, 21.65, 21.62, 21.25.

Analytical data for **25-Chloride**: $^{1}$H NMR (600 MHz, $CDCl_3$): δ 9.05 (s, 1H), 8.71 (d, *J* = 7.7 Hz, 1H), 8.51 (d, *J* = 7.7 Hz, 2H), 7.51 (d, *J* = 7.6 Hz, 2H), 7.30 (d, *J* = 7.3 Hz, 1H), 2.50 (s, 3H), 2.26 (s, 2H).; $^{13}$C NMR ($CDCl_3$, 150 MHz): δ 169.22, 164.92, 147.20, 146.66, 131.30, 130.93, 130.84, 129.26, 128.88, 126.13, 114.01, 22.05, 21.88.

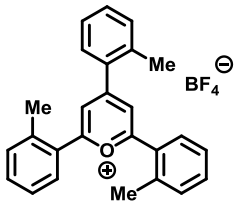


2,4,6-tri-*o*-tolylpyrylium tetrafluoroborate (**28**)

2,4,6-Tri(*o*-tolyl)pyrylium tetrafluoroborate (**28**) was synthesized in identical fashion as to 2,4,6-tri(*p*-tolyl)pyrylium tetrafluoroborate (**25**), in an isolated yield of 2.8 g (35% yield relative to starting *o*-tolualdehyde) using 2-methylacetophenone instead of 4-methylacetophenone, and *o*-tolualdehyde instead of *p*-tolualdehyde.[100] The product was precipitated from acetone using diethyl ether.

Analytical data for **28**: $^{1}$H NMR (600 MHz, $CDCl_3$): δ 8.04 (s, 2H), 7.94 (d, *J* = 6.5 Hz, 2H), 7.76 – 7.72 (m, 1H), 7.61 – 7.56 (m, 2H), 7.53 (t, *J* = 7.5 Hz, 1H), 7.50 – 7.39 (m, 6H), 2.66 (s, 6H), 2.62 (s, 3H).; $^{13}$C NMR ($CDCl_3$, 150 MHz): δ

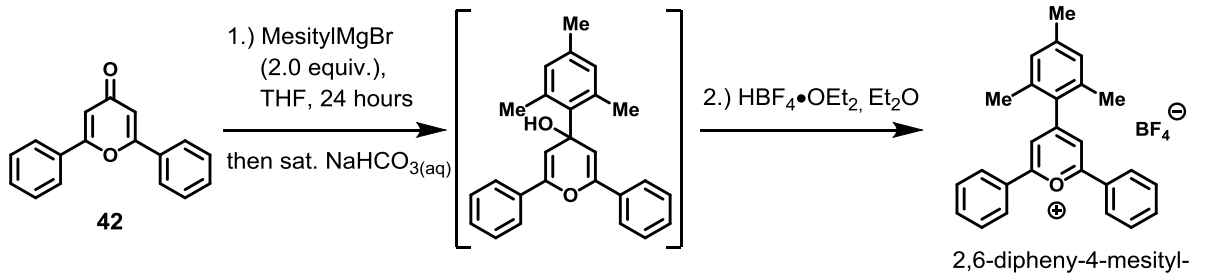


The synthesis of 2,6-diphenyl-4-mesitylpyrylium tetrafluoroborate (**29**) was adapted from literature procedures.[106,107] 2,6-diphenyl-4H-pyran-4-one (**42**) was synthesized in two steps from methylbenzoate according to a literature procedure in an 82% overall yield. To a 100 mL rbf was added 155 mg **41** followed by ~40 mL anhydrous THF. The flask was sealed with a rubber septum, kept under positive nitrogen pressure, and cooled to 0 °C in an ice bath. To this solution was added 1.8 mL of a 1.0 M solution of mesitylmagnesium bromide (1.8 mmol) in THF. The solution was allowed to come to ambient temperature and stirred for 24 hours. Then, the solution was quenched with ~ 50 mL of saturated sodium bicarbonate, and extracted with 3x 50mL of diethyl ether. The organic layer was separated, dried with anhydrous magnesium sulfate, and gravity filtered through filter paper into a 250 mL Erlenmeyer flask. To this solution was added several drops of tetrafluoroboric acid diethyletherate with vigorous agitation between drops. The yellow precipitate was collected via filtration, and after drying under vacuum, 225 mg (60% yield) of 2,6-diphenyl-4-mesitylpyrylium tetrafluoroborate was isolated.

Analytical data for **42**: $^{1}$H NMR (600 MHz, $CDCl_3$): δ 7.93 – 7.81 (m, 4H), 7.54 (m, 6H), 6.82 (s, 2H).; $^{13}$C NMR ($CDCl_3$, 150 MHz): δ 180.23, 163.35, 131.46, 131.42, 129.15, 125.94, 111.42

Analytical data for **29**: $^{1}$H NMR (600 MHz, $CDCl_3$): δ 8.28 (d, *J* = 8.0 Hz, 4H), 8.12 (s, 2H), 7.76 (t, *J* = 7.4 Hz, 2H), 7.70 (t, *J* = 7.7 Hz, 4H), 7.06 (s, 2H), 2.37 (s, 3H), 2.29 (s, 6H).; $^{13}$C

NMR ($CDCl_3$, 150 MHz): δ 171.68, 141.46, 140.88, 135.73, 134.98, 132.25, 130.28, 129.68, 128.93, 128.59, 120.24, 21.25, 20.63

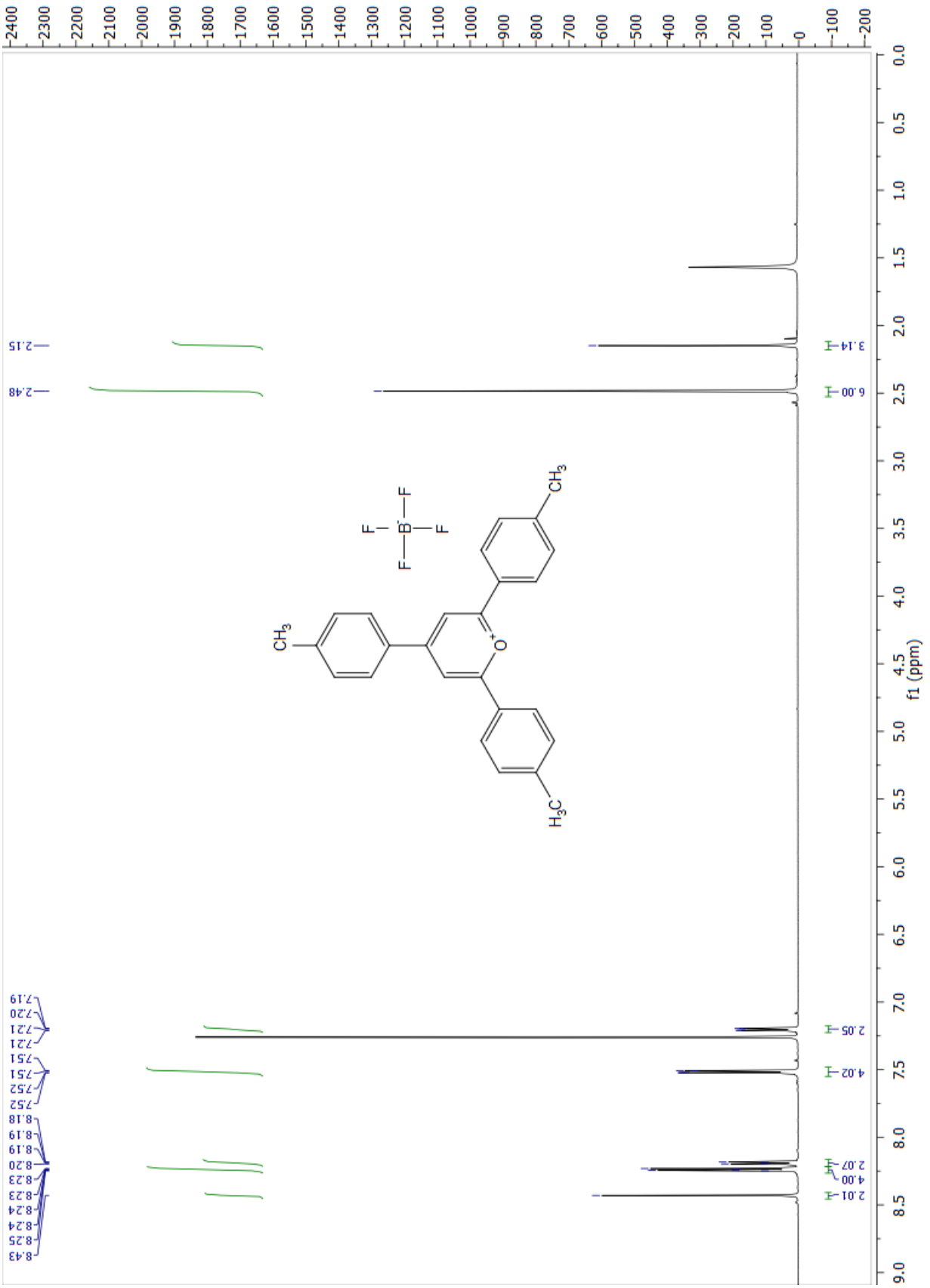
f1 (ppm)
2.15
2.48
3.14
6.00
2.05
4.02
2.07
4.00
2.01
8.43
8.25
8.24
8.24
8.23
8.23
8.20
8.19
8.19
8.18
7.52
7.52
7.51
7.51
7.21
7.21
7.20
7.19
CH3
CH3
H3C
B
F
F
F
F
O+

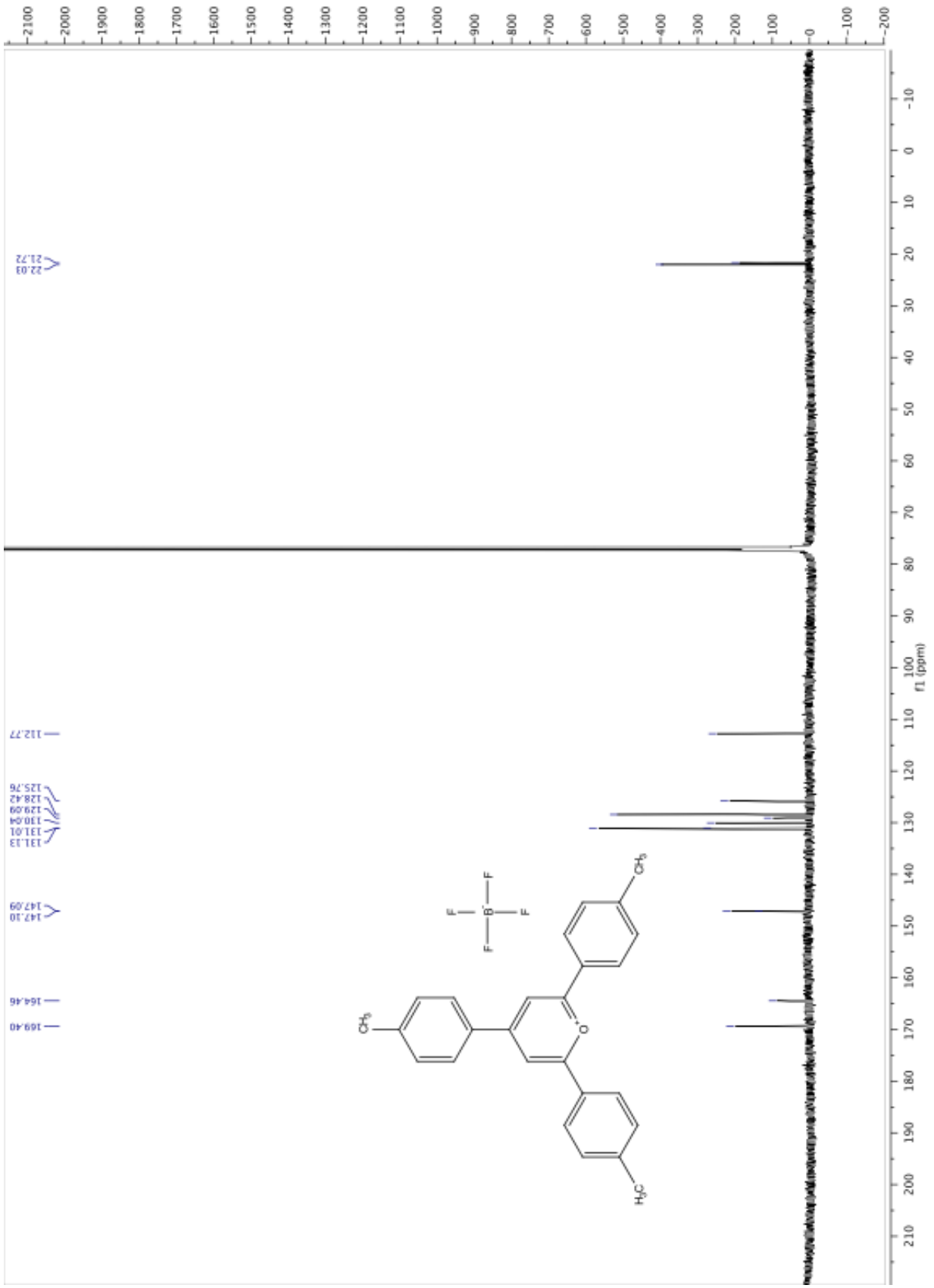
22.03
21.72
112.77
125.76
128.42
129.09
130.04
131.01
131.13
147.09
147.10
164.46
169.40
f1 (ppm)

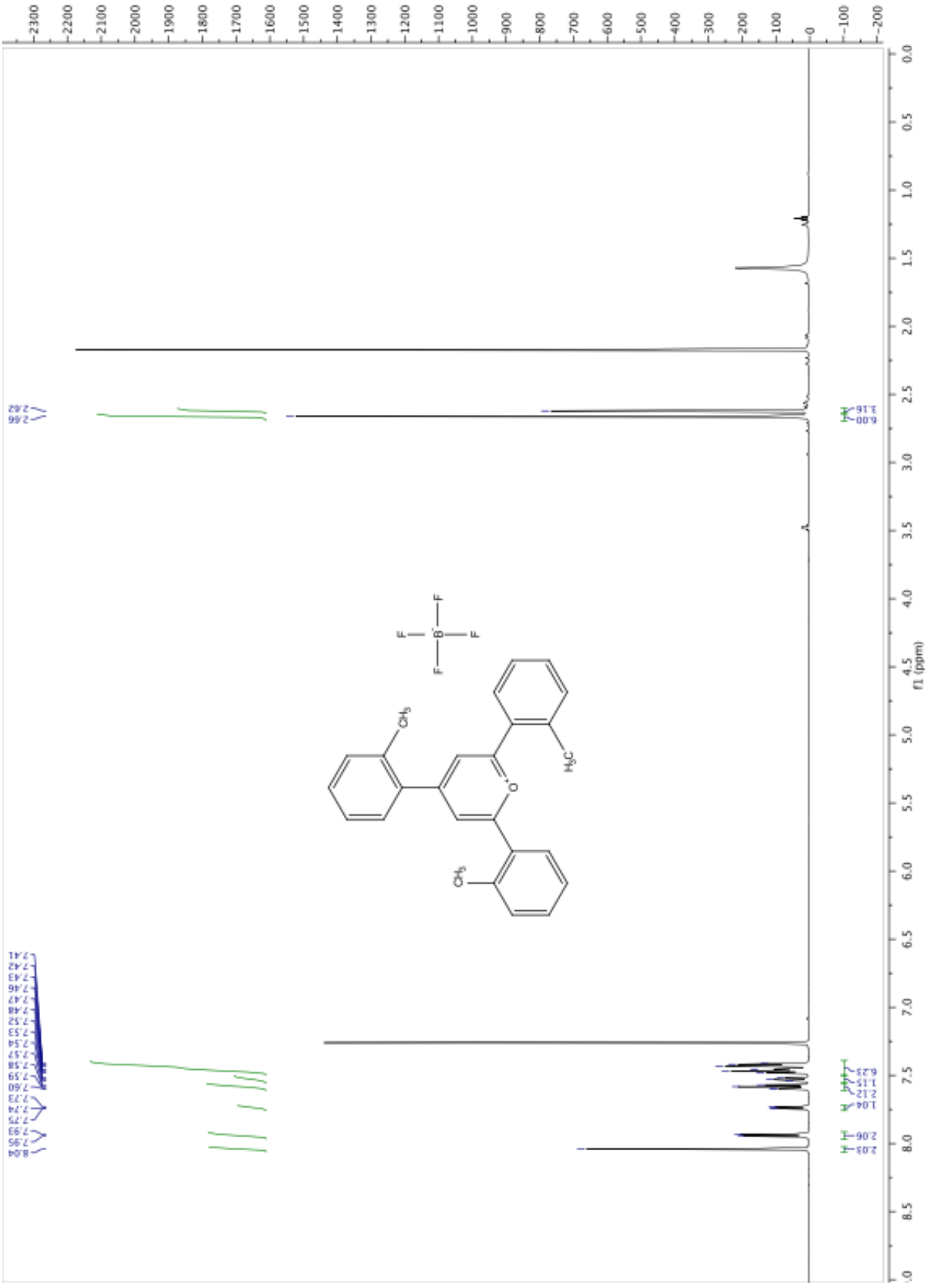
f1 (ppm)

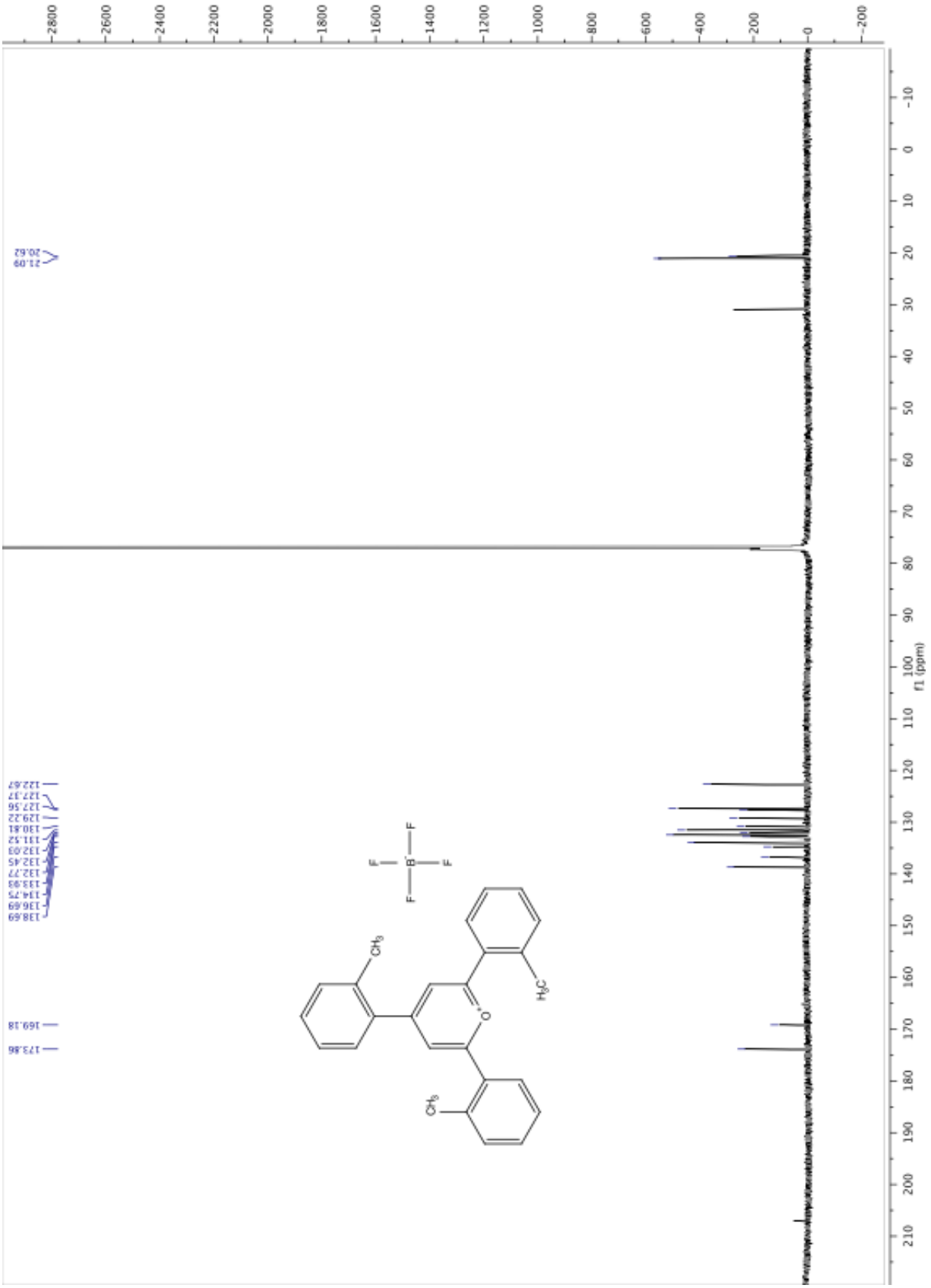
f1 (ppm)

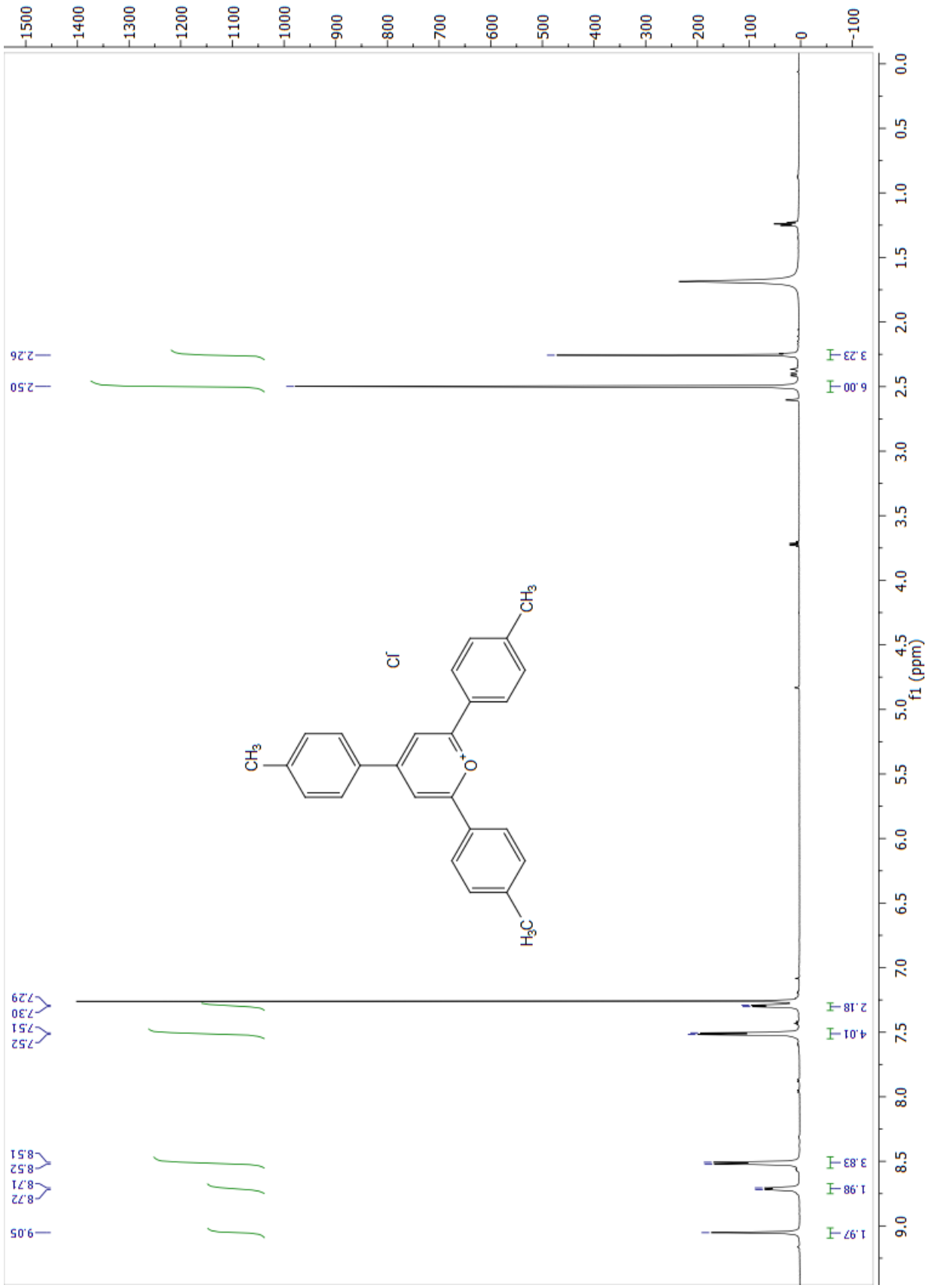
f1 (ppm)
2.26
2.50
7.29
7.30
7.51
7.52
8.51
8.52
8.71
8.72
9.05
3.23
6.00
2.18
4.01
3.83
1.98
1.97
CH3
CH3
H3C
O+
Cl-

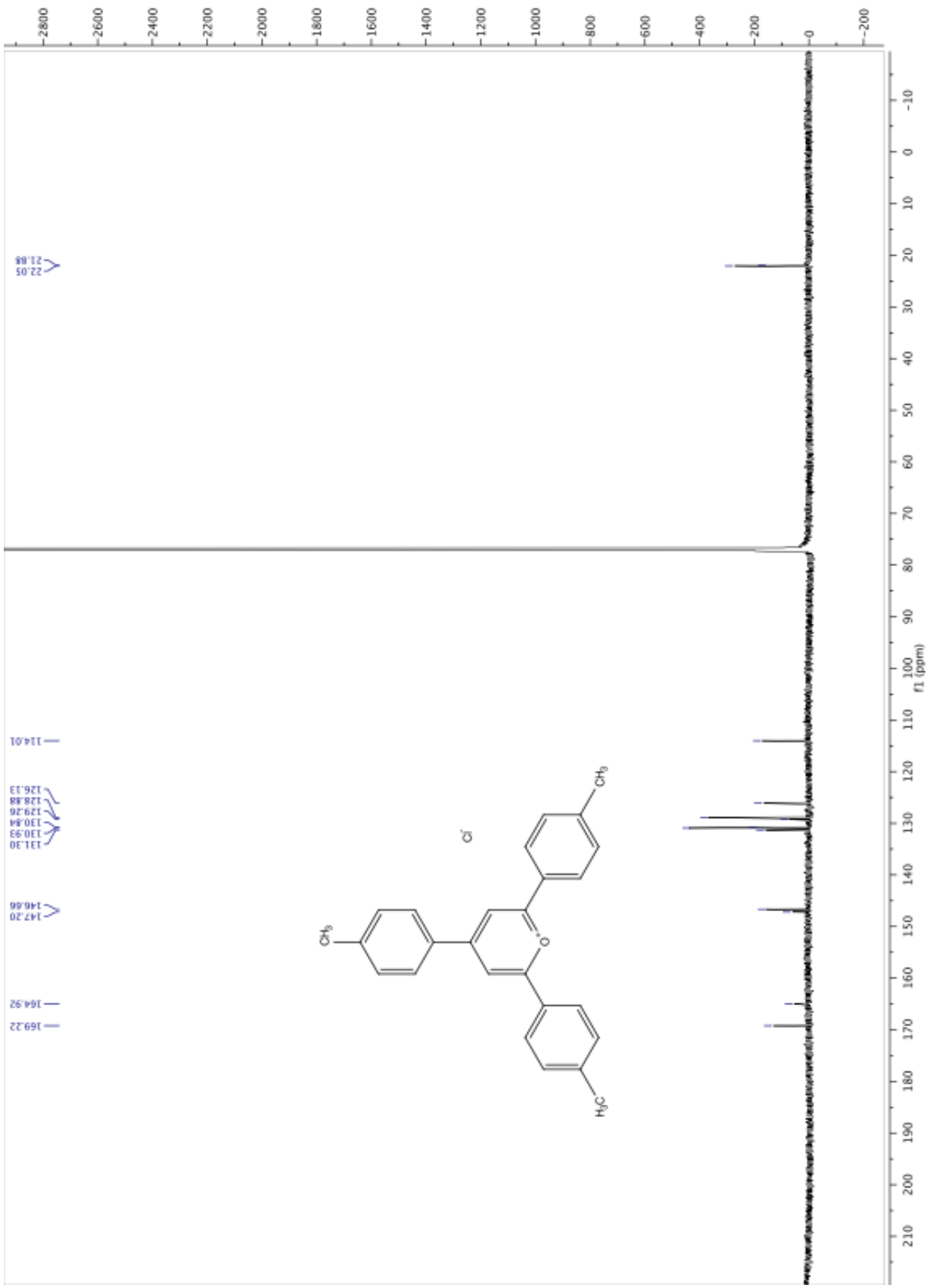
22.05
21.88
114.01
126.13
128.88
129.26
130.84
130.93
131.30
146.66
147.20
164.92
169.22
f1 (ppm)
CH3
Cl-
O+
CH3
H3C

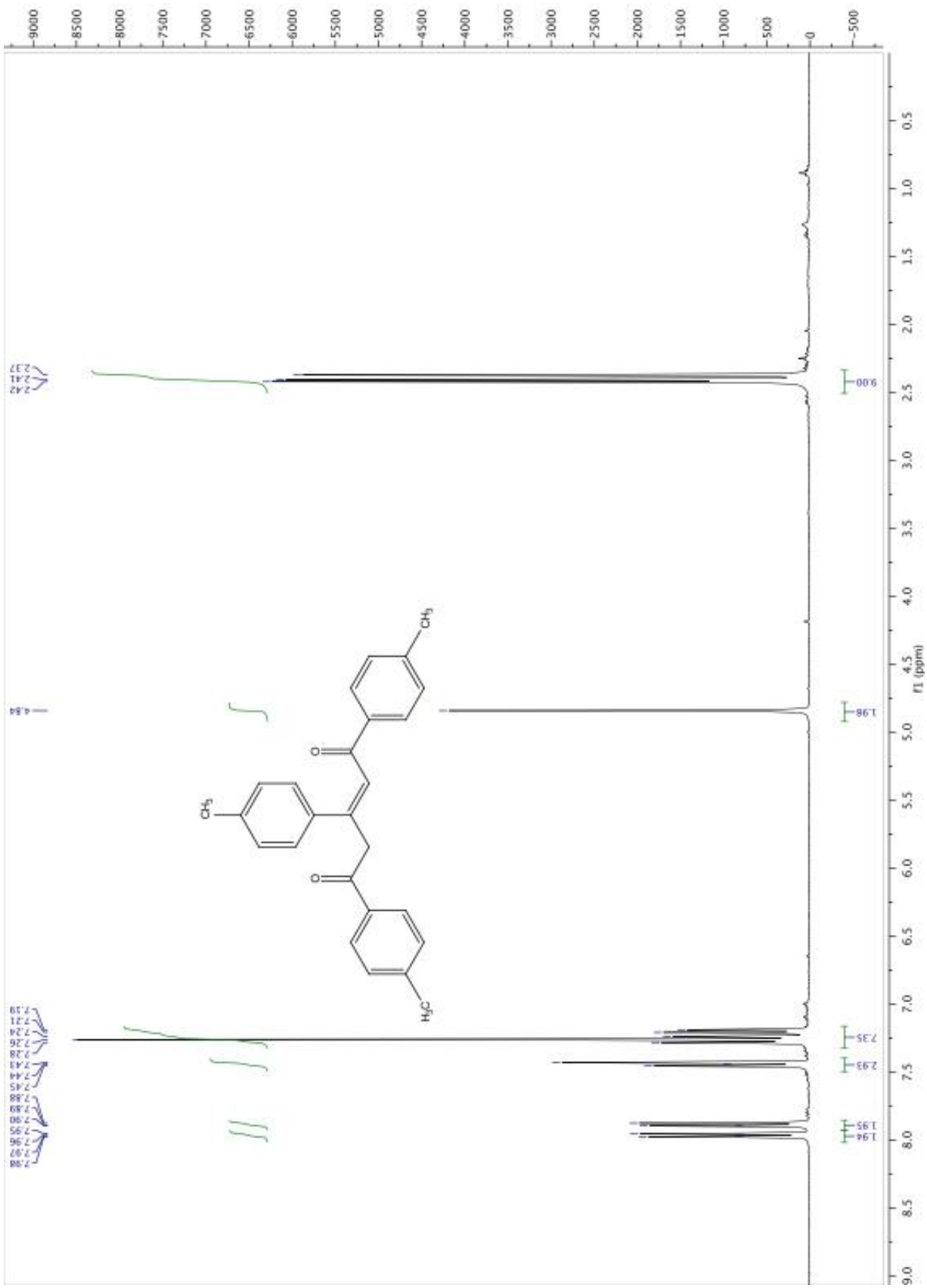
f1 (ppm)
9.00
1.98
7.35
2.93
1.95
1.94
4.84
2.42
2.41
2.37
CH3
H3C
O
O

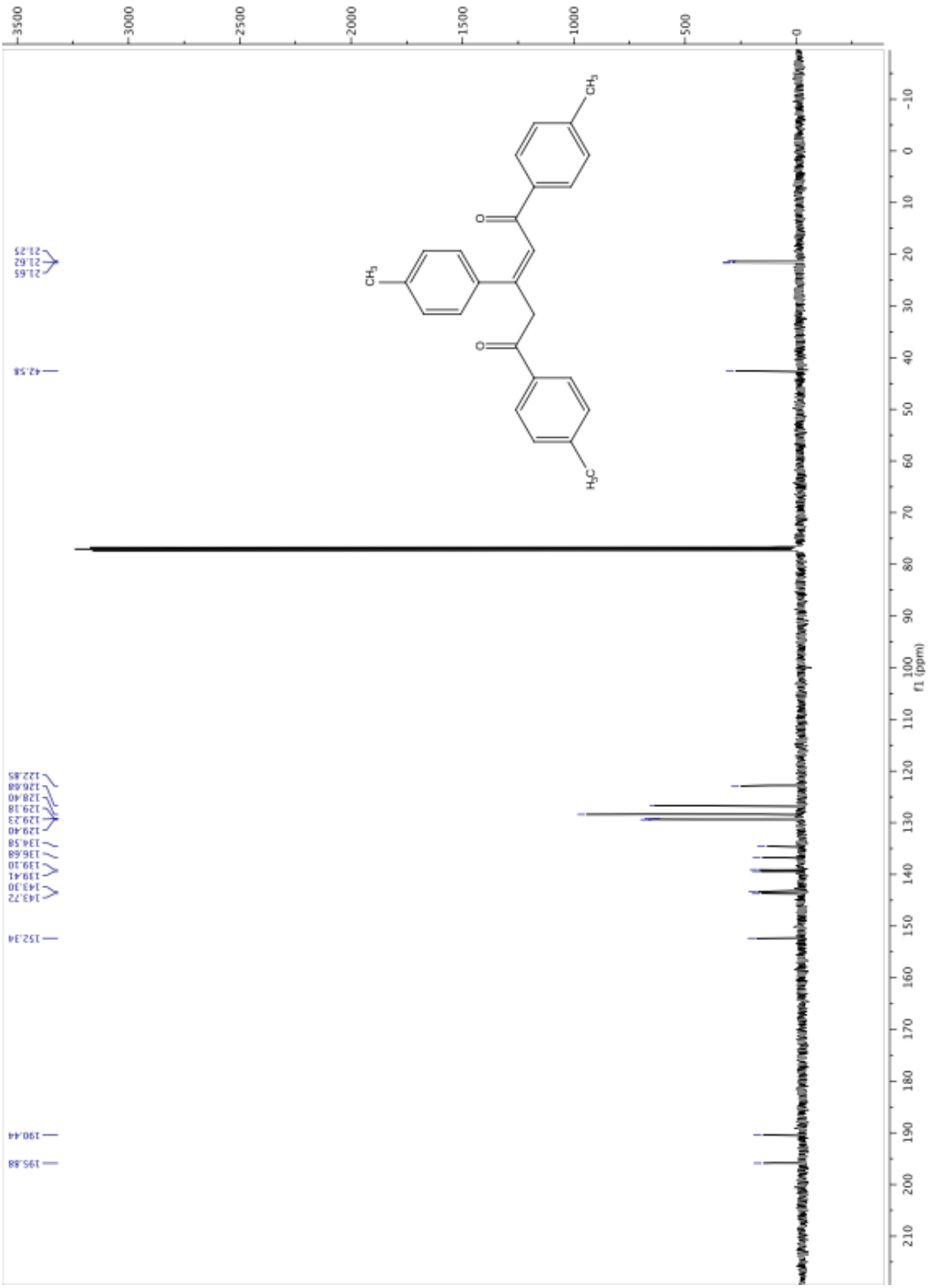
f1 (ppm)
CH3
H3C
O
O
21.25
21.62
21.65
42.58
122.85
126.68
128.40
129.18
129.23
129.40
134.58
136.68
139.10
139.41
143.30
143.72
152.34
190.44
195.88

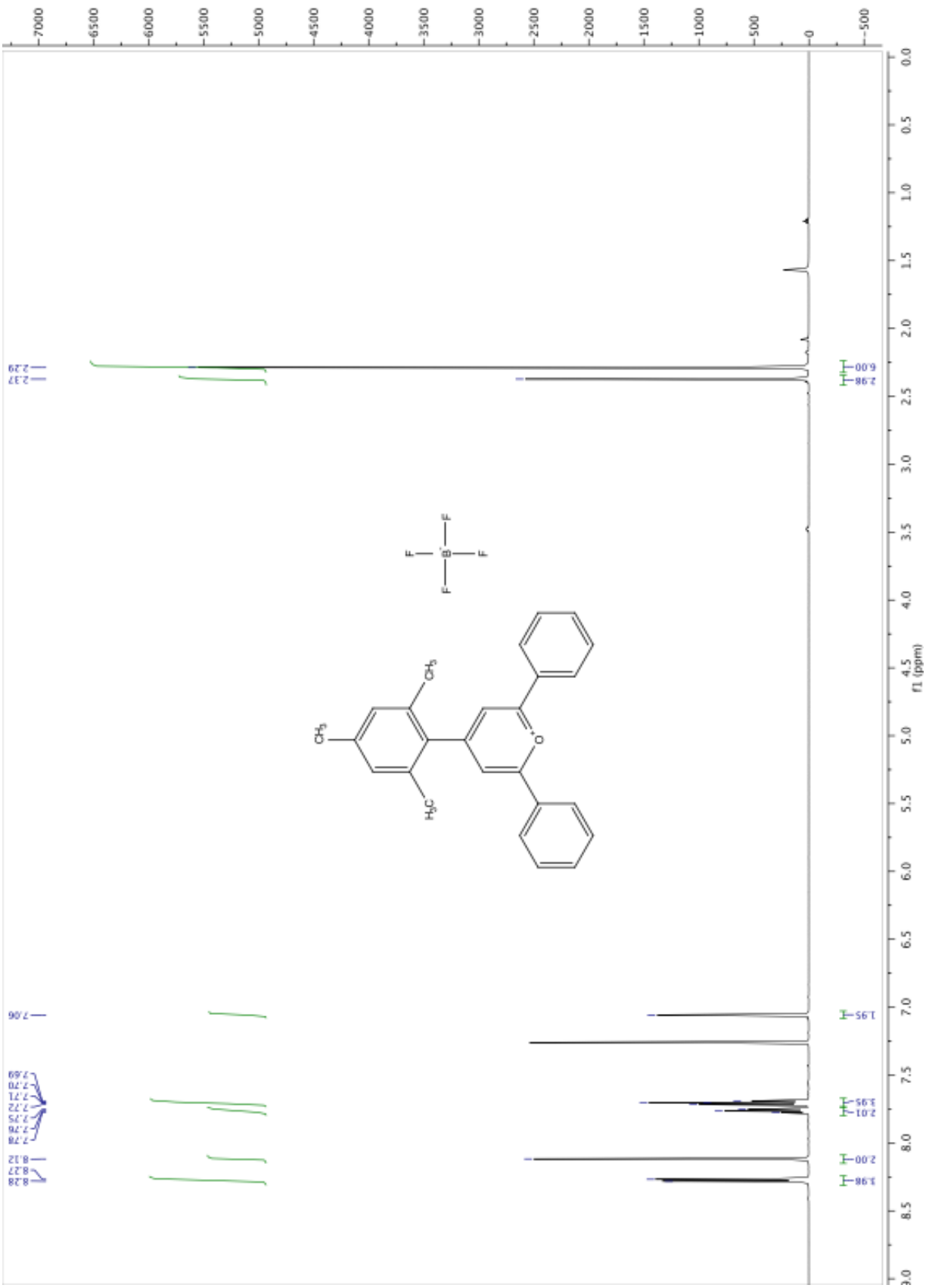

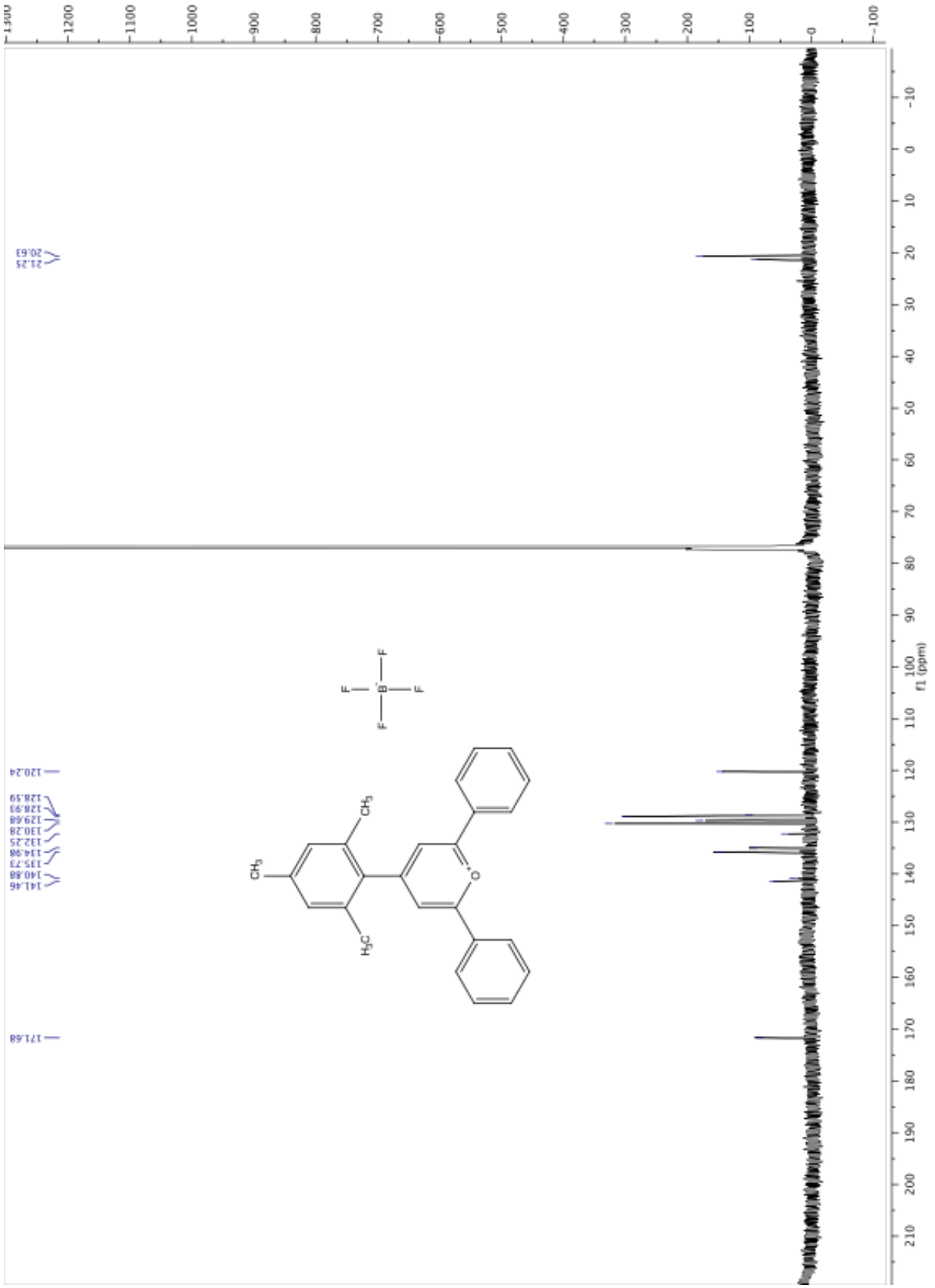
171.68
141.46
140.88
135.73
134.98
132.25
130.28
129.68
128.93
128.59
120.24
21.25
20.63
f1 (ppm)

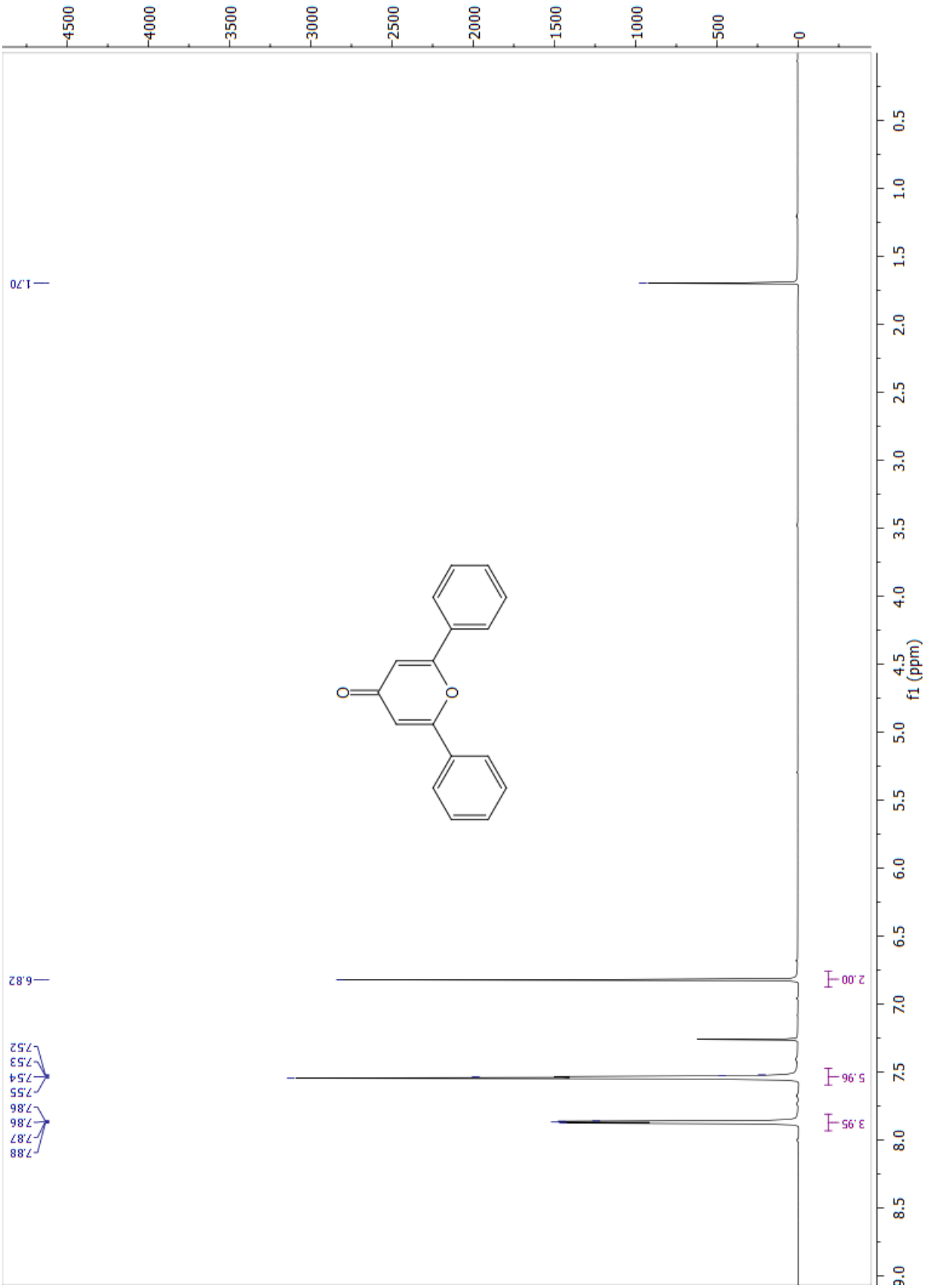
1.70
6.82
7.52
7.53
7.54
7.55
7.86
7.86
7.87
7.88
2.00
5.96
3.95
f1 (ppm)


111.42
125.94
129.15
131.42
131.46
163.35
180.23
f1 (ppm)

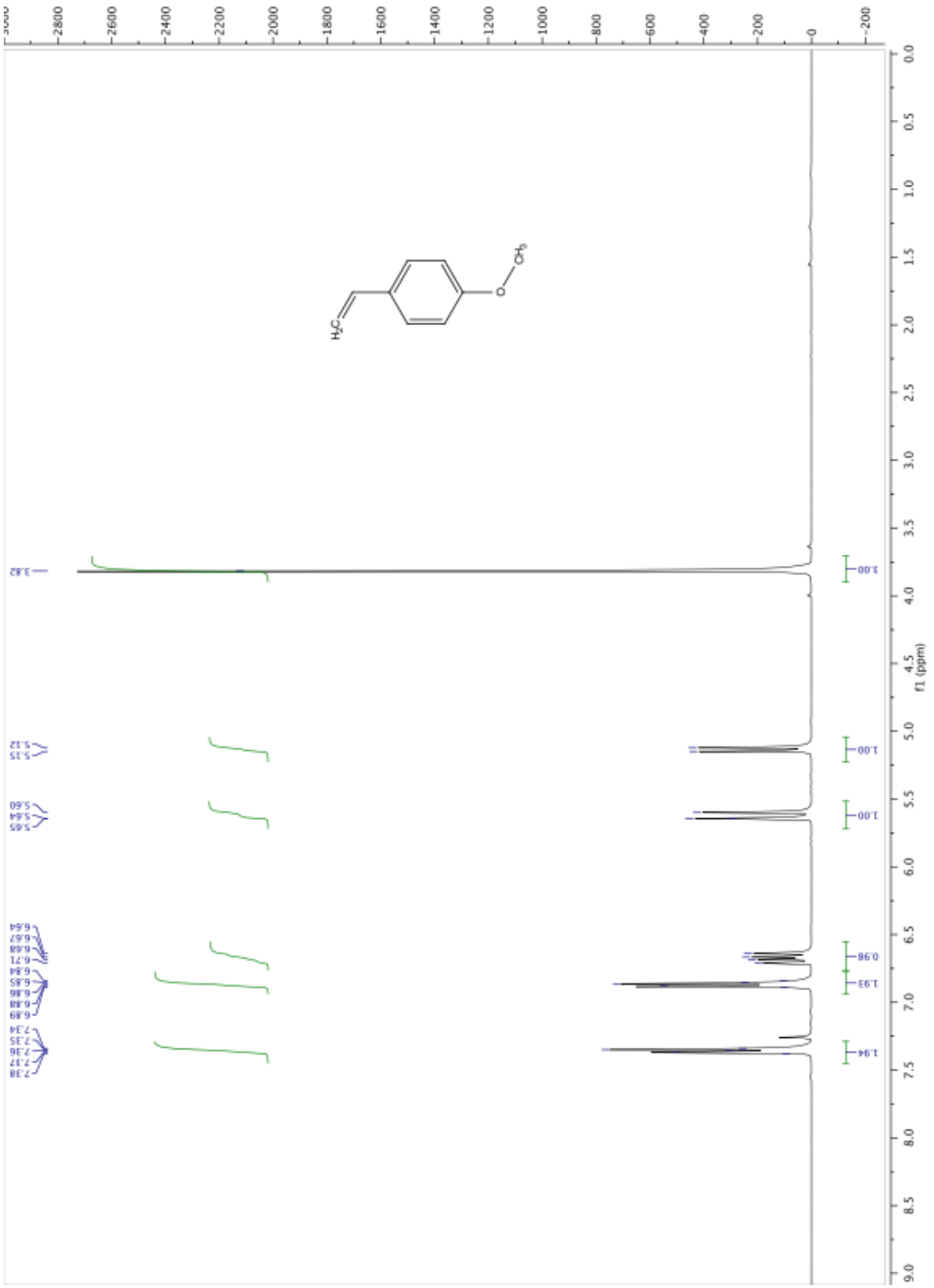
f1 (ppm)

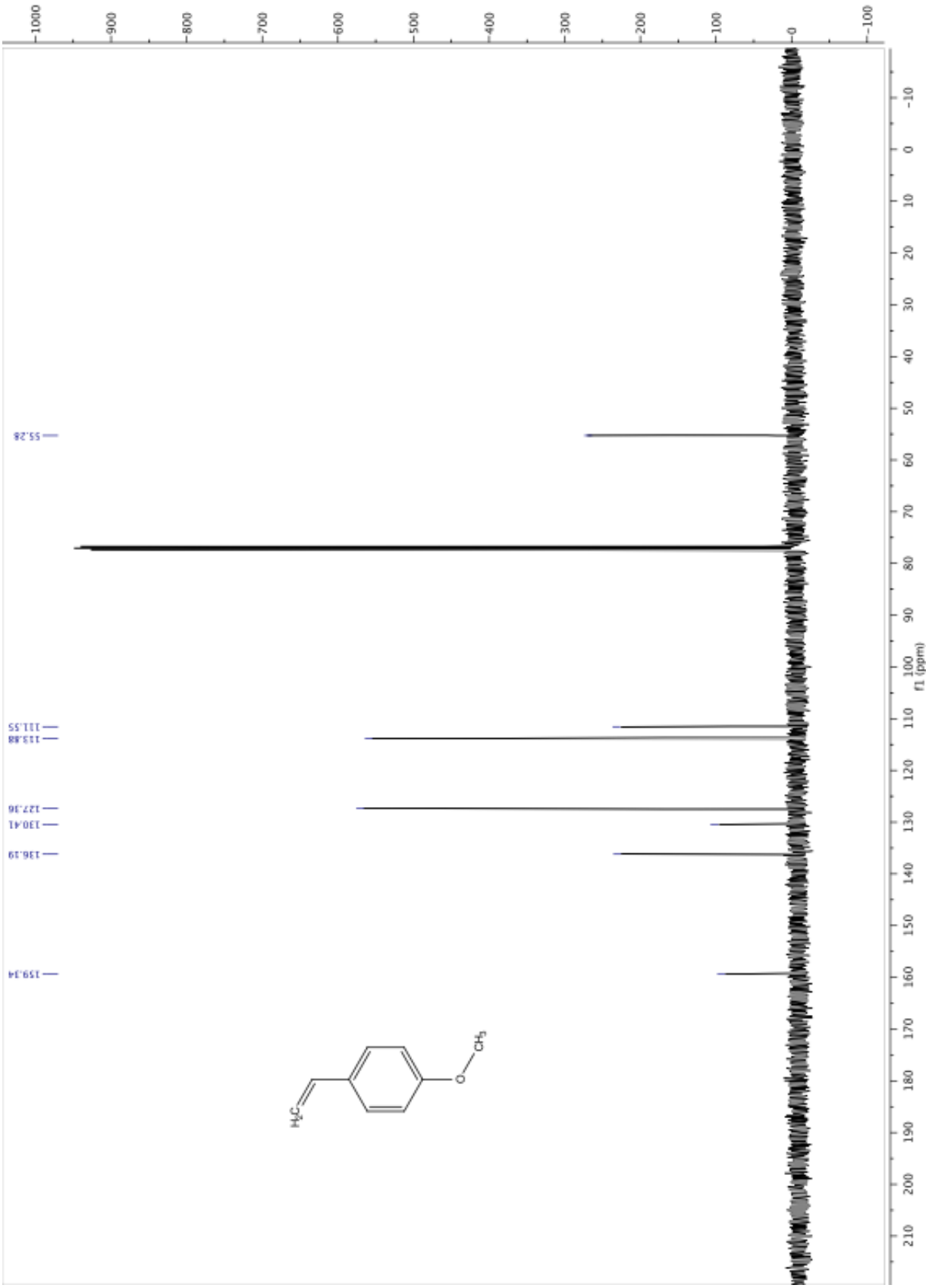
55.28
111.55
113.88
127.36
130.41
136.19
159.34
f1 (ppm)

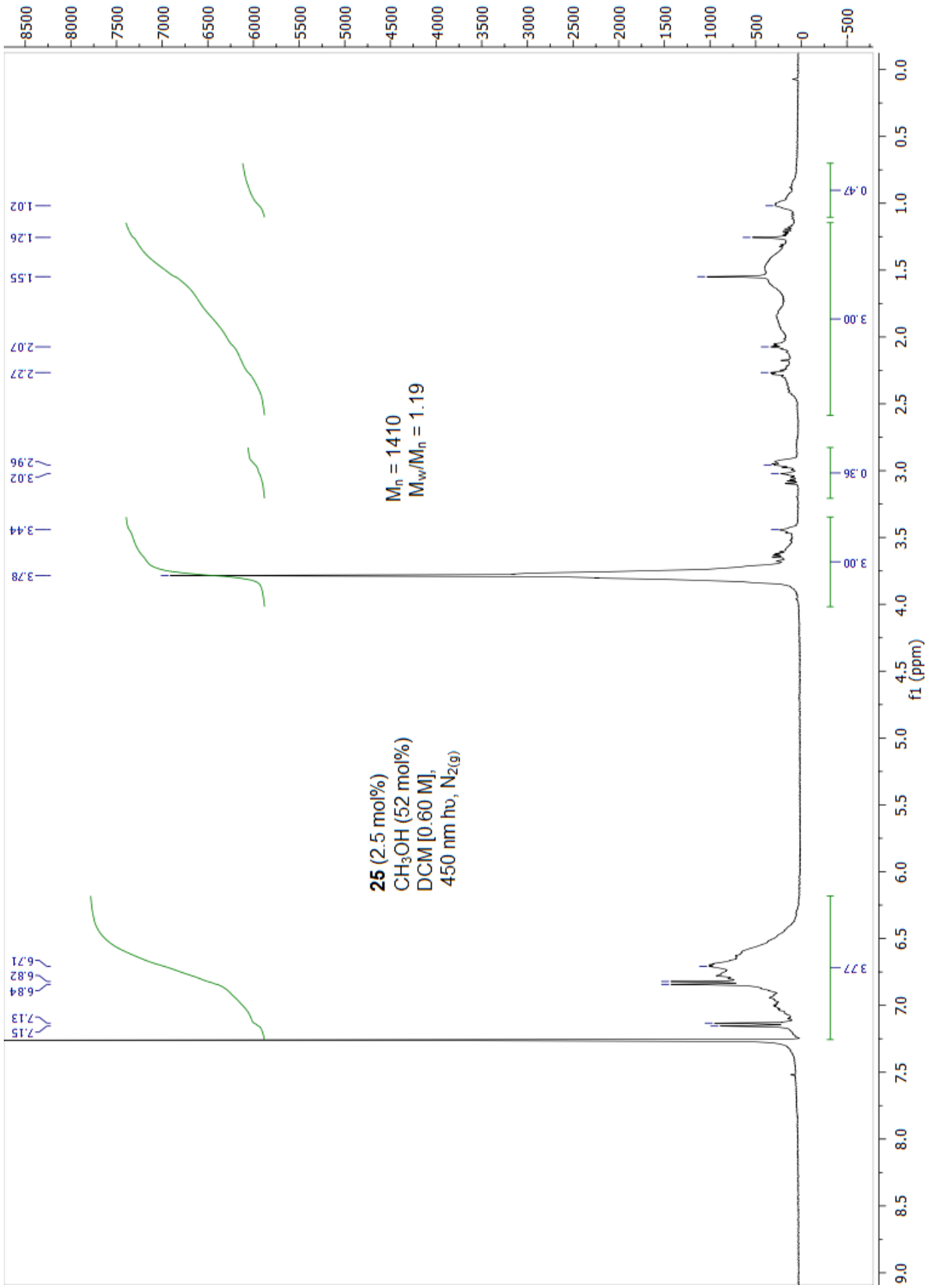
25 (2.5 mol%)
CH3OH (52 mol%)
DCM [0.60 M],
450 nm hυ, N2(g)
Mn = 1410
Mw/Mn = 1.19
f1 (ppm)

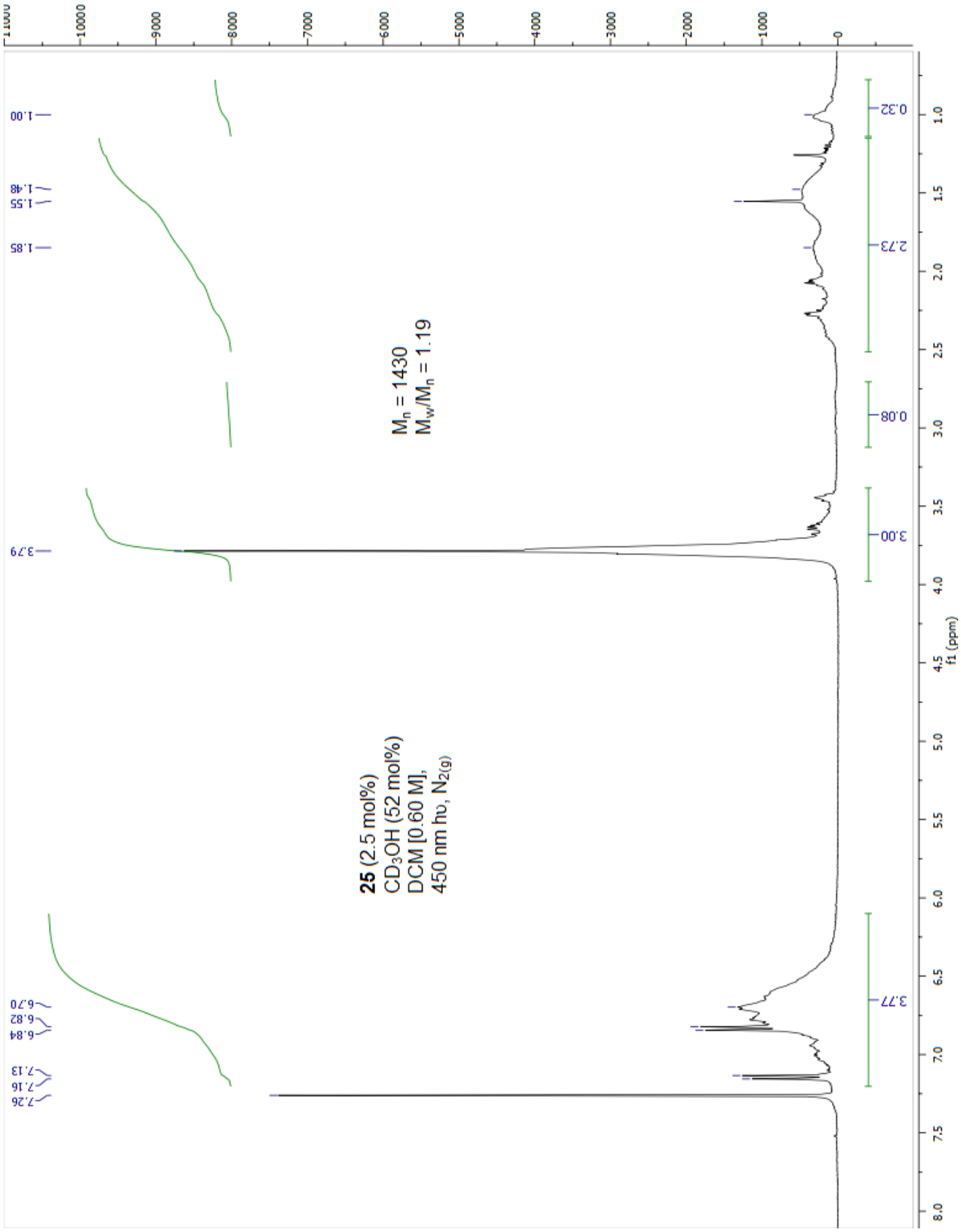
25 (2.5 mol%)
CD3OH (52 mol%)
DCM [0.60 M],
450 nm hυ, N2(g)
Mn = 1430
Mw/Mn = 1.19
f1 (ppm)

## GPC Traces

Figure 4.5, Entry 1

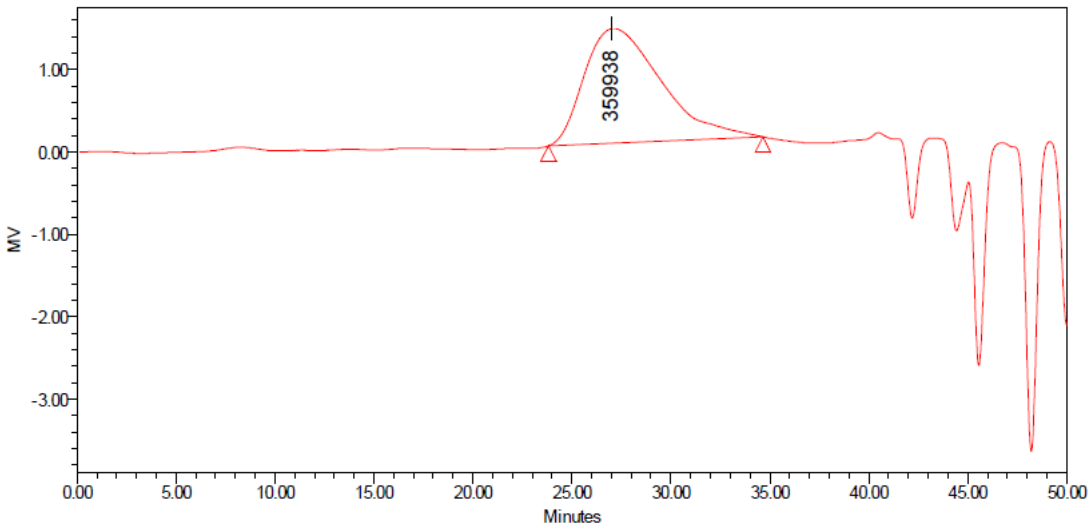


**GPC Results**

| | Dist Name | Mn | Mw | MP | Mz | Mz+1 | Mv | Polydispersity | MW Marker 1 | MW Marker 2 |
|---|---|---|---|---|---|---|---|---|---|---|
| 1 | | 140023 | 298916 | 359938 | 444280 | 549581 | | 2.134759 | | |

Figure 4.5, Entry 2

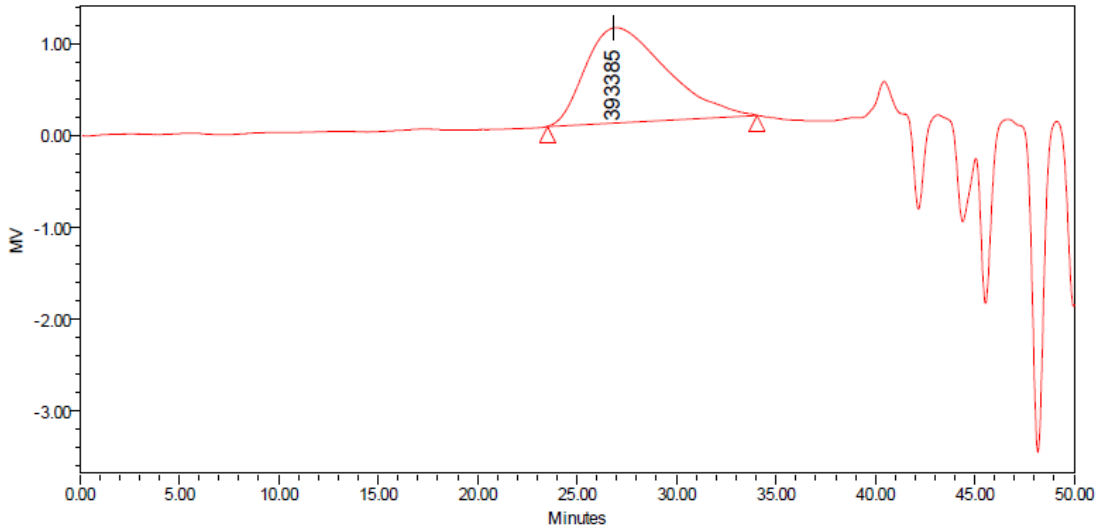


**GPC Results**

| | Dist Name | Mn | Mw | MP | Mz | Mz+1 | Mv | Polydispersity | MW Marker 1 | MW Marker 2 |
|---|---|---|---|---|---|---|---|---|---|---|
| 1 | | 148668 | 307785 | 393385 | 459418 | 566286 | | 2.070286 | | |

Figure 4.5, Entry 3

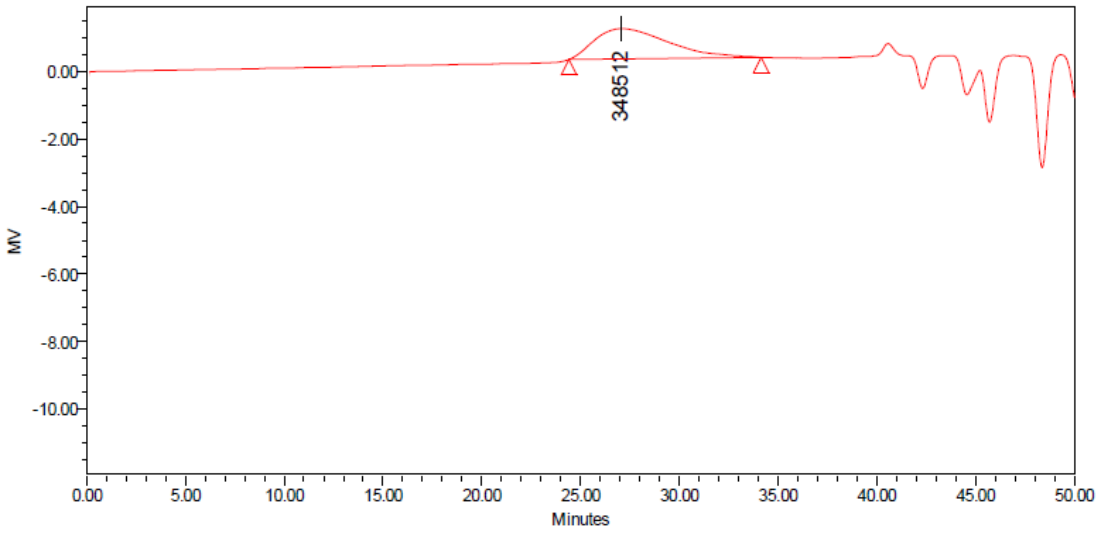


**GPC Results**

| | Dist Name | Mn | Mw | MP | Mz | Mz+1 | Mv | Polydispersity | MW Marker 1 | MW Marker 2 |
|---|---|---|---|---|---|---|---|---|---|---|
| 1 | | 152683 | 300016 | 348512 | 440050 | 543826 | | 1.964959 | | |

Figure 4.5, Entry 4

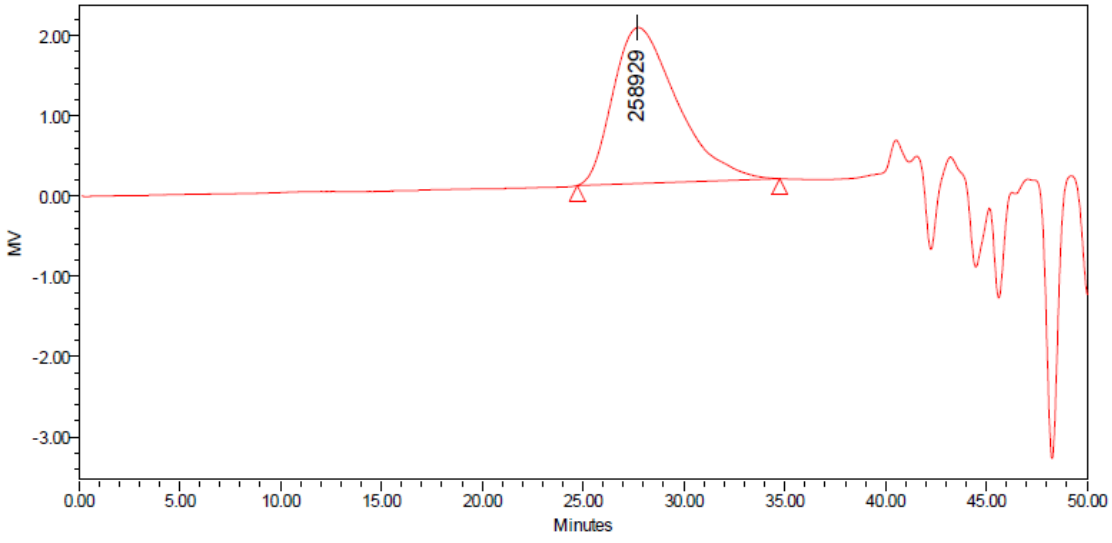


**GPC Results**

| | Dist Name | Mn | Mw | MP | Mz | Mz+1 | Mv | Polydispersity | MW Marker 1 | MW Marker 2 |
|---|---|---|---|---|---|---|---|---|---|---|
| 1 | | 134260 | 238534 | 258929 | 340822 | 430510 | | 1.776652 | | |

Figure 4.5, Entry 5

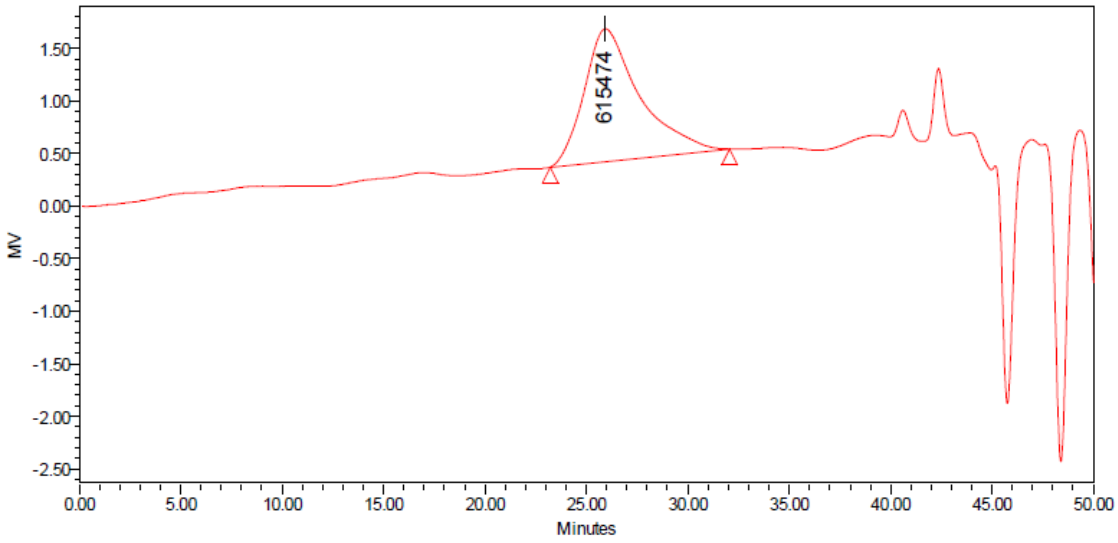


**GPC Results**

| | Dist Name | Mn | Mw | MP | Mz | Mz+1 | Mv | Polydispersity | MW Marker 1 | MW Marker 2 |
|---|---|---|---|---|---|---|---|---|---|---|
| 1 | | 292290 | 445412 | 615474 | 558473 | 631910 | | 1.523870 | | |

Figure 4.6, Entry 1

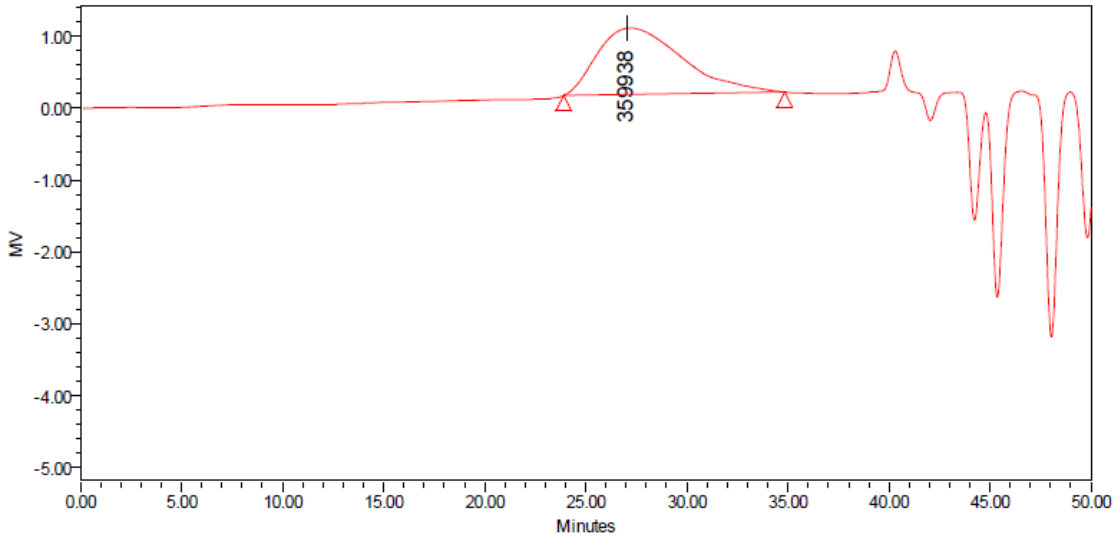


**GPC Results**

| | Dist Name | Mn | Mw | MP | Mz | Mz+1 | Mv | Polydispersity | MW Marker 1 | MW Marker 2 |
|---|---|---|---|---|---|---|---|---|---|---|
| 1 | | 129002 | 289158 | 359938 | 444241 | 555350 | | 2.241507 | | |

Figure 4.6, Entry 2

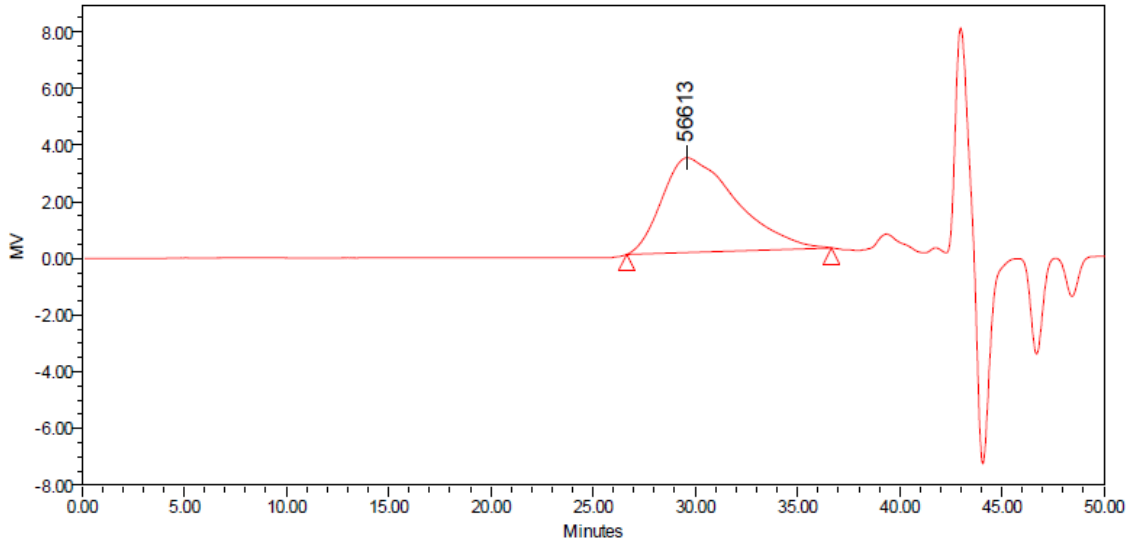


GPC Results

| | Dist Name | Mn | Mw | MP | Mz | Mz+1 | Mv | Polydispersity | MW Marker 1 | MW Marker 2 |
|---|---|---|---|---|---|---|---|---|---|---|
| 1 | | 22636 | 48555 | 56613 | 78408 | 105924 | | 2.145030 | | |

Figure 4.6, Entry 6

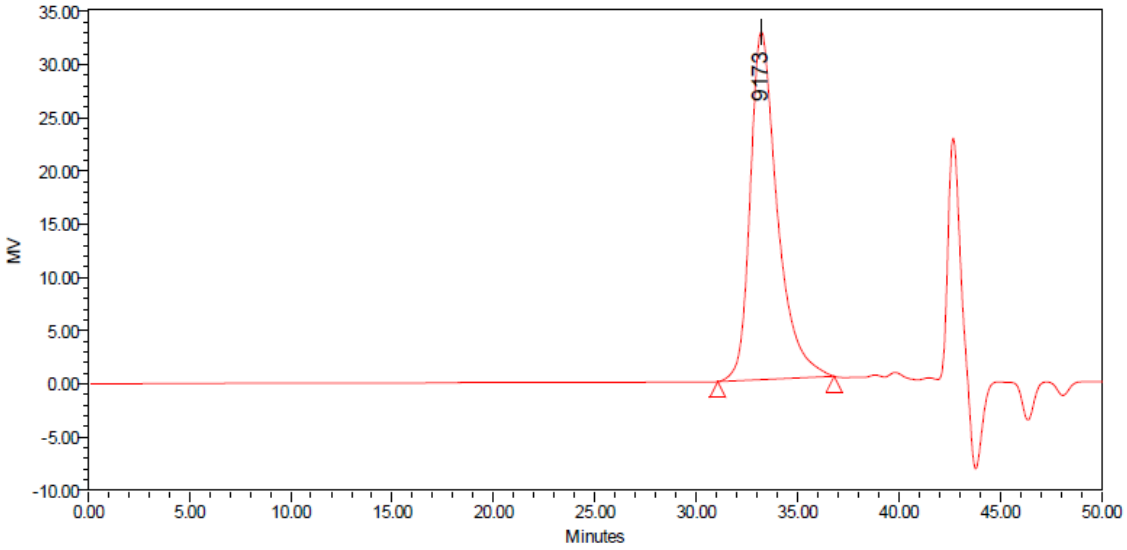


GPC Results

| | Dist Name | Mn | Mw | MP | Mz | Mz+1 | Mv | Polydispersity | MW Marker 1 | MW Marker 2 |
|---|---|---|---|---|---|---|---|---|---|---|
| 1 | | 7507 | 8593 | 9173 | 9541 | 10436 | | 1.144559 | | |

Figure 4.7, 1.3 mol% Methanol

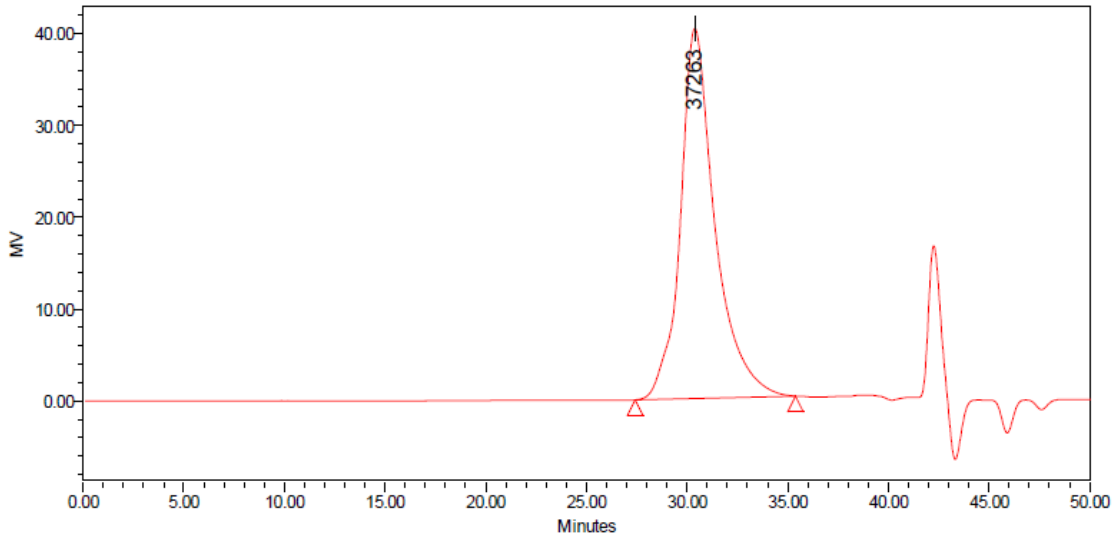


**GPC Results**

| | Dist Name | Mn | Mw | MP | Mz | Mz+1 | Mv | Polydispersity | MW Marker 1 | MW Marker 2 |
|---|---|---|---|---|---|---|---|---|---|---|
| 1 | | 27818 | 36120 | 37263 | 44454 | 53863 | | 1.298427 | | |

Figure 4.7, 3.3 mol% Methanol

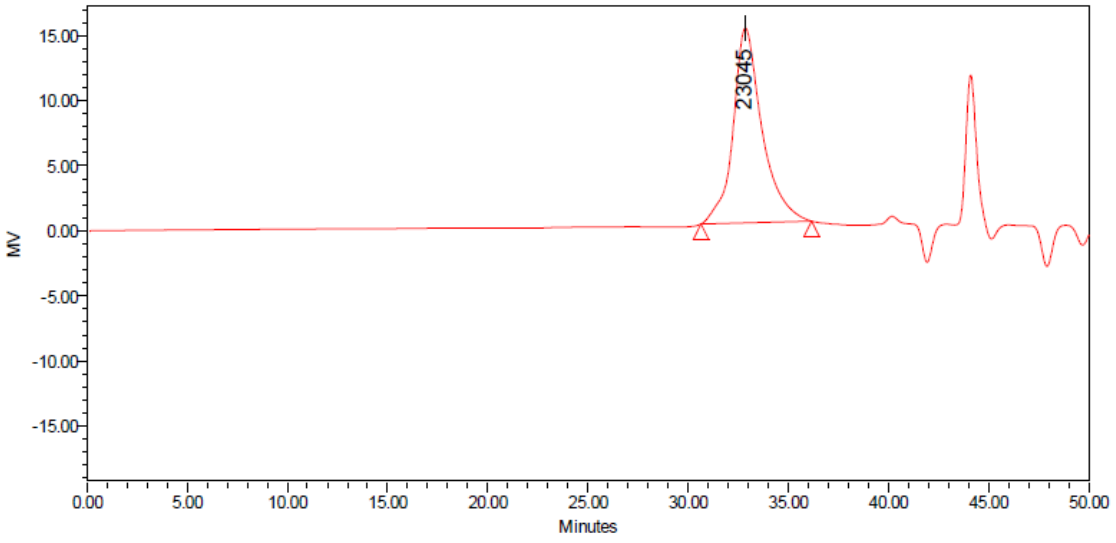


**GPC Results**

| | Dist Name | Mn | Mw | MP | Mz | Mz+1 | Mv | Polydispersity | MW Marker 1 | MW Marker 2 |
|---|---|---|---|---|---|---|---|---|---|---|
| 1 | | 19431 | 22357 | 23045 | 25309 | 28448 | | 1.150579 | | |

Figure 4.7, 6.5 mol% Methanol

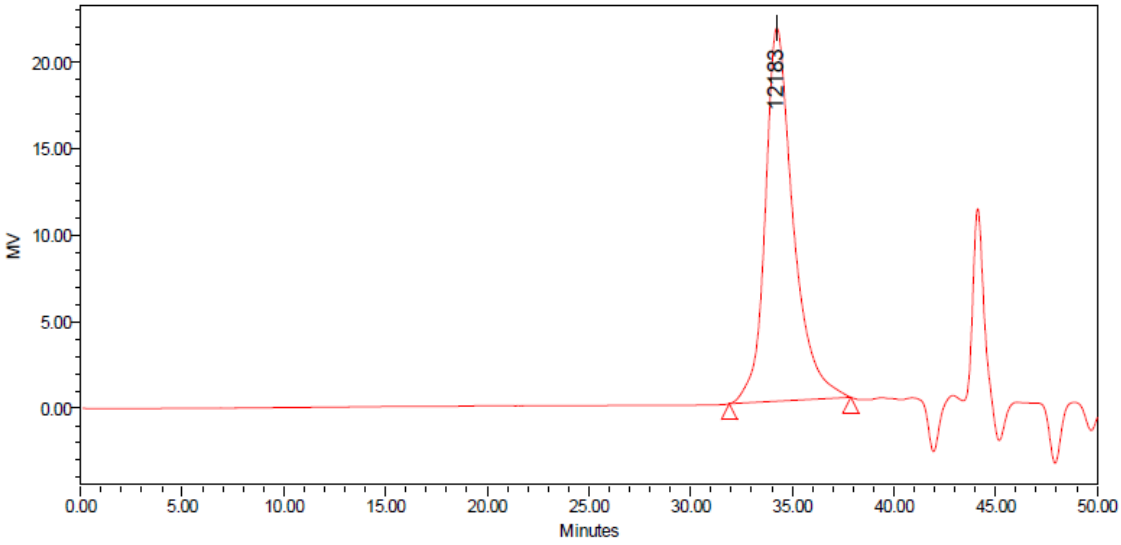


GPC Results

| | Dist Name | Mn | Mw | MP | Mz | Mz+1 | Mv | Polydispersity | MW Marker 1 | MW Marker 2 |
|---|---|---|---|---|---|---|---|---|---|---|
| 1 | | 10150 | 11601 | 12183 | 12949 | 14326 | | 1.142901 | | |

Figure 4.7, 13 mol% Methanol

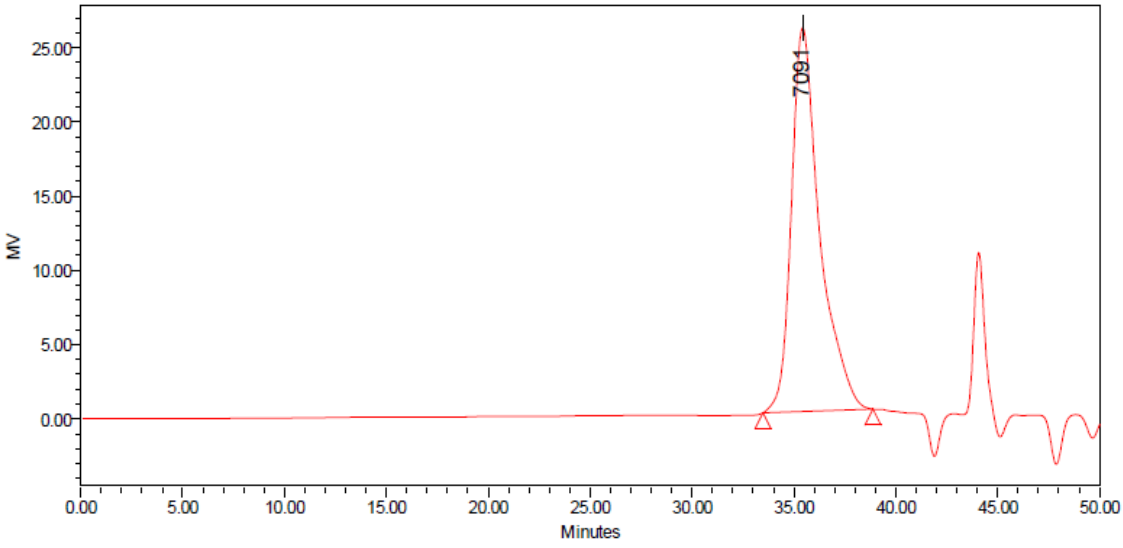


GPC Results

| | Dist Name | Mn | Mw | MP | Mz | Mz+1 | Mv | Polydispersity | MW Marker 1 | MW Marker 2 |
|---|---|---|---|---|---|---|---|---|---|---|
| 1 | | 5778 | 6543 | 7091 | 7228 | 7858 | | 1.132303 | | |

Figure 4.7, 26 mol% Methanol

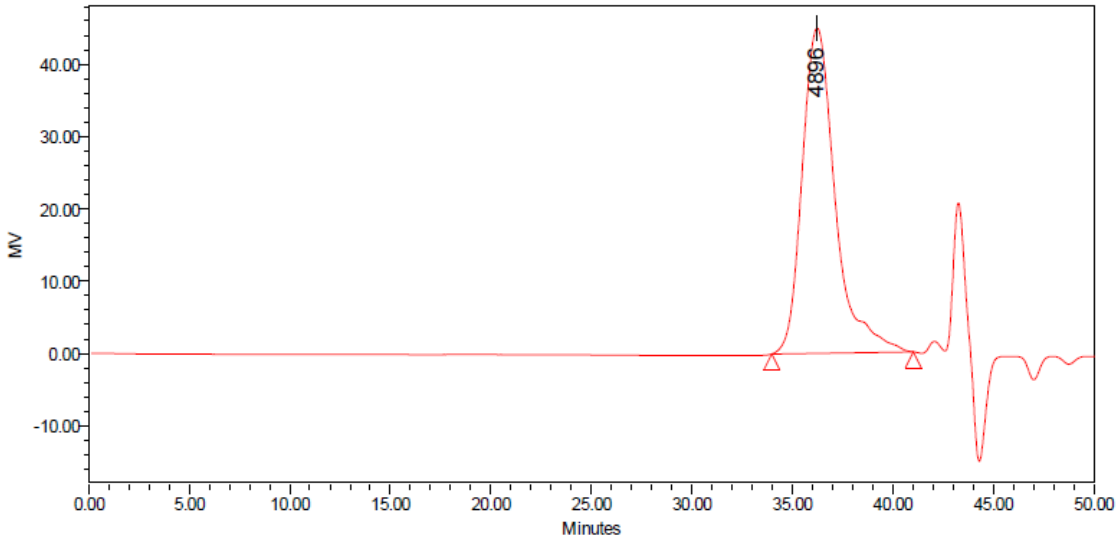


GPC Results

| | Dist Name | Mn | Mw | MP | Mz | Mz+1 | Mv | Polydispersity | MW Marker 1 | MW Marker 2 |
|---|---|---|---|---|---|---|---|---|---|---|
| 1 | | 3973 | 4765 | 4896 | 5417 | 6001 | | 1.199325 | | |

Figure 4.7, 52 mol% Methanol

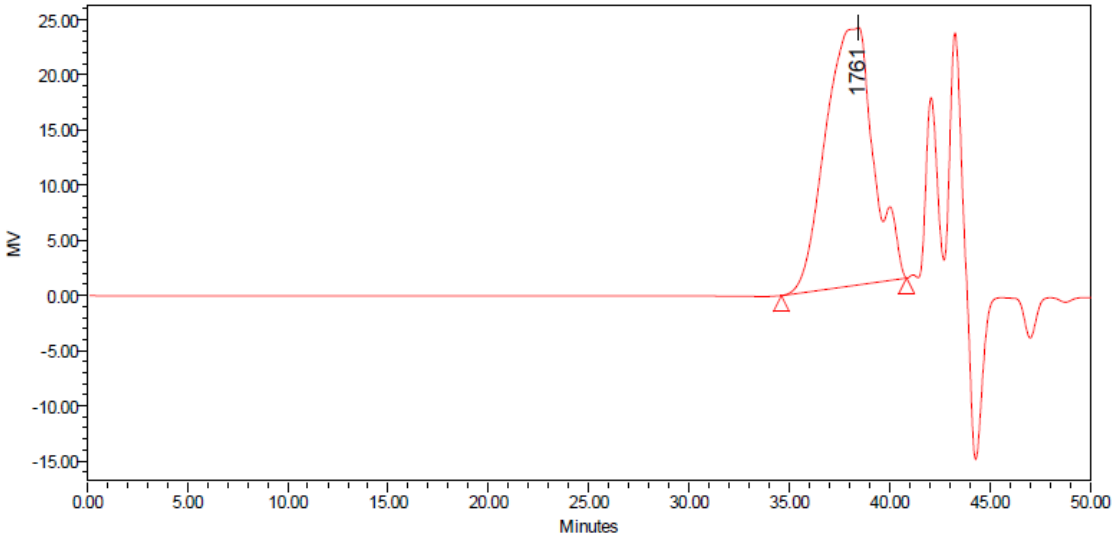


GPC Results

| | Dist Name | Mn | Mw | MP | Mz | Mz+1 | Mv | Polydispersity | MW Marker 1 | MW Marker 2 |
|---|---|---|---|---|---|---|---|---|---|---|
| 1 | | 2076 | 2511 | 1761 | 3042 | 3632 | | 1.209498 | | |

Figure 4.8, a.

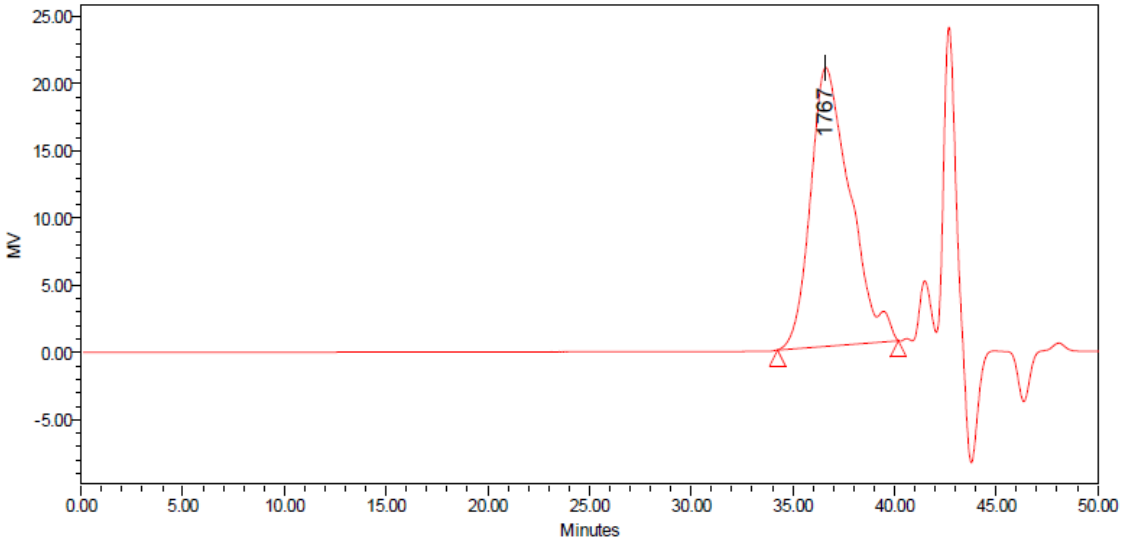


**GPC Results**

| | Dist Name | Mn | Mw | MP | Mz | Mz+1 | Mv | Polydispersity | MW Marker 1 | MW Marker 2 |
|---|---|---|---|---|---|---|---|---|---|---|
| 1 | | 1412 | 1675 | 1767 | 1960 | 2251 | | 1.186244 | | |

Figure 4.8, b.

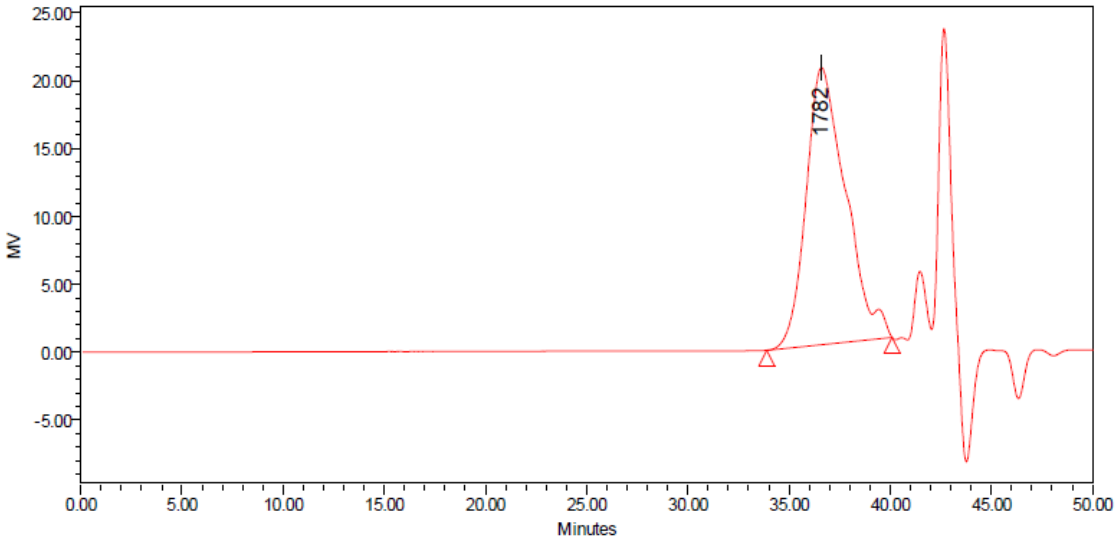


**GPC Results**

| | Dist Name | Mn | Mw | MP | Mz | Mz+1 | Mv | Polydispersity | MW Marker 1 | MW Marker 2 |
|---|---|---|---|---|---|---|---|---|---|---|
| 1 | | 1429 | 1702 | 1782 | 2000 | 2313 | | 1.190549 | | |

Figure 4.9, Entry 1

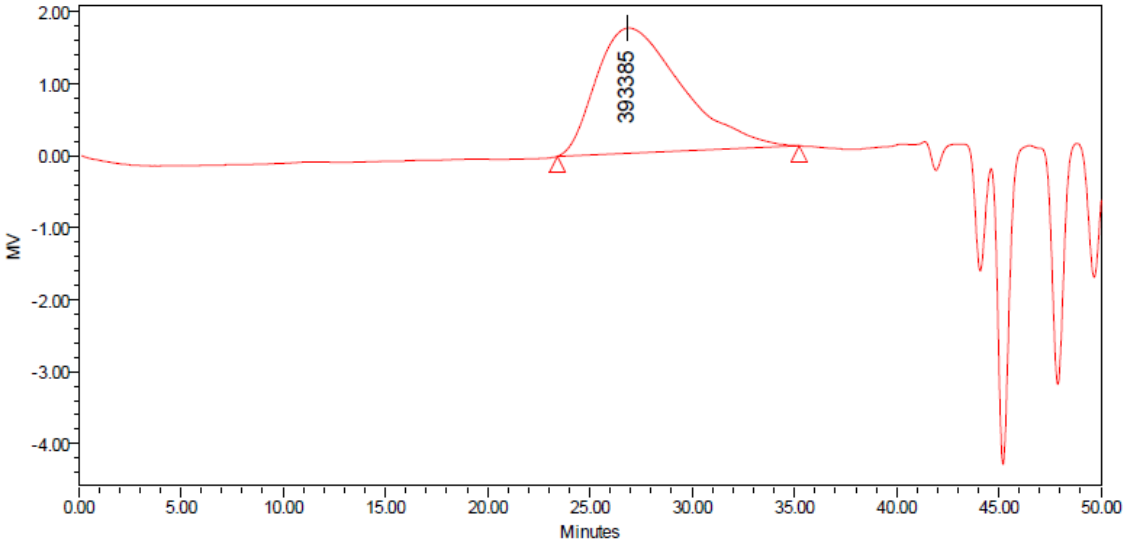


**GPC Results**

| | Dist Name | Mn | Mw | MP | Mz | Mz+1 | Mv | Polydispersity | MW Marker 1 | MW Marker 2 |
|---|---|---|---|---|---|---|---|---|---|---|
| 1 | | 135092 | 309499 | 393385 | 467306 | 574306 | | 2.291022 | | |

Figure 4.9, Entry 2

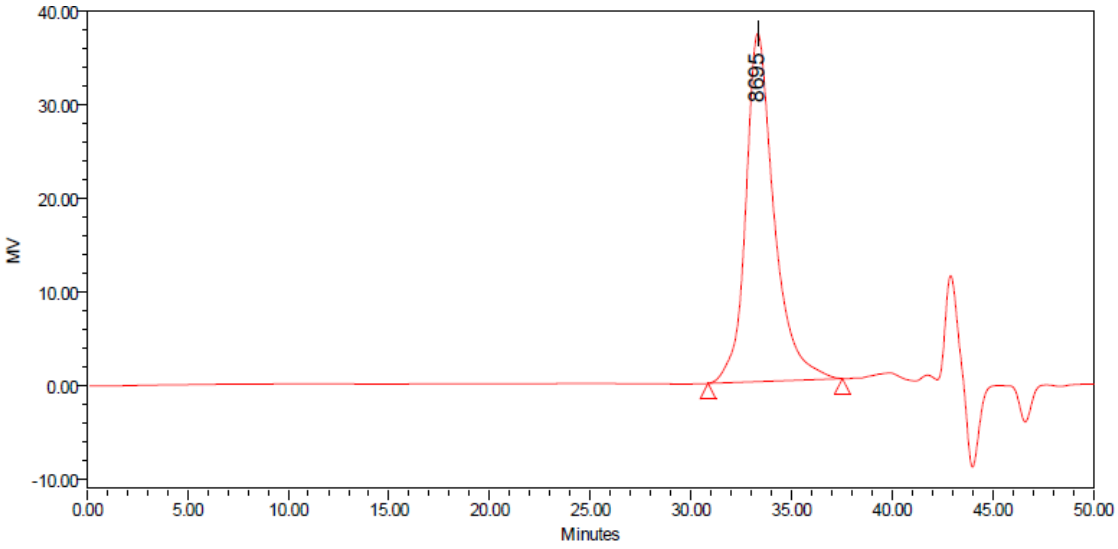


**GPC Results**

| | Dist Name | Mn | Mw | MP | Mz | Mz+1 | Mv | Polydispersity | MW Marker 1 | MW Marker 2 |
|---|---|---|---|---|---|---|---|---|---|---|
| 1 | | 7085 | 8351 | 8695 | 9519 | 10749 | | 1.178617 | | |

Figure 4.9, Entry 3

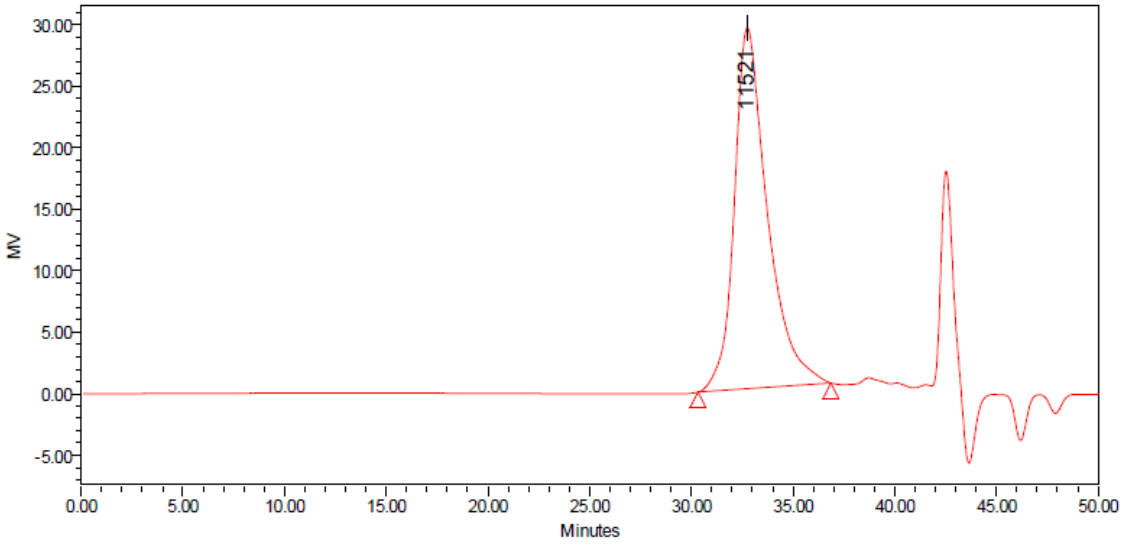


**GPC Results**

| | Dist Name | Mn | Mw | MP | Mz | Mz+1 | Mv | Polydispersity | MW Marker 1 | MW Marker 2 |
|---|---|---|---|---|---|---|---|---|---|---|
| 1 | | 8727 | 10679 | 11521 | 12494 | 14332 | | 1.223724 | | |

Figure 4.9, Entry 4

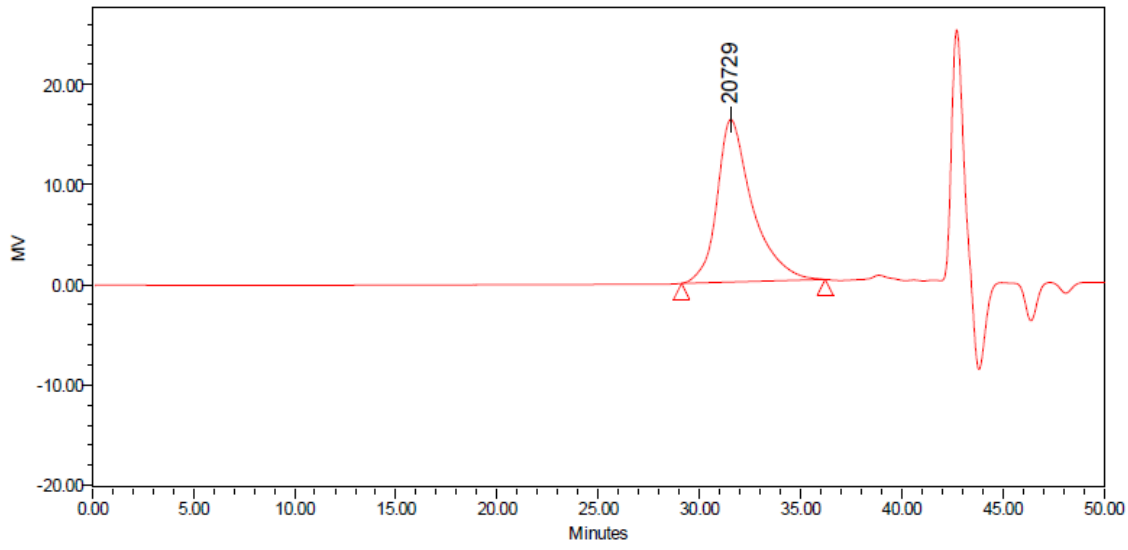


**GPC Results**

| | Dist Name | Mn | Mw | MP | Mz | Mz+1 | Mv | Polydispersity | MW Marker 1 | MW Marker 2 |
|---|---|---|---|---|---|---|---|---|---|---|
| 1 | | 15081 | 19183 | 20729 | 23007 | 26849 | | 1.271983 | | |

Figure 4.9, Entry 5

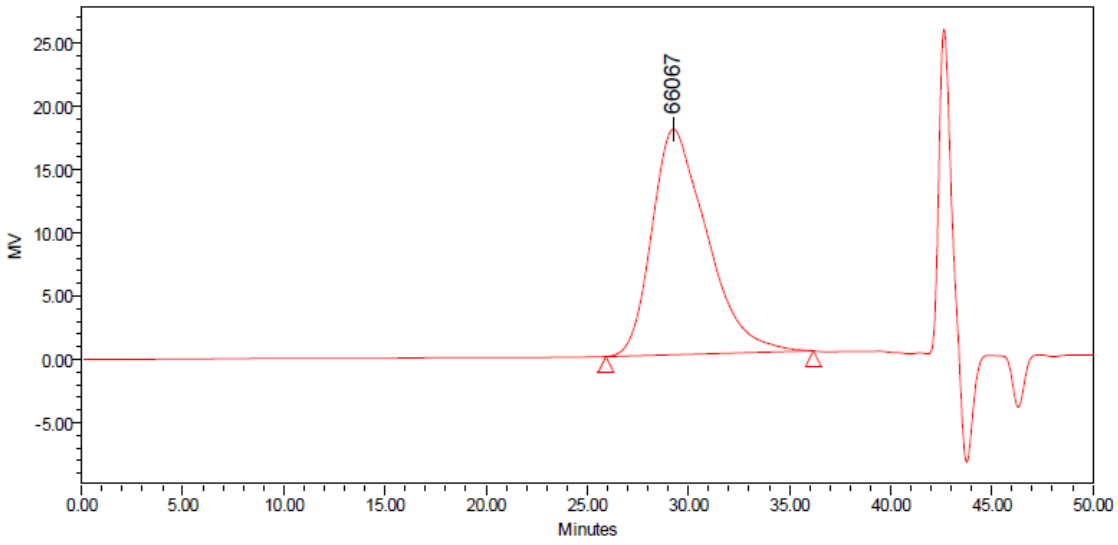


**GPC Results**

| | Dist Name | Mn | Mw | MP | Mz | Mz+1 | Mv | Polydispersity | MW Marker 1 | MW Marker 2 |
|---|---|---|---|---|---|---|---|---|---|---|
| 1 | | 37486 | 62956 | 66067 | 89444 | 117105 | | 1.679467 | | |

Figure 4.9, Entry 6

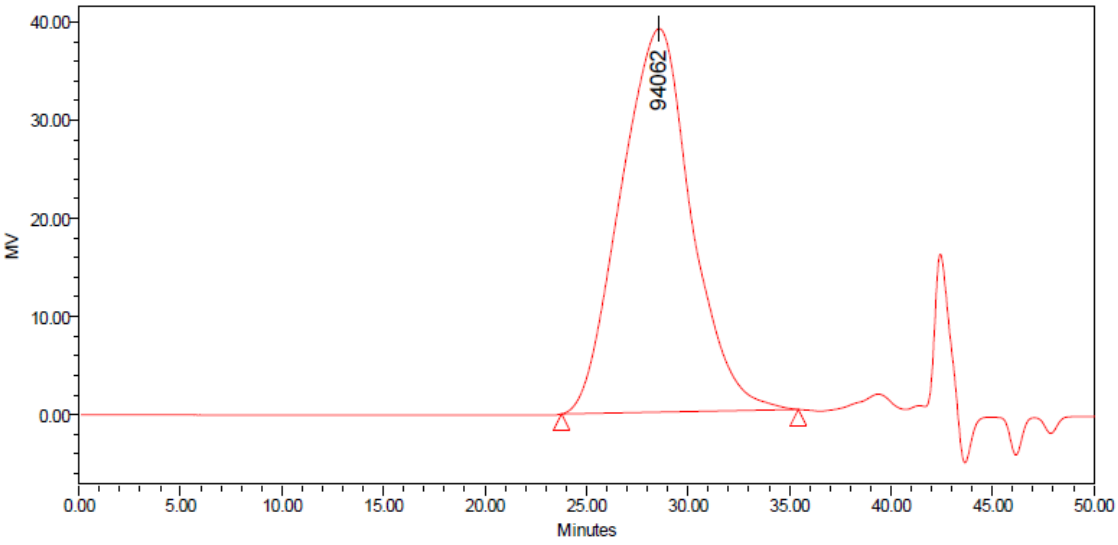


**GPC Results**

| | Dist Name | Mn | Mw | MP | Mz | Mz+1 | Mv | Polydispersity | MW Marker 1 | MW Marker 2 |
|---|---|---|---|---|---|---|---|---|---|---|
| 1 | | 65862 | 140973 | 94062 | 254454 | 381769 | | 2.140437 | | |

Figure 4.9, Entry 7

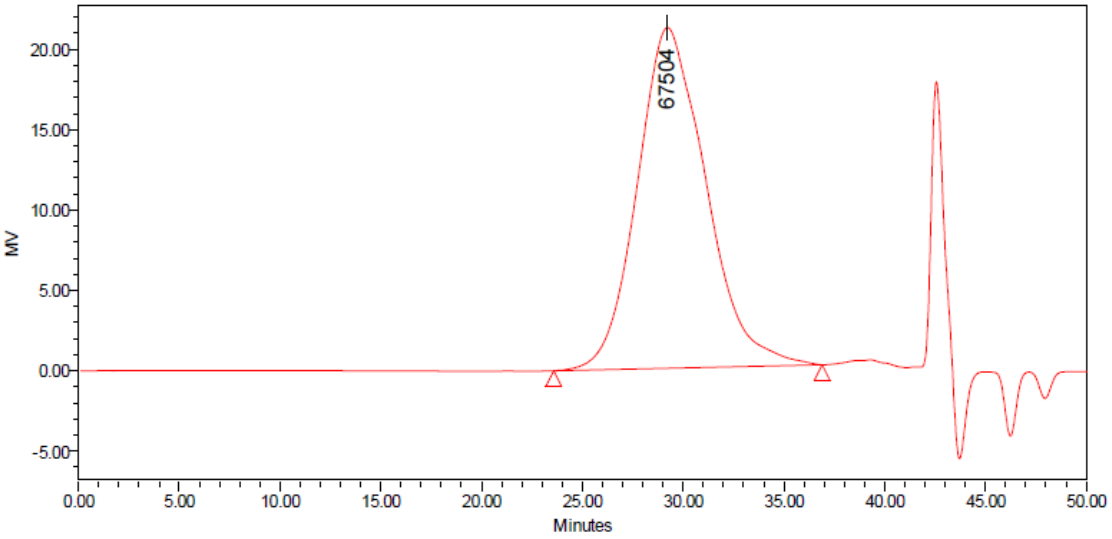


**GPC Results**

| | Dist Name | Mn | Mw | MP | Mz | Mz+1 | Mv | Polydispersity | MW Marker 1 | MW Marker 2 |
|---|---|---|---|---|---|---|---|---|---|---|
| 1 | | 36629 | 80601 | 67504 | 153640 | 268930 | | 2.200482 | | |

Figure 4.9, Entry 8

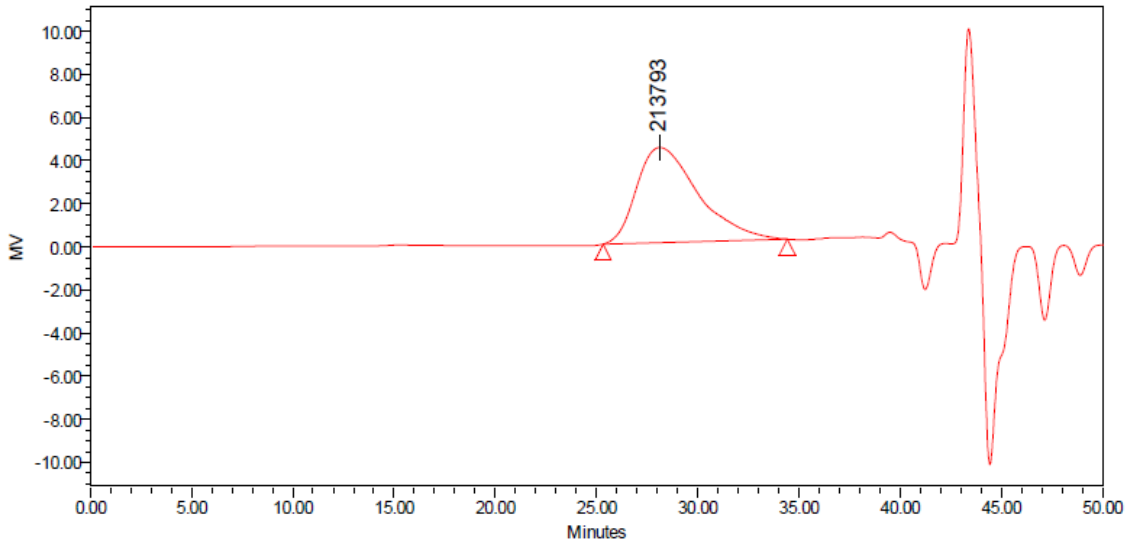


**GPC Results**

| | Dist Name | Mn | Mw | MP | Mz | Mz+1 | Mv | Polydispersity | MW Marker 1 | MW Marker 2 |
|---|---|---|---|---|---|---|---|---|---|---|
| 1 | | 114454 | 191129 | 213793 | 265855 | 332414 | | 1.669917 | | |

Figure 4.10, 0.13 mol% **25**

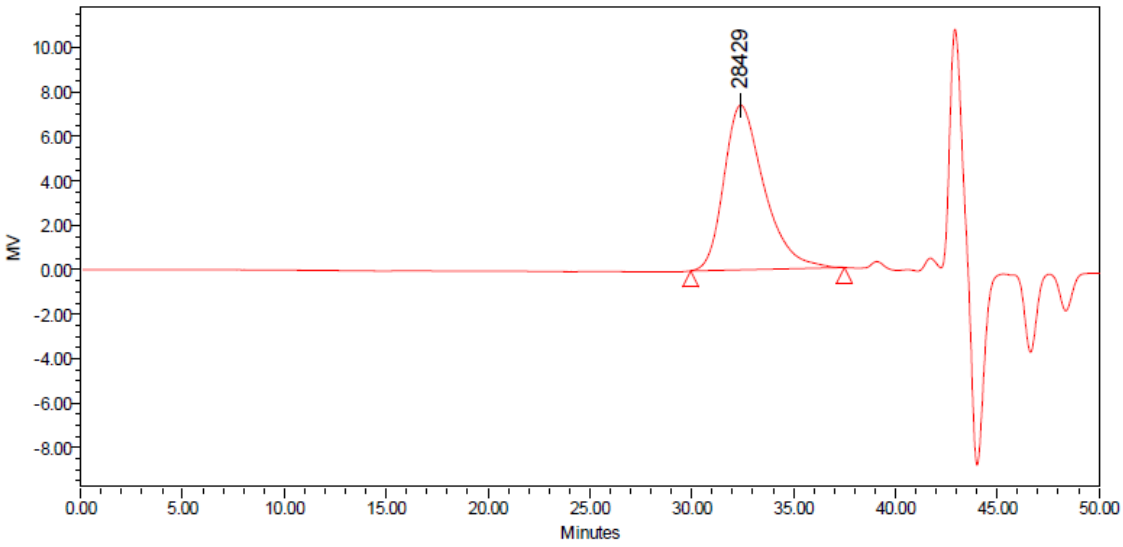


**GPC Results**

| | Dist Name | Mn | Mw | MP | Mz | Mz+1 | Mv | Polydispersity | MW Marker 1 | MW Marker 2 |
|---|---|---|---|---|---|---|---|---|---|---|
| 1 | | 21460 | 26950 | 28429 | 31872 | 36470 | | 1.255840 | | |

Figure 4.10, 0.25 mol% **25**

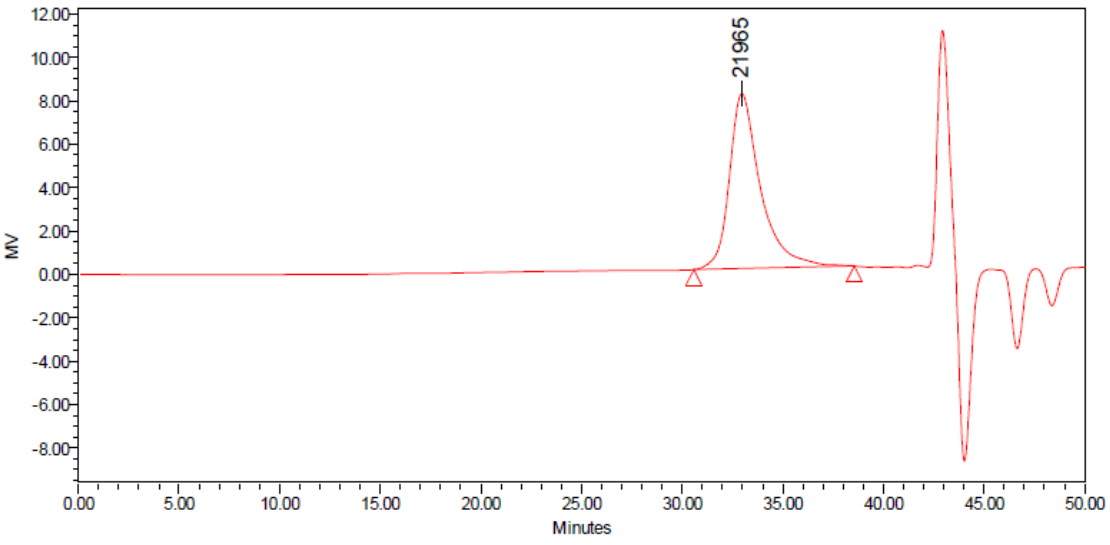


**GPC Results**

| | Dist Name | Mn | Mw | MP | Mz | Mz+1 | Mv | Polydispersity | MW Marker 1 | MW Marker 2 |
|---|---|---|---|---|---|---|---|---|---|---|
| 1 | | 16475 | 20298 | 21965 | 23250 | 25966 | | 1.232026 | | |

Figure 4.10, 0.5 mol% **25**

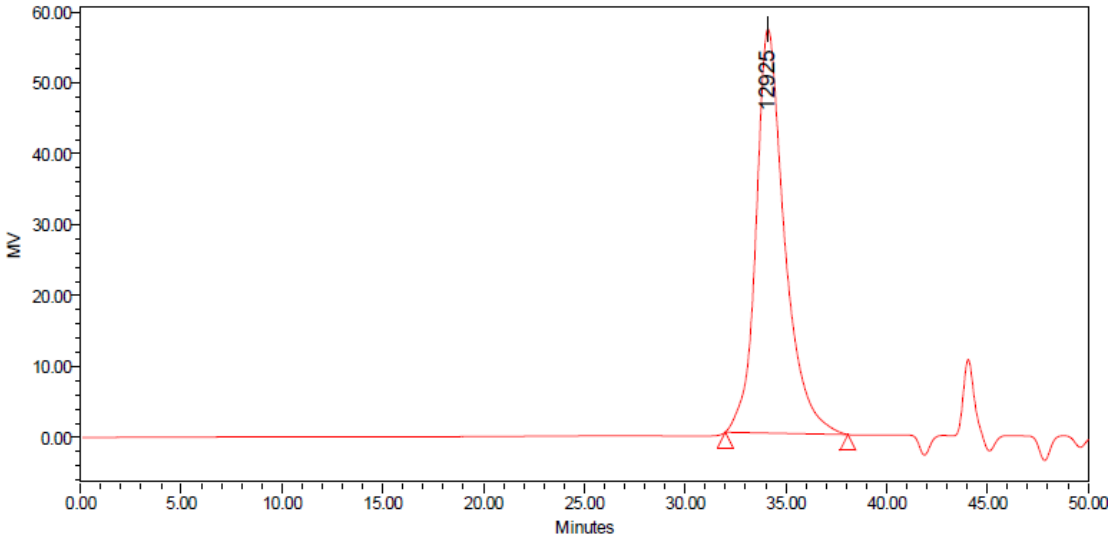


**GPC Results**

| | Dist Name | Mn | Mw | MP | Mz | Mz+1 | Mv | Polydispersity | MW Marker 1 | MW Marker 2 |
|---|---|---|---|---|---|---|---|---|---|---|
| 1 | | 10759 | 12351 | 12925 | 13818 | 15281 | | 1.148002 | | |

Figure 4.10, 1.0 mol% **25**

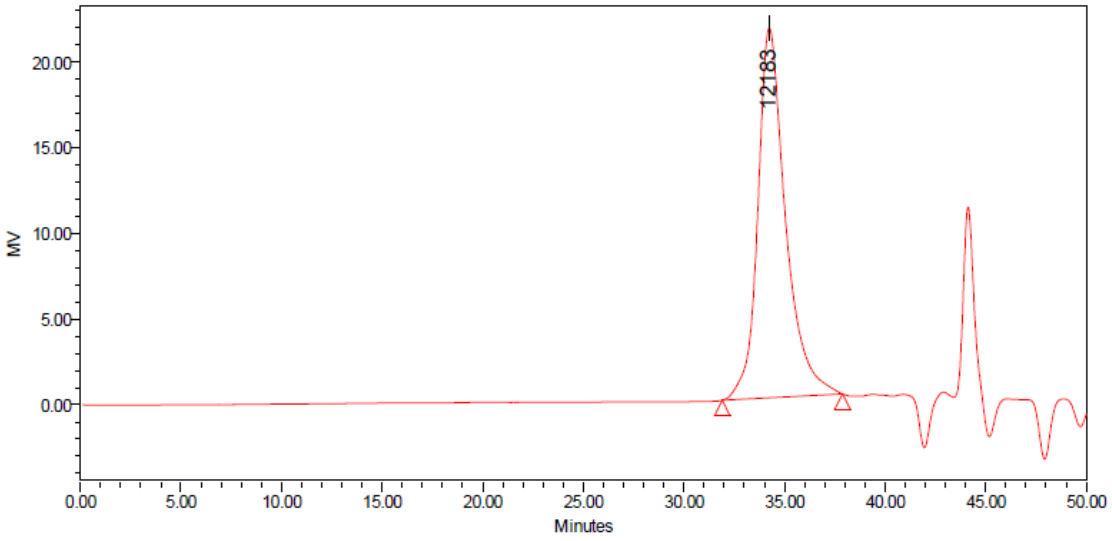


**GPC Results**

| | Dist Name | Mn | Mw | MP | Mz | Mz+1 | Mv | Polydispersity | MW Marker 1 | MW Marker 2 |
|---|---|---|---|---|---|---|---|---|---|---|
| 1 | | 10150 | 11601 | 12183 | 12949 | 14326 | | 1.142901 | | |

Figure 4.10, 2.5 mol% **25**

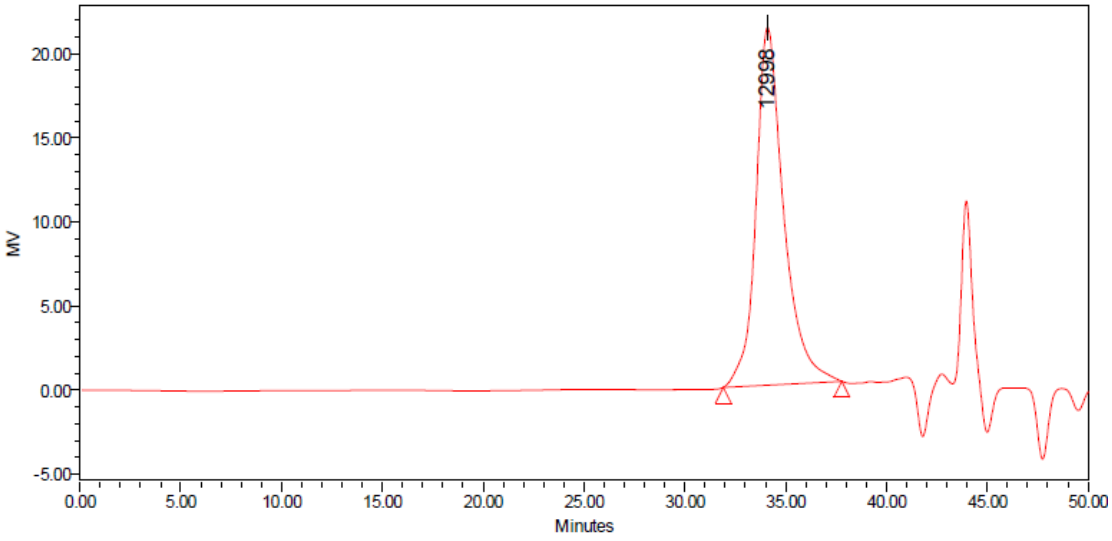


**GPC Results**

| | Dist Name | Mn | Mw | MP | Mz | Mz+1 | Mv | Polydispersity | MW Marker 1 | MW Marker 2 |
|---|---|---|---|---|---|---|---|---|---|---|
| 1 | | 10878 | 12436 | 12998 | 13882 | 15353 | | 1.143212 | | |

Figure 4.11, **25**

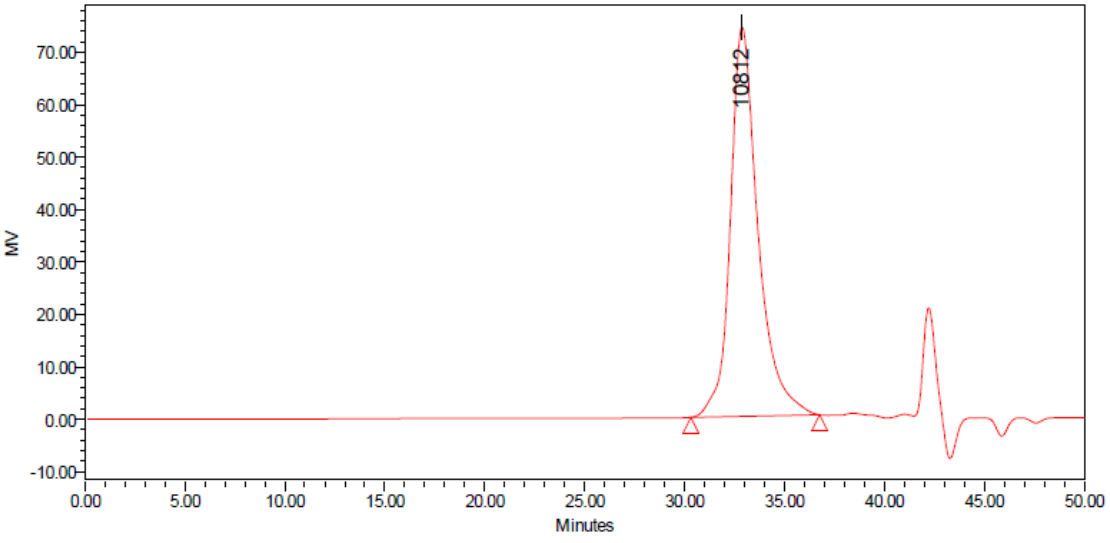


**GPC Results**

| | Dist Name | Mn | Mw | MP | Mz | Mz+1 | Mv | Polydispersity | MW Marker 1 | MW Marker 2 |
|---|---|---|---|---|---|---|---|---|---|---|
| 1 | | 8899 | 10400 | 10812 | 11840 | 13411 | | 1.168681 | | |

Figure 4.11, **28**

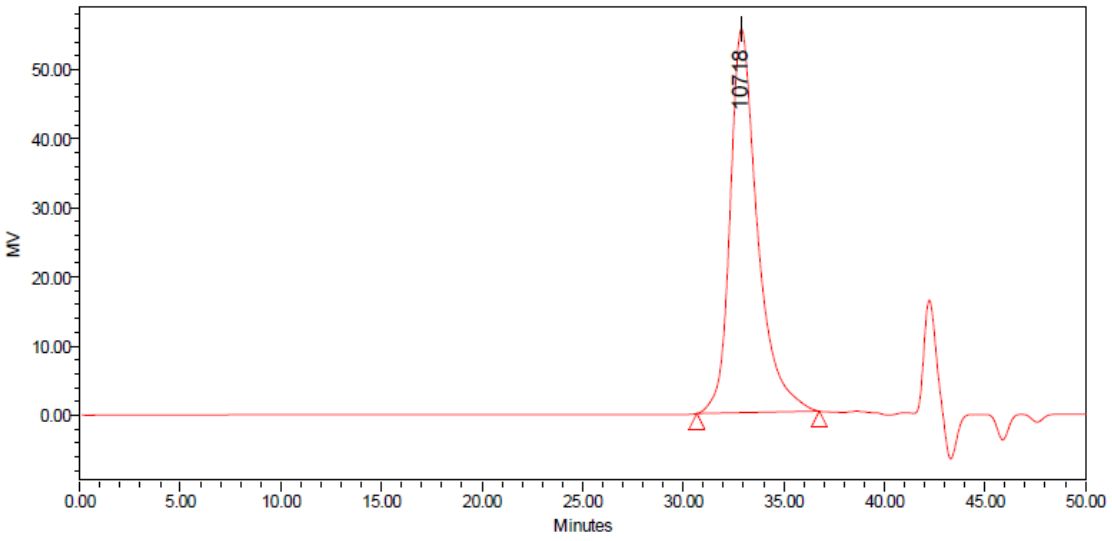


**GPC Results**

| | Dist Name | Mn | Mw | MP | Mz | Mz+1 | Mv | Polydispersity | MW Marker 1 | MW Marker 2 |
|---|---|---|---|---|---|---|---|---|---|---|
| 1 | | 8710 | 10109 | 10718 | 11346 | 12557 | | 1.160587 | | |

Figure 4.11, **29**

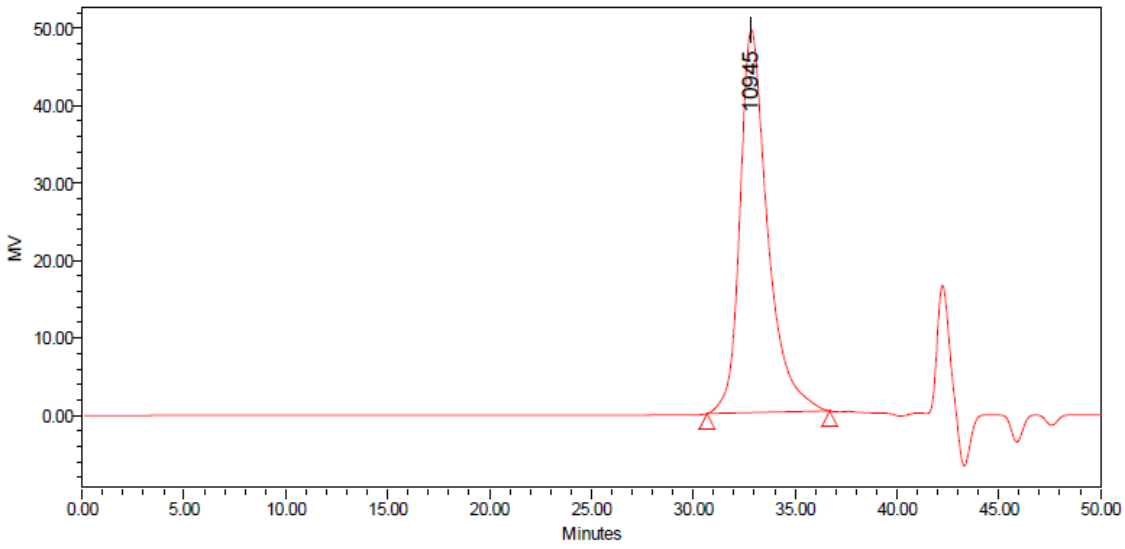


**GPC Results**

| | Dist Name | Mn | Mw | MP | Mz | Mz+1 | Mv | Polydispersity | MW Marker 1 | MW Marker 2 |
|---|---|---|---|---|---|---|---|---|---|---|
| 1 | | 8887 | 10301 | 10945 | 11547 | 12761 | | 1.159025 | | |

Figure 4.15, Entry 2

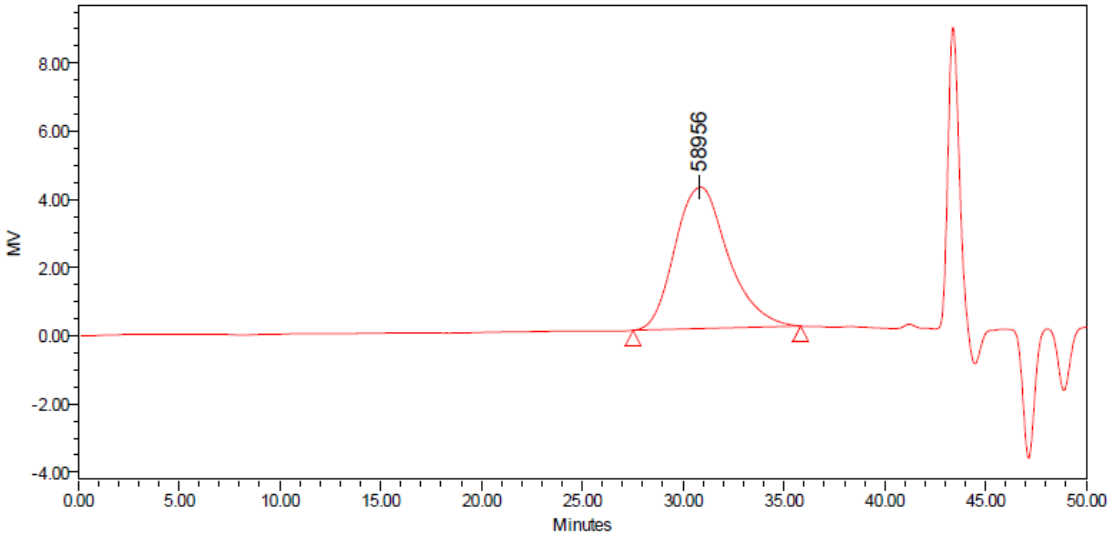


**GPC Results**

| | Dist Name | Mn | Mw | MP | Mz | Mz+1 | Mv | Polydispersity | MW Marker 1 | MW Marker 2 |
|---|---|---|---|---|---|---|---|---|---|---|
| 1 | | 44280 | 62349 | 58956 | 81555 | 101017 | | 1.408072 | | |

Figure 4.15, Entry 3

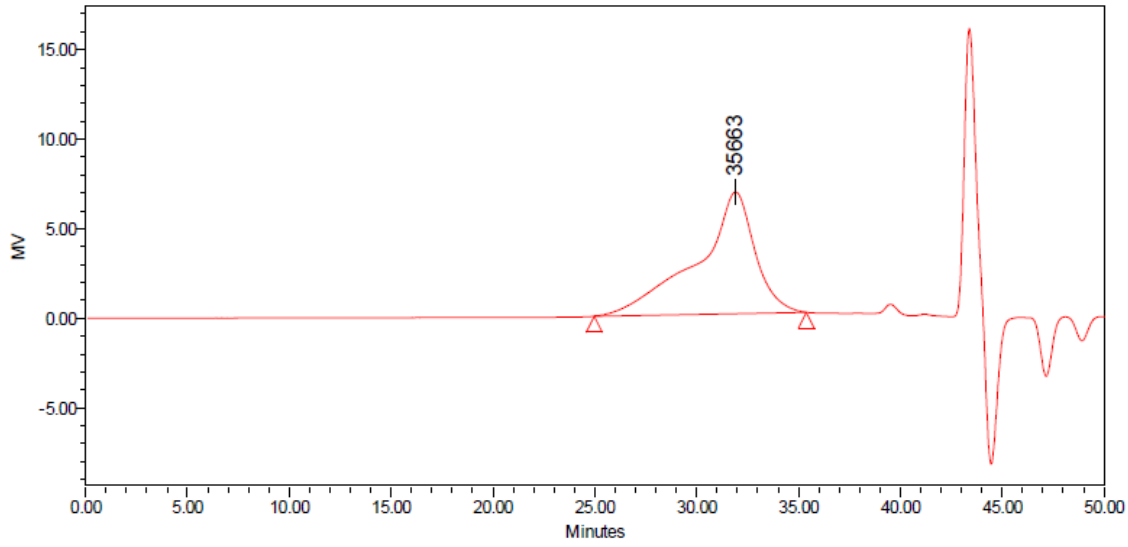


**GPC Results**

| | Dist Name | Mn | Mw | MP | Mz | Mz+1 | Mv | Polydispersity | MW Marker 1 | MW Marker 2 |
|---|---|---|---|---|---|---|---|---|---|---|
| 1 | | 42066 | 84350 | 35663 | 193303 | 337945 | | 2.005169 | | |

Figure 4.15, Entry 4

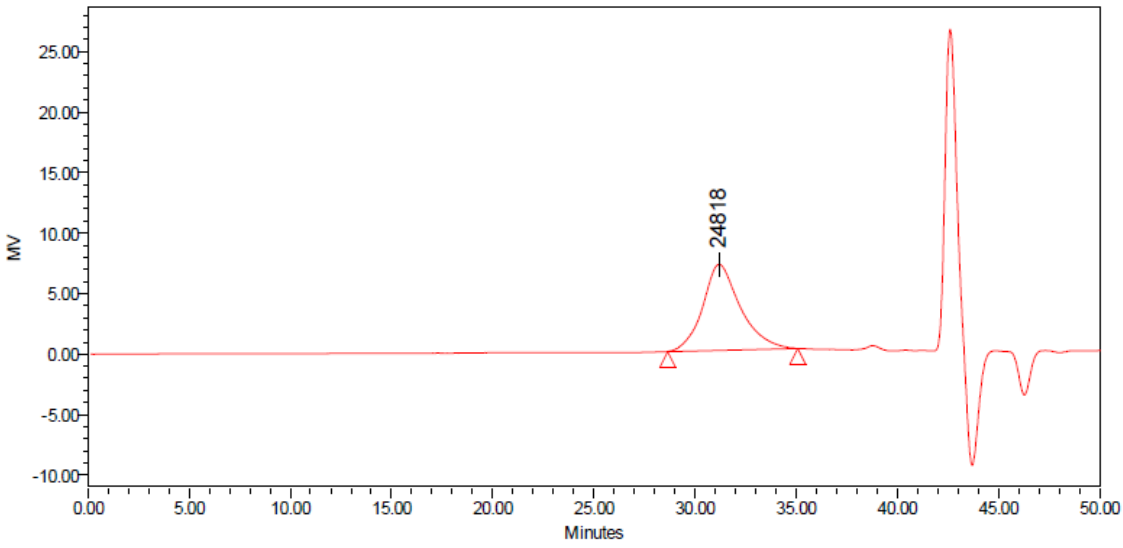


**GPC Results**

| | Dist Name | Mn | Mw | MP | Mz | Mz+1 | Mv | Polydispersity | MW Marker 1 | MW Marker 2 |
|---|---|---|---|---|---|---|---|---|---|---|
| 1 | | 19559 | 24724 | 24818 | 30143 | 35871 | | 1.264082 | | |

Figure 4.15, Entry 5

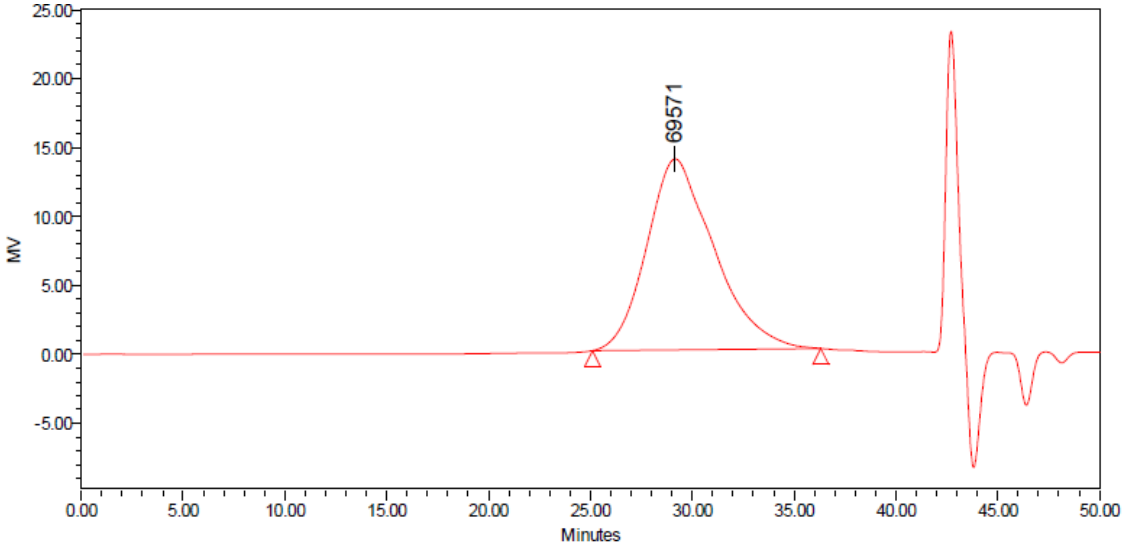


**GPC Results**

| | Dist Name | Mn | Mw | MP | Mz | Mz+1 | Mv | Polydispersity | MW Marker 1 | MW Marker 2 |
|---|---|---|---|---|---|---|---|---|---|---|
| 1 | | 36764 | 76160 | 69571 | 130395 | 196464 | | 2.071610 | | |

Figure 4.15, Entry 6

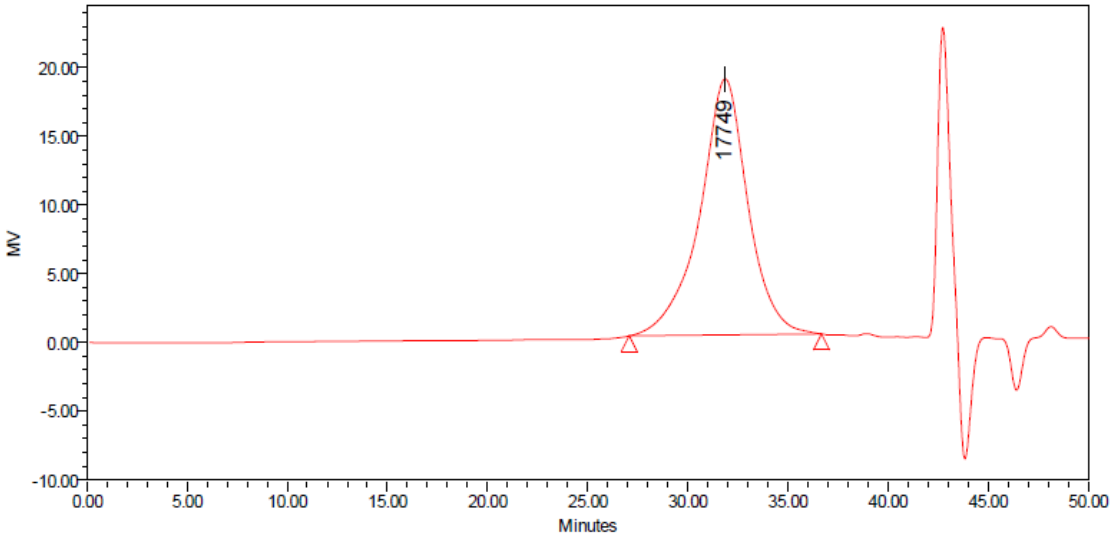


**GPC Results**

| | Dist Name | Mn | Mw | MP | Mz | Mz+1 | Mv | Polydispersity | MW Marker 1 | MW Marker 2 |
|---|---|---|---|---|---|---|---|---|---|---|
| 1 | | 15306 | 23355 | 17749 | 38035 | 62325 | | 1.525841 | | |

Figure 4.15, Entry 7

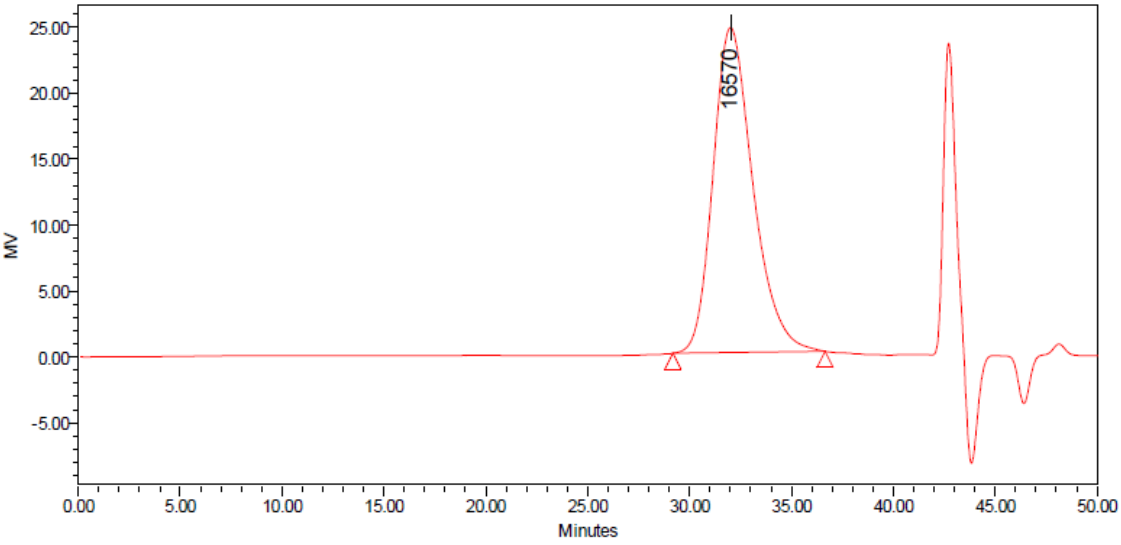


**GPC Results**

| | Dist Name | Mn | Mw | MP | Mz | Mz+1 | Mv | Polydispersity | MW Marker 1 | MW Marker 2 |
|---|---|---|---|---|---|---|---|---|---|---|
| 1 | | 12853 | 16311 | 16570 | 19716 | 23193 | | 1.269070 | | |

## REFERENCES


(1) Markovnikov, V. *Justus Liebigs Ann. Chem.* **1870**, *153*, 228.

(2) Carey, F. A.; Sundberg, R. J. In *Advanced Organic Chemistry Part A: Structure and Mechanisms*; Springer, 2008; pp. 389–459.

(3) Brown, H. C. *Tetrahedron* **1961**, *12*, 117.

(4) Brown, H. C. *Hydroboration*; W. A. Benjamin, Inc.: New York, 1962.

(5) Brown, H. C.; Rao, B. C. S. *J. Am. Chem. Soc.* **1959**, *81*, 6423.

(6) Johnson, J. R.; Van Campen, M. G. *J. Am. Chem. Soc.* **1938**, *60*, 121.

(7) Brown, H. C.; Subba Rao, B. C. *J. Org. Chem.* **1957**, *22*, 1137.

(8) Pauling, L. *J. Am. Chem. Soc.* **1932**, *54*, 3570.

(9) Allred, A. L. *J. Inorg. Nucl. Chem.* **1961**, *17*, 215.

(10) Strom, A. E.; Hartwig, J. F. *J. Org. Chem.* **2013**, *78*, 8909.

(11) Rucker, R. P.; Whittaker, A. M.; Dang, H.; Lalic, G. *J. Am. Chem. Soc.* **2012**, *134*, 6571.

(12) Takemiya, A.; Hartwig, J. F. *J. Am. Chem. Soc.* **2006**, *128*, 6042.

(13) Utsunomiya, M.; Hartwig, J. F. *J. Am. Chem. Soc.* **2004**, *126*, 2702.

(14) Utsunomiya, M.; Kuwano, R.; Kawatsura, M.; Hartwig, J. F. *J. Am. Chem. Soc.* **2003**, *125*, 5608.

(15) Zhu, S.; Niljianskul, N.; Buchwald, S. L. *J. Am. Chem. Soc.* **2013**, *135*, 15746.

(16) Nguyen, T. M.; Manohar, N.; Nicewicz, D. A. *Angew. Chem. Int. Ed. Engl.* **2014**, DOI: 10.1002/anie.201402443.

(17) Bronner, S. M.; Grubbs, R. H. *Chem. Sci.* **2014**, *5*, 101.

(18) Chou, C. M.; Guin, J.; Muck-Lichtenfeld, C.; Grimme, S.; Studer, A. *Chem. Asian J.* **2011**, *6*, 1197.

(19) Beller, M.; Seayad, J.; Tillack, A.; Jiao, H. *Angew. Chem. Int. Ed. Engl.* **2004**, *43*, 3368.

(20) Campbell, A. N.; White, P. B.; Guzei, I. A.; Stahl, S. S. *J. Am. Chem. Soc.* **2010**, *132*, 15116.

(21) Ackermann, L.; Beck, E. M.; Bouffard, J.; Daugulis, O.; Davies, H. M. L.; Dick, A. R.; Du Bois, J.; Fagnou, K.; Gaunt, M. J.; Itami, K.; Larock, R. C.; Lautens, M.; Li, C. J.; Liu, G.; Mariampillai, B.; Martins, A.; Shi, F.; Vicente, R.; Wu, Y.; Xia, J. B.; Yoo, W. J.; You, S. L.; Zalatan, D. N. *Topics in Current Chemistry: C-H Activation*; Yu, J. Q.; Shi, Z., Eds.; Heidelberg, 2010.

(22) Takahashi, K.; Yamashita, M.; Ichihara, T.; Nakano, K.; Nozaki, K. *Angew. Chem. Int. Ed. Engl.* **2010**, *49*, 4488.

(23) Kranenburg, M.; Burgt, Y. E. M. Van Der; Kamer, P. C. J.; Leeuwen, P. W. N. M. Van. *Organometallics* **1995**, *14*, 3081.

(24) Ito, M.; Ikariya, T. *Chem. Commun. (Camb).* **2007**, 5134.

(25) Dong, G.; Teo, P.; Wickens, Z. K.; Grubbs, R. H. *Science* **2011**, *333*, 1609.

(26) Zeng, M.; Li, L.; Herzon, S. B. *J. Am. Chem. Soc.* **2014**, *136*, 7058.

(27) Neunteufel, R. A.; Arnold, D. R. *J. Am. Chem. Soc.* **1973**, *95*, 4080.

(28) Fox, M. A. *Photochem. Photobiol.* **1990**, *52*, 617.

(29) Anslyn, E. V.; Dougherty, D. A. In *Modern Physical Organic Chemistry*; University Science Books: Sausalito, CA, 2006; pp. 935–999.

(30) Yasuo, S.; Arnold, D. R. *J. Chem. Soc. Chem. Commun.* **1975**, 407.

(31) Gassman, P. G.; Bottorff, K. J. *Tetrahedron Lett.* **1987**, *28*, 5449.

(32) Inoue, Y.; Yamasaki, N.; Tai, A. *J. Chem. Soc. Chem. Commun.* **1993**, 718.

(33) Asaoka, S.; Kitazawa, T.; Wada, T.; Inoue, Y. *J. Am. Chem. Soc.* **1999**, *121*, 8486.

(34) Fukuhara, G.; Mori, T.; Inoue, Y. *J. Org. Chem.* **2009**, *74*, 6714.

(35) Mangion, D.; Arnold, D. R. *Acc. Chem. Res.* **2002**, *35*, 297.

(36) Borg, R. M.; Arnold, D. R.; Cameron, T. S. *Can. J. Chem.* **1984**, *62*, 1785.

(37) Mcmanus, K. A.; Arnold, D. R. *Can. J. Chem.* **1995**, *73*, 2158.

(38) Arnold, D. R.; McManus, K. A.; Chan, M. S. W. *Can. J. Chem.* **1997**, *75*, 1055.

(39) Chan, M. S. W.; Arnold, D. R. *Can. J. Chem.* **1997**, *75*, 1810.

(40) De Lijser, H. J. P.; Arnold, D. R. *J. Org. Chem.* **1997**, *62*, 8432.

(41) Arnold, D. R.; Mcmanus, K. A. *Can. J. Chem.* **1998**, *76*, 1238.

(42) Narayanam, J. M. R.; Stephenson, C. R. J. *Chem. Soc. Rev.* **2011**, *40*, 102.

(43) Nicewicz, D. A.; Nguyen, T. M. *ACS Catal.* **2014**, *4*, 355.

(44) Prier, C. K.; Rankic, D. A.; MacMillan, D. W. C. *Chem. Rev.* **2013**, *113*, 5322.

(45) Yoon, T. P.; Ischay, M.; Du, J. *Nat. Chem.* **2010**, *2*, 527.

(46) Hamilton, D. S.; Nicewicz, D. A. *J. Am. Chem. Soc.* **2012**, *134*, 18577.

(47) Kotani, H.; Ohkubo, K.; Fukuzumi, S. *J. Am. Chem. Soc.* **2004**, *126*, 15999.

(48) Ohkubo, K.; Mizushima, K.; Iwata, R.; Fukuzumi, S. *Chem. Sci.* **2011**, *2*, 715.

(49) Ohkubo, K.; Mizushima, K.; Iwata, R.; Souma, K.; Suzuki, N.; Fukuzumi, S. *Chem. Commun. (Camb).* **2010**, *46*, 601.

(50) Ohkubo, K.; Nanjo, T.; Fukuzumi, S. *Bull. Chem. Soc. Jpn.* **2006**, *79*, 1489.

(51) Benniston, A. C.; Harriman, A.; Li, P.; Rostron, J. P.; van Ramesdonk, H. J.; Groeneveld, M. M.; Zhang, H.; Verhoeven, J. W. *J. Am. Chem. Soc.* **2005**, *127*, 16054.

(52) Fukuzumi, S.; Kotani, H.; Ohkubo, K.; Ogo, S.; Tkachenko, N. V; Lemmetyinen, H. *J. Am. Chem. Soc.* **2004**, *126*, 1600.

(53) Ohkubo, K.; Kotani, H.; Fukuzumi, S. *Chem. Commun. (Camb).* **2005**, 4520.

(54) Fukuzumi, S.; Kotani, H.; Ohkubo, K. *Phys. Chem. Chem. Phys.* **2008**, *10*, 5159.

(55) Benniston, A. C.; Harriman, A.; Li, P.; Rostron, J. P.; Verhoeven, J. W. *Chem. Commun. (Camb).* **2005**, 2701.

(56) Verhoeven, J. W.; Ramesdonk, H. J. Van; Zhang, H.; Groeneveld, M. M.; Benniston, A. C.; Harriman, A. *Int. J. Photoenergy* **2005**, *07*, 103.

(57) Benniston, A. C.; Harriman, A.; Verhoeven, J. W. *Phys. Chem. Chem. Phys.* **2008**, *10*, 5156.

(58) Benniston, A. C.; Elliott, K. J.; Harrington, R. W.; Clegg, W. *European J. Org. Chem.* **2009**, 253.

(59) Baldwin, J. E. *J. Chem. Soc. Chem. Commun.* **1976**, 734.

(60) Bordwell, F. G.; Zhang, X.; Cheng, J. *J. Org. Chem.* **1991**, *56*, 3216.

(61) Roberts, B. P. *Chem. Soc. Rev.* **1999**, *28*, 25.

(62) Crich, D.; Grant, D.; Krishnamurthy, V.; Patel, M. *Acc. Chem. Res.* **2007**, *40*, 453.

(63) Guin, J.; Mück-Lichtenfeld, C.; Grimme, S.; Studer, A. *J. Am. Chem. Soc.* **2007**, *129*, 4498.

(64) Pan, X.; Lacôte, E.; Lalevée, J.; Curran, D. P. *J. Am. Chem. Soc.* **2012**, *134*, 5669.

(65) Blanksby, S. J.; Ellison, G. B. *Acc. Chem. Res.* **2003**, *36*, 255.

(66) Nguyen, T. M.; Nicewicz, D. A. *J. Am. Chem. Soc.* **2013**, *135*, 9588.

(67) Bordwell, F. G.; Zhang, X.-M.; Satish, A. V.; Cheng, J.-P. *J. Am. Chem. Soc.* **1994**, *116*, 6605.

(68) Tyson, E. L.; Ament, M. S.; Yoon, T. P. *J. Org. Chem.* **2013**, *78*, 2046.

(69) Tyson, E. L.; Niemeyer, Z. L.; Yoon, T. P. *J. Org. Chem.* **2014**, *79*, 1427.

(70) Clennan, E. L.; Liao, C.; Ayokosok, E. *J. Am. Chem. Soc.* **2008**, *130*, 7552.

(71) Clennan, E. L.; Warrier, A. K. S. *Org. Lett.* **2009**, *11*, 685.

(72) Roberts, J. C.; Pincock, J. A. **2006**, 2453.

(73) Caldwell, R. A.; Creed, D.; Demarco, D. C.; Melton, L. A.; Ohta, H.; Wine, P. H. *J. Am. Chem. Soc.* **1980**, *102*, 2369.

(74) McNulty, J.; Keskar, K. *Tetrahedron Lett.* **2008**, *49*, 7054.

(75) Prediger, P.; Barbosa, L. F.; Génisson, Y.; Correia, C. R. D. *J. Org. Chem.* **2011**, *76*, 7737.

(76) Simone, F. De; Gertsch, J.; Waser, J. *Angew. Chemie Int. Ed.* **2010**, *0804*, 5767.

(77) Acetti, D.; Brenna, E.; Fuganti, C. *Tetrahedron: Asymmetry* **2007**, *18*, 488.

(78) Mangas-Sánchez, J.; Busto, E.; Gotor-Fernández, V.; Gotor, V. *Org. Lett.* **2010**, *12*, 3498.

(79) Kerti, G.; Kurtán, T.; Illyés, T.-Z.; Kövér, K. E.; Sólyom, S.; Pescitelli, G.; Fujioka, N.; Berova, N.; Antus, S. *European J. Org. Chem.* **2007**, 296.

(80) Hatzakis, N. S.; Smonou, I. *Bioorg. Chem.* **2005**, *33*, 325.

(81) Chauhan, K. K.; Frost, C. G.; Love, I. *Synlett* **1999**, *11*, 1743.

(82) Yang, C.-G.; He, C. *J. Am. Chem. Soc.* **2005**, *127*, 6966.

(83) Meyer, C.; Marek, I.; Courtemanche, G.; Normant, J. F. *Tetrahedron* **1994**, *50*, 11665.

(84) Huh, N.; Thompson, C. M. *Tetrahedron* **1995**, *51*, 5935.

(85) Chen, L.; Shi, E.; Liu, Z.; Chen, S.; Wei, W.; Li, H.; Xu, K.; Wan, X. *Chem. a Eur. J.* **2011**, *17*, 4085.

(86) Riener, M.; Nicewicz, D. A. *Chem. Sci.* **2013**, *4*, 2625.

(87) Bauld, N. L.; Pabon, R. *J. Am. Chem. Soc.* **1983**, *105*, 633.

(88) Schepp, N. P.; Johnston, L. J. *J. Am. Chem. Soc.* **1994**, *116*, 7356.

(89) Rooney, J. M. *J. Macromol. Sci. Part A - Chem.* **1986**, *23*, 823.

(90) Gómez, M. L.; Previtali, C. M.; Montejano, H. A. *Int. J. Photoenergy* **2012**, 1.

(91) Yagci, Y.; Durmaz, Y. Y.; Aydogan, B. *Chem. Rec.* **2007**, *7*, 78.

(92) Sangermano, M. *Pure Appl. Chem.* **2012**, *84*, 2089.

(93) Kahveci, M. U.; Yilmaz, A. G.; Yagci, Y. In *Photochemistry and Photophysics of Polymer Materials*; Allen, N. S., Ed.; John Wiley & Sons, Inc.: Hoboken, New Jersey, 2010; pp. 421–478.

(94) Yagci, Y.; Jockusch, S.; Turro, N. J. *Macromolecules* **2010**, *43*, 6245.

(95) Crivello, J. V. *J. Polym. Sci. Part A Polym. Chem.* **1999**, *37*, 4241.

(96) Schlesinger, S. I. *Polym. Eng. Sci.* **1974**, *14*, 513.

(97) Dektar, J. L.; Hacker, N. P. *J. Org. Chem.* **1991**, *56*, 1838.

(98) Dektar, J. L.; Hacker, N. P. *J. Org. Chem.* **1990**, *55*, 639.

(99) Miranda, M. A.; Gar, H. *Chem. Rev.* **1994**, *94*, 1063.

(100) Martiny, M.; Steckhan, E.; Esch, T. *Chem. Ber.* **1993**, *126*, 1671.

(101) Wang, Y.; Haze, O.; Dinnocenzo, J. P.; Farid, S.; Farid, R. S.; Gould, I. R. *J. Org. Chem.* **2007**, *72*, 6970.

(102) Kumli, E.; Montermini, F.; Renaud, P. *Org. Lett.* **2006**, *8*, 5861.

(103) De, P.; Faust, R. *Macromolecules* **2004**, *37*, 7930.

(104) Denmark, S. E.; Butler, C. R. *J. Am. Chem. Soc.* **2008**, 3690.

(105) Dinculescu, A.; Balaban, T. S.; Popescu, C.; Toader, D.; Balaban, A. T. *Bull. des Sociétés Chim. Belges* **1991**, *100*, 665.

(106) Knight, J. D.; Metz, C. R.; Beam, C. F.; Pennington, W. T.; VanDerveer, D. G. *Synth. Commun.* **2008**, *38*, 2465.

(107) Hamilton, D. S.; Nicewicz, D. A. *J. Am. Chem. Soc.* **2012**, *134*, 18577.